# THE JOURNAL OF SOLAR ENERGY SCIENCE AND ENGINEERING

VOLUME 1 | APRIL-JULY, 1957 | NUMBERS 2, 3


## The Proceedings of the Solar Furnace Symposium

### Held January 21 and 22, 1957, at Phoenix, Arizona

### Table of Contents


On High Temperatures and New Materials ..... 3
LESLIE E. SIMON

Solar Furnaces and Their Applications ..... 9
FELIX TROMBE

Design of the Quartermaster Solar Furnace ..... 16
JOHN M. DAVIES AND EUGENE S. COTTON

The Design of the Heliostat Mirror for a Solar Furnace ..... 23
PAUL D. JOSE

Economic Factors in Furnace Design ..... 28
NEVIN K. HIESTER, THOMAS E. TIETZ AND ROBERT DE LA RUE, JR.

Fuel for Solar Furnaces ..... 44
A. RICHARD KASSANDER, JR.

A Solar Furnace for Research in Nonferrous Metallurgy ..... 48
W. M. TUDDENHAM

Industrial Considerations of Solar Furnaces ..... 52
FRANK E. EDLIN

Designing Solar Furnaces for Specific Performance ..... 55
RAYMOND BLISS

A Solar Furnace for Use in Applied Research ..... 63
PETER E. GLASER

The Uses of Solar Energy ..... 68
C. C. FURNAS

Control of Thermal Radiation from a High Temperature Source ..... 75
BERTRAM BUSSELL, K. G. LINDH, R. D. KOPA AND G. E. GWYNNE

Temperature and Flux vs. Geometrical Perfection ..... 78
TIBOR LASZLO

Materials and Surfaces for Solar Furnaces ..... 84
RALPH H. WIGHT

Flux Distribution Near the Focal Plane ..... 94
ROBERT DE LA RUE, JR., EUGENE LOH, JOEL L. BRENNER AND NEVIN K. HIESTER

Construction and Operation of the ASC Solar Furnace ..... 99
C. J. KEVANE

A Method for Manufacturing Parabolic Mirrors ..... 102
PAUL B. ARCHIBALD

Measurement of the Spectral Intensity Distribution of a Convergent High-Intensity Light Beam with a Magnesium-Oxide-Smoked Plate ..... 104
F. W. BROWN, III

Design Problems of a Solar Furnace ..... 108
NOBUHEI HUKUO AND HISAO MII

A Survey of Solar Furnace Installations in the United States ..... 115
RAYMOND K. COHEN AND NEVIN K. HIESTER



OL.
1
957

Copyright 1957
By Association For Applied Solar Energy

$5.00

VOL.
1
1957

# ON HIGH TEMPERATURES AND NEW MATERIALS

By MAJOR GENERAL LESLIE E. SIMON (Ret.)

Vice President and Director, Research and Development, The Carborundum Company
Niagara Falls, N.Y.

**Increased velocities and extended times of flight of guided missiles, increased velocities of passenger-carrying aircraft, and demands for more efficient turbines and for competitive atomic power reactors have placed temperature-strength requirements on materials which exceed the best that can be reasonably hoped for from metals. Controlled high temperatures and uncontaminated atmospheres are indispensable conditions for the development of, and testing of, critically needed new high temperature materials to meet these ends. The solar furnace promises to be a very helpful research tool for meeting this need. The kinds of materials whose need can be anticipated, some of their characteristics, useful applications, and their probable place in future development are described.**

## STEPS TO DISCOVERY

### Procedure

The world is full of phenomena wherein one needs the fruits of a program before one has the proper means of going about the program. In a college curriculum, it is so desirable to take certain courses of study before undertaking others that it has been said it is best to take everything before taking anything. Similarly, in the problem of achieving high temperatures, and of discovering or devising high temperature materials, with the exception of the solar furnace (and partial exception of some other techniques), high temperature materials are needed to produce the high temperatures required for a program of development of the high temperature materials. This anomalous inversion applies with special cogency when one considers the temperatures and the materials which will be required for such prospective new things as gas-cooled nuclear reactors; and one may be even more baffled if he tries to visualize going about making a controlled fusion device. Historically, seemingly insoluble problems of this sort have yielded to stepwise procedures and clever intuitive stratagems. Fortuitous results have often derived from the cross-fertilization of ideas in circumstances where the orderly planning of procedure would have been too difficult to attempt.

### Questions

Another anomalous aspect of our high temperature and high materials efforts is the habitual scientific phenomenon of discovering answers to questions before the questions are, or can be, asked. How often do we say in the laboratory (albeit with some degree of facetiousness and exaggeration), "We know the answers: it is the questions that we do not understand." In scientific work, one frequently has a mass of uncollated answers to questions that have not been articulated and that at the time one perhaps does not even know how to articulate. If one had the prescience of a Leonardo Da Vinci, perhaps this condition would lose some of its wry humor, but even Da Vinci's answers and questions about engines and machines were very poorly related timewise. It is probably impossible to frame questions with regard to unknown concepts. Like the detective in a "whodunit", we must first gather the facts, i.e. the answers and partial answers, and then reason back to the theory. This, of course, is tantamount to actually asking the question in the first instance.

### Order

However, in a world of increasing complexity and specialization, the scientist in one field is less and less adequate to the task of collating his answers with those of scientists in other fields; and even a group of scientists must look for additional support if they are to relate their tentative questions in logical temporal order to the expanding technical and technological needs of civilization. Undoubtedly, the communication between heterogeneous groups afforded by this Solar Furnace Symposium will contribute much to these three problems: (1) experimental procedure, (2) enunciation of questions, and (3) logical ordering of questions. Accordingly, I should like to suggest some possible frames of reference for use in considering needs for high temperatures and high temperature materials.

## THE HISTORICAL RELATIONSHIP BETWEEN TEMPERATURE AND MATERIALS

The history of the world's material progress is markedly linked to the scale at which man could convert heat energy to his use and additionally to the efficiency of that conversion. Whereas the growth curve of total energy converted to man's use as a function of time is consistent with so many other exponentially increasing curves depicting progress, its positive first derivative is due to the scale of conversion. I have shown here in Fig. 1 in a very approximate way the world consumption of energy from 1900

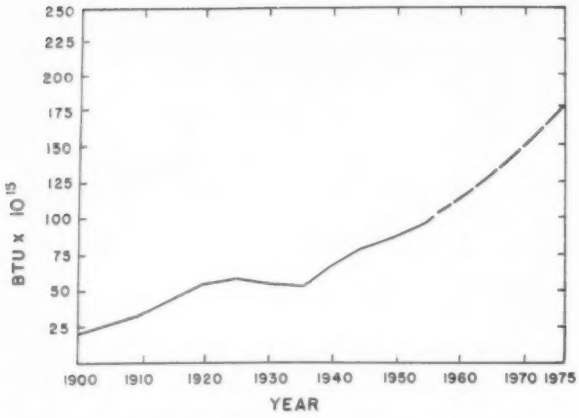


FIG. 1 — World energy consumption (all sources).[1]

up to the present time with an extrapolation to 1975. Quite obviously, if controlled fusion were to become a reality there would be a marked increase in slope of the slope of the curve.[1]

Meanwhile, thermodynamic efficiency, hampered by the nonavailability of structural materials adequate to function under the required temperatures and other environmental conditions, leaves much to be desired.

In a scientific sense, it seems irregular to speak of high temperatures in discussing a range of only 1000° or 2000°K, when this range constitutes such a minuscule portion of the total range of temperature which in the proton-proton chain and carbon cycle reactions in the sun and stars is of the order of millions of degrees K.[2] The relation of this range to the total is clearly shown in Fig. 2, which places the service limits of present-day materials in their appropriate segment of the entire Kelvin Scale.[3]

I wish in no way to detract from the vision of those daring scientists who believe that the almost incredibly high temperatures of fusion may some day be "contained"; however, in order to clarify our view of relatively short-term objectives, I believe it desirable to take a quick glance backward at the historical relationship between temperature and materials for the purpose of noting the things that have influenced the time-scale of past progress.

FIG. 2 — Place of service limit of present materials in the temperature range.

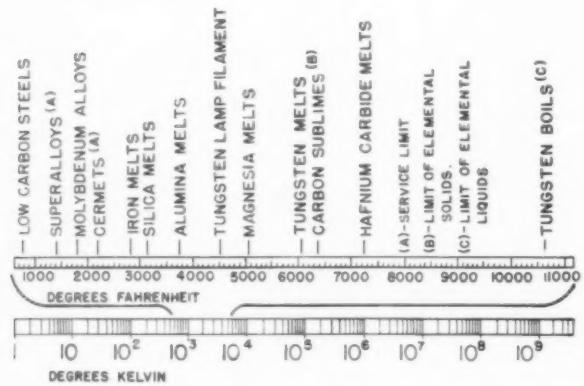


This should permit some prognosis as to what may be expected in the near future.

When Watt made the first steam engine in 1764, there was no materials problem. Available ferrous materials were quite sufficient for the moderate steam pressures and temperatures of the time. In fact it was not until the close of World War I, when the operating temperatures of the most advanced steam turbines reached about 1050° F that serious practical problems began to arise from the inadequacy of materials. During the intervening period of approximately forty years the operating temperatures of turbine design have progressed in an amount of only about 600°F. As design requirements grew in severity stress-wise, they also increased in severity temperature-wise, so that cast iron had to give way to plain carbon steel, which in turn gave way to alloy steels. As the temperature requirement moved steadily upward it was necessary for the austenite steels to be used in place of the ferritic steels because the strength of the latter falls off badly above 1200°F. There are, of course, many alloys including the cobalt-based alloys which exhibit attractive properties at relatively high temperature, but none are likely to have high strength, and marked resistance to creep and erosion at temperatures approaching 2000°F, which seems to be about the limit of operating temperature that can be satisfactorily withstood by alloys of iron, nickel, chromium and cobalt. Among the possible metals that might be used beyond this limit are molybdenum, tungsten, tantalum, and columbium. However, they all have intrinsic limitations which at present, at least, exhibit little likelihood of being circumvented in an economically feasible way.[4] Fig. 3 illustrates the strength versus temperature behavior of a number of high temperature alloys.[5]

## THE CURRENT AND POSSIBLE FUTURE RELATIONSHIP BETWEEN TEMPERATURE AND MATERIALS

Since World War II and particularly more recently, the compulsion of the Second Law of Thermodynamics has driven designers of engineering devices to higher and

FIG. 3 — Degradation of strength with increasing temperature for some selected types of materials.

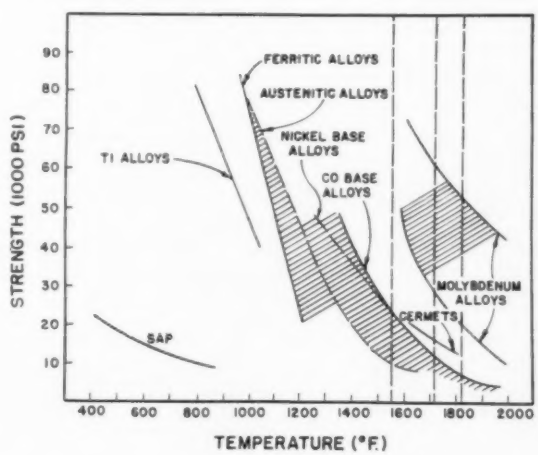


VOL.
1
1957

higher temperatures. In addition, there have arisen the problems of very peculiar atmospheres and the effects of intense neutron and beta-gamma radiation fluxes.[6] Consequently, the problems in testing of materials have increased immensely. Not only do we need to measure physical constants of materials under temperatures and other environmental factors which are difficult of achievement and which render measurement almost impossible, but we encounter many instances in which mere traces of impurities have a marked effect on physicals, and where the impurities may well be introduced by the test method. Perhaps the current demands for new materials can be outlined most briefly by a few examples.

### Gas Turbines

Currently, modern gas turbines can operate about 1650°F. Because even moderate increases in operating temperature are accompanied by substantial improvements in efficiency of fuel utilization, there is continued pressure for development of material to stand higher temperatures.[5] Cermets, especially the titanium carbide bodies bonded with nickel and containing additions of other carbides to improve oxidation resistance, have performed as buckets at temperatures up to 2000°F. Ceramics used as stator blades face less drastic service requirements than when used as buckets. If high temperature materials can be developed to operate satisfactorily in the gas turbine environment, the prospects from the standpoint of presently enunciated requirements are exciting. Such a development could lead to making power plants for really cheap power, utilizing gas-cooled reactors operating at much higher temperatures than are now possible. These two developments should be capable of producing a nationwide or worldwide economic improvement of a whole order.

### Rocket Motors

All large rockets such as the German V-2 and the Redstone are regeneratively cooled; that is, the rocket combustion chamber and nozzle are made of relatively thin metal around which fuel and oxidizers circulate to preheat the liquids before entering the combustion chamber, thereby improving combustion efficiency and preventing excessive heating of the metal parts of the nozzle. This construction is suitable only for liquid propellant rockets. Lately there has been an increasing use of ceramic nozzles and combustion chamber liners in the smaller liquid propellant rockets. A silicon nitride-bonded silicon carbide body, known as NIAFRAX® has proved to very successful for these uses. The current trend in rocket motors is to an increase in use of solid propellants. Where the entire burning time of the propellant is only a few seconds, even very large solid propellant rockets need only metal nozzles. However, long-range rockets require both large size and long-burning times (scores of seconds). For longer burning times, ceramic nozzles provide the only possible solution to the materials problem. Therefore there is increasing demand for lightweight, erosion- and oxidation-resistant ceramic materials capable of withstanding the conditions imposed by prolonged burning times in solid propellant rockets. For these and comparable conditions, graphite, either plain or coated with a material such as silicon carbide or aluminum oxide, is being studied as are a variety of other ceramic materials, most of them based on silicon carbide.[7,8]

### Nose Cones for Missiles

Whereas the tendency of missiles to burn up their tails has been brought somewhat under control, increased velocities, ranges, and times of flight have introduced a new and much more difficult problem of how to keep them from burning up their noses. It is comparatively simple to get missiles and satellites away from the earth where the early travel through the earth's atmosphere is at relatively low velocities; it is much more complex to get them back again.

In the missile field the complex relationship of temperature due to aerodynamic heating and the time of exposure thereto has an important bearing on the probable usefulness of any given material or combination of materials in this application. The temperature reached in the nose cone of a missile is primarily a function of the velocity of the missile and the length of time it is in the earth's atmosphere. It is an unfortunate and painful fact, that as a general rule the velocity and time-of-exposure parameters are maxima for the same missile designs, so that temperature and time of exposure are simultaneously maximized.

It can be readily calculated that the maximum temperature of the nose cone of a long-range missile such as the ICBM will be many thousands of degrees and that the period during which materials in the nose cone will be subjected to such temperatures will be in the order of tens of seconds. Accordingly, the high temperatures and heat fluxes to be experienced are likely to make the use of high temperature ceramic bodies a necessity. But, ceramic bodies as we know them are not strong in an engineering sense. At the same time the need to restrict weight places practical limitations on the mass of material which can be used to absorb heat, to achieve structural strength, and to yield other properties. These become uncomfortable restrictions for large size nose cones. Consequently, there are anomalies in a specification which calls for a lightweight, structurally strong, thermal shock-, oxidation- and erosion-resistant ceramic body several feet in width or diameter and a number of feet in height. Practical fabrication techniques are almost wholly unexplored. Designers are limited to a handful of materials which will satisfy the basic conditions of strength, oxidation- and erosion-resistance, and many of these would appear to warrant little consideration in the temperature ranges projected. Nevertheless, suitable nose cone materials must be developed to meet these requirements if a long-range missile capable of accurate and reliable delivery to a target is to become a reality.

With smaller missiles the problems tend to scale down in all dimensions. Maximum temperatures and periods of exposure reduce with size. The operating specifications

for weapons such as the intermediate-range (1500 miles) missile still appear extremely severe for anything developed to date. A satisfactory solution to the nose cone problem may not only involve new high temperature materials, but a knowledge of how to vary specific heat and thermal conductivity of a body in a controlled manner from inside to outside, so as to combine economically the effects of a heat-sink with refractory characteristics and benefit from radiation. Test methods that include well-controlled high temperatures without contaminating atmospheres appear indispensable to such developments.

### Radomes for Missiles

Radomes are nose cones with an additional requirement, that of transparency to radar beams used for missile guidance. Radomes are not apt to be used on re-entry missiles but rather on defensive missiles, which must seek out and destroy targets, and on research vehicles. Therefore, the anticipated temperatures are not as high, but the imposition of electrical requirements greatly narrows down the possible materials. Likewise, permissible thicknesses are less than in the case of nose cones, and manufacturing tolerances must be much higher. Some available materials such as hot-pressed boron nitride and aluminum oxide appear to answer this requirement, at least in part.[9,10]

### Airfoils

It appeared unnecessary to mention the need for new materials for control surfaces for missiles because it is rather widely recognized that even manned aircraft now under development will burn up their much less severely taxed control surfaces, if they are made of ordinary materials such as dural and stainless steel.[11] Thus far, flame-spraying of the metal with ceramics such as aluminum oxide has proved ineffective. While maximum temperatures reached will be far lower for manned aircraft than for missiles, the long period of exposure to these high temperatures — hours instead of minutes — and the repetitive heating and cooling cycles which materials in this service must withstand, create problems of no mean proportion. Temporarily, the incorporation of small sections of ceramic materials in the airfoil or control surface of an aircraft, while presenting some difficulties, should not be a major problem; but as the over-all performance of the aircraft is increased and larger sections, or perhaps entire airfoils and control surfaces of ceramic materials are indicated, then the problem becomes a titanic one. Even the problem of self-lubrication of hot hinge points is interesting. At the same time, the need to insure the safety of its crew in the case of the manned aircraft adds a consideration which is nonexistent in the case of a missile. Consequently, a high degree of certainty with regard to structural strength under diverse load conditions will be necessary in addition to temperature stability and resistance to oxidation, erosion, and thermal shock.

Here again we encounter a major contradiction in the specifications which establish an absolute requirement that ceramic materials be used for thermal reasons and at the same time establish physical strength requirements which are quite beyond the known capabilities of ceramic bodies. Consequently, there is a strong motivation to explore composite materials — ceramic bodies reinforced with metal for structural strength, ceramic coatings on metal structures, and laminate or sandwich structures, to name a few of the possible approaches.[12] Fibrous, porous, or similar lightweight forms of ceramic materials will be of real importance in providing desirable thermal properties. The list of selected refractory materials in Table I affords a brief view of presently available high temperature materials and their melting points.

TABLE I

SELECTED MATERIALS FOR HIGH TEMPERATURE ENVIRONMENTS*

| Material | | Melting Temp. Deg. C. | Material | | Melting Temp. Deg. C. |
|---|---|---|---|---|---|
| Nonmetal | Metal | | Nonmetal | Metal | |
| $4TaC \cdot ZrC$** | | 3942 | | Nb | 2500 |
| HfC** | | 3887 | | Ir | 2440 |
| C | | 3700 | $B_4C$ | | 2350 |
| | W | 3370 | SiC*** | | 2200 |
| $ThO_2$ | | 3220 | $Al_2O_3$ | | 2050 |
| ZrC | | 3175 | | Rh | 1966 |
| TiC | | 3140 | $Si_3N_4$*** | | 1900 |
| $ZrB_2$ | | 3040 | | Zr | 1900 |
| BN*** | | 3000 | $2MgO \cdot SiO_2$ | | 1890 |
| | Ta | 2996 | $3Al_2O_3 \cdot 2SiO_2$ | | 1810 |
| $TiB_2$ | | 2980 | | Ti | 1800 |
| $HfO_2$ | | 2812 | | V | 1720 |
| MgO | | 2800 | $SiO_2$ | | 1710 |
| $ZrO_2$ | | 2720 | | Cr | 1615 |
| | Mo | 2620 | | Co | 1480 |
| CaO | | 2570 | | Ni | 1452 |
| BeO | | 2510 | | Si | 1420 |
| $ZrO_2 \cdot SiO_2$ | | 2500 | | Be | 1350 |

* Data compiled from various authoritative sources.
** A. F. Wells, *Structural Inorganic Chemistry*, 2nd ed. Oxford University Press.
*** Dissociates without melting.

### Test Methods

Extensive testing of materials under conditions of simulated physical environment and stress loading equal to expected operational loads is mandatory. The design of facilities and test methods for so doing presents a formidable challenge. Whereas some small hypersonic wind tunnels are running at velocities of the order of Mach 10, the construction of a tunnel to go to velocities to simulate re-entry (Mach 15-20) and at the same time to approximate the heat of re-entry appears wholly impractical. Nose cone materials have been tested in the exhaust stream of jet engines and rocket motors, but these atmospheres are highly contaminated and have gross temperature gradients, among other undesirable characteristics.

Solar furnaces, on the other hand, are one of our potentially most valuable tools for the development of data on the high temperature properties of materials. Their use precludes the complicating environmental factors—high neutron and beta-gamma radiation density, high velocity gas streams, combustion products—which tend to plague other means for obtaining high temperatures. These extraneous testing conditions often obscure or prevent the acquisition of fundamental data of particular interest such as strength and creep, emissivity, specific heat and conductivity, electrical properties, and corrosion mechanics of materials at high temperature. However, even solar fur-

nace tests admit of improvement to avoid highly localized heating which can cause spalling of the test piece. The use of high intensity carbon arcs, which can now go up to 50,000°K, offers promise insofar as mere achievement of temperature is concerned, but attempts to heat the volume of gas of a hypersonic tunnel have not succeeded. The achievement of velocity by means of the wind tunnel and independent heating of the point of the model by means of a high intensity arc or by solar energy may offer a solution.[13, 14] The arc technique is under experimentation at the Carborundum Laboratories. At the present time a materials designer is forced to accept inadequate approaches to simulation of operating conditions and to make educated guesses as to behavior of his materials under missile service conditions.

A comparable situation exists in connection with materials for nuclear reactor construction, although in this instance the completion of some facilities is being rushed and present problems should be solved, at least in part, within a short time. Temperatures now under consideration for reactors are far less extreme than those for missiles, but in exchange, major problems are introduced that pertain to stability of materials in high neutron flux fields at sustained operating temperatures. Radiation damage, oxidation and corrosion, retention of fission products, and resistance to structural failure must be evaluated. Reactor facilities suitable for high temperature tests in flowing gas are now receiving much attention.

### Gas-Cooled Nuclear Reactors

Great Britain was the first proponent of the gas-cooled nuclear reactor. The dual purpose plutonium-producing power reactor at Calder Hall, which began operation this past fall, is a gas-cooled machine. This reactor, however, like the first gas-cooled units being considered in the United States, operates in what we might call the conventional temperature range, a few hundred degrees centigrade, and while there are materials problems of some magnitude, they are not primarily thermal in character.[15]

It is inevitable, however, that in time the thermodynamic efficiency of higher operating temperatures and the attendant economies in power generation will force an upward revision in the operating temperature objectives of gas-cooled reactors. The economies in space and weight resulting from the high specific power achieved through high temperature operation of propulsion-type gas-cooled reactor power plants will demand progress in this direction.

In addition, the gas-cooled reactor offers an exciting possibility to the chemical and metallurgical processing industries where it may be possible to furnish high temperature process heat economically. This could permit revolutionary advances in chemical synthesis, petroleum cracking and refining, coal carbonization, and concurrent ore reduction and production of refined metal. Such a reactor would operate in the range of 1500-3000°C, and would utilize any one of several gases, the principal ones under consideration being He, $H_2$, $H_2O$, air, $Co_2$ or $N_2$.

Helium or nitrogen are the two gases most generally considered for use in the power reactors. With the exception of helium, all of these gases introduce corrosion problems of varying magnitudes. The nitride reactions with metals, for example, are a matter of considerable concern in those circumstances where temperatures are low enough to permit use of metals.

Two other parameters besides temperature and corrosion severely limit the number of materials suitable for use in a gas-cooled nuclear reactor: the nuclear capture cross-section, and radiation damage characteristics. For structural use in the range of 800-2000°C, in helium-cooled reactors, molybdenum and tungsten can be considered. Helium handling at elevated temperatures, on the other hand, is beset with considerable difficulties. Once the move is made to other gases at the high temperature level, choice of structural materials of necessity shifts to the ceramics. The number of materials having a combination of the properties required for such service is extremely limited. Silicon carbide, graphite, beryllium oxide, zirconia, and alumina appear to be of principal interest from a structural standpoint and also as possible matrix or protective coatings for uranium oxide or uranium carbide fuel elements.[16]

### The Fusion Reactor

In the long-range future the temperature levels with which we will have to contend in the thermonuclear or fusion reactor will dwarf anything discussed heretofore in this paper. Perhaps here is an area in which we need not bother about first getting the material to hold the material that we need to make. The containment of the plasma, in which form the reactants will exist at this temperature level, and its thermal insulation, seems feasible only by use of a magnetic field.

The prospect of really abundant nuclear power by fusion, rather than by fission, with its attendant fission products, is indeed engaging. However, until the method of sustaining the controlled thermonuclear reactor has been demonstrated, along with the means of containing and insulating the reactants, the nature and magnitude of the materials problems associated with utilization of the resultant energy will not be evident. That they will be unique and difficult seems highly probable. On the other hand, this apparent ultimate in man's mastery of energy could come through the direct conversion of nuclear energy to electrical energy. It might even be suggested that power under these conditions might be so abundant or in such a form that it will require no conductors for its transmission, and distributional problems would disappear. Perhaps when this time comes we shall exchange our engaging scientific activities for contemplative and philosophical ones and concentrate on our spiritual well-being instead of on an understanding of nature.

## REFERENCES


1. W. E. Pratt, "The petroleums, an enduring source of energy." Atomic Industrial Forum Report, no. 11, 1956.
2. F. Hoyle, "Ultrahigh temperatures." *Scientific American* 191(3): 144-54, Sept. 1954.

3. P. Duwez, "High temperatures: materials." *Scientific American* 191 (3): 99-106, Sept. 1954.
4. L. D. Richardson, "Ceramics in aviation." *News in Engineering* (Engrg. Expt. Sta., Ohio State Univ.) 28: 34-40, July, 1956.
5. J. J. Harwood, "Advances in gas turbine materials." *Aero Digest* 73: 20-27, Aug. 1956.
6. W. Finkelnberg, "Behavior of matter at high temperatures." *Research & Engineering* 11: 24-26, Aug. 1956.
7. G. M. Butler, "Jets, reactors, missiles, need ceramic parts." *Ceramic Industry* 64: 70-74, 101, March 1955.
8. H. M. Kilmar and W. L. Wroten, "Special ceramic materials of construction for rocketry." *Ceramic Industry* 66: 93-96, May 1956.
9. K. M. Taylor, "Boron nitride, a new ceramic material." *Materials & Methods* 43: 88-90, Jan. 1956.
10. P. S. Hessinger, "Ceramic radomes for aircraft." *American Ceramic Society Bulletin* 34: 145-50, May 1955.
11. T. von Karman, "Aerodynamic heating, the temperature barrier in aeronautics." *Research & Engineering* 11: 31-33, Aug. 1956.
12. F. R. Shanley, W. J. Knapp, and R. A. Needham, "Prestressed ceramics for airplane wings." *Ceramic Industry* 66: 113-16, June 1956.
13. A. Kantrowitz, "Very high temperatures." *Scientific American* 191: 132-42, Sept. 1954.
14. T. S. Laszlo, "Solar furnaces in high temperature research." *Science* 124: 797-800, Oct. 26, 1956.
15. F. Daniels, "Small gas cycle reactor offers economic promise." *Nucleonics* 14: 34-44, March 1956.
16. L. R. McCreight and H. G. Sowman, "Ceramics for nuclear power applications." *American Ceramic Society Bulletin* 35: 176-79, May 1956.

VOL.
1
1957

# SOLAR FURNACES AND THEIR APPLICATIONS

By FELIX TROMBE

Director of Research, Centre National de la Recherche Scientifique
Paris, France

**Problems encountered in focusing the solar energy in the construction of the large solar furnace at Montlouis are discussed, and the 1000-kw unit now being built is described. A short review of solar furnace applications and of the economics of their operations indicates increased importance and use for this type of furnace.**

## INTRODUCTION

A number of papers have already been presented by the author and by other authors on the general subject of solar furnaces. This paper will be limited to a discussion of new techniques developed at the Solar Laboratory of Montlouis and to a discussion of the future industrial possibilities of these furnaces.

## TECHNICAL PROBLEM OF FOCUSING SOLAR ENERGY

We have discussed in a previous paper[1] the solutions which we have adopted in the construction of the large furnace at Montlouis. We shall now briefly review some of our conclusions.

### Mirror Surface

It is preferable to use glass surfaces in a solar furnace with a distant heliostat requiring reflections over long distances. One might be able to use a plastic surface, but we have never tried it. A metallic reflecting surface exhibiting the same flatness as glass is hard to manufacture and certainly more expensive.

Our experience indicates that it is preferable to use glass with the back surface silvered, the silver being protected by deposited copper and varnish. The mirrors of Montlouis which have been in operation since 1949 have proven that such mirrors will resist a harsh climate for many years.

Until now no one has tested over a long period of time and in actual operating conditions an aluminized glass surface with the aluminum deposit protected by a varnish. Such an experiment would be of interest.

### Mirror Size

The size of the mirrors selected for the heliostat at Montlouis is 50 x 50 cm. It does not seem practical to us to build flat reflectors with much larger mirrors. A mirror 50 x 50 cm and 6 or 7 mm thick is sufficiently rigid and will not be elastically deformed under its own weight or by the forces of average winds. Larger and thicker glass will be affected by thermal dilatations, and if a mirror 1 m by 1 m and 7 mm thick is used, it is probably going to be broken before too long. Smaller mirrors, of less than 50 x 50 cm, would add little to their rigidity and flatness while the number of supports would be increased.

We have already mentioned the problem of reflecting sunlight over a long distance. A flat mirror reflects a central beam of constant intensity which is surrounded by zones of increasing shadow and decreasing energy. These zones will increasingly spill over the central beam as the target is further away from the mirror. It is important that the zones of shadow do not reach the paraboloid. One must therefore carefully calculate the dimensions of the reflectors so that only the central beam of energy reaches the paraboloid.

### Guiding Mechanism

We have concluded that the simplest and most reliable guiding mechanism is a photoelectric cell device composed of four photoelectric cells. The one used at Montlouis is shown schematically in Fig. 1.

FIG. 1 — Schematic diagram of tilt director.

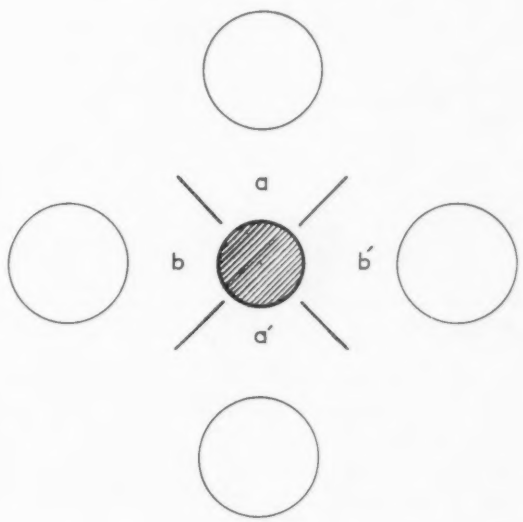

FIG. 2 — Supports and control jacks of heliostat of 70-kw furnace.

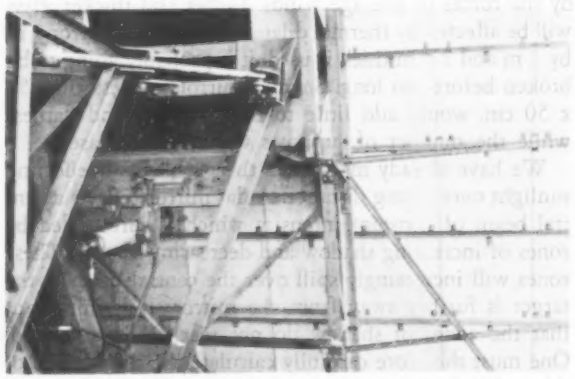

FIG. 3 — Frame and control jacks of one of the heliostats for 1000-kw furnace.

We also believe that hydraulic mechanisms will operate the heliostat with a minimum of energy expense, and a minimum of maintenance costs. We use at Montlouis constant oil pressure obtained with simple weighted accumulators. The oil pressure is controlled by rotary valves actuated by amplified signals from the photoelectric cells. The oil pressure then operates the hydraulic azimuthal and elevation jacks that move the heliostat (see Figs. 2 and 3). The photoelectric signals are amplified electronically and operate solenoid and mechanical actuating arms. This system, which is already in use on the 35-ft furnace, has been adopted for the new 1000 kw unit. Fig. 3 shows the jacks and supports of one of the 6 x 7 m heliostats that will be used in this new unit. About 100 to 120 watts are sufficient to operate this heliostat during a full day.

We have also developed in recent months a new photoelectric tilt director with a much larger focal field. This director is able to place the heliostat in correct position even after solar interruption of several hours.

## THE 1000-KW UNIT UNDER CONSTRUCTION AT MONTLOUIS

### General Arrangement

The 1000-kw unit is already under construction. The general arrangements of the heliostats and of the paraboloid are shown in Figs. 4 and 5.

The heliostat arrangement permits the use of a large number of independent units that are each guided by their own photoelectric tilt director. These will be adjusted so that all the heliostats will reflect parallel rays on the concentrator.

### Heliostats

Sixty-two heliostats, each 6 m high by 7 m wide, will reflect sunlight into the concentrator. The size of these heliostats was determined by calculating their optimum economic size. For example, these heliostats can be transported from the factory to the site with a minimum of assembly work.

The size of the heliostats selected permits each heliostat to slightly cover the neighboring unit when they are facing the paraboloid (see Fig. 4). Thus at any time of the day a continuous beam of energy will be reflected into the paraboloid. The energy density of the beam is not continuous. Fig. 6 illustrates partial shadowing of part of the beam reflected by the heliostats, but these losses of energy are calculated for the 1000 kw unit to be relatively low.

Thus the 62 heliostats will be able to reflect a beam of about 1500-kw strength.

### Concentrator

The concentrator will be of the same type as the existing unit at Montlouis. The focal distance will be about 18 to 20 m. As shown in Fig. 5, we are planning to cut out

FIG. 4 — General arrangement for 1000-kw furnace.

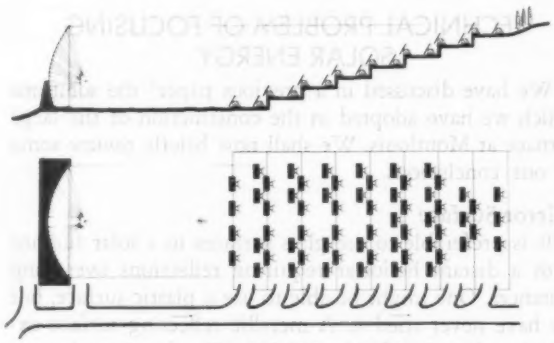

FIG. 5 — Paraboloid for 1000-kw furnace.

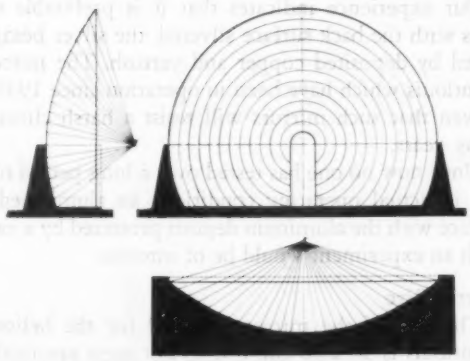

VOL. 1 1957

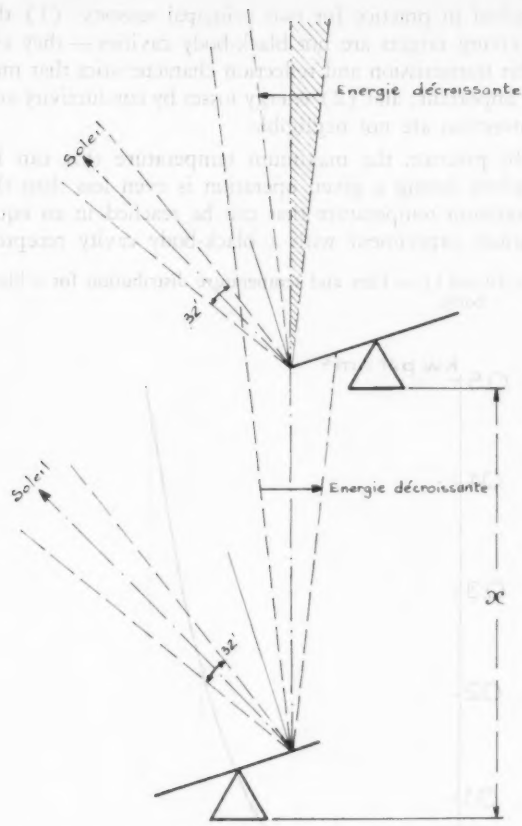


FIG. 6 — Shadowing effect caused by superposition of various heliostats.

the lower part of the paraboloid and to build it slightly off from the vertical so that the focal point will be at a lower elevation. The concentrator will be 40 m high and 54 m wide. We intend to use a larger aperture than for the existing Montlouis furnace, and the ratio of the diameter to focal length, *n*, will be equal to 3.

The inclined concentrator should also permit us to work at times in direct fusions without crucibles, especially when the material can be kept in a pyramid with a slope of about 40°.

Since the surface of the paraboloid must be made from a multitude of mirrors, we have decided to use again the arrangement adopted for the existing large furnace. As shown in Fig. 7, we shall use small mirrors placed on successive crowns. These crowns are composed of identical segments. Each of these segments supports a number of flat mirrors bent to approximate the curvature of the paraboloid (see Fig. 8).

This solution to the problem of obtaining a large paraboloid is more economical than others. Naturally, it is possible, instead of using glass, to use aluminum segments curved on a matrix. (This was done for the Algerian furnace.) It is also possible to make these crown segments in optical glass ground into the shape of the paraboloid. Naturally, such surfaces would yield excellent concentration results but would also cost much more. We have adopted a technique that gives excellent results and is sufficiently economical to permit us to plan the industrial utilization of the furnace.

One of the glass segments used in the present Montlouis furnace is shown in Fig. 9. We are now able, by bending ordinary flat mirrors into an approximation of the paraboloid, to concentrate with 3500 mirrors the energy reflected by the heliostat. This concentration is as

FIG. 7 — Schema of paraboloid at Montlouis.

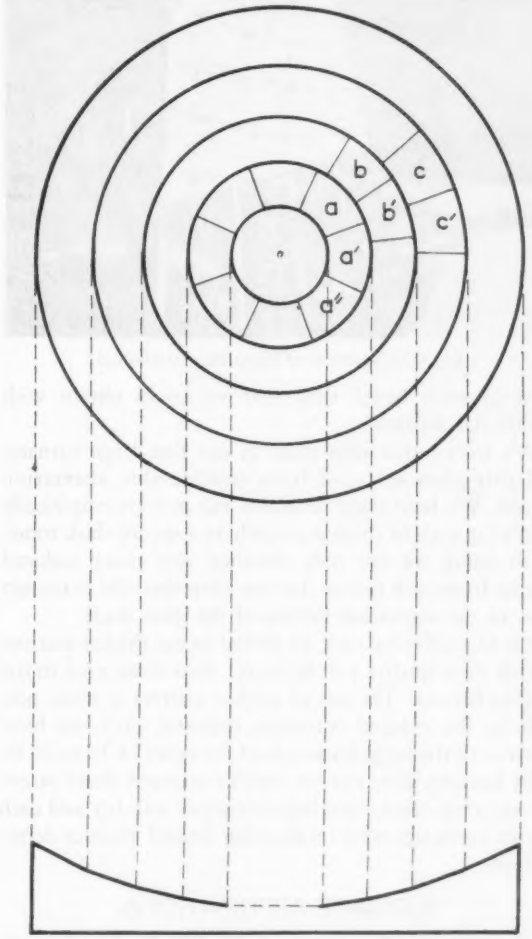


FIG. 8 — Points of support for glass of paraboloid at Montlouis.

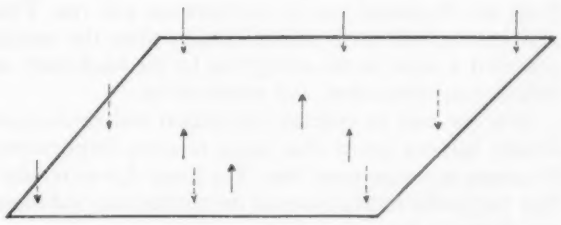

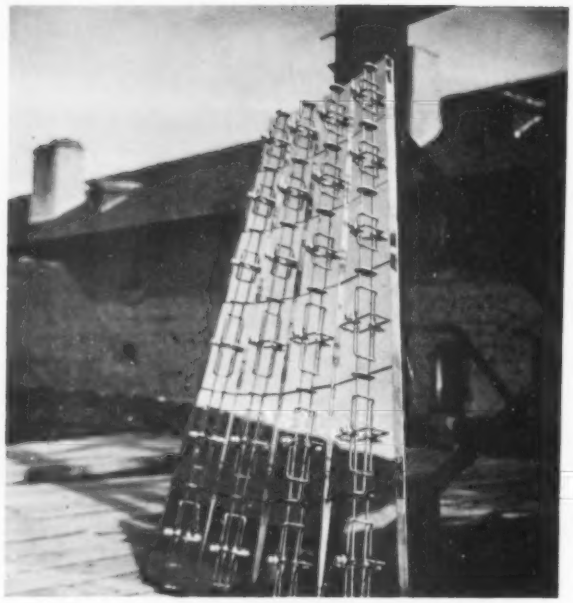

FIG. 9 — Segment of Montlouis paraboloid.

good or even better than that we could obtain with 20,000 flat mirrors.

We used rather thin glass in our first large furnace, and this glass suffered from considerable aberration defects. We bent these defective flat mirrors empirically by testing each of them separately in a special dark room. In so doing we not only obtained very much reduced images from each mirror, but we were also able to correct most of the aberration defects of the glass itself.

For our 1000-kw unit we intend to use thicker mirrors so that their quality will be better than those used in the smaller furnace. The use of thicker mirrors is made possible by the reduced curvature required, since the focal distance of the large furnace is of the order of 18 to 20 m.

By keeping these mirrors under continued elastic stress, we naturally obtain excellent curvature stability and each mirror keeps the exact focalization desired without deformations.

## FURNACE APPLICATIONS

The beam which is concentrated at the focal point must, if it is going to furnish energy, be absorbed by an adequate target.

If we place a black body perpendicular to the rays, this body will be heated, and its temperature will rise. This temperature will reach an equilibruim when the energy absorbed is equal to the energy lost by the black body as reradiation, convection, and conductivity.

It is not easy to estimate convection and conduction losses, but we know that their relative importance decreases as temperature rises. The losses due to reradiation vary as the fourth power of the temperature and these are shown in Figs. 10 and 11.

If we consider only reradiation losses, it can be easily shown that a furnace with a large aperture should reach 5000°K. Unfortunately, this temperature cannot be reached in practice for two principal reasons: (1) the receiving targets are not black-body cavities — they exhibit transmission and reflection characteristics that may be important; and (2) energy losses by conductivity and convection are not negligible.

In practice, the maximum temperature that can be reached during a given operation is even less than the maximum temperature that can be reached in an equilibrium experiment with a black-body cavity receptor.

FIG. 10 and 11 — Flux and temperature distribution for a black body.

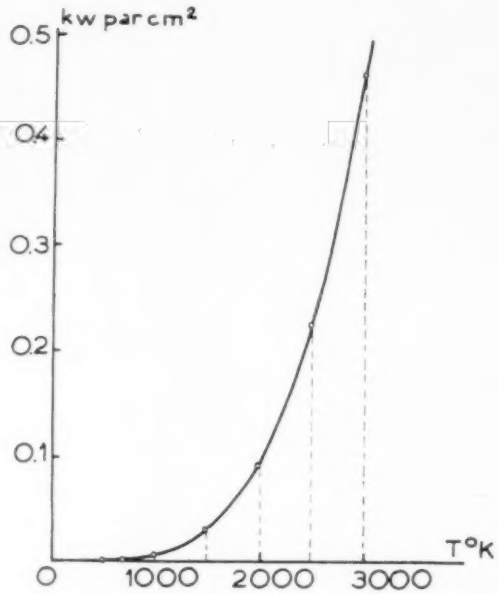


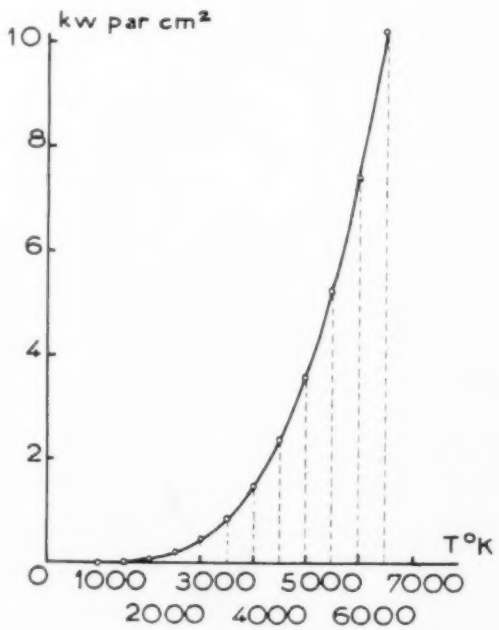


VOL.
1
1957

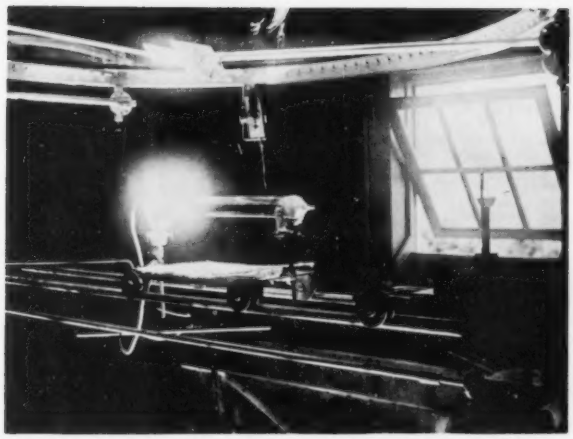

FIG. 12 — Fusion of iron in hydrogen performed on small Montlouis horizontal furnace.

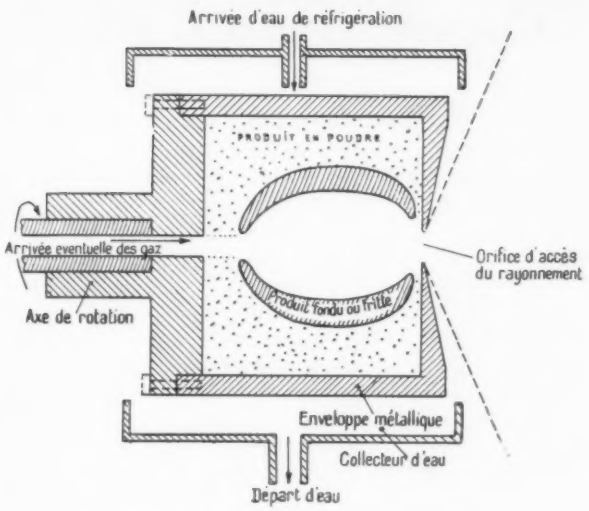


FIG. 13 — Schema of a rotating furnace.

FIG. 14 — Rotating furnace in action.

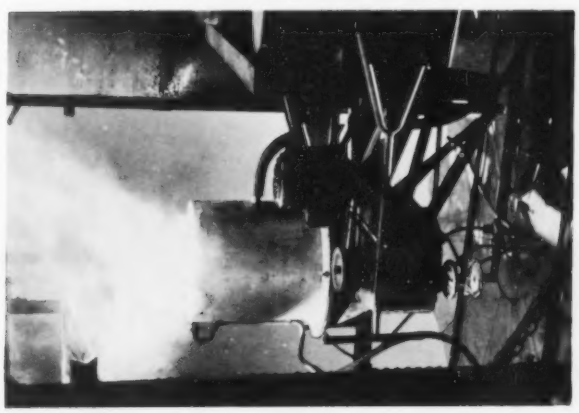

Indeed, if we want to obtain a certain effect (such as sintering, fusing, distillation, or chemical reaction), we must create in the mass of the substances being handled a temperature gradient of importance. This means that working temperatures are evidently lower than maximum temperatures.

For example, a solar furnace that might, under certain perfect conditions, give a maximum temperature of 4000°K will only be used and be useful at 3500°K. The concept of temperature gradients must be considered with care if one wants to obtain economic results from the operation of solar furnaces.

We have already described[2] the techniques developed at Montlouis for using the solar furnace. These techniques include heating products in direct sunlight (for example, Fig. 12 shows a fusion of iron in a tube filled with hydrogen), and the utilization of rotating black-body cavities (see Figs. 13 and 14). We have continued to develop these techniques, and at the present time the rotating cavities are used each day to produce with the large furnace about 60 kgm of sintered refractories such as zirconium oxide, calcium zirconate, chromium, dolomite, alumina, and others. These treatments permit, if certain operating conditions are adopted, considerable purification of the base material.

We may observe in direct treatment of a substance two simultaneous effects: volatilization on the surface and migration into colder regions of certain impurities. These effects can be increased and accelerated by adding certain compounds to the product. In the rotating furnace one obtains similar results with large quantities of material.

Purification in the solar furnace can be applied to metals. It gives remarkable results for many oxides.

It is also possible to use the furnaces in the production of crucibles. The process shown in Fig. 15 permits us to manufacture, by rotating an inclined furnace, a refractory crucible the composition of which is determined by the metal that must be melted. This operation permits manufacturing the crucible inside a metallic container, the crucible being created in a zone which is fritted while the

FIG. 15 — Fusion of a metal in a refractory crucible prepared by previous treatment in the furnace.

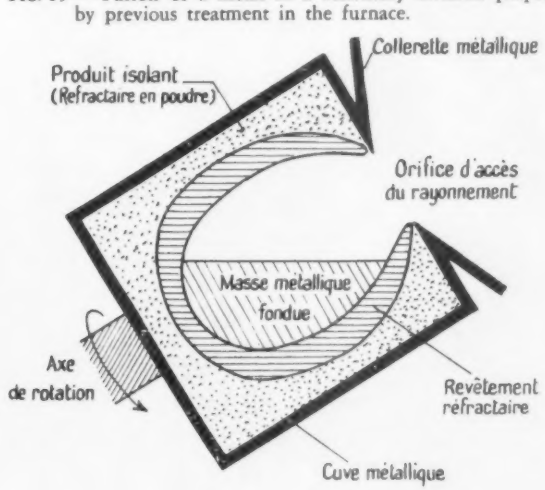

FIG. 16 — Iron melt of 80 kgm and part of the crucible used to melt it.

metal is still protected by unfritted and colder powder.

These crucibles are manufactured at about 2000°C or more and are used with metals in operations with temperatures of the order of 1500° to 1600°C.

We have made fusions of pure iron in crucibles of alumina, which are not attacked in the process. Fig. 16 shows an iron block of 80 kgm beside a piece of the crucible in which it was melted.

These crucibles in alumina (Fig. 17), in mullite (Fig. 18), and in quartz (Fig. 19) can be used a large number of times. Even if they are cracked during the beginning of the heat treatment, the metal will quickly plug the cracks.

We may finally indicate that large mineral masses

FIG. 17 — Alumina crucible.

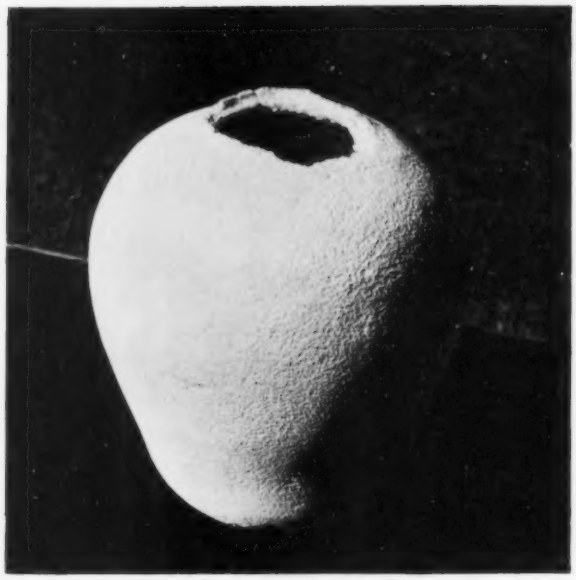

FIG. 18 — Mullite crucible.

(100 kgm at one time) can react with appropriate compounds in the rotating furnaces. Fig. 20 shows a block of zircon $SiO_2ZrO_2$ reacted with sodium carbonate.

This short review of solar furnace applications indicates that they may be useful in a variety of processes.

## ECONOMICS OF OPERATION

We estimate that the 1000-kw prototype furnace will cost 300 million francs. This price will be lowered somewhat once a number of installations are built. We can assume that a solar furnace of 1000-kw capacity would cost about 200 million francs.

The amortization of this cost at 10 per cent per year would cost about 20 million francs per year.

Such a furnace could produce up to two and one-half

FIG. 19 — Quartz crucible.

VOL.
1
1957

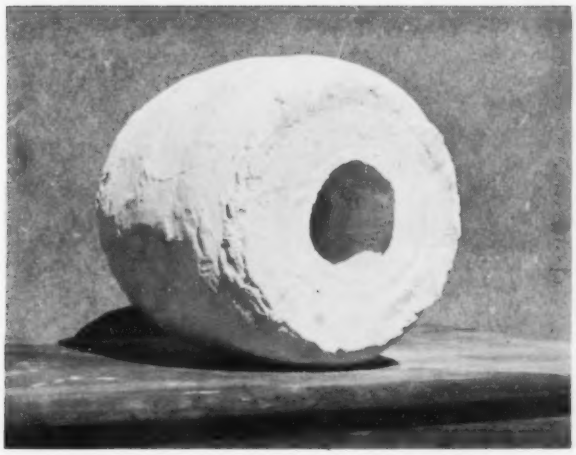

FIG. 20 — Zircon reacted with sodium carbonate.

million kwh per year. The amortization of the furnace would therefore cost less than 10 francs per kwh. But the solar furnace kilowatt-hour must be compared to the kilowatt-hours consumed by a high frequency electric furnace or an arc furnace to produce a kilowatt-hour of heat. In these terms the solar furnace is definitely cheaper than a high frequency furnace and competitive with electric arc furnaces.

Evidently the industrial beginnings of the solar furnace must proceed slowly, but their utilization seems suited to discontinuous operations, without crucible, and particularly in oxidizing atmospheres. As their market expands, solar furnaces could be used in the manufacture of sintered products and of special refractories.

Solar furnaces can also be used in metallurgical operations, competing directly with high frequency furnaces. They are naturally most useful in the production of pure products. We are using our furnaces with these possibilities in mind, and we have already sintered ultra-refractories for industrial users (see Fig. 21).

The interest of industrial and government research

FIG. 21 — Typical oxide of zirconia treated in the solar furnace.

organizations in the solar furnace indicates that their use should become quite widespread in the near future. To this end a realistic and intelligent dissemination of the facts concerning their real possibilities is needed. In this way the researcher and the industrialist will discover the real utility of these tools.

We must be optimists, and at the same time that we seek to enlarge the field of solar energy research, we must also seek to find industrial applications for our work.

## REFERENCES


1. Félix Trombe, "High temperature furnaces." (In *Proceedings of the World Symposium on Applied Solar Energy, Phoenix, Arizona, 1955,* Stanford Research Institute, 1956, pp. 63-72.)
2. Félix Trombe and M. Foex, "Traitements à haute température au moyen de fours centrifuges chauffés par l'énergie solaire." (To be published in the *Transactions of the Tucson Conference on the Use of Solar Energy — The Scientific Basis.)*

# DESIGN OF THE QUARTERMASTER SOLAR FURNACE

By JOHN M. DAVIES and EUGENE S. COTTON

Quartermaster Research & Development Command, Natick, Massachusetts

**The U.S. Army Quartermaster Research & Development Laboratories are charged with the responsibility for developing protection for men and materials against thermal radiation from nuclear and other weapons. This paper describes a large solar furnace now being erected at Natick, Massachusetts, for the purpose of producing a radiation flux sufficiently high to destroy materials and burn protected skin with exposure times shorter than one second. The concentrating element for the furnace consists of an area of spherical mirrors arranged on an approximate surface so that all of the images are superimposed at the target. Since a continuous reflecting surface is not required, identical mirrors produced by mass production methods are used with significant savings in cost.**

## INTRODUCTION

The U.S. Army Quartermaster Research and Development Laboratories are conducting a continuing program to develop protection for the soldier against the thermal radiation from nuclear and other weapons. Ideally, these studies require a source providing a high, uniform intensity over a large area. The sources which are available, such as high-current carbon arcs, gas-fired panels, burning magnesium, and incandescent lamps, are not adequate. In considering the improvement which might be made in sources, it seemed that a solar furnace offered the best hope of meeting the requirements.

The area should be large enough to produce realistic flaming of materials and to provide at least an approximation to one dimensional heat transfer conditions. The flux should be high enough to produce destruction of materials and burning of protected skin with exposure times of much less than one second. As a compromise, the minimum requirement was set at 60 cal/cm$^2$/sec over a circular area 4 in. in diameter in a vertical plane.

A solar image of this size will be formed by an array of spherical concentrating mirrors arranged on a sperical surface so that the images of all of them are superimposed at the target. This array resembles to some extent a large paraboloid such as has been used previously, but the performance is somewhat different. It does not require a continuous reflecting surface, so that identical mirrors produced by mass production methods can be used with a significant saving in cost.

## GENERAL CHARACTERISTICS OF THE QM FURNACE

The general appearance of the QM furnace is similar to other large furnaces, such as at Montlouis. An artist's conception of the installation is shown in Fig. 1. An immediately obvious departure from usual design is the square shape of the concentrator array. This is not a necessary feature, but it seemed practical to fill the corners of the framework with mirrors and take advantage of the extra area, even though such mirrors are less efficient. The use of the corners increases the maximum rim angle from 23° to 32°; these mirrors may not be used in all exposures, since a small angle of convergence is desirable for much of our work.

The horizontal distance from the concentrator to the heliostat is 96 ft, which avoids shadowing of the heliostat by the other components. The concentrating area is 28 ft by 28 ft, with a central hole 8 ft by 8 ft, where the target chamber obscures the parallel beam. The heliostat frame is to be approximately 40 ft by 36 ft, with a smaller central hole to allow for the target chamber. A venetian blind-type shutter is mounted so that it can be used to attenuate the parallel light without obscuring the convergent beam. The measuring apparatus, shutters, controls, and laboratory facilities will be housed in the target chamber, which will be reached by a small elevator platform.

The effective focal length of the concentrating surface is 35.8 ft, giving a solar image of 4 in. diameter if perfectly imaged. The projected area of the concentrator perpendicular to the parallel beam is 710 sq ft. This gives a theoretical concentration factor of about 8160. Assuming a nominal furnace efficiency of 50 per cent, and an *average* solar constant at the site of 0.020 cal/cm$^2$/sec, we could then obtain an average of 82 cal/cm$^2$/sec at the center of a uniform image, which is greater than the intensity we have set as a design objective. These calculations can be made more accurate and detailed, as will be shown later. However, such order-of-magnitude constants enabled us

VOL. 1 1957

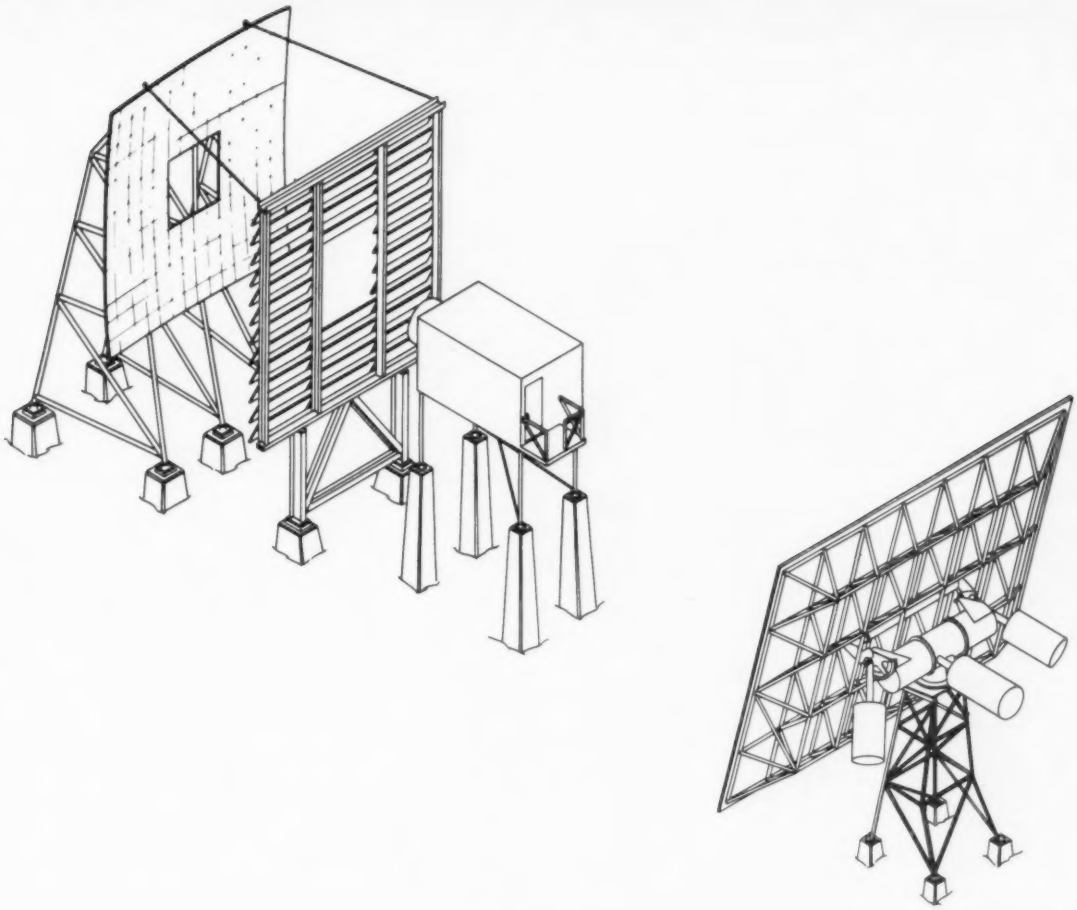

FIG. 1 — Drawing of furnace.

to arrive at practical sizes of the components. If we were to use this furnace for power applications we could expect an output power of 25-30 kilowatts under average conditions.

## CONCENTRATING ARRAY

The use of an array of individual focusing mirrors was originally suggested by R. Gardon.[1] A similar concept has been employed in the MIT furnace through the use of flat mirrors.[2] Although the mirrors in the MIT instrument did not focus the light, nevertheless superposition of the beams from individual mirrors was used to form a composite beam. The objective of the MIT furnace was essentially the same as for the QM furnace, to produce a nearly uniform area of irradiation. Extrapolation of the flat mirror design to larger area and higher intensity, however, was found to be impractical owing to the large number of separate mirrors requiring alignment, and to the loss of energy from flat mirrors due to beam "spread". The use of individual focusing mirrors permits a longer effective focal length and a smaller angle of convergence. Also, the total number of individual mirrors is reduced considerably. Ideally, from such an array, all of the radiation is focused within the 4-in. diameter solar image. The area is not uniformly irradiated, however; this will be treated in a later section.

The size and shape of the individual curved mirrors are determined by quite practical considerations. It is desired that the mirrors fit closely on the array without wasting area. This condition suggests a polygon, and for the sake of simplicity in manufacture we have chosen a square, 2 ft on a side. With this choice, the number of mirrors mounted on the array is 180. Each mirror will be mounted on an aluminum ring which has a diameter of 23.5 in. The ring adds symmetrical rigidity to the mirror, and also provides a support for fastening to the framework and adjusting the angle of inclination to the incoming beam.

The early design of the concentrator was based upon a paraboloidal shape, or an approximation to it, by means of several zones with different radii of curvature. This scheme is obviously costly, regardless of the method of mirror formation. Our final design is based upon the use of individual spherical mirrors, all having the same radius of curvature, and mounted on the array in such a way that the best image from each occurs at the target position.

This arrangement was evolved through many stages, but the principal considerations were cost and optical aberration. The first is quite obvious; we aimed at a single mirror which can be mass-produced. The second consideration concerns the optical performance of the spherical mirrors, and deserves a brief explanation.

Instead of considering the concentrator as a single reflecting surface, it is viewed as an arrangement of individually focusing spherical mirrors. The mirror which is placed in the on-axis position, or at the center of the array, must focus at

$$f = \frac{d}{\alpha}$$

where $d$ is the image diameter and $\alpha$ is the angle subtended by the sun. In our case, $d = 4$ in. and $\alpha$ is .00931 radians, which gives $f = 429.6$ in. (35.8 ft). The radius of curvature of a spherical mirror is twice its focal length, or 859.2 in.

Actually, there is no mirror at the center of the array; all of the mirrors are operated off-axis, since all of them are required to produce a solar image at a point on-axis 35.8 ft from the center of the array. Our task is to devise a surface which will make this possible for all mirrors.

The first approximation to such a surface is obtained by a consideration of the third order aberrations which apply to a spherical mirror. For an object at infinity (i.e. the sun) the image distance due to spherical aberration for an extreme ray parallel to the axis is

$$a = -\frac{R}{(2 + h^2/R^2)}$$

where $R$ is the radius of curvature and $h$ is the distance from the axis where the ray is incident. For a square mirror, 24 in. on a side, the maximum value of $h$ is $12\sqrt{2}$, or about 17 in. The value of $R$ is 859.2, so that

$$\begin{aligned} a &= -\frac{859.2}{2 + (17)^2/(859.2)^2} \\ &= -\frac{859.2}{2.004} \\ &= -429.5 \text{ in.} \end{aligned}$$

Thus, the image from the extreme rays is formed 0.1 in. closer to the mirror than that from axial rays. As will be seen, this aberration is quite small.

The coma produced in the solar image due to the lack of uniformity in lateral magnification by this mirror can be shown to be quite small. Third-order theory for a mirror results in the following formula for the radius of the comatic circle:

$$r_c = \frac{3yh^2}{4f^3}$$

where $y$ is the distance of the image from the mirror axis. For our extreme mirror, i.e. a corner of the array, $y$ is about 110 in., and as before, $h = 17$ in., $f = 429.6$ in.

Thus,

$$\begin{aligned} r_c &= \frac{3\,(110)\,(17)^2}{4\quad(429.6)^3} \\ &= 0.0003 \text{ in.} \end{aligned}$$

The tangential coma is $3r_c$, or about .001 in., so that the image of a point source at infinity would become a circle of diameter .0006 in., with a .001 in. "tail" extending to the true image position. Such an aberration is completely negligible in the case we are considering.

Next we must calculate the principal aberration due to the off-axis operation of our mirrors. This effect is known as astigmatism. A point source at infinity which is not on the axis of the mirror will produce two line images which are not at the same point in space. These lines are perpendicular to one another, and are separated by a distance which depends upon the angle which the incoming beam makes with the axis. The tangential, or primary, focus for a spherical mirror is formed at a distance

$$a_t = \frac{R \cos \beta}{2}$$

from the center of the mirror, where $\beta$ is the angle which the incoming beam makes with the principal axis. The sagittal, or secondary, focus is formed at

$$a_s = \frac{R}{2 \cos \beta}$$

In our case, the maximum value of the angle $\beta$ is about 15°, so that

$$\begin{aligned} a_t &= \frac{(859.2)\,(.966)}{2} \\ &= 415.0 \text{ in.} \end{aligned}$$

and

$$\begin{aligned} a_s &= \frac{(859.2)}{2\,(.966)} \\ &= 444.7 \text{ in.} \end{aligned}$$

The maximum astigmatic difference is $(a_s - a_t)$, or 29.7 in. The best image is difficult to define for a system suffer-

FIG. 2 — Astigmatic image position.

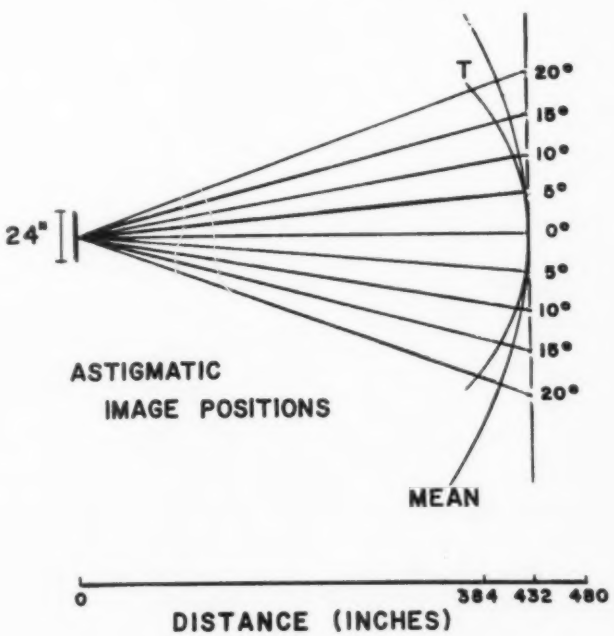




VOL.
1
1957

ing from astigmatism; the loci of the mean positions form a nearly spherical surface about the mirror center. In our case, at $\beta = 15°$, the mean position is at 429.8 in. from the center; this differs by only 0.2 in. from $R/2$. A "mean focus" is the position where the image of a point source is spread out into a minimum illuminated area which has the approximate outline of the mirror itself. In our case, this is nearly a square; if the image is formed on a vertical plane, as in the system under study, the square image becomes a trapezoid. The effect of the astigmatic aberration for a mirror of these dimensions is shown in Fig. 2.

The other classical aberrations, distortion, and curvature of the field, do not concern us here, since the sun as an object has such a small lateral extent. Also, a mirror is not subject to chromatic aberration.

In summary, each individual mirror forms an image which is subject to two aberrations of consequence. As a result of spherical aberration, a mirror of these dimensions would form a mean image between 429.5 in. and 429.6 in. from the mirror center, if used on-axis. The operation of the same mirror 15° off-axis produces a "mean" image at about 429.8 in., also measured from the mirror center. The astigmatic difference is quite large, however, so that significant changes in image size would be detected only by moving several inches away from the mean position.

Since these estimates of mean image position were calculated using only the results of third-order aberration theory, it seemed advisable to consider higher order aberrations and also to use more exact methods. The operation of a spherical mirror of this radius at off-axis angles of 15° or less was investigated by Davis[3] using ray tracing techniques. This method reduces the number of approximations involved and treats all aberrations simultaneously. Davis found that the distance from the mirror center to the mean image position decreased very slightly with off-axis angle. The outermost mirror, according to this result, would need to be advanced from a spherical surface in the direction of the incoming beam less than 2 in.; such a correction can easily be made in adjustment of the mirror on the array. Using ray tracing, the best image is calculated by obtaining the spread of an image of a point source in the vertical plane, and minimizing the area. In third-order theory, we merely assumed that the best image occurred at the mean between the astigmatic images, and found the deviation from a spherical surface to be negligible.

These optical considerations yielded a result which defined a design criterion. If the best image position for each mirror is approximately at $R/2$, then the centers of all mirrors must lie on a surface which is part of a spheroid of radius $R/2$. The slope of the spheroidal surface is not coincident with the slope of the mirror, since its purpose is only to position the mirror for best imaging. Fig. 3 shows the shape of the surface and the approximate mirror positions in a vertical section.

It is desired that the mirrors used in this furnace be quite efficient optically, and that they preserve the solar spectrum as far as practicable. In order to achieve these goals we have chosen front-surface aluminized plate glass as the concentrator mirror material. The aluminum surface will be protected by silicon monoxide. It is planned to cover the mirrors when they are not in use. The plate glass is ¼ in. thick, and the desired curvature will be produced by slumping over an accurate mold, with grinding and polishing only if necessary. A standard deviation of 2.5 per cent in the mean radius of curvature has been set as our allowable tolerance.

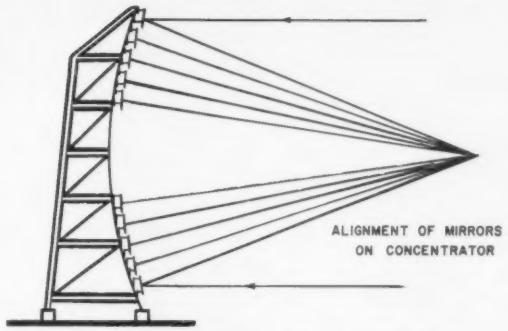


FIG. 3 — Location of mirrors on concentrator.

Each mirror will be fastened securely to the aluminum ring, which will be mounted on the array by means of three universal-type joints to provide adjustment in depth and angle. The mirrors will be aligned individually so that their images are completely coincident, probably through the use of an artificial source at the focus.

## HELIOSTAT

Our need for a solar image at a fixed point on a vertical plane virtually dictated the use of an auxiliary heliostat. Heliostatic arrays of this size are not common, the largest in use being at Mont Louis.[4] The basic requirement placed upon the heliostat is that it maintain the reflected beam in a fixed position parallel to the principal axis of the concentrator. This results in a movement of the heliostat such that its normal bisects the angle between the sun and the concentrator at all times.

This constraint does not completely define the motion of the heliostat plane; it is defined, however, when the set of axes about which the plane will move is chosen. Astronomical instruments often use an equatorial type of mounting to reduce the motion so that a constant speed drive about one axis is almost sufficient. In such a mounting, one axis is perpendicular to the earth's equatorial plane and the other is parallel to it; the tracking of celestial objects is accomplished by a constant speed about the first axis, while the other is adjusted periodically for changes in the declination. Our heliostat does not track a celestial object, but is oriented toward a point moving on the celestial sphere in both azimuth and elevation. However, we calculated the motion required for an equatorial mounting to see whether any advantage could be obtained from it. The results showed that the total motion about one axis was somewhat reduced, but that an undesirable tilting of the heliostat frame with respect to the horizontal plane was encountered. This

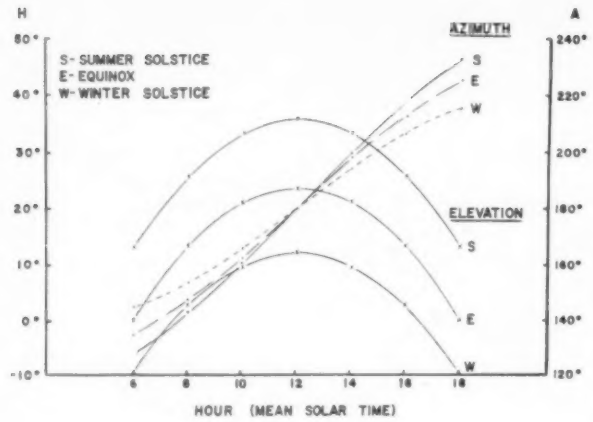


FIG. 4 — Angles of heliostat.

would require a larger mirror surface and also would force the whole array to a greater height above the ground.

Since there is no set of axes for a heliostat which permits motion to be restricted to a single rotation, a conventional azimuth-elevation mounting referred to the horizontal plane was chosen for its simplicity. The actual mounting to be used is one which has been utilized for radio telescopes and radar antennas, developed by the D S. Kennedy Co. of Cohasset, Mass. The approximate azimuth and elevation angles which occur at various hours of the day are shown in Fig. 4. These angles were computed using a "mean sun" — the heliostat will actually track according to the apparent motion of the true sun. A sensing element which keeps the reflected beam incident upon the concentrator will position the heliostat automatically about both axes. It is hoped that we can control the position of the heliostat within ½ minute of arc, so that the motion of the image will be less than 1/16 in. away from the target position.

The over-all size of a heliostat array can be calculated by projecting the small cone of light from the sun so that it uniformly illuminates the concentrator at all positions of the heliostat. This has been done in an elegant manner by Jose,[5] using two different locations of the elevation axis in the mirror surface. The concentrator discussed in the previous section is square, so that it is not practical to provide full illumination at all usable hours. However, nearly full illumination can be provided on the longest day of the year for about 8 hours if a heliostat size of 40 ft by 36 ft is employed. This size is computed through the use of Jose's method, which assumes that the axes are in the reflecting plane. In practice, this will not be the case; engineering requirements result in an offset of the axes from the heliostat plane. Such an offset would require an increase in area if full illumination of the concentrator were needed for the entire period.

The heliostat framework will be constructed of aluminum, to which the mirrors will be attached directly. The flat mirrors will be ¼ in. polished water-white plate glass, again in the form of squares, 2 ft on a side. The reflecting surface will be the back surface of the glass, silvered and protected with copper plating and paint. Each mirror will be supported at three points on a centered circle by means of screws which are fitted into oversized holes in the glass. A spring behind each support will keep the mirror correctly positioned but will permit thermal expansion in the plane of the mirror. It is not necessary that all mirrors be exactly in the same plane, only that they remain parallel.

The heliostat will not be required to track accurately in winds exerting a force over 5 lb per sq ft, and is designed to survive winds of hurricane velocity, which sometimes occur at our location. The furnace site is at the edge of a small lake so that the western horizon for the heliostat is very low. The eastern horizon is somewhat limited by buildings and trees, so that early morning operation is restricted.

## OTHER COMPONENTS

In order to secure efficient operation and use of the furnace certain auxiliary components will be needed. Our first consideration is, of course, for the safety of personnel working near the focal point. A method of shutting off the concentrator is needed in case the solar image moves or begins to damage material within the test chamber. To accomplish this we have planned a venetian shade-type attenuator (shown in Fig. 1) which will be closed automatically in case of power failure, incorrect tracking, excessive image movement, lack of cooling in shutters, and other emergencies. The operator will also be able to close the attenuator suddenly if he thinks it advisable.

Such an attenuator can obviously be used also to control the total radiation which is incident upon the concentrator. The attenuator will be placed so that it regulates the amount of parallel light from the heliostat, but does not interfere with the convergent beams from the concentrator. The blades will be electrically operated so that the operator can select the desired intensity attenuation while inside the test chamber.

The test chamber will be 8 ft by 8 ft in a cross section presented to the parallel light, and almost 16 ft in the direction of this beam. Inside the test chamber will be the sample-holding equipment, heliostat control panel, and instruments for measuring effects on samples. Also mounted inside the chamber will be a fast exposure shutter, giving exposures as short as 0.1 seconds, and a water-cooled, protective shutter which is designed to shield the exposure shutter and sample apparatus until just before the exposure is made. Shutters of this type are now in use with the QM carbon arc and have been found to be quite satisfactory. The chamber will be temperature controlled. Access will be gained by means of an elevator at the rear. The incoming parallel radiation will be monitored for available intensity at any time, and the concentrated radiation will be measured by means of copper button calorimeters.

## EXPECTED PERFORMANCE

The requirement placed upon the QM furnace is the formation of a uniformly irradiated 4-in. diameter spot.

VOL.
1
1957

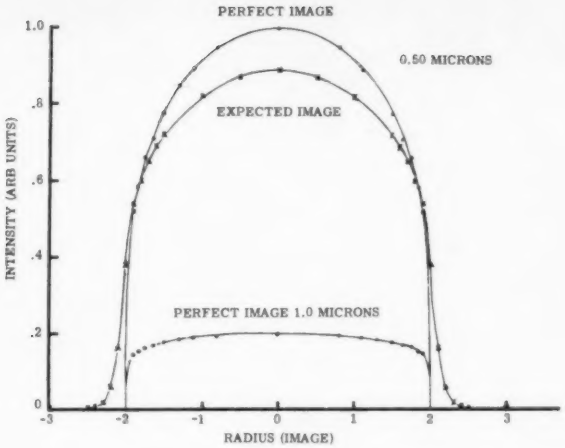


FIG. 5 — Quality of solar image.

A perfect solar image will not, of course, have this property of uniformity. The radiancy of the solar disk is shown in Fig. 5 for wave lengths of 0.5 microns and 1.0 microns.[6] No single image of the sun can be more uniform than this at the same wave length. Various arrangements for defocusing some of the elemental mirrors could be devised which would redistribute the radiation, but in any such scheme some of the radiation must be discarded from the desired image area. It is therefore felt necessary to align the furnace for the best possible composite image, measure its radiancy as a function of distance from the center, and then utilize auxiliary stops, or some other means, to make the irradiance more uniform if it is desirable.

One can arrive at an approximation to the image shape by a consideration of the astigmatic aberration discussed earlier. Each object point is imaged as an area, whose size is dependent upon the off-axis angle obtaining for that particular mirror. The methods of ray tracing[3] provide a simple way of determining the size of this area; the image from the mirror is then thought of as the sum of these areas which have a one-to-one correspondence with each point in the sun. In addition, the image from each mirror is spread into an ellipse as a result of the angle which the incoming ray makes with the vertical target plane.

For this purpose, the array surface was considered to be composed of mirrors in seven zones, each zone conimage from the mirror is then thought of as the sum of tributing a composite image of a different radius. The zonal image was then calculated using the "spread" due to the aberration and the angle of incidence on the target for that zone. The images from the seven zones were weighted according to their contribution to the total image. This expected image, shown in Fig. 5, is spread over a larger diameter, about 5.8 in.

As a result of image enlargement the intensity of the radiation at the center of the image will be reduced. We showed earlier than an average of 82 cal/cm²/sec might be expected from the furnace using the theoretical concentration factor and an approximate estimate of furnace efficiency. This assumed a uniform image intensity; actually, at 50 per cent efficiency, the intensity near the center of a perfect image would be higher, about 106 cal/cm²/sec. The actual image will give a central intensity of approximately 94 cal/cm²/sec and it will fall to about 40 cal/cm²/sec at the 2-in. radius. Thus we have already achieved a somewhat more uniform image over the 4-in. diameter, but, as expected, at the expense of radiation thrown beyond the 4-in. diameter. Further improvement of this intensity profile toward uniformity may be achieved by the judicious use of stops in the central part of the beam, at a distance where the temperature would not become excessive. These stops could be silvered to keep their temperature low, and they would simply remove radiation from the beam which was destined to contribute principally at the center of the image.

In order to present a comparative picture of this furnace, some of the essential characteristics[7,8] are tabulated in Table I.

TABLE I

CHARACTERISTICS OF THE QUARTERMASTER SOLAR FURNACE

| | |
|---|---|
| Number of reflectors | 2 |
| Aperture | 28 ft x 28 ft (square) |
| Focal length | 35.8 ft |
| Ratio of aperture to focal length | 0.78 - 1.11 |
| Effective concentrating surface | 710 sq ft |
| Theoretical diameter of image | 4.0 in. |
| Expected diameter of image | 5.8 in. |
| Theoretical concentration ratio | 8161 |
| Estimated over-all concentrating efficiency | 50 per cent |
| Probable concentration ratio | 4080 |
| Average image flux density (sun at .08 watts/cm²) | 326.4 watts/cm² |
| Input power | 53 kilowatts |
| Output power (over perfect image) | 27 kilowatts |
| Maximum flux density in expected image | 94 cal/cm²/sec |

All of the performance characteristics in Table I are based on an average solar constant at sea level of .08 watts/cm², (or .019 cal/cm²/sec), as used by Benveniste.[7]

## CONCLUSION

The QM solar furnace is planned for initial alignment and operation during the summer of 1957. It will be the first large furnace of the focusing type to utilize an effective aperture to focal length ratio of less than one. We hope that it will furnish much valuable information on the effects of high intensity thermal radiation of materials. In addition, it may contribute to the general solar energy field by its use of front-surface mirrors, prefocused and mass-produced, on a nonparabolic array. Such experience, added to that of the many other furnaces in use and under construction, may assist in the application of solar energy concentration to the problems of dwindling sources of power on earth.

## REFERENCES

1. R. Gardon, private communication, 1955.
2. R. Gardon, "A segmented-mirror solar furnace for high intensity thermal radiation studies." *Rev. Sci. Inst.* 25: 459, 1954.
3. W. Davis, private communication, Oct. 29, 1956.

4. F. Trombe, "High temperature furnaces." (In *Proceedings of the World Symposium on Applied Solar Energy, Phoenix, Arizona,* 1955, p. 63.)
5. P. D. Jose, "The design of a heliostat mirror for a solar furnace." Report No. HDR(RM)-TM-56-3, Holloman Air Force Base, July 1956.
6. C. G. Abbot, "The sun as a source of continuous radiation." (In *Sources of Radiant Energy,* ed. by W. E. Forsythe, N.Y., McGraw-Hill, 1937, p. 75.)
7. G. Benveniste, "Solar energy furnaces." Menlo Park, Stanford Research Institute, 1955.
8. G. Benveniste and N . K. Hiester, "The solar furnace—new tool for high temperature work." *Mech. Eng.* 78:915, 1956.

VOL.
1
1957

# THE DESIGN OF THE HELIOSTAT MIRROR FOR A SOLAR FURNACE

By PAUL D. JOSE

Holloman Air Development Center
Alamogordo, New Mexico

**An analysis is made of the size and shape required for a heliostat mirror as a function of: latitude, hours of operation, angular diameter of the sun, the distance between the parabolic condenser and heliostat, and the arrangement of the axes. All these parameters enter into a general equation from which the shape of the heliostat mirror may be exactly determined. Two arrangements of axes are considered for the alt-azimuth arrangement. The Trombe mount is discussed.**

In solar furnaces of large dimensions the arrangement of the various elements is similar to that shown in Fig. 1. Although other arrangements are possible, they are not practical in large installations. The model shown in Fig. 1 was built by Holloman Air Development Center. The condenser at the left is shaped from a solid aluminum slab. The reflecting surface is spherical, since a parabolic surface would have been more difficult to machine. The observation tower and the flux density shutter are built separately, although in a full scale structure they could be built into a single unit. The heliostat at the right is of an unconventional design; its azimuth axis is at the center of the turn table on which the elevation axis rests. This arrangement of the axes made the model easier to build. The shape of the heliostat mirror was computed so as to completely illuminate the aperture of the condenser during eight hours of operation.

This discussion deals with the determination of the precise size and shape of the reflecting surface of the heliostat mirror for any given set of conditions. The axis of the furnace is taken horizontal in a due north-south direction. Any other direction would have required a mirror of unsymmetrical shape. An array of individual small heliostats is not considered since it is impossible to illuminate uniformly the parabolic condenser in any other manner than with one continuous surface.

FIG. 1 — Model of solar furnace.

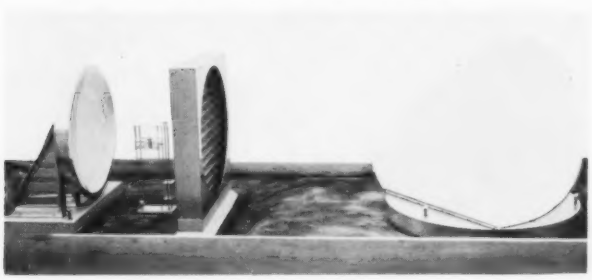

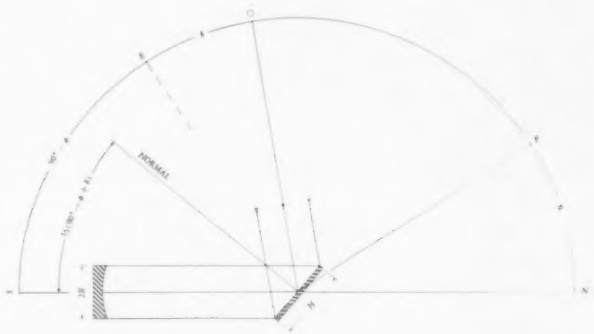

FIG. 2 — Dependence of over-all height of heliostat mirror on the latitude ($\phi$) and maximum declination of the sun ($\delta$). Approximate over-all height $= H = 2R \sec \frac{1}{2}(90° - \phi + \delta)$.

The quantities involved in determining the size and shape of the heliostat mirror are:

(1) the latitude of the furnace site,
(2) the declination of the sun at the summer solstice ($\delta = +23\frac{1}{2}°$)
(3) the limits on the hour angle of the sun,
(4) the maximum apparent angular diameter of the sun which occurs in January (32′32″),
(5) the distance between the parabolic condenser and the azimuth axis of the heliostat carriage,
(6) the location of the axes of the heliostat relative to the optical axis of the parabolic condenser.

The requirements for (1) and (2) are illustrated in Fig. 2. The latitude, ($\phi$), and the maximum declination of the sun, ($\delta$), determine the approximate over-all height of the mirror surface. $H = 2R \sec \frac{1}{2}(90° - \phi + \delta)$.

Requirement (3) will become apparent later in the discussion.

Fig. 3 illustrates the requirements (4) and (5). In order to illuminate fully the parabolic condenser, light from every point on the sun's surface must be reflected

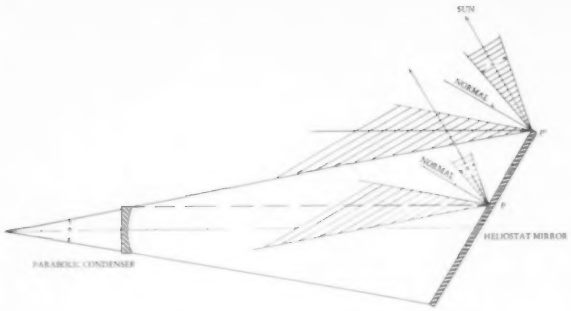


FIG. 3 — Dependence of the size of the heliostat mirror on the angular diameter of the sun and the distance between the condenser and the heliostat.

through every point of the aperture of the condenser. The apparent angular diameter of the sun is $\alpha$. Any point on the heliostat mirror receives light from the sun in a bundle of rays which are enveloped in a right circular cone whose vertex is at the reflecting point on the mirror. The light reflected from this point is also a right circular cone. Two points of reflection are shown in Fig. 3. If only the light rays reflected from points below $P$ are considered, it is noticed that no rays which are reflected downward will pass through the top of the condenser — only light reflected upward and horizontally will pass through. In order to get all the light possible through the top of the condenser it is necessary to go up to the point $P'$ on the heliostat mirror. In three dimensions the boundary rays reflected from all the points as $P'$ outline a right circular cone about the parabolic condenser. The generating angle of this cone is $\alpha/2$. The vertex of the cone will lie at a considerable distance to the rear of the condenser. From Fig. 3 it is apparent that the area outlined on the heliostat mirror depends also on the separation of the parabola and the heliostat. The greater the separation the greater will be the cross section of the enveloping cone. At latitude 33°N, the over-all height of the mirror increases by about 1.3 ft for each 100 ft of separation of condenser and heliostat mirror.

The requirement (6) will be apparent later.

The law of reflection and the orientation of a plane surface are referred to the normal to the surface. For any given position of the sun, the sunlight must be reflected due south by the heliostat mirror. The normal to the mirror surface is the bisector of the angle between the direction of the sun and the direction of the horizontal line directed toward the south.

The altitude and azimuth of the sun are given by:

$$\sin h_s = \sin \delta \sin \phi + \cos \delta \cos \phi \cos t \qquad [1]$$

$$\sin A_s = \frac{\cos \delta \sin t}{\cos h_s} \qquad [2]$$

where $\phi$ = the latitude of the station
$\delta$ = the declination of the sun
$t$ = the hour angle of the sun
$h_s$ = the altitude of the sun
$A_s$ = the azimuth of the sun.

From the spherical triangles in Fig. 4 the altitude and azimuth of the normal to the heliostat mirror can be found. $A$ and $h$ will indicate the azimuth and altitude of

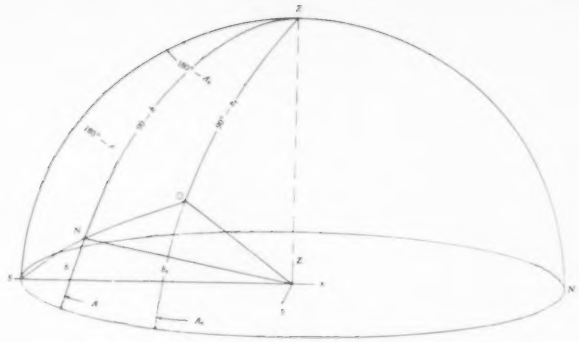

FIG. 4 — Altitude and azimuth of the normal to the heliostat.

the normal to the mirror. $\odot$, $N$ and $S$ indicate the sun, the normal, and the south point. From the laws of reflection we have:

$$SN = \tfrac{1}{2}\,(S\odot) \qquad [3]$$

In the spherical triangle $ZS\odot$ we have

$$\cos S\odot = -\cos h_s \cos A_s \qquad [4]$$

$$\sin ZS\odot = \frac{\sin A_s \cos h_s}{\sin S\odot} \qquad [5]$$

In the spherical triangle $ZSN$ we have

$$\sin h = \sin SN \cos ZSN \qquad [6]$$

$$\sin A = \frac{\sin SN \sin ZSN}{\cos h} \qquad [7]$$

Equations [6] and [7] give the altitude and the azimuth of the normal to the heliostat mirror. For purposes of computing, the orientation of the normal will be given in terms of its direction cosines

$$\begin{aligned} \lambda &= \cos h \cos A \\ \mu &= \cos h \sin A \\ \nu &= \sin h \end{aligned} \qquad [8]$$

The general arrangement of the elements of a solar furnace are shown in Fig. 5. The coordinate axes are chosen with $x$-positive to the right or north, $y$-positive forward or toward the east, and $z$-positive upward. The $x$-axis coincides with the axis of the parabola. The coordinates of the center of the aperture of the parabola (not the vertex) are $(L, 0, 0)$. The azimuth axis of the heliostat intersects the $x$-axis at $(P, 0, 0)$. The elevation axis lies in a horizontal plane which is at a distance $f$ from the $xy$-plane. The azimuth axis intersects the plane of the elevation axis

FIG. 5 — Arrangement of the axis.

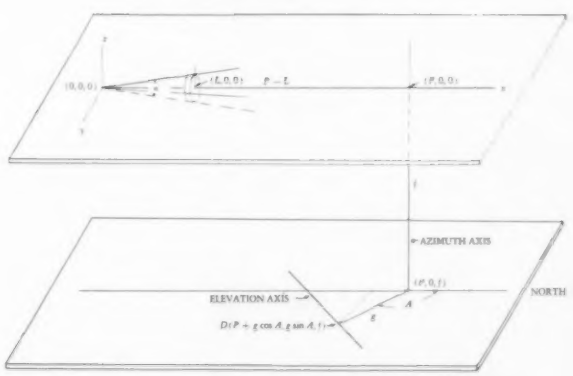

at the point $(P, 0, f)$. The distance from the elevation axis to the point $(P, 0, f)$ is denoted $g$. $g$, which is always considered positive in length, is the radius of a circle to which the elevation axis is always tangent as the heliostat rotates in azimuth. The point of intersection of the elevation axis and $g$ is $D(P+g \cos A, g \sin A, f)$. The line $g$ has the same azimuth as the normal to the heliostat mirror.

The equation of the plane which passes through $D$, contains the elevation axis, and whose normal has the direction cosines given by Equation [8] is:

$$x \cos A \cos h + y \sin A \cos h + z \sin h = (P \cos A + g) \cos h + f \sin h \qquad [9]$$

The equation of the right circular cone with vertex at the origin and axis coincident with the positive $x$-axis and generating angle $a/2$ is:

$$y^2 + z^2 = m^2 x^2 \qquad m = \tan a/2 \qquad [10]$$

The intersection of the plane (Equation [9]) and the cone (Equation [10]) is an ellipse. (The parabolic and hyperbolic cross sections are of no importance.) For any given orientation of the heliostat mirror this ellipse outlines the area on the mirror which contributes light to fully illuminate the aperture of the parabola.

To derive the explicit equation of this ellipse, the origin of coordinates will be translated to the point $D$ and the axes will then be rotated so that the new $x$-axis is parallel to the normal to the heliostat and the new $y$-axis is the elevation axis through $D$.

The equations of translation are:

$$x = x' + (P + g \cos A) \qquad y = y' + g \sin A \qquad z = z' + f \qquad [11]$$

The equations of rotation are:

$$x' = -x'' \cos A \cos h + y'' \sin A - z'' \cos A \sin h$$
$$y' = -x'' \sin A \cos h - y'' \cos A - z'' \sin A \sin h$$
$$z' = -x'' \sin h + z'' \cos h \qquad [12]$$

Applying these transformations to the equations of the plane we get $x'' = 0$. Applying these transformations to the equation of the cone and substituting $x'' = 0$ we obtain; (Note the double primes are omitted.)

$$\begin{aligned} &y^2 [1 - (1 + m^2) \sin^2 A] \\ &+ z^2 [1 - (1 + m^2) \cos^2 A \sin^2 h] \\ &+ yz [2(1 + m^2) \sin A \cos A \sin h] \\ &- y [2 \sin A] [m^2 P + g(1 + m^2) \cos A] \\ &- z \{2g \sin h [1 - (1 + m^2) \cos^2 A] \\ &- 2f \cos h - 2m^2 P \cos A \sin h\} \\ &+ [g^2 + f^2 - m^2 P^2 - 2gm^2 P \cos A \\ &- (1 + m^2) g^2 \cos^2 A] = 0 \end{aligned} \qquad [13]$$

Equation [13] is the general expression for the ellipse which bounds the area which contributes light to the parabola. $A$ and $h$ are the azimuth and altitude of the normal to the heliostat mirror, $m$ is the tangent of the sun's semidiameter, $f$ is the distance from the axis of the parabola to the horizontal plane in which the elevation axis lies, $g$ is the horizontal distance between the elevation and azimuth axes, $P$ is the distance of the azimuth axis from the vertex of the cone.

Two different locations of the elevation axis will be considered. In the conventional heliostat $f = g = 0$ and

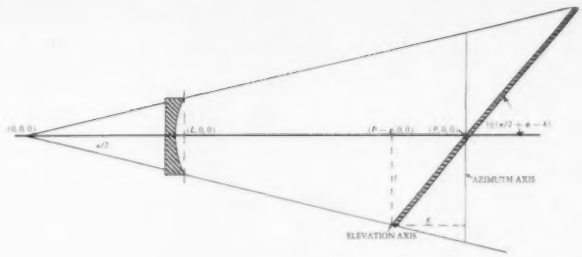


FIG. 6 — When the normal to the heliostat is in the plane of the meridan, the elevation axis is taken perpendicular and tangent to the cone.

Equation [13] becomes:

$$\begin{aligned} &y^2 [1 - (1 + m^2) \sin^2 A] \\ &+ z^2 [1 - (1 + m^2) \cos^2 A \sin^2 h] \\ &+ yz [2 (1 + m^2) \sin A \cos A \sin h] - y [2m^2 P \sin A] \\ &+ z [2m^2 P \cos A \sin h] - m^2 P^2 = 0 \end{aligned} \qquad [14]$$

For the unconventional location of the axes, values of $f$ and $g$ will be determined according to the following restrictions. The heliostat will be positioned for zero hour angle and maximum declination of the sun. Moreover, it will be moved along the $x$-axis so that its surface passes through the point $(P, 0, 0)$. The elevation axis is chosen in the plane of the mirror so that it is tangent to the lowest element of the cone. In this position the inclination of the mirror surface is $\frac{1}{2}[90° + \phi - \delta]$.

From Fig. 6 we have

$$\tan [\pi + \tfrac{1}{2} (90° + \phi - \delta] = f/g$$

or

$$f = g \tan \tfrac{1}{2} (90° + \phi - \delta) \qquad [15]$$

$$m = \frac{f}{P - g} = \frac{g \tan \tfrac{1}{2} (90° + \phi - \delta)}{P - g}$$

or

$$g = \frac{Pm}{m + \tan \tfrac{1}{2} (\pi/2 + \phi - \delta)} \qquad [16]$$

In order to illustrate the use of these equations it will be assumed that the radius of the aperture of the condenser is $R = 9$; that $P - L = 48$, $\phi = 33°$, $\delta = +23\tfrac{1}{2}°$, $a = 32'32''$, $m = \tan a/2 = .00473176$. Since $m = \tan a/2 = R/L$ we have:

$$L = R/m = 1902.0407$$
$$P = 48 + L = 1950.0407$$

and Equation [14] for the ellipses for the conventional heliostat becomes:

$$\begin{aligned} &y^2 [1 - 1.000022 \sin^2 A] \\ &+ z^2 [1 - 1.000022 \cos^2 A \sin^2 h] \\ &+ yz [2.000045 \sin A \cos A \sin h] \\ &- y [0.087322 \sin A] \\ &+ z [0.087322 \cos A \sin h] - 85.140726 = 0 \end{aligned} \qquad [17]$$

For the unconventional heliostat, the values of $f$ and $g$ are, from Equations [15] and [16]:

$$g = \frac{Pm}{m + \tan \tfrac{1}{2} (\pi/2 + \phi - \delta)} = 7.780172$$
$$f = g \tan \tfrac{1}{2} (\pi/2 + \phi - \delta) = -9.190310$$

and the equations of the ellipses become

$$y^2\,[1 - 1.000022 \sin^2 A] + z^2\,[1 - 1.000022 \cos^2 A \sin^2 h] + yz\,[2.000025 \sin A \cos A \sin b] - y\,[.087322 + 15.1560692 \cos A] \sin A - z\,\{15.560344 \sin b\,[1 - 1.000022 \cos^2 A] + 18.380620 \cos b - .087322 \cos A \sin b\} + [59.852148 - .679380 \cos A - 60.532431 \cos^2 A] = 0 \qquad [18]$$

From Equations [1] to [7] the entries in Table I were found.

TABLE I

ALTITUDES AND AZIMUTHS OF SUN AND MIRROR NORMAL

| | $t^h$ | $A_s$ | $b_s$ | $A$ | $b$ | Tilt of mirror surface |
|---|---|---|---|---|---|---|
| $\delta = 23\frac{1}{2}°$ | 0 | 180°00′ | 80°30′ | 180°00′ | 40°15′ | 49°45′ |
| | 1 | 121 59 | 73 45 | 168 19 | 39 19 | 50 41 |
| | 2 | 102 06 | 62 02 | 157 20 | 36 35 | 53 25 |
| | 3 | 91 37 | 49 33 | 148 26 | 31 32 | 58 28 |
| | 4 | 83 57 | 37 00 | 139 04 | 26 24 | 63 36 |
| $\delta = -23\frac{1}{2}°$ | 0 | 180 00 | 33 30 | 180 00 | 16 45 | 73 15 |
| | 1 | 163 48 | 31 43 | 172 33 | 16 01 | 73 59 |
| | 2 | 149 08 | 26 40 | 165 27 | 13 49 | 76 11 |
| | 3 | 136 41 | 19 04 | 158 49 | 10 14 | 79 46 |

It is interesting to note from Table I that the altitude of the sun when it is four hours from the meridian in the summer is greater than the meridian altitude in the winter (Latitude 33°).

Substituting the values of $A$ and $b$ from Table I, for the summer sun, into Equations [17] and [18] and plotting the resulting ellipses we get Figs. 7 and 8 for the conventional and unconventional heliostats respectively. By reflecting all these ellipses across the vertical axis and then drawing the envelope which encompasses them, we arrive at the shape of the reflecting surface of the heliostat which is required for an eight hour day. The shape

FIG. 7 — Shape of conventional heliostat.
8 hours———
6 hours---------

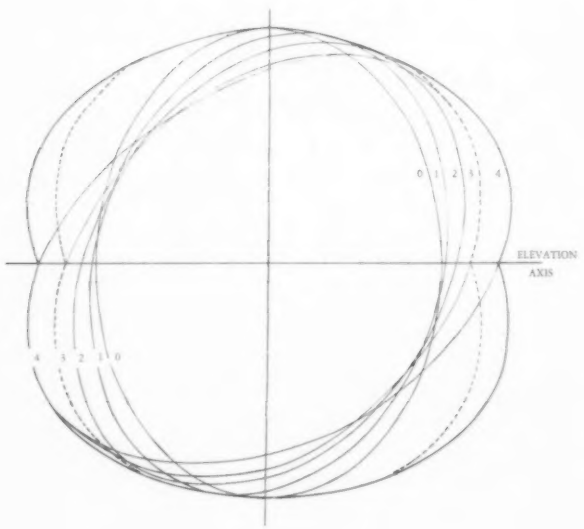


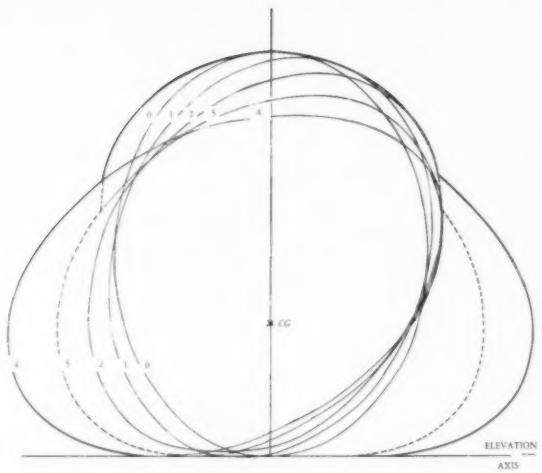


FIG. 8 — Shape of unconventional heliostat mirror.
8 hours———
6 hours---------

for a six hour day is readily found by neglecting the ellipses for $t = 4$ hrs. The dotted envelopes represent the shape required for a six hour day. It should be noted that it is not necessary to plot ellipses for any other time of year than the summer, since all other ellipses will lie within the bounds determined by $\delta = 23\frac{1}{2}°$.

The wooden models of Fig. 9 show the general appearance of the two types of mounts and mirror shapes which have been discussed above.

The heliostat used by Trombe on his furnace in the Pyrenees has a type of mount which is considerably different from the two which have been described above. In the French furnace the primary axis is placed due east and west. The bearing ends rest on stationary piers. At the center of this axis and perpendicular to it is the secondary axis to which the heliostat mirror is attached. The mirror is tilted about the primary east-west axis and rotated about the secondary axis which always remains in the plane of the meridian.

The general equation from which the shape of the Trombe heliostat mirror may be determined is found in a similar manner to that used above. The stationary east-

FIG. 9.

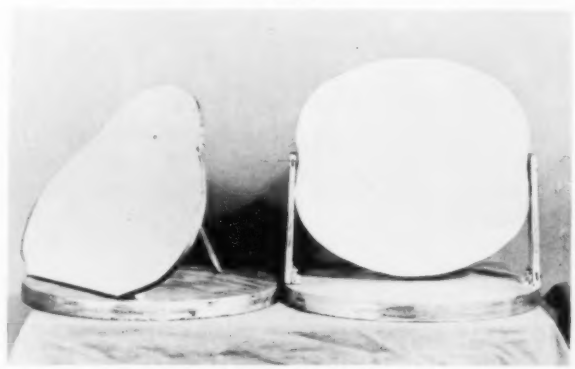

VOL.
1
1957

west axis occupies the position of the elevation axis as shown in Fig. 6. The point of intersection of the two axes is stationary and has the coordinates $(P - g, 0, f)$. The plane of the mirror passes through this point of intersection. In practice the primary axis must be below the cone shown in Fig. 6, since lobes on the lower edge of the mirror must clear the primary axis. This requirement will slightly alter the shape of the surface from that which is to be described. The equation of any plane through this point, whose normal has the direction cosines given in Equation [8] is:

$$x \cos h \cos A + y \cos h \sin A + z \sin h = (P - g) \cos h \cos A + f \sin h \quad [19]$$

As in the above discussion the origin of coordinates will be translated to the new origin $(P - g, 0, f)$ and rotated so that the $x$-axis is parallel to the normal to the mirror surface. The equations of translation are:

$$\begin{aligned} x &= x' + (P - g) \\ y &= y' \\ z &= z' + f \end{aligned} \quad [20]$$

By applying these equations for translation the equations of the plane (Equation [19]) and the cone (Equation [10]) become:

$$x' \cos h \cos A + y' \cos h \sin A + z' \sin h = 0 \quad [21]$$

$$z'^2 + y'^2 - m^2 x'^2 + 2fz' - 2m^2 (P - g) x' + f^2 - m^2 (P - g)^2 = 0 \quad [22]$$

From Equation [16] it is seen that $f^2 - m^2 (P - g)^2 = 0$, so that the equation of the translated cone is

$$z'^2 + y'^2 - m^2 x'^2 + 2fz' - 2m^2 (P - g) x' = 0 \quad [23]$$

The tilt of the secondary axis at any instant is found from Equation [21], by setting $y = 0$, *i.e.*

$$x \cos h \cos A + z \sin h = 0 \quad [24]$$

The slope of the secondary axis is $-\cot h \cos A$. This furnishes the clue for finding the direction cosines in the equations for rotation. The equations for rotation are:

$$\begin{aligned} x' &= -x'' \cos h \cos A - y'' \frac{\cos^2 h \sin A \cos A}{\sqrt{1 - \cos^2 h \sin^2 A}} + z'' \frac{\sin h}{\sqrt{1 - \cos^2 h \sin^2 A}} \\ y' &= -x'' \cos h \sin A + y'' \sqrt{1 - \cos^2 h \sin^2 A} \\ z' &= -x'' \sin h - y'' \frac{\sin h \cos h \sin A}{\sqrt{1 - \cos^2 h \sin^2 A}} - z'' \frac{\cos h \cos A}{\sqrt{1 - \cos^2 h \sin^2 A}} \end{aligned} \quad [25]$$

Applying these equations for rotation to Equation [23] and setting $x'' = 0$ we have, for the family of ellipses which delineate the shape of the Trombe heliostat mirror, (Note the double primes are omitted.)

$$\frac{a}{d} y^2 + \frac{b}{d} yz + \frac{c}{d} z^2 + \frac{e}{\sqrt{d}} y - \frac{k}{\sqrt{d}} z = 0 \quad [26]$$

where

$$\begin{aligned} a &= 1 + \cos^2 h \sin^2 A (1 - \cos^2 h \cos^2 A) - \cos^2 h \sin^2 A (2 + m^2 \cos^2 h \cos^2 A) \\ b &= 2 (1 + m^2) (\sin h) (\cos h \sin A) (\cos h \cos A) \\ c &= \cos^2 h \cos^2 A - m^2 \sin^2 h \\ d &= 1 - \cos^2 h \sin^2 A \end{aligned}$$

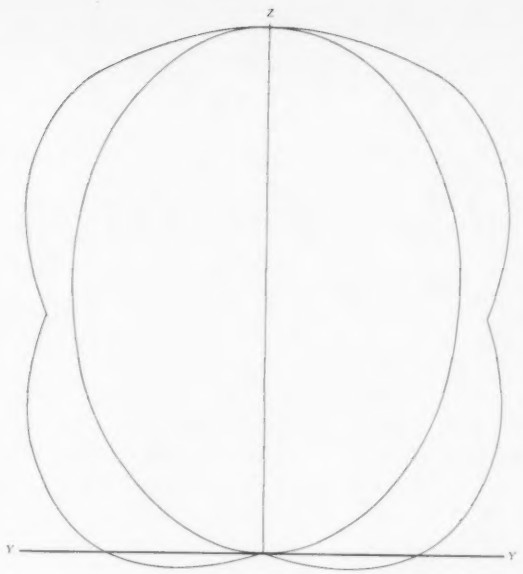


FIG. 10.— Trombe heliostat.

$$\begin{aligned} e &= 2 \cos h \sin A [-f \sin h + m^2 (P - g) \cos h \cos A] \\ k &= 2 [f \cos h \cos A + m^2 (P - g) \sin h] \end{aligned}$$

The constants $P$, $f$, $g$, and $m$ and the values of $h$ and $A$ were taken as above and the corresponding ellipses drawn. Fig. 10 shows the ellipse for $t = 0$ hrs, and the envelope for an eight hour day. A value of $f = -10$ would permit the lobes on the lower edge of the mirror to clear the primary axis as the mirror rotates about the secondary axis. With this value of $f$ the mirror shape would be slightly altered. Several points to consider in comparing the three types of mounts are:

(1) The over-all heights of the three mirrors are essentially the same. The lobes on the lower edge of the Trombe heliostat make it a very little greater in height.

(2) The over-all widths vary. The unconventional type has the greatest width, while the Trombe type has the least width.

(3) The area of the unconventional shape is about 10 per cent greater than the area of the conventional shape. The Trombe heliostat has the least area.

(4) The centers of gravity of the Trombe and the conventional heliostat mirrors are very close to the centers of the mirrors, whereas the center of gravity of the unconventional shape is about 1/3 of the way from the base to the top.

(5) The conventional type is pivoted close to the center of gravity and permits balancing the mirror so that relatively little power is required for turning in elevation. The other two mirrors lie above their primary axes and require power to raise them.

(6) The relative effect of strong winds on the three types of mounts should be investigated.

(7) Consideration must be given to the relative merits of the three types of mounts as to the advantages of adjusting and maintaining the small flat mirrors which would compose their surfaces.

# ECONOMIC FACTORS IN FURNACE DESIGN*

By NEVIN K. HIESTER, THOMAS E. TIETZ, and ROBERT E. DE LA RUE, Jr.

Stanford Research Institute
Menlo Park, California

The theoretical and practical factors which affect the specific performance characteristics and costs of solar furnaces are reviewed in detail. Technical and economic considerations indicate that the best design for a large solar furnace should incorporate the following features:

(1) a parabolic concentrator consisting of adjustable curved-mirror segments,

(2) a stationary concentrator with its axis horizontal, using an auxiliary movable mirror to follow the sun,

(3) an angle between the image area and the rim of the concentrator of between 50° to 70°,

(4) a reflecting surface consisting of back-silvered glass. The actual heat flux available at the target is expressed as

$$p = 46.1 \times 10^3 \, E \, p_o \sin^2 \theta$$

where $E$ is the over-all efficiency factor of the solar furnace, $p_o$ is the solar constant, and $\theta$ is the rim angle. $E$ is defined as

$$E = \eta_a \, \eta_r \, \eta_s \, \gamma$$

where $\eta_a$ accounts for loss of radiant energy due to the atmosphere, $\eta_r$ is the combined reflectivity coefficient of the reflecting surfaces of the concentrator and auxiliary mirrors, $\eta_s$ accounts for the nonreflecting portions of the concentrator because of shadowing and open areas between mirror segments, and $\gamma$ is an index which represents the degree of geometrical perfection of the parabolic concentrator. A tabulation of calculated $E$ and $\gamma$ values for a number of actual solar furnaces is presented.

The design study and cost estimate, given in Appendix A, include a preliminary structural design and relative cost estimates for a solar furnace system having a 100-ft parabolic concentrator with a movable auxiliary mirror to follow the sun. The results of this study were extrapolated to give cost curves for furnace systems having concentrators with diameters from 50 to 200 ft.

## INTRODUCTION

The use of a solar furnace to obtain high temperature has been a subject of interest for many centuries. Recent investigations, particularly the work of Félix Trombe in France since 1946, have been especially fruitful. These studies, revealing new promise for practical applications of this technique to obtain high temperatures have aroused the interest of both scientists and engineers.

The features which make solar furnaces attractive as research tools can be placed in four general categories.

**(1) High Temperatures in a Controlled Atmosphere**

In contrast to the usual techniques for obtaining high temperatures, a solar furnace can have an oxidizing, reducing, or neutral atmosphere as desired. Temperatures exceeding 3000°C can be obtained with solar furnaces.

**(2) Cavity Heating by Radiation**

Spot melting in a cavity offers distinct advantages over other methods in that it avoids contamination at high temperatures and eliminates requirements for ultrahigh temperature crucible materials. With this technique, it is possible to use the material under study as its own susceptor and to produce materials of extremely high purity. No other method of heating can provide results as free from contamination at ultrahigh temperatures.

**(3) High Heat Flux**

The solar furnace is unique in its ability to provide a source of high heat flux. The furnace can deliver heat to a surface at a rate exceeding that found in any engineering application, including rocket motors, and thus is a most powerful tool. For example, new materials could be subjected to severe thermal shock by this means, and high-rate heat transfer investigations could be undertaken.

**(4) Absence of Large Electric or Magnetic Fields**

A solar furnace offers the advantage of allowing studies to be conducted at extremely high temperatures in the absence of large electric or magnetic fields.

Stanford Research Institute is engaged in research in several fields involving high temperature technology. Studies have been conducted in metallurgy and ceramics with the purpose of developing materials with improved high temperature properties. Through these activities, the Institute became keenly interested in the unique applications made possible by solar furnaces in the field of high temperature research. The Institute obtained support from the United States Air Force through the Air Force Office

* This paper is published by permission of the Air Force Office of Scientific Research of the Air Research and Development Command, who supported the work, and is based on ASTIA Document No. AD-95818 (AFOSR-TN-382), June 21, 1956.

VOL.
1
1957

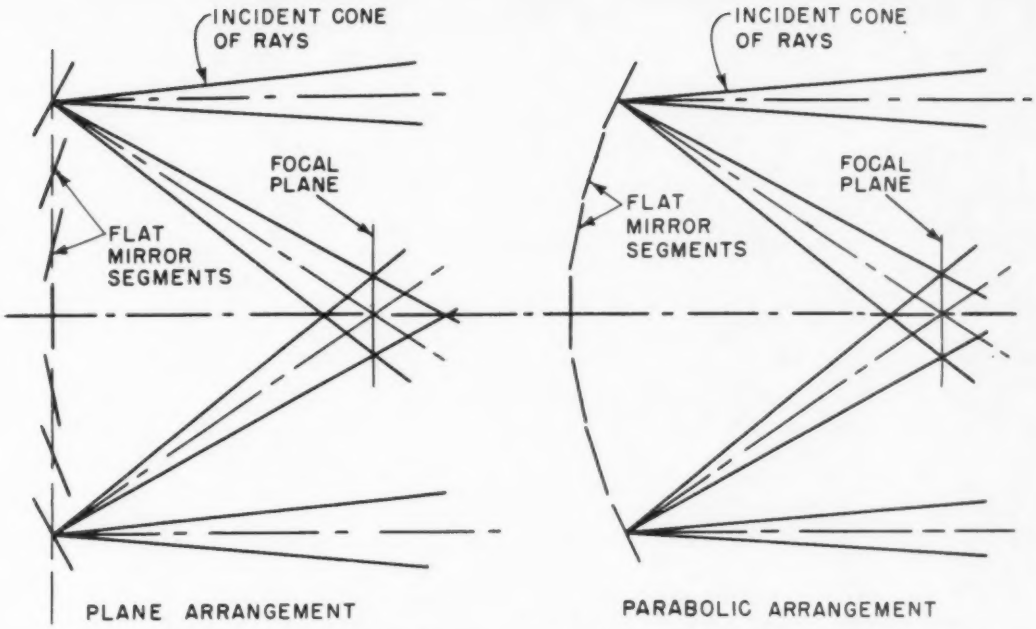


FIG. 1 — Schematic diagram showing arrangements of mirror segments in a flat-plate concentrator.

of Scientific Research in order to undertake the present study on the application of solar furnaces for research on solids at high temperatures. Arrangements were made to use the lens-type solar furnace located at the California Institute of Technology (CIT) in Pasadena for the experimental phase of the program.

The general objective of the program was to study the application of solar furnaces for research on solids at elevated temperatures. The work was divided into three specific areas: (a) theoretical study (1); (b) design study and cost estimate; and (c) experimental study (2, 3, 4). The results of the second program are the basis for this paper.

## GENERAL DISCUSSION

In determining the most suitable solar furnace system on both an economic and a technical basis, there are a number of factors which must be considered. Since many of these factors are interrelated, a design study should include their effects on specific and over-all performance characteristics and costs. The theoretical considerations presented by Loh, Duwez, Hiester and Tietz[1] are used to relate the performance characteristics and costs of certain solar furnace systems.

## FACTORS AFFECTING SOLAR FURNACE PERFORMANCE CHARACTERISTICS AND COSTS

The specific items which affect the performance characteristics and costs of solar furnace systems can be classified in six general categories. These are: the type of furnace, methods of mounting the concentrator and tracking the sun, optics, materials and accuracy of construction, site, and types of target or use. Two other factors which affect the over-all cost of an installation, namely the facilities and staff and the operational costs, are not considered in this report.

### (1) Type of Furnace

Included in the category covering the type of furnace is the method of concentrating the sun's rays. There are three principal forms of concentrators: the lens, oriented flat plates, and the parabolic surface. For each form of concentrator different methods of construction are possible. The parabolic concentrator can consist of either a single reflecting surface or a series of curved-mirror segments. Flat-plate reflectors can be arranged in a number of ways. As shown in Fig. 1, the segments can be arranged so that the center of each segment lies on a plane or so that the segments are tangent to a parabolic surface.

The factors which should be evaluated to determine the relative costs of the various types of concentrators are the number, size, and cost of the reflecting segments (or lens), the cost of the segment support brackets, the cost of adjustments of the segments, and the proportional size and cost of the components of the concentrator (concentrator primary frame, supporting structure, and foundation).

In comparing the different types of reflecting concentrators, there are two factors which indicate that the cost of a segmented parabolic concentrator would be lower than that of the flat-plate type. These are the number of reflecting segments and the size of the concentrator required to obtain a given concentration. Trombe[5] stated, in reference to the 35-ft solar furnace at Montlouis, that an energy concentration at the focal point obtained by approximately 20,000 flat mirrors could be obtained by

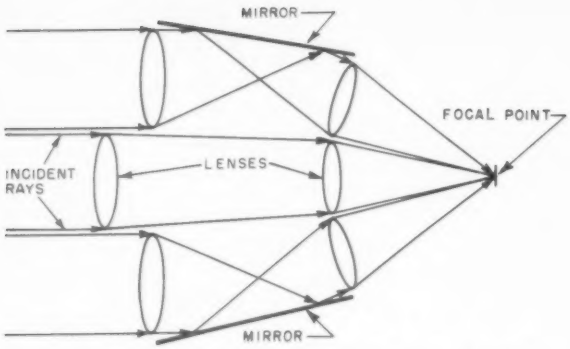


FIG. 2 — Schematic diagram of lens-type furnace at California Institute of Technology.

using 3,500 curved mirror segments.* Reference to the results obtained with the Massachusetts Institute of Technology Fresnel-type flat-plate mirror described by Gardon[6] gives somewhat similar results. For example, that furnace obtained a flux of 5.35 cal/cm²/sec over an area of 5 sq in. with a concentrator of 30 sq ft. A paraboloidal mirror to provide the same performance would require about 22.5 sq ft.

A single-surface parabolic concentrator is not considered here, since for large concentrators over about 10 ft in diameter, the single-surface type is much more difficult and expensive to construct than the segmented type.

Thus, a preliminary evaluation of these factors indicates that the cost of an oriented flat-plate concentrator would be about twice that of a segmented parabolic concentrator having equal performance characteristics. This is based on the cost of the reflecting surfaces alone, assuming the mirrors to be of the same material. If consideration is given to the number of mirror-supporting brackets, relative size of the supporting structures and foundations, and other factors, the cost differential would probably be greater.

In comparing the relative costs of the lens-type concentrator** and parabolic concentrator, there are several factors which indicate that the cost of a large solar furnace employing a lens-type concentrator would be higher. These are the size and shape of the lenses, the nontransmitting area between the lenses, and the optical losses. Lenses of high quality obtained by simple manufacturing procedures would be circular in shape and small in size. Because of the shape and size, the nontransmitting portion of an array of lenses would be greater than the nonreflecting portion of a parabolic concentrator composed of rectangular segments. The over-all size of an array of lenses, and thus the cost of a lens-type concentrator, would therefore be higher than a segmented-parabolic concentrator having the same performance characteristics.

The other factor which indicates that the cost of a lens-type concentrator would be higher than a parabolic type is the optical losses. For the two types of mountings that employ lenses, there is a total of three reflecting and/or transmitting units. Thus, for the type of mounting used at the California Institute of Technology (shown in Fig. 2) there are two transmitting units and one reflecting unit, while for the Cassegrainian type of mounting there are two reflecting units and one transmitting unit. This compares with one reflecting surface for the parabolic-type concentrator. As will be shown later, as the number of reflecting and/or transmitting units increases, the over-all size and cost of a solar furnace system of a given performance increase. A preliminary evaluation of this factor thus indicates that the cost of a lens-type concentrator would be higher than a parabolic concentrator having the same performance characteristics.

### (2) Mounting and Tracking

The second item which influences the performance and cost of solar furnaces is the method of mounting the concentrator and tracking the sun. There are at least four methods of mounting the reflector-type of concentrator, each of which has certain advantages depending upon the size of the solar furnace and the intended use. In one, the individual flat-plate mirror segments each track the sun and horizontally reflect the sun's rays which are superimposed on the target.[7] A second type is a unit in which the entire concentrator follows either the entire, or a limited, portion of the sun's path. A third type is composed of a fixed concentrator with a horizontal axis and a movable flat mirror (heliostat) which is used to track the sun and direct the rays into the concentrator. In this case the rays are reflected and concentrated to the target, on the horizontal axis. In the last type, the concentrator and one flat mirror are fixed, with the concentrator faced toward the ground. In this case a second flat mirror or heliostat is required, which tracks the sun. The last two cases are illustrated in Fig. 3. The fixed mirror can be

FIG. 3 — Methods of mounting reflector-type concentrators.

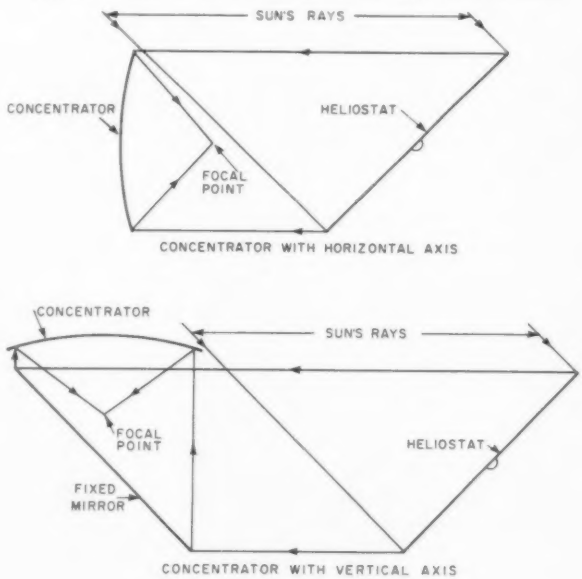


* The concentrator of this furnace is composed of flat mirrors which were mechanically deformed to give them a curvature approximating that of a paraboloid.

** A discussion of the lens-type solar furnace at the California Institute of Technology is presented by Hiester, Loh, and Tietz.[2]

VOL. 1 1957

dispensed with in the vertical arrangement if the concentrator is mounted high enough to prevent shadowing of the movable heliostat under it, but this is normally impractical. On June 21, at Menlo Park's latitude, a 100-ft mirror would have to be approximately 400 ft above the heliostat.

Although the latter types of mounting can be used with either an oriented flat-plate or a segmented parabolic-type concentrator, in the first type, where the individual segments track the sun, only flat-plate mirrors are technically feasible.* As has already been shown, such concentrators are more expensive than the parabolic type, so the first type of mounting can be dismissed.

In determining the relative costs of mountings which employ auxiliary mirrors, the effect of additional reflecting surfaces as well as the effect of the types of mounting and tracking equipment have to be considered. This is because no surface is 100 per cent efficient as a reflector, but varies in performance depending on the material.[8] A system employing more reflecting surfaces would therefore require a larger concentrator and larger auxiliary mirrors to give the same performance characteristics. For furnace systems employing parabolic concentrators and having the same performance characteristics, but a different number of auxiliary mirrors, the following relationship holds:[1]

$$(\eta_r')_1^2 \sin^2 \theta_1 = (\eta_r')_2^3 \sin^2 \theta_2 \qquad [1]$$

where $\eta_r'$ is the individual reflectivity efficiency factor taking into account losses by reflectivity or absorptivity of the optical parts of the furnace and $\theta$ is the rim angle of a parabolic concentrator. Subscript 1 and 2 refer to the systems employing one and two auxiliary mirrors, respectively. Also

$$\frac{D_2}{D_1} = \frac{\sin \theta_2 \, (1 + \cos \theta_1)}{\sin \theta_1 \, (1 + \cos \theta_2)} \qquad [2]$$

where $D$ is the diameter of the paraboloid.

Assuming the furnace system which employs one auxiliary mirror to have a concentrator with a diameter of 100 ft, a rim angle of 50°, and all reflecting surfaces constructed of the same material with $\eta_r = 0.85$, then the required diameter of the concentrator using two auxiliary mirrors is obtained from Equations [1] and [2].

$$\theta_2 = \sin^{-1}\left[\frac{(0.85)^2}{(0.85)^3} \sin 50^\circ\right] = 64.5^\circ$$

Therefore

$$D_2 = 100 \, \frac{\sin 64.5 \, (1 + \cos 50)}{\sin 50 \quad (1 + \cos 64.5)}$$

$$D_2 = 135 \text{ ft}$$

and it is immediately apparent that system 2 is more costly.

The selection between the two types of mounting, namely the type where the entire concentrator tracks the sun and the type employing a fixed concentrator and a movable heliostat to track the sun, should be on a technical rather than a cost basis. Although no cost estimate was made for the tracking type of concentrator, it appears that the cost of the two mounting systems having the same performance characteristics would be comparable. This is based on the fact that although the size and therefore the cost of the tracking concentrator would be less than the fixed concentrator, because of the smaller number of reflecting surfaces employed in the tracking system, the additional cost of the turntable and the tilting device would offset the difference, due to the additional load requirements for the tracking concentrator.

The technical factors which indicate the disadvantages of a large unit employing a tracking-type concentrator are the inconvenience of the location of the target area and the shutter design. Two methods can be used in constructing the target platform: (1) by using a cantilever-type construction and having the target platform at one end, or (2) by having a movable target tower which is designed to follow the path of the reflected image. For the first method, access to the target area would be poor, and in the second case the mechanism required to move the tower would be very complex, making the cost prohibitive. For the method employing a cantilever to support the target platform, the shutter design would be difficult because of the interference of the cantilever. Thus on a technical basis, the system employing a fixed concentrator and a movable heliostat appears to be more desirable.

### (3) Optics

The next design category to be considered is the optics or the optical geometry of the concentrator. In this group there are five important variables: the aperture, ratio of aperture to focal length, image or target diameter, average target flux, and uniformity of flux distribution at the target. The theoretical analysis and relationships relating to the optical geometry and performance characteristics of a parabolic-type concentrator were presented by Loh *et al.*[1]

The first factor in this category which will be evaluated from both a technical and an economic standpoint is the rim angle, or the ratio of aperture to focal length of the concentrator, since this affects the relation between mirror and image size and determines the flux. To determine the

FIG. 4 — Variation of concentration ratio with rim angle.

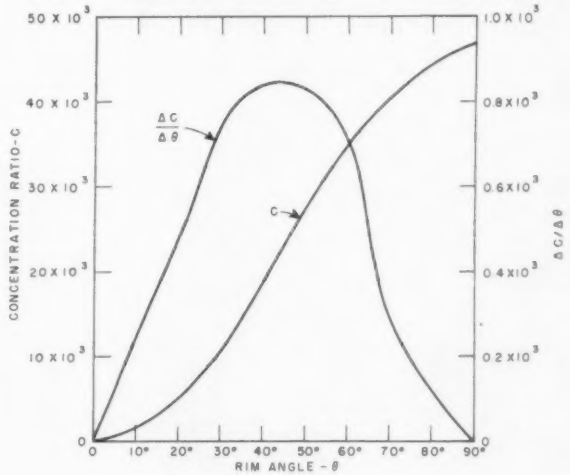


* In curved segments the angle between the incident ray and the focused ray can vary only slightly if the image is to be of good quality. In tracking the sun individually, this angle changes greatly, and to retain quality flat segments must be used.

optimum rim angle $\theta$, the effect of increasing rim angle on the flux delivered by the concentrator will be determined.

For the case of a parabolic-type concentrator, the optimum rim angle depends upon the basis on which it is chosen. For example, the maximum change in the contration ratio with respect to a change in $\theta$, and thus in the flux at the image, occurs at the inflection point of the curve, as seen in Fig. 4, where concentration ratio $C$ is plotted versus rim angle $\theta$. This inflection point occurs at a rim angle of 45°. In this case, as shown in Fig. 4, any dollar invested to increase the rim angle by one degree returns the most flux at 45°.

From a cost viewpoint, there are three bases on which the optimum rim angle may be selected. These are: (1) the amount of flux per unit cost, assuming that the useful value of the flux is constant; (2) the amount of flux per unit cost, assuming that the value of flux increases as the total quantity of flux delivered by the concentrator increases (so that value/cost equals flux/cost multiplied by flux); and (3) the rate of change of flux per unit cost. An illustration of the variation of the optimum rim angle using these three bases is given in Fig. 5. For this example, two assumptions were made, first, that the cost of a solar furnace system consisting of a fixed parabolic concentrator and a movable heliostat varies with the diameter of the diameter of the concentrator to the 1.5 power (the results of the design study given in Appendix A indicate that the cost varies approximately with the diameter to the 1.5 power), and second, that the focal length of the concentrator is constant, so that the size of the sun image at the focal plane would be constant. If the purpose of the solar furnace in a particular application is to replace a conventional type of furnace, i.e. electric or gas-fired, then from an engineering viewpoint the flux per unit cost is one of the most important factors. For this case, as can be seen from the flux/cost versus rim angle curve in Fig. 5 (curve $B$) the maximum ratio occurs at a rim angle of approximately 45°.

FIG. 5 — Variation of flux and cost of a solar furnace employing a parabolic concentration with rim angle.

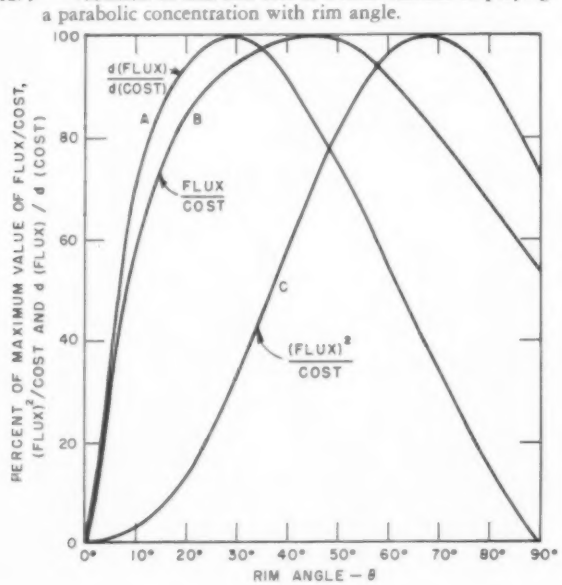


When the maximum temperature obtainable (i.e. maximum flux) is taken to be the prime factor, then the unit value of the flux can be taken to be related to the total quantity of flux delivered by the furnace. Specifically, the optimum rim angle was determined by assuming the value of the flux to be equivalent to the total flux delivered. For this case, from the flux$^2$/cost curve in Fig. 5 (curve $C$), the optimum value of the rim angle is approximately 70°.*

In the last case, shown by curve $A$ in Fig. 5, the maximum differential change in flux with cost occurs at a rim angle of 30°. In this case, therefore, a dollar invested for a degree increase in rim angles greater than 30° would not supply as much flux as a degree increase at 30°. Since the first two cases are the practical limits of interest, it appears that the optimum value of the rim angle of a parabolic concentrator is between 50° to 70°.

Although the rim angle is an important factor with respect to furnace design, it may be necessary for certain applications to provide other heat flux levels and image diameters than the design values. In a system employing parabolic concentrators there are four methods which can be used to achieve different flux levels and/or image diameters. These are: (1) the use of a control shutter placed between the focal plane and the concentrator; (2) shading of a portion of the concentrator and/or the heliostat; (3) position adjustment and deformation of the individual mirror segments of the concentrator to obtain a different focal length; and (4) movement of the target off-focus.

The first two methods, the use of a control shutter and the shading of the concentrator and/or heliostat, can be used to reduce the heat flux level without loss of uniformity in the flux at the focal plane or without a change in the image size. A control shutter can also be designed to reduce the image size. The third method, adjustment and deformation of the individual mirror segments, can be used to achieve either higher or lower flux levels and larger or smaller images by increasing or decreasing the focal length of the paraboloid. For a given aperture, a smaller image diameter and higher flux are obtained by decreasing the focal length, whereas increasing the focal length will result in a larger image size and lower flux.

The last method, moving the target off-focus, will result in a larger or smaller image size, but this is accompanied with some loss of uniformity of heat flux within the image. During the present program there was not sufficient time to make a detailed technical evaluation of the change in image size and the flux intensity distribution over the image for targets moved away from the focal plane. An independent study was undertaken to determine

* Another way of considering this is to define the unit value of flux as unit value $= \gamma$ (flux)$^n$.

If $n$ is zero, or the unit value constant, one gets curve $B$, Fig. 5. For the unit value proportional to the flux ($n = 1$) the resultant curve is $C$, and the peak of the curve moves towards 90° with increasing $n$. If $n$ is infinity, i.e. if one is willing to pay any price to get flux, the peak of the curve is at 90° as one would expect.



VOL. 1 1957

the variation of the flux intensity distribution and image size with distance from the focal plane of a paraboloid, and the results are reported elsewhere.*

### (4) Construction Factors

The next design category which will be considered is the materials of construction and the method of construction. Selection of structural materials will depend upon the strength-weight relations and the corrosion resistance required. The choice of reflector materials will be governed by reflectivity and corrosion resistance as well as by the optics and the spectrum desired. Ghai[8] has determined the reflectivity and corrosion of several common surfaces. Of the three types of reflecting materials, metal, front-silvered glass, and back-silvered glass, the latter has been determined to be the most favorable.

The disadvantages of metal as a reflecting surface are poor corrosion resistance and the inability of any resulting oxide coating to reflect the entire spectrum. Although the reflecting qualities of front-silvered glass are good, corrosion is again a problem. The reflecting surface of back-silvered glass can be protected from corrosion by various means. One factor which is a disadvantage for back-silvered glass is the addition of an absorption loss by the glass. This loss can be minimized, however, by the use of a good grade of optical glass.

The accuracy of construction of the reflecting surfaces, i.e. how closely they approach the perfect geometrical shape, will affect the performance characteristics of the furnace system. Therefore, consideration will be given to variation of cost with estimated degrees of accuracy of the reflecting surfaces. For this purpose an efficiency factor $E$, and the index of geometrical perfection $\gamma$, were determined for a number of furnaces employing parabolic concentrators. The efficiency term includes all of the sources of inefficiency in furnace construction and is defined by

$$E = \eta_r \, \eta_s \, \eta_a \, \gamma \qquad [3]$$

where $\gamma$ is the index of geometric perfection, $\eta_r$ is the over-all reflectivity efficiency of the reflecting surface, $\eta_s$ is the shadowing efficiency factor which accounts for the nonreflecting surfaces, and $\eta_a$ is the fraction of the solar constant which is available at the site. These losses are covered in more detail later.

Another definition of the efficiency factor can be obtained from Loh *et al.*[1]

$$E = \frac{p_{\text{actual}}}{46.1 \times 10^3 \, p_o \sin^2 \theta} = \frac{p_{\text{actual}}}{C_{\text{theoretical}} \, p_o} \qquad [4]$$

where $p_{\text{actual}}$ is the heat flux actually received per unit area within the sun image at the focus, and $p_o$ is the solar constant, measured above the atmosphere.

In Table I, the efficiency factor and index of geometrical perfection are given for seven furnaces. Where flux measurements were reported in the literature, these data were used to determine the efficiency factor and index of geometrical perfection. Where only the temperature obtained by the particular furnace was reported, the efficiency factor and index of geometrical perfection were estimated by computing the heat flux required to obtain the reported temperature, assuming cavity heating and black-body radiation. The heat flux as a function of temperature for a cavity is given by

$$p = \sigma \, T_m^4 \qquad [5]$$

where $\sigma$ is the Stefan-Boltzmann constant and $T_m$ is the temperature of the body. Because of the lack of data concerning the type, size, and material of the sample and the method used to measure the temperature, two other assumptions were necessary. In Case I, it was assumed the only heat loss was by radiation from a cavity, and for Case II, it was assumed that heat loss by conduction and convection was equal to 20 per cent of the heat loss by radiation. Values of the reflectivity efficiency factor $\eta_r$ and transmission factor $\eta_a$ were estimated, based on the knowledge of the materials of the reflecting surface and furnace locations, respectively. $p_o$ was taken as 0.033 cal/sec/cm$^2$ or 2 cal/min/cm$^2$.

As can be seen from Table I, the index of geometrical perfection for two of the three large furnaces, Montlouis 35 ft and Algiers 27.6 ft, are approximately the same,

* See R. E. De La Rue *et al*, "Flux distribution near the focal plane," pp. 95-99.

TABLE I

EFFICIENCY FACTOR AND INDEX OF GEOMETRICAL PERFECTION FOR VARIOUS SOLAR FURNACES

| Furnace | Diameter (ft) | Reflector Material | $\theta$ (degrees) | Temp. (°K) | Flux (cal/sec/cm$^2$) | $\eta^a$ | $\eta^r$ | Case I | | Case II | | Reference |
|---|---|---|---|---|---|---|---|---|---|---|---|---|
| | | | | | | | | $E$ % | $\gamma$ % | $E$ % | $\gamma$ % | |
| Montlouis | 35 | glass | 41 | 3270 | .... | 0.85 | (0.82)[a] | 24.0 | 41.9 | 30.6 | 52.5 | 9 |
| Algiers | 27.6 | aluminum | 36.5 | 3270 | .... | 0.85 | 0.80 | 30.3 | 43.2 | 36.7 | 54.0 | 10 |
| Fordham | 5 | glass | 60 | 3610 | .... | 0.76 | 0.80 | 21.3 | 33.7 | 25.6 | 42.1 | 11 |
| Japan | 6.5 | aluminum | 75 | 2370 | .... | 0.76 | 0.80 | 3.3 | 5.4 | 4.0 | 6.6 | 12 |
| Convair | 5 | glass | 60 | .... | 665* | 1.0 | 0.80 | 57.6 | 71.5 | .... | .... | 13 |
| Convair | 10 | aluminum | 83 | .... | 96* | 1.0 | 0.80 | 10.8 | 13.5 | .... | .... | 13 |
| Nat. Bur. St. | 5 | rhodium | 60 | 3570 | | 0.76 | (0.85)[a] | 23.5 | 42.8 | 29.4 | 53.5 | 14 |

* Value of flux corrected from value given in reference indicated because flux meter used to obtain data had an opening larger than the sun image. The original values had also been corrected to $\eta^a$ of unity.

having an average value of about 53 per cent. Actually, this value should be higher because no consideration was given to the losses due to shadowing. If a 5 to 10 per cent shadowing loss is assumed, it appears that these furnaces have indexes of geometrical perfection of approximately 60 per cent.

The effects of shadowing of the reflecting surfaces and the reduction in performance caused by nonreflecting portions of the furnace also should be included in the category dealing with the method of construction. Shadowing losses are caused by structures and other portions of the furnace, i.e. mirror-adjustment brackets and shutters, which block the sun's rays from the reflectors and target. The percent of the voids (spaces between the reflecting segments of the concentrator and auxiliary mirrors) should be considered in the furnace design. Both of these factors tend to reduce the performance characteristics and should be kept to a minimum.

**(5) Location**

The fifth category which should be considered is the location or site of the furnace. Selection of a site should be considered from two viewpoints, the solar climate and the over-all cost of the installation. The solar climate should be investigated to determine the average solar radiation and the fraction that is direct radiation. The portion of the sun's energy which is received as direct radiation and can be concentrated is affected by many factors. A study of the relative importance of these factors has indicated that water vapor and atmospheric pollutants have more effect on the energy available for solar furnace work than has the altitude. The effects these factors have on the atmospheric transmission coefficient $\eta_a$ will be discussed in the next section.

**(6) Type of Target and Use**

The last category is the type of target and intended applications of the solar furnace. In designing a furnace, consideration must be given to the types of targets that will be used. The emissivity or absorptivity of the target and the heat losses by convection and conduction affect the maximum attainable temperature. Also, the intended use of the furnace, i.e. as a high temperature source or a production unit, must be considered to determine the type of mounting, the required work space at the focus, and other related factors.

**(7) Conclusions**

In summary, the technical and economic considerations indicate that the best design of a large solar furnace should consist of:

(1) a parabolic concentrator made up of adjustable curved mirror segments,

(2) a fixed concentrator with its axis horizontal, using a heliostat to follow the sun,

(3) a rim angle between 50° to 70°, depending upon the economic value of flux increments,

(4) a reflecting surface of back-silvered glass.

## THEORETICAL CONSIDERATIONS IN SOLAR FURNACE DESIGN

In this section the various factors limiting the degree of concentration of energy and consequently the maximum attainable temperature will be related to the design of a solar furnace, making use of the theoretical considerations presented by Loh *et al.*[1]

**(1) Location of Furnace**

In the design of a solar furnace to meet certain specifications of maximum flux (or temperature), one of the prime considerations is the effect of the location or site on the performance characteristics. These effects influence the percentage and quality of the sun's energy available for concentration.

The radiant energy which reaches the surface of the earth is composed of two components, direct radiation that can be concentrated with lenses and mirrors, and diffused radiation that cannot be concentrated. The factors which affect the amount of the sun's energy which is diffused include scattering and absorption effects of the gas molecules, dust particles, and water vapor. The latitude, elevation, and weather of the site influence the amount of the sun's energy available for concentration.

Because it would be difficult to evaluate each of these factors separately, their effects are grouped into a single term, the atmospheric transmission coefficient, $\eta_a$. The actual flux received at the site that can be concentrated is given by

$$p_a = \eta_a p_o \qquad [6]$$

where $p_o$ is the solar constant, measured above the atmosphere.

**(2) Heat Flux Delivered to the Target**

In designing a solar furnace for a specified heat flux at the target, there are two classes of factors (theoretical and operational) which should be considered. Both affect the maximum flux (or temperature) a solar furnace can achieve.

The first class is related to the optical geometry of the concentrator and includes six important design variables: the aperture, ratio of aperture to focal length, image diameter, average heat flux at the image, uniformity of flux distribution at the image, and the efficiency at which the energy received by the concentrator is concentrated. Equations relating these variables for a parabolic-type concentrator were derived by Loh *et al*[1] and will be repeated here for reference. The relation between the diameter, $d$, of the sun image, and the focal, $f$, is

$$d = 2f \tan 16' = \frac{f}{107.3} \qquad [7]$$

The term "sun image" is used to refer to the circular image formed on the focal plane by the part of the mirror at the axis. The relationship between the aperture ratio, $D/f$, and azimuthal angle, $\theta$, is given by

$$\frac{D}{f} = \frac{4 \sin \theta}{1 + \cos \theta} = \tan \frac{\theta}{2} \qquad [8]$$

where $D$ is the diameter of the paraboloid at the edge. The total power which is concentrated within the sun



VOL. 1 1957

image is given by

$$P = \pi \eta_a p_o f^2 \sin^2 \theta \qquad [9]$$

where $\theta$ is the maximum angular aperture or the rim angle of a parabolic concentrator. The heat flux per unit area within the sun image is

$$p = 46.1 \times 10^3 \eta_a p_o \sin^2 \theta \qquad [10]$$

The concentration ratio, $C$, is defined as the ratio of the heat flux at the sun image of a furnace to the actual flux received from the sun by the receiver at normal incidence after reflection, both per unit area, and is given by

$$C = \frac{p}{\eta_a p_o} = 46.1 \times 10^3 \sin^2 \theta \qquad [11]$$

The operational class includes those factors which reduce the performance of the furnace because of inefficiencies related to the optical losses. These are the reflectivity loss of the mirrors, the shadowing loss, and loss due to the deviation of the concentrator and heliostat from their ideal geometrically correct shapes.

In the derivation of Equations [9] and [10] it was assumed that all of the energy available at the furnace site is received by the mirror and is reflected without loss. This is of course impossible, and the power and heat flux given by Equations [9] and [10], respectively, must be multiplied by a reflectivity factor less than unity which is characteristic of the material from which the reflecting surface is made. If the furnace has several reflecting surfaces (such as the case where a heliostat is used for tracking the sun) or has a combination of lenses and reflecting mirrors, a single coefficient less than unity may be used to take all the refractive or reflective losses into account. This coefficient is designated by $\eta_r$.

The shadowing losses are caused by the target and the supporting structure of the furnace blocking the sun's rays from the concentrator. The effects of these shadowing losses must be subtracted from the total power and heat flux available at the sun image; therefore Equations [9] and [10] become

$$P = \pi \eta_r \eta_s \eta_a p_o f^2 \sin^2 \theta \qquad [12]$$

and

$$p = 46.1 \times 10^3 \eta_r \eta_s \eta_a p_o \sin^2 \theta \qquad [13]$$

where $\eta_s$ is the fraction of the sun's rays which is available for concentration, accounting for losses due to shadowing effects of the target and furnace structure. If the concentrator is composed of mirror segments, consideration must be given to the loss due to the nonreflecting surface between the mirrors. Also the portion of the mirror which is lost due to the shielding of the mounting brackets for the segments has to be taken into account and contributes to the shadowing losses. The effects of these factors are all included in the shadowing loss term $\eta_s$.

The last operational factor involves the inefficiencies that the degree of accuracy of construction of the concentrator surface introduces. In the equations above it was assumed that the parabolic reflecting surface was a geometrically perfect paraboloid. This is of course impossible to obtain, and the performance of any solar furnace will be less than that predicted by Equations [12] and [13]. The geometrical imperfection of a mirror, i.e., unevenness of the mirror surface and its deviation from the correct profile, will reduce the actual concentration of the heat flux at the sun image. The index of geometrical perfection, $\gamma$, of a concentrator may be defined as the quotient of the actual concentration ratio to the theoretical concentration ratio after correction for atmospheric, reflective, and shadowing losses. In designing a solar furnace, the index of geometrical perfection should be known as a function of the angular aperture and the diameter of the concentrator. Therefore, the actual heat flux available at the target, accounting for the various factors which reduce the performance, is

$$p = 46.1 \times 10^3 \eta_r \eta_s \eta_a \gamma p_o \sin^2 \theta \qquad [14]$$

To compare the degree of efficiency of solar furnaces, either in existing or proposed furnaces, or to determine the degree of efficiency needed to obtain a specified heat flux, a single term is useful, the efficiency factor $E$, previously defined in Equations [3] and [4]. This term, which includes the three factors which reduce the performance of a furnace because of inefficiences related to optical losses and the atmospheric transmission factor, is defined as the product of the index of geometrical perfection, the over-all reflectivity efficiency factor, shadowing efficiency factor, and the fraction of the solar constant

FIG. 6 — Variation of heat flux with rim angle for various degrees of efficiency for a parabolic concentrator.

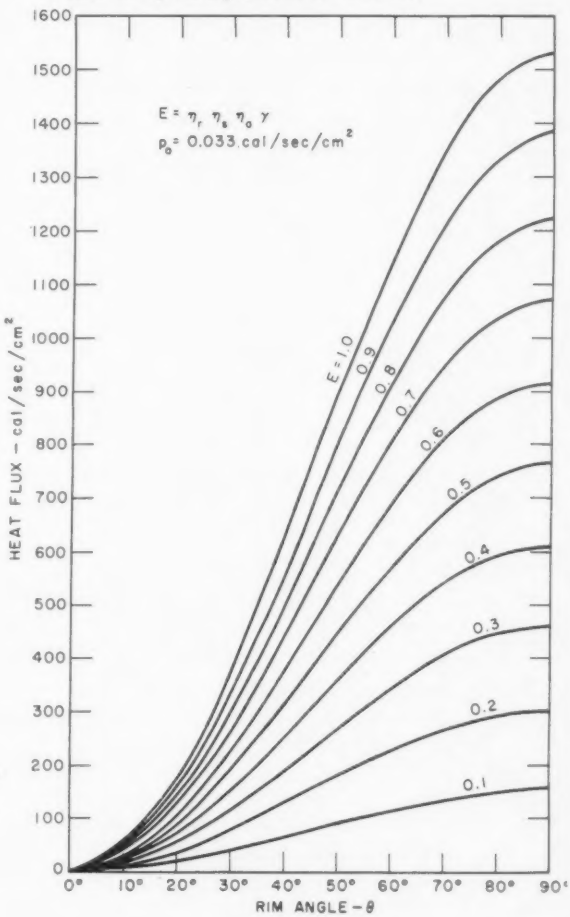

available at the site. Curves showing the variation of heat flux delivered by a parabolic concentrator with the rim angle of the paraboloid for various degrees of efficiency are given in Fig. 6.

**(3) Heat Flux Utilized by the Target**

The heat flux utilized by the target is of interest when knowledge of the theoretical and actual temperatures attainable is desired. Also, when a temperature is specified, the minimum heat flux necessary to obtain the temperature has to be determined in order to design the furnace properly.

To determine the maximum theoretical temperature a target can obtain, the geometry of the target and the absorptivity of the target material must be considered. Relationships were developed by Loh *et al*[1] relating the heat flux received by a body to the maximum theoretical attainable temperature for a cavity-type and a flat-plate type receiver.

In estimating the actual temperature attainable the additional heat losses from the receiver over and above the loss by radiation at the sun image must be evaluated. These include the effect of the emissivity and absorptivity of the sample and the losses from the target by convection and conduction to the surroundings and support structure of the receiver. Therefore, the actual temperature is a function of the total heat input minus the various losses by radiation (in addition to that from the area of the sun image), conduction, and convection. The relations between the various heat losses are complex and depend upon the shape, size, and material of the receiver; they will not be evaluated here.

The actual attainable temperature of the target can be decreased by shielding a portion of the total power received or transmitted by the concentrator. This shielding can be the result of the furnace structure or of a shutter designed to control the heat flux and thus the temperature of the sample.

## DESIGN PROCEDURE

To illustrate the recommended procedure in designing a solar furnace, the various factors which affect the performance characteristics will be considered in order to show the effect they have on the size requirements of a furnace.

**(1) Specifications**

(a) Performance

The solar furnace must be able to attain a thermal flux density of approximately 300 cal/sec/cm$^2$ over an area of uniform irradiance 6 in. in diameter. This flux density would be required when the level of direct radiation at the site is 0.0285 cal/sec/cm$^2$.

(b) General Design

The solar furnace will consist of a fixed parabolic concentrator with a horizontal axis, a heliostat mirror to track the sun, and a target tower.

(c) Parabolic Concentrator Design

The concentrator should be designed to keep the size to a minimum because the dimensions of the concentrator govern the size of the heliostat and other structures. The concentrator should be constructed of curved segments of back-silvered glass which has a minimum reflectivity coefficient of 0.85.

(d) Heliostat Mirror Design

The size and tracking capabilities of the heliostat must be such as to keep the concentrator filled with solar radiation under the following conditions: (1) the heliostat must be able to track the sun during the day over an angle of 120°; (2) the elevation must be sufficient to cover seasonal variations in the sun's elevation of a minimum of 32° and a maximum of 80°; (3) the heliostat must be able to assume angles with the horizontal ranging from 50° to 74°. The heliostat reflecting surface should be constructed of flat, back-silvered glass having a minimum reflectivity coefficient of 0.85.

(e) Miscellaneous

All structures erected between the heliostat and concentrator must offer minimum obstruction to the transmission of the sun's ray. The total allowable shadowing losses, including the loss due to nonreflecting surfaces, must be less than 10 per cent.

**(2) Design**

For the specified heat flux, 300 cal/sec/cm$^2$, the required rim angle $\theta$ of the furnace may be evaluated using Equation [14]:

$$\sin\theta = \left[\frac{p}{46.1 \times 10^3\,(\eta_r')^2\,\eta_s\,\gamma\,\eta_a\,p_o}\right]^{1/2}$$

The individual reflectivity coefficient in this equation is squared to account for the two reflecting surfaces, the concentrator and heliostat. If the values given in the specifications for the reflectivity coefficient, the direct radiation flux density received at the furnace site, and shadowing losses, are substituted in the above equation and a value of 0.60 is used for the index of geometrical perfection, the required rim angle is the angle $\theta$ whose sine is

$$\left[\frac{300}{46.1 \times 10^3\,(0.85)^2\,(0.90)\,(0.60)\,(0.0285)}\right]^{1/2}$$

$$\theta = 50^\circ$$

A value for the index of geometrical perfection of 0.60 was selected because, as determined earlier, it appears to be the highest value which has been achieved for solar furnaces which have been constructed.

For the specified image diameter, 6 in., the required focal length $f$ and the aperture of the concentrator $D$ can be determined from Equations [7] and [8], respectively. The focal length is

$$f = 107.3 \times d$$

$$f = \frac{107.3 \times 6}{12} = 53.7 \text{ ft}$$

From Equation [8], the aperture of the concentrator may be obtained using the value of the rim angle previously determined:

$$D = f \times 4 \tan\frac{\theta}{2}$$

$$D = 53.7 \times 4 \tan 25^\circ = 100 \text{ ft}$$

The surface area of the concentrator is obtained by



VOL. 1 1957

the following formula for the surface area of a parabolic surface:

$$\text{Area} = \frac{\pi}{3f}\left[(4f^2 + \frac{D^2}{4})^{3/2} - 8f^3\right] \qquad [15]$$

This surface area can also be expressed in terms of the projected area of the concentrator as

$$\text{Area} = \beta\,(\frac{\pi D^2}{4}) \qquad [15a]$$

where $\beta$ is a function only of $D/f$ (or $\theta$)

$$\beta = \frac{32}{3\,(D/f)^2}\left\{\left[1 + \frac{(D/f)^2}{16}\right]^{3/2} - 1\right\}$$

or [16]*

$$\beta = \frac{2}{3}\cot^2\frac{\theta}{2}(\sec^3\frac{\theta}{2} - 1)$$

Substituting the value of the diameter $D$ and the correction factor $\beta$, the surface area of the specified concentrator is

$$\text{Area} = (1.052)\,\frac{\pi\,(100)^2}{4} = 8280 \text{ sq ft}$$

The determination of the height and width of the heliostat and the required distance between the concentrator and heliostat are standard trigonometric and geometric problems and only the results will be presented here:

Heliostat dimensions: height = 261 ft, width = 231 ft, and minimum distance between concentrator and heliostat = 360 ft.

A structural design and cost study of a solar furnace system of the size determined in this illustration is presented in Appendix A.

The authors wish to express their appreciation for the invaluable technical advice of Messrs. J. U. Landis, B. W. O. Dickinson, and W. L. Dickey of Bechtel Corporation, San Francisco, and Messrs. D. Mayer and C. Finninger of Consolidated Western Steel Company, Los Angeles, in the structural design and cost estimation phase of this report.

## NOMENCLATURE

- $C$ . . . Concentration ratio, ratio of the heat flux at the sun image of the furnace to the actual flux received by the concentrator from the sun
- $d$ . . . Diameter of the circular image in the focal plane produced by the central portion of the parabolic concentrator. This image is called the "sun image."
- $D$ . . . Diameter of the paraboloid at the edge or length of a side of a flat-plate concentrator
- $E$ . . . Efficiency factor, the product of the index of geometrical perfection, the over-all reflectivity efficiency factor, the shadowing efficiency factor, and fraction of the solar constant available at the site
- $f$ . . . Focal length of the paraboloid
- $L$ . . . Length of a side of a flat-plate mirror
- $N$ . . . Number of mirror segments
- $p$ . . . Heat flux received per unit area within the sun image at the focus
- $p_s$ . . . Actual flux per unit area received at furnace site, $p_s = \eta_s\, p_o$
- $p_o$ . . . Solar constant, measured above the atmosphere, 2 cal/cm$^2$/sec
- $P$ . . . Total power or flux passing through the sun image
- $T$ . . . Absolute temperature
- $\beta$ . . . Ratio of surface area of paraboloid to projected area of the mirror opening
- $\gamma$ . . . Index of geometrical perfection of a parabolic concentrator
  This index is given by the ratio of the actual measured flux within the sun image to the theoretical flux computed on the assumption that the paraboloid is geometrically perfect.
- $\gamma'$ . . . Index of geometrical perfection of a flat-plate concentrator
- $\epsilon$ . . . Emissivity coefficient
- $\eta_s$ . . . Fraction of ideal constant which is available at the furnace site, taking into account losses through the atmosphere
- $\eta_r$ . . . Reflectivity efficiency factor taking into account losses by reflectivity or absorptivity of the optical parts of the furnace
- $\eta'_r$ . . . Reflectivity efficiency factor of individual reflecting surfaces
- $\eta_s$ . . . Reflecting efficiency factor taking into account losses due to shadowing and nonreflecting portions of the optical parts of the furnace
- $\theta$ . . . Angular aperture or rim of angle of a parabolic concentrator
  Angle between the axis and the line joining the focus to the edge of the parabolic concentrator
- $\sigma$ . . . Stefan-Boltzmann constant

* Typical values of $\beta$ are:

| $\theta$ | 0 | 10 | 30 | 50 | 70 | 90 |
|---|---|---|---|---|---|---|
| $\beta$ | 1 | 1.002 | 1.016 | 1.052 | 1.114 | 1.219 |

## REFERENCES

1. E. Loh, P. Duwez, N. K. Hiester, and T. E. Tietz, "Theoretical considerations on performance characteristics of solar furnaces." ASTIA Document No. AD 81521 (AFOSR TN-56-69), Jan. 16, 1956. (Accepted for publication by *Jet Propulsion.*)
2. N. K. Hiester, E. Loh, and T. E. Tietz, "The operation and use of the California Institute of Technology lens-type solar furnace." ASTIA Document No. AD 88368 (AFOSR-TN-56-248), April 24, 1956. (To be published in the *Transactions of the Conference on the Use of Solar Energy — the Scientific Basis.* Tucson, University of Arizona Press, 1957.)
3. P. Duwez and E. Loh, "Phase diagram studies of the zirconia-thoria system and titanium-zirconium-oxygen system." ASTIA Document No. AD 97076 (AFOSR-TN-459), Sept. 4, 1956. (Submitted to the *Journal of the American Ceramic Society* for publication.)
4. E. Loh, N. K. Hiester, and T. E. Tietz, "Heat flux measurements at the sun image of the California Institute of Technology lens-type solar furnace." ASTIA Document No. AD 110383 (AFOSR-TN-56-587), Sept. 14, 1956. (Submitted to the *Journal of Solar Energy Science and Engineering* for publication.)
5. F. Trombe, "Development of large-scale solar furnaces." (In F. Daniels and J. A. Duffie, eds., *Solar Energy Research,* Madison, University of Wisconsin Press, 1955, p. 170.)
6. R. Gardon, "Segmented-mirror solar furnace for high-intensity thermal radiation studies." *Rev. Sci. Inst.* 25: 459, 1954.
7. D. H. Lyons, R. D. Cooper, and E. S. Cotton, "Solar furnace design." Report T-7, Quartermaster Research and Development Center, 1956.
8. M. L. Ghai, "Design of reflector-type direct solar cooker." *J. Sci. Ind. Res.* 12A(4): 168.
9. F. Trombe, "L'utilisation de l'énergie solaire, état actuel et perspectives d'avenir." *J. Recherches* (CNRS) 25: Dec. 1953.
10. A. Guillemonat, "Un essai industriel de captation de l'énergie solaire à Alger." World Power Conference, Rio de Janeiro, tit. 5.

11. *New York Times*, June 29, 1955.
12. T. Hisada, "Construction of solar furnaces." Nagoya, Japan, Government Industrial Research Institute, 1955.
13. J. Farber, "Images of very high temperature sources." High Temperature Symposium, Berkeley, California, June 25, 1956.
14. S. Zerfoss, private communication, 1956.

## Appendix A

## DESIGN AND COST STUDY

To evaluate the various solar furnace systems from an economic viewpoint, a preliminary structural design and cost study was undertaken. The purpose of this study was to determine relative and order-of-magnitude costs for a 100-ft, paraboloidal concentrator with a movable heliostat. The study also included relative cost estimates of various components of the solar furnace. The results for the 100-ft furnace were extrapolated to include furnaces with 50-ft to 200-ft concentrators. The results of this cost study will be compared with another cost study (independently made) for a solar furnace system employing a 120-ft parabolic concentrator.

## COST ESTIMATES FOR 100-FOOT CONCENTRATOR

### (1) Specifications

The specifications used for the design study of a solar furnace consisting of a fixed parabolic concentrator with a heliostat for tracking the sun and a target tower are given below.

(a) Parabolic Concentrator (see Fig. A-1)

Aperture (diameter) = 100 ft
Focal length = 53.7 ft
Ratio of aperture to focal length = 1.86
Surface area of mirror = 8,280 sq ft

The concentrator reflecting surface is to be formed from curved 3 ft x 3 ft back-silvered glass 0.25 in. in thickness. Each segment is to be a section of a paraboloid having the same focal point as the principal mirror. The curved sections are each to be distorted into a paraboloidal form by adjusting screws.

FIG. A-1 — Parabolic concentrator.

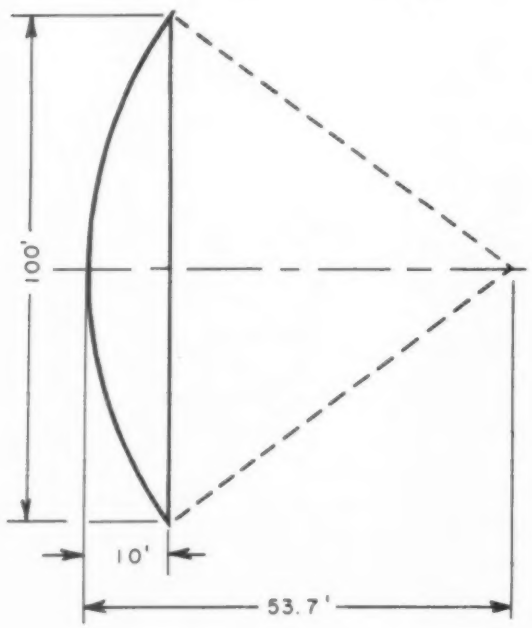


(b) Heliostat for Tracking Sun

Rectangular:
Height = 132 ft
Width = 126 ft
Area = 16,000 sq ft

The heliostat requirements with respect to tracking the sun are: (1) ability to track the sun during the day over an angle of 120° (use of servomechanism for tracking); (2) sufficient elevation to cover seasonal variation in sun's elevation of a minimum of 32° and a maximum of 80°;* (3) ability to assume angles with the horizontal ranging from 50° to 74°.

The heliostat reflecting surface is to be constructed of 3 ft x 3 ft x 0.25 in., flat, back-silvered glass. Provision for adjustment in order to assure that the reflected light is parallel must be included.

(c) Minimum Distance between Concentrator and Heliostat

The minimum distance between the plane of aperture of the parabolic concentrator and the center of the heliostat is to be 180 ft to prevent interference of concentrator with the sun's rays to heliostat when the sun is at its minimum elevation.

(d) Tower at Focus

A tower is to be provided at the focus of the concentrator to provide working area. The height of structure must be such as to position the center of the floor area approximately 5 ft beneath the focal spot. The size of platform is 10 ft wide by 20 ft long; the probable load on platform is 20 tons. An elevator must be provided.

(e) Soil Conditions

The soil conditions were taken as the average type encountered in the Livermore, California area, i.e. moderately hard to stiff clay to a depth of 40 ft, and gravel below 40 ft with good bearing conditions.

### (2) Structural Design Study

To determine relative and order-of-magnitude costs of a parabolic-type solar furnace and its various parts, a preliminary design study was made. The purpose of this design study was to determine the general layout, the size, and the basic type of construction of the various parts. The results of this design study were used to estimate the costs of various parts of the solar furnace.

The general layout of the 100-ft solar furnace showing the necessary clearances and basic size requirements of the elements is given in Fig. A-2. Interesting features shown in this drawing are the shape of the heliostat reflecting surface envelope and the method used for tracking the sun.

The shape of the heliostat reflecting surface is determined by the minimum portion of the specified rectangular shape mirror which would reflect the sun's rays into

* Sun's elevation at approximate latitude of Livermore, California.



VOL. 1 1957

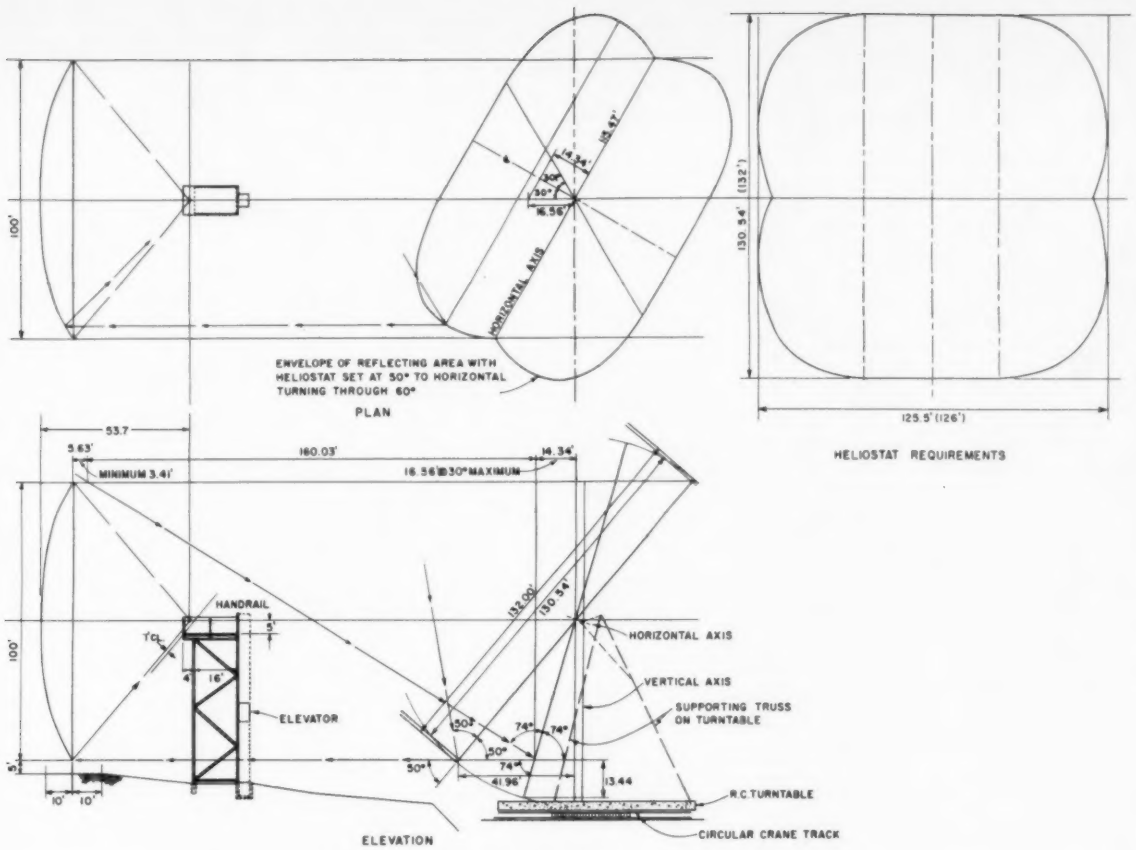


FIG. A-2 — General layout of 100-ft solar furnace.

FIG A-3 — Structural details of concentrator.

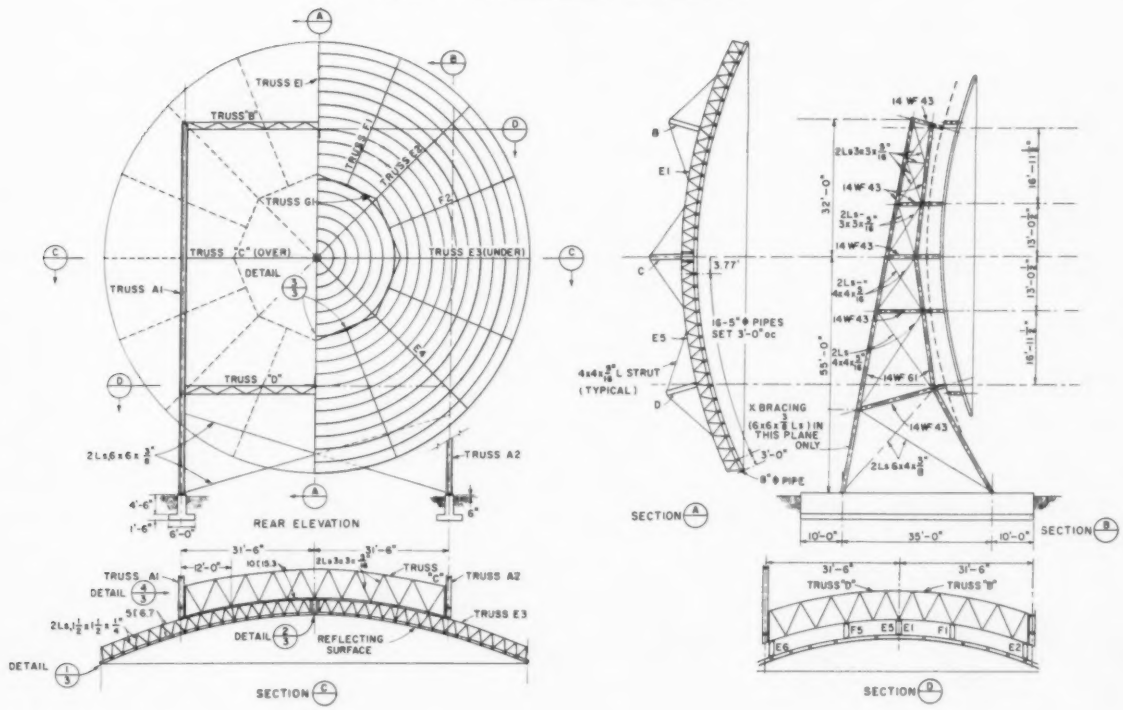

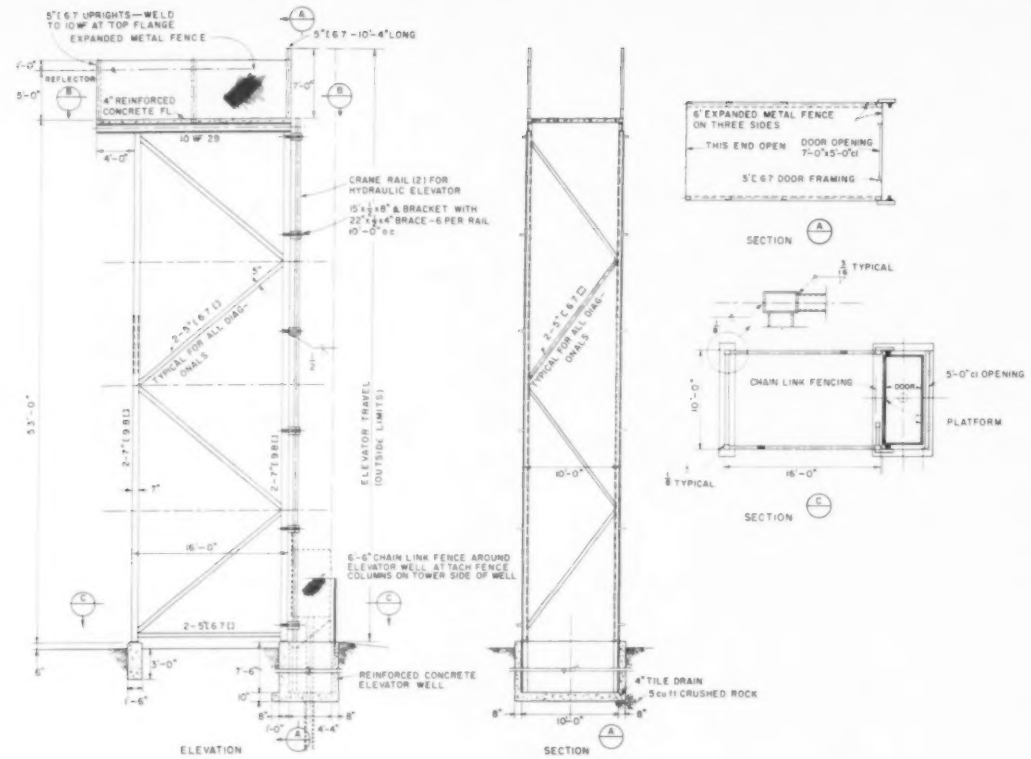


FIG. A-4 — Furnace target tower.

FIG. A-5 — Heliostat.

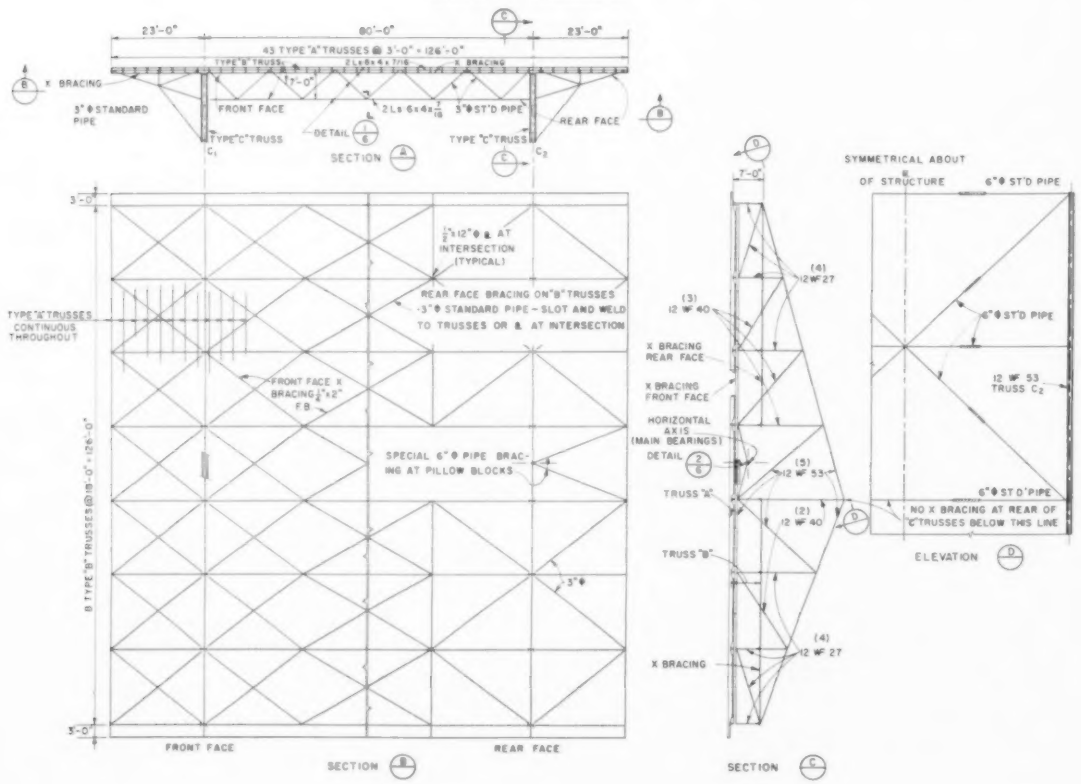




VOL. 1 1957

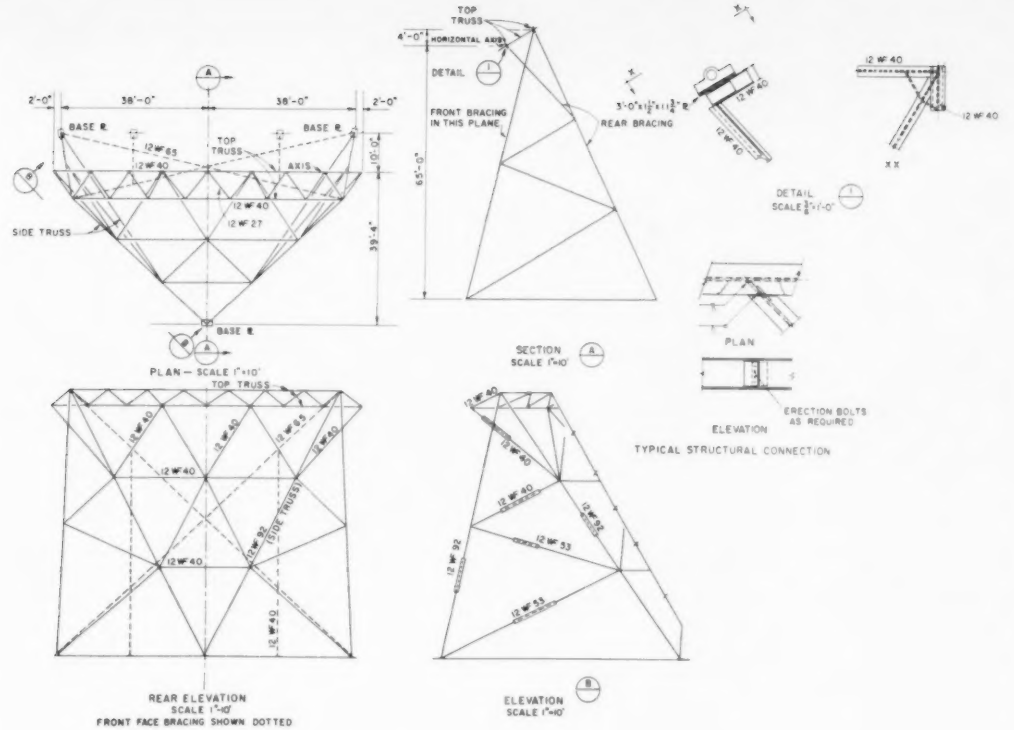


FIG. A-6 — Heliostat tower.

the concentrator. To obtain the desired tracking characteristics the heliostat reflecting surface and support tower is mounted on a turntable allowing rotational motion. The angular motion is obtained by pivoting the heliostat mirror frame at the junction of the frame with the heliostat support tower.

Fig. A-3 shows the general structural details of the concentrator's foundation, tower, and reflecting surface supports. The details of furnace target tower are shown in Fig. A-4. The three main structural parts of the heliostat, the mirror, tower, and turntable and foundation are shown in detail in Fig. A-5 to A-7.

FIG. A-7 — Heliostat turntable and foundation.

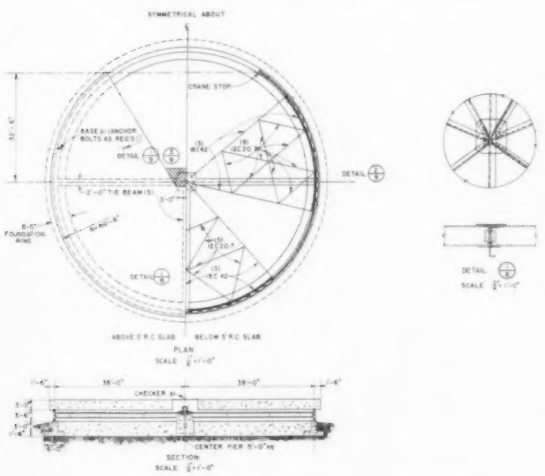


### (3) Cost Study

The cost study consists of an estimation of the total cost of a 100-ft solar furnace and the effect the size of the concentrator has on the relative cost of the major components (concentrator, heliostat, target tower, and equipment). The total cost of the 100-ft solar furnace was obtained by estimating the costs of the various parts. Whenever the cost of equipment or materials could be obtained from the current literature or supplier's quotations, these figures were used. Otherwise, the cost of the part was calculated using estimated cost-per-square-foot or per-weight factors.

The results obtained for the 100-ft furnace were extrapolated to other size furnaces by estimating the effect of size on the three types of elements of the furnace system. The three types of elements are: (1) the reflecting surfaces and their support; (2) the structures and foundations; and (3) the equipment, which includes the turntable, drives, and controls. The total cost for each element was divided into two portions, a constant or fixed cost to indicate a limiting cost for small concentrators, plus a variable cost, which was assumed to be a function of the diameter of the concentrator. For the reflecting surface and supports, the variable cost was assumed to vary as the square of the diameter of the concentrator. For the structure and foundations, the cost was taken to vary as the diameter cubed, and for the equipment to the one-half power. Fig. A-8 shows graphically how these costs vary with the diameter of the concentrator. The costs of the various parts of the 100-ft solar furnace are given in Table A-I.

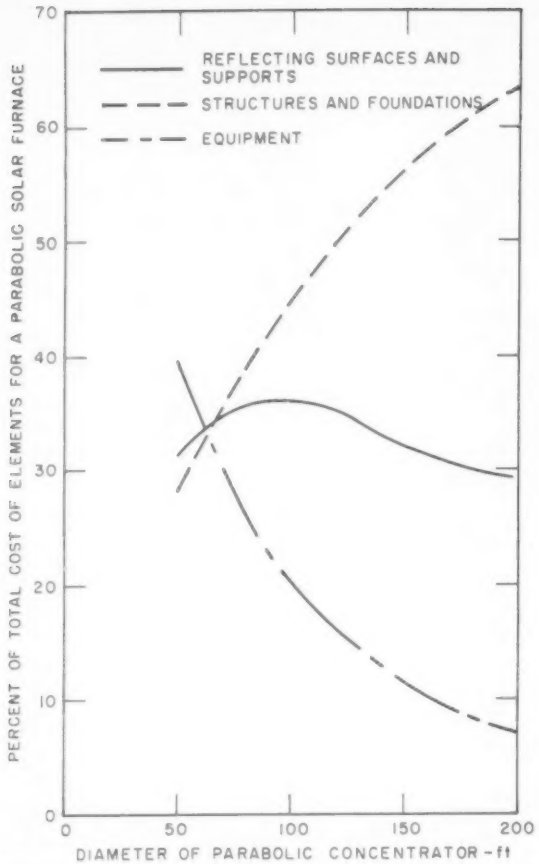


FIG. A-8 — Variation of costs of elements of a parabolic solar furnace with diameter.

TABLE A-I

RELATIVE COSTS OF PARTS OF A SOLAR FURNACE

consisting of a 100-ft fixed parabolic concentrator, focal furnace tower, and a tracking heliostat

| Component | Per cent of total cost of materials and construction | Cost of materials and construction |
|---|---|---|
| *Concentrator* | | |
| Reflecting surfaces and primary supports | 14.5 | $113,800 |
| Structure | 8.0 | 66,800 |
| Foundation | 2.0 | 15,700 |
| Subtotal | 25.0 | $196,300 |
| *Heliostat* | | |
| Reflecting surfaces and primary supports | 20.5 | $160,900 |
| Structure | 26.0 | 204,100 |
| Foundation | 3.5 | 27,500 |
| Subtotal | 50.0 | $392,500 |
| *Equipment* | | |
| Turntable | 15.0 | $117,800 |
| Drives and controls | 5.0 | 39,200 |
| Subtotal | 20.0 | $157,000 |
| *Tower* | | |
| Structure and foundation | 2.0 | $ 15,700 |
| Elevator | 3.0 | 23,500 |
| Subtotal | 5.0 | $ 39,200 |
| Total | 100.0 | $785,000 |

The estimated costs obtained for the 100-ft solar furnace were:

| | |
|---|---|
| Materials and Construction | $785,000 |
| Engineering and Design | 80,000 |
| Adjustment of Reflecting Segments | 8,000 |
| Total Cost | $863,000 |

The total cost is based on the solar furnace alone with no consideration of supporting facilities and appurtenances such as laboratory buildings, housing, storage, grading, site development, etc. Also, no allowance was made for a safety shutter and flux density control shutter.

The variation of the total construction and materials cost for solar furnaces with concentrators from 50 to 200 ft in diameter is shown in Fig. A-9. The relative costs of the major components (concentrator, heliostat, equipment, and target tower) are presented in Fig. A-10 for various size systems.

The engineering and design cost was estimated to vary linearly from approximately $65,000 for the 50-ft furnace to $90,000 for the 200-ft furnace. The cost of adjusting the individual segments of the reflecting surfaces was estimated to vary as the square of the diameter of the furnace from $2,000 to $32,000 for the 50-ft and 200-ft furnaces, respectively.

The above relative cost information, together with a technical study, would be useful in selection of the most suitable solar furnace design on an economic basis.

FIG. A-9 — Variation of cost of a parabolic solar furnace with diameter.

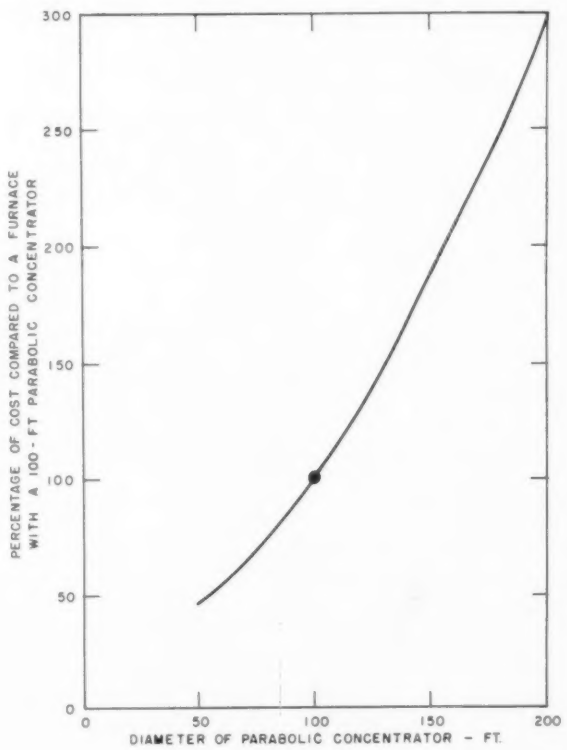


VOL. 1 1957

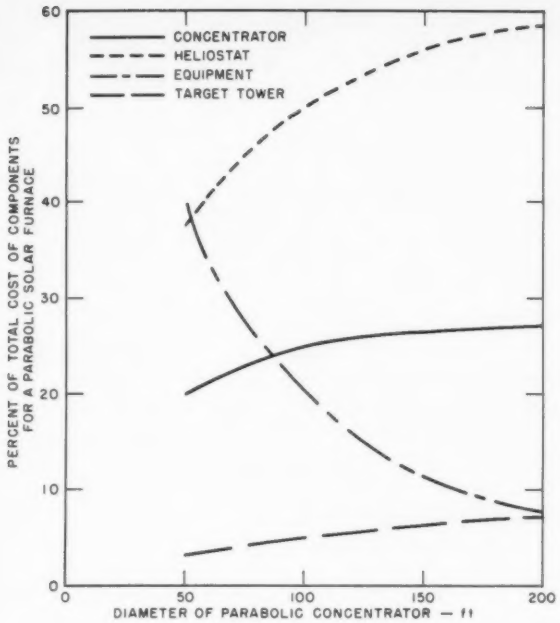


FIG. A-10 — Variation of costs of major components of a parabolic solar furnace with diameter.

## COST ESTIMATE FOR 120-FOOT CONCENTRATOR

An independent cost estimate was made for a solar furnace system consisting of a 120-ft fixed parabolic concentrator, movable heliostat, and a target tower. The results of this cost study are shown in Table A-II together with the results of the cost study presented in this report for the 100-ft solar furnace extrapolated to a 120-ft furnace.

TABLE A-II

COMPARISON OF COST ESTIMATES FOR 120-FT PARABOLIC SOLAR FURNACE

consisting of a fixed parabolic concentrator, movable heliostat, and target tower

| Elements | Estimate A (extrapolated) Per cent of total cost | Estimate B Per cent of total cost |
|---|---|---|
| Concentrator | 25.6 | 36.0 |
| Heliostat | 69.4 | 61.0 |
| Target Tower | 5.0 | 3.0 |
| Total | 100.0 | 100.0 |
| Estimated Total Cost | $1,216,000 | $2,160,000 |
| Cost per sq ft of concentrator surface $/sq ft | 100 | 174 |

As can be seen in Table A-II, the total cost and therefore the cost per square foot of concentrator surface of Estimate B is 74 per cent greater than Estimate A at the 120-ft aperture level. This difference is, in part, due to the variation of design specifications, structural design, and site of the two methods. Therefore, an absolute comparison cannot be made of the results, but the results can be used to indicate the possible limits of costs of a solar furnace system of this size. The relative costs of the elements are in close agreement and therefore an average value of the two methods should give a fairly reliable value.

# FUEL FOR SOLAR FURNACES

By A. RICHARD KASSANDER, JR.

Director, Institute of Atmospheric Physics
University of Arizona, Tucson, Arizona

**A basically nontechnical discussion is presented of the similarities and differences between the solar source of energy for high temperature furnaces and conventional fuels. Certain basic physical considerations of the sun are pointed out, as well as the geometry of the earth-sun relationship. Data are presented showing the seasonal, geographical, and meteorological effects on the daily totals of solar energy incident on a horizontal surface.**

Although the Institute of Atmospheric Physics is not doing any work in the general area of solar furnace research, we are routinely recording the total solar radiation that falls on a horizontal surface and the direct incident solar radiation measured normal to the solar beam. In addition, we have undertaken certain studies using solar radiation as a measurement tool to give fundamental information about the atmosphere and to learn more about the driving forces which influence weather processes. These include infrared spectroscopic measurements, radiometric studies, and investigations of the relative reflectivity of portions of the earth's surface.

Being associated with such studies hardly puts me in the position of being able to bring original and significant information to a group of scientists and engineers engaged in research with solar furnaces. In fact, the work that has been done on the nature of solar radiation that would appropriately be reviewed in a paper on "Fuel for Solar Furnaces" is probably very well known to all of the participants in the conference. On the other hand, it occurs to me that there are many interested persons and friends of science who have not had the opportunity to review this material. It is, therefore, my intention, at the risk of being repetitious to the technical members of the audience, to review the very basic aspects of the source of energy for solar furnaces in the hope of helping these friends to understand better our technology and to appreciate better the vast energy at our disposal.

When we think of fuels for furnaces we generally think of taking certain materials in which nature, over a period of millions of years, has stored potential energy, and chemically or physically combining them in some way so as to release the potential energy in the form of heat. An example of this would be the use of organic fuels such as coal or oil. Here nature has taken vegetable or animal material which potentially has no fuel value and through heat and pressure over long periods of time has distilled them into fixed carbon or combustible hydrocarbons so that by fairly simple techniques we can ignite them and realize the contained heats of combustion. Generally, since the combustion process produces barely enough heat for the purpose at hand, particularly if this is a so-called "high temperature furnace," the material to be melted, vaporized, or smelted is placed in as close contact with the fuel as is chemically or physically possible.

Recently, man has learned to control certain nuclear reactions and has achieved the utilization of the release of large amounts of heat in nuclear reactors. However, due to the violence of the reaction and the undesirable effects of radioactivity, these reactions have been used so far only to produce power through auxiliary transfer agents rather than for the production of high temperature.

Somewhat of the order of four billion years ago nature started such a nuclear reaction in what we call the sun. This reaction is that of the hydrogen bomb with the exception that, rather than being explosive, an equilibrium has been reached so that enormous amounts of energy are being released at a constant rate. Ever since the discovery of the burning glass, man has been using this source of energy to produce high temperatures in a basically simple, although technically complicated, way as he tries to get higher and higher temperatures.

The main difference between conventional fuels and the sun as a fuel for a furnace is that in the latter case our fuel is 93 million miles from the furnace. Nevertheless, appreciable amounts of energy do arrive at the earth's surface and the main purpose of this conference is to discuss the ways it can best be concentrated at the furnace site. Usually the scientist or engineer building a furnace chooses a site noted for clear skies. Since the quality of the radiation doesn't differ much and since he cannot control it anyway, he accepts his fuel as it is delivered and starts from that point. From a fundamental interest point of view, I propose to review what happens to these solar radiations in their trip to the earth and to discuss a little their spatial and temporal variations at the earth's surface.

For the balance of my discussion I shall talk about solar energies in terms of "langleys", one langley being defined as one gram-calorie per square centimeter. However, if you prefer to use more practical units you will be very close to my numbers if you translate one langley per minute to one horsepower per square yard. Studies of

VOL.
1
1957

the spectral distribution of the solar radiation tell us that the sun behaves approximately like a "black body" or perfect radiator whose temperature is about 6000° absolute. This 6000°K surface temperature of the sun means that the sun's surface is radiating about 100,000 langleys per minute. If you considered the 93 million miles that separate the sun and the earth, and the total surface area of the sun, you would find that, according to most recent estimates, about 2.00 langleys per minute reach the outer edge of the earth's atmosphere, measured on a surface perpendicular to the solar beam.

The earth's atmosphere actually plays a very minor role, on the average, in the degradation of the energy. The earth as a whole intercepts about one two-billionth of the total energy output of the sun, by virtue of the geometrical relationships between the earth and the sun. The earth's atmosphere, through various scattering phenomena, absorption, and reflection from clouds, further depletes the solar beam on the average of about 40 per cent depending on the latitude of the furnace location and the state of the atmosphere over the location. Of course, the term "on the average" is a little deceptive since obviously complete cloudiness can shut down the furnace and even relatively diffuse clouds can substantially reduce its efficiency.

In considering the temporal and spatial distribution of solar energy, we are limited by the fact that normal incidence solar radiation measurements are systematically reported by the U.S. Weather Bureau for a very few locations. Moreover, it is the standard Weather Bureau practice to omit any data in which clouds interfered with the observation even in a small way. We are therefore obliged to rely on measurements reported for total incident radiation on a horizontal surface, and although these measurements include an average of around 25 per cent diffuse skylight, this is more than made up for by the reduction of the energy density measurement on a horizontal surface when the sun's rays are oblique to the surface. However, these data, at least, give us some idea of the relative roles of the latitude and transparency effects of the atmosphere at various locations in the United States. Fig. 1 shows a comparison of the normal and horizontal radiation receipts on a clear June day in Tucson.

The accompanying eight figures will give some idea of the distribution of solar fuel over the United States during June and December. Figs. 2 and 6 show the daily total solar energy per unit area on a horizontal surface at the outer limit of the earth's atmosphere at, let us say, 100 miles out, to use a very round number. These receipts, of course, depend only on the latitudes. The most interesting feature of these figures is that the daily total reaching the earth is more than twice as much at the southern border as it is at the northern border in December while in June there is less than three per cent difference. This is a result of the fact that the sun's rays are perpendicular to the earth at 23½° south latitude in December and 23½° north latitude in June, and to the differing lengths of days at the two latitudes in question.

Of further interest is the fact that in June there is a larger daily total of solar energy in the northern United States than the southern United States. This is due to the fact that although noon solar radiation decreases systematically to the north in June there are about two more daylight hours at the northernmost points than there are in the southernmost points of the United States. The reverse is true in December, so that the southward increase in hourly values is further increased in daily total values since the day is about two hours longer at the southern boundary.

Figs. 3 and 7 show the daily total radiation on a horizontal surface for the 15th of June and 15th of December using the average of cloudless days. Comparison of these curves with those of Figs. 2 and 6 show the fraction of the solar beam that is absorbed by the atmosphere and its water vapor and scattered by dust, haze, etc.

The most noteworthy feature of these latter two figures is the change in the June pattern at the surface from the pattern outside the atmosphere. This is due to the fact that when upper level moisture content is relatively high,

FIG. 1 — Comparison of records of direct solar radiation and total solar radiation on a horizontal surface.

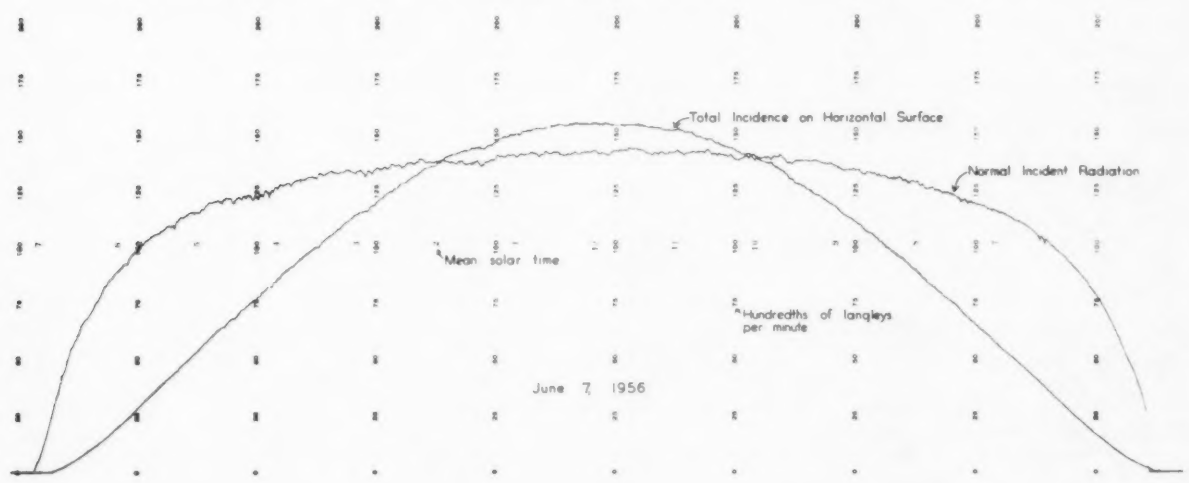

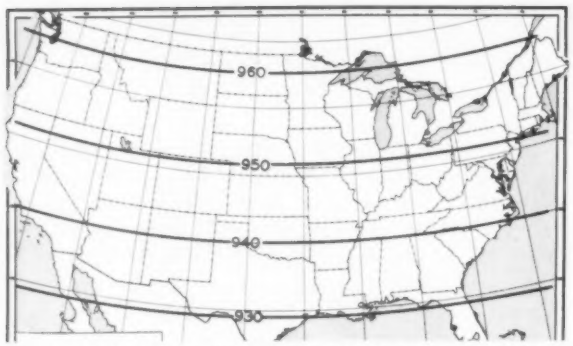


FIG. 2 — Daily total radiation (in langleys) on a horizontal surface outside the earth's atmosphere for June. (After List.)

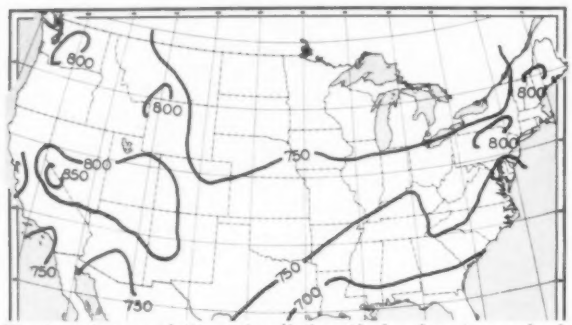


FIG. 3 — Average daily total radiation (in langleys ) on a horizontal surface of the earth for a cloudless June 15. (After Fritz.)

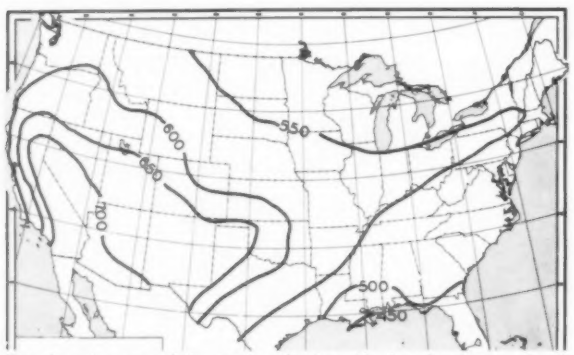


FIG. 4 — Average daily total radiation (in langleys) on a horizontal surface of the earth for June. (After Fritz.)

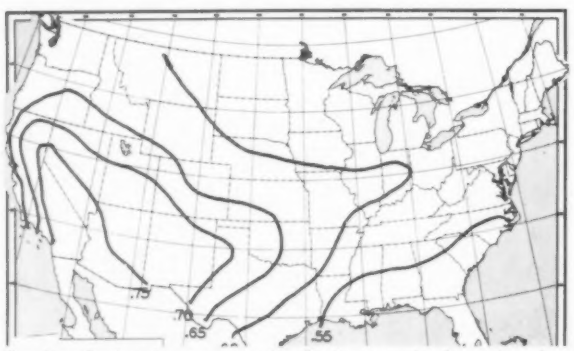


FIG. 5 — Ratio of average total radiation on a horizontal surface of the earth to that received outside the atmosphere for June.

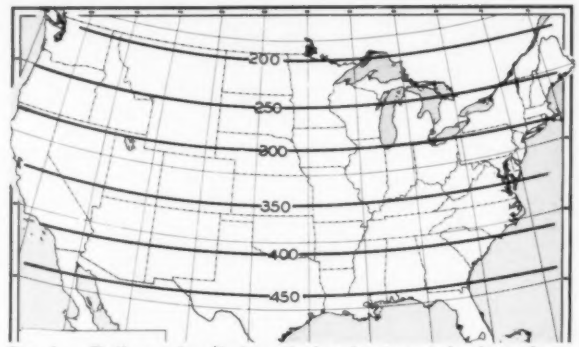


FIG. 6 — Daily total radiation (in langleys) on a horizontal surface outside the earth's atmosphere for December. (After List.)

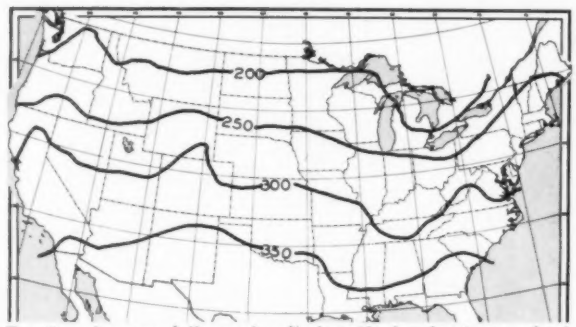


FIG. 7 — Average daily total radiation (in langleys) on a horizontal surface of the earth for a cloudless December 15. (After Fritz.)

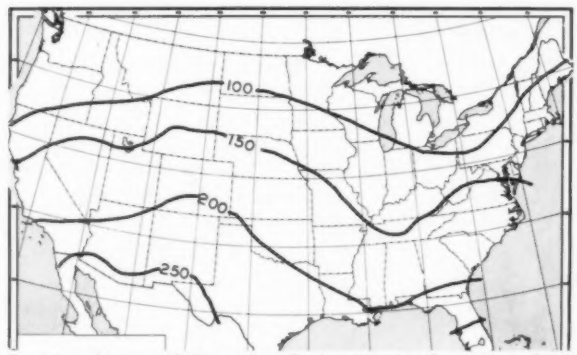


FIG. 8 — Average daily total radiation (in langleys) on a horizontal surface of the earth for December. (After Fritz.)

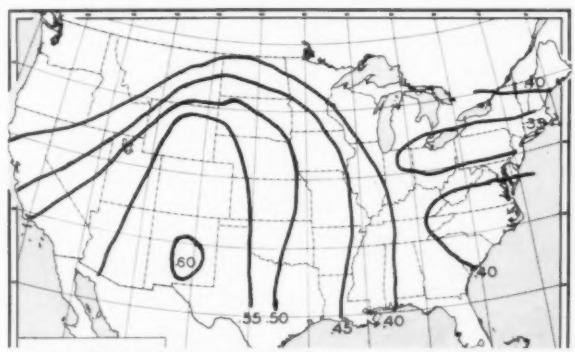


FIG. 9 — Ratio of average total radiation on a horizontal surface of the earth to that received outside the atmosphere for December.

VOL.
1
1957

as it is in June, small changes do not as greatly affect the amount of water vapor absorption, so that the maximum radiation receipts are at the higher land elevations where there is a smaller thickness of the atmospheric absorbing layer.

Figs. 4 and 8 show the June and December averages of daily total radiation on a horizontal surface for all types of days. Here we note particularly that there are relatively low values in the Great Lakes region in both winter and summer due to a combination of relatively high cloudiness and important cloudless-day losses. In the Southwest we find maximum values due to a combination of relatively sparse cloud cover and slight clear-air depletions.

Figs. 5 and 9 essentially summarize these other figures. They were obtained by combining Figs. 2 and 4 and Figs. 6 and 8 to find the fraction of the solar energy received outside the atmosphere that actually reaches the surface during June and December. In June, we see that about 45 per cent of the total solar fuel is depleted before reaching the surface of the earth in the southeastern United States, whereas about 25 per cent is depleted in the southwestern portion, the balance of the country having an average depletion perhaps halfway between these values. In December, on the other hand, losses seem to be roughly radially distributed around central New Mexico, which receives 60 per cent of the energy incident on the outer atmosphere, the rest of the country's receipts falling off fairly systematically to around 35 per cent in the northeastern and northwestern corners.

In conclusion, it should be pointed out again that absolute reliance should not be placed on these data. They have all been expressed in terms of daily totals of radiation on a horizontal surface. The scientist using a solar furnace is frequently interested in a relatively few hours of maximum intensity of radiation normal to the solar beam. Unfortunately, systematic measurements of the latter type are not available. Nevertheless, the data presented do give an indication of the relative abundance of solar fuels at various locations in the United States for the extremes of the operating seasons.

## BIBLIOGRAPHY


R. J. List, ed., *Smithsonian Meteorological Tables,* 6th ed. Washington, Smithsonian Institution.

S. Fritz, "Solar radiation during cloudless days." *Heating and Ventilating* 46: 69-74, Jan. 1949.

S. Fritz and T. H. MacDonald, "Average solar radiation in the United States." *Heating and Ventilating* 46: 61-64, July 1949.


OL.
1
957

# A SOLAR FURNACE FOR RESEARCH IN NONFERROUS METALLURGY

By W. M. TUDDENHAM

Research Center, Kennecott Copper Corporation, Salt Lake City, Utah

**Pyrometallurgical and physical metallurgical research often require high temperatures, controlled atmospheres, and freedom from contamination. To obtain such conditions at the Kennecott Research Center, a high temperature solar furnace was constructed using the 60-in. rhodium-plated mirror from an Army surplus searchlight. For maximum flexibility in sample handling, a modified heliostat-type mounting with two auxiliary mirrors was used. A traversing mechanism for zone refining experiments and a totally enclosed sample chamber have been provided. The installation and its characteristics as well as some of its projected uses are described.**

The general subject of solar energy furnaces has been well reviewed;[1,2,3] therefore, this paper is limited to a discussion of the unit at the Kennecott Research Center. It does seem worthwhile, however, to reiterate some of the features of a solar furnace that inspired a copper company to construct one as a research tool.

The principal objectives of the Kennecott Research Center are:

(1) to develop techniques for increasing the recovery of copper and other minerals from Kennecott's operating properties,

(2) to improve methods of recovering valuable by-products,

(3) to assist the company's Exploration Department by evaluating new sources of metals,

(4) to find better and less costly methods of extracting metals from ore,

(5) to improve the quality of refined copper.

In all of these phases of activity, pyrometallurgical techniques play an important role. The effects of various furnace atmospheres on smelting procedures and results are of particular interest to the pyrometallurgist. Specialized techniques such as vacuum fusion and zone refining are becoming increasingly more important in research and in the production of high purity metals. Molybdenum, rhenium, and niobium are examples of important metals that require special purification and fabrication techniques because of their high melting temperatures and

FIG. 1 — Diagram of solar furnace installation.

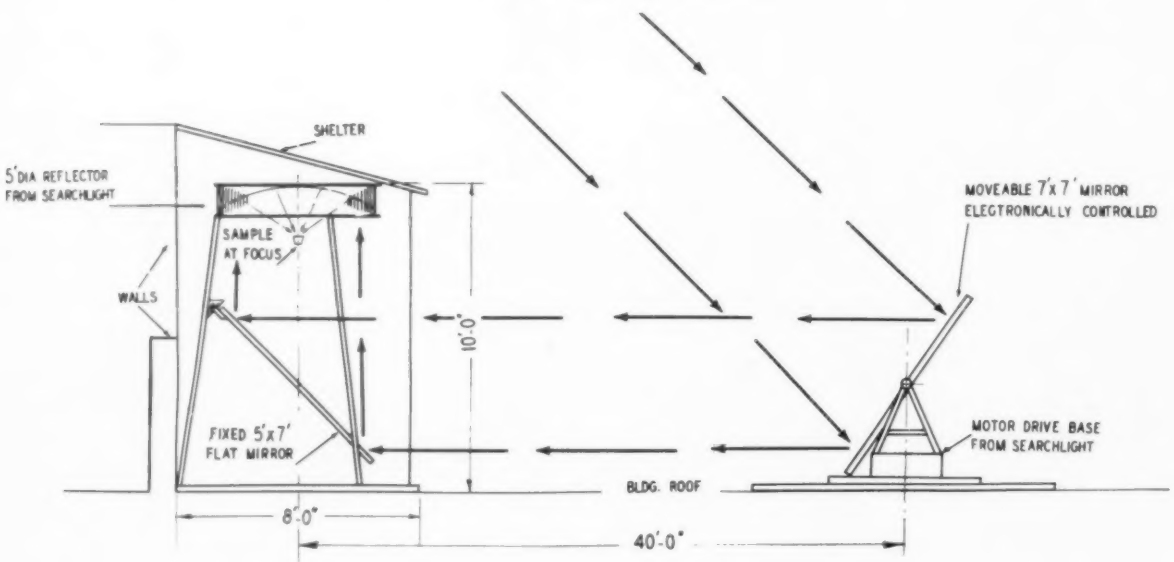


VOL. 1 1957

affinity for gases such as oxygen and nitrogen.

It was felt that a solar furnace, being a high intensity source of pure heat under controlled conditions of pressure and furnace atmosphere, would be valuable for research not only in the fields mentioned above but also in other projects. The additional feature of being able to fuse samples in such a way as to avoid contamination from the container was also of interest. One of the most appealing features of the solar furnace as a research tool was its apparent adaptability to problems of many different types. Experience, thus far, has shown this adaptability to be a most valuable feature.

The idea of building a solar furnace at the Kennecott Research Center was conceived in the spring of 1955. Upon investigation, it was found that a 60-in. war surplus searchlight was available from a local salvage yard at scrap price, and plans were made to utilize this searchlight as the nucleus for a solar furnace unit. Consideration of the type of problem that was expected, coupled with discussions with others in the field, led to the conclusion that a modified heliostat mounting should be used. This type mounting was decided upon because it offered maximum flexibility and convenience in sample handling even though it was recognized that the maximum temperatures to be expected would be lowered because of increased aberration and reflection losses. Research Center personnel designed and constructed the unit. The cost of the unit exclusive of research time has been approximately $3400, including $1400 for materials and $2000 for labor.

Fig. 1 is a diagram of the furnace installation. The sun's rays are reflected from the 7 ft by 7 ft heliostat to a fixed 5 ft by 7 ft flat mirror and thence to the horizontally mounted 5-ft diameter parabolic reflector. As far as possible, those portions of the original searchlight that were adaptable were used. Since the unit was installed in the roof, relatively lightweight construction was necessary. The partially dismantled searchlight base was used to hold the heliostat. Fig. 2 is a photograph of the completed installation.

FIG. 2 — Kennecott solar furnace installation.

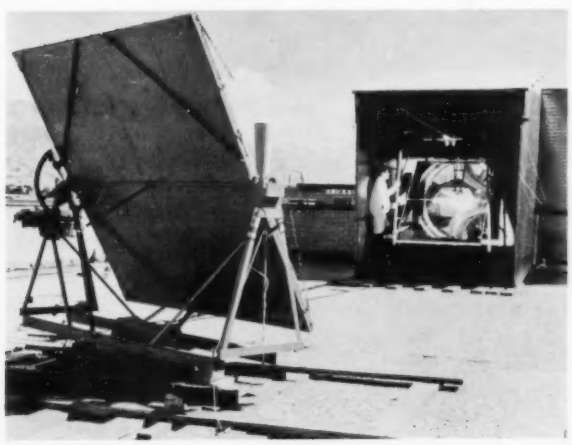

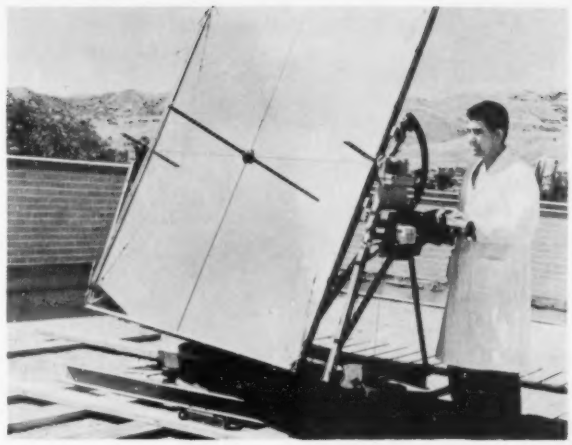

FIG. 3 — Front view of heliostat.

## FURNACE CHARACTERISTICS

### Parabolic Mirror

It was possible to obtain a new parabolic mirror that had never before been in service. The mirror is front-surfaced and is constructed of copper with a rhodium plating. The characteristics of this type of searchlight reflector as summarized by Conn[3] are presented in Table I.

TABLE I
CHARACTERISTICS OF PARABOLIC REFLECTOR FROM A 60-IN. SEARCHLIGHT

| | |
|---|---|
| Aperture | 60 in. |
| Focal length | 25¾ in. |
| Focal length/aperture | 0.43 |
| Effective conc. surface | 19.6 ft sq |
| Theoretical image diameter | 0.24 in. |

Benveniste and Hiester[2] have reviewed the dimensions listed in Table I and their meanings in terms of solar furnace efficiency. It is worthy of mention that these searchlight reflectors are, generally speaking, quite satisfactory for small solar furnace applications.

### Auxiliary Mirrors

As shown in Figs. 1 and 2, the furnace has two auxiliary reflectors. These reflectors are commercial plate glass mirrors with electrolytic copper backing. The frames are constructed of welded 1-in. angle iron with ¾-in. plywood backing. Two 3½ ft by 5 ft mirrors are used for the fixed reflector and four 3½ ft by 3½ ft mirrors are used for the heliostat.

Fig. 3 is a photograph of the heliostat installation. As is seen in the photograph, wires and turnbuckles are used for mirror alignment. This arrangement has not been entirely satisfactory, and a modified mounting is under consideration which would not only be more rigid but would allow individual alignment of the mirrors. Following the suggestion of Trombe,[5] we plan to decrease the size of the individual mirror elements to 20 in. square.

The searchlight base was modified as is seen in Figs. 2 and 3 and used as a mount for the heliostat. The original drive motors were replaced with reversible, fractional horsepower Barcol PYAZ motors geared down to approximately 1 rpm. A further reduction of 150 to 1 was

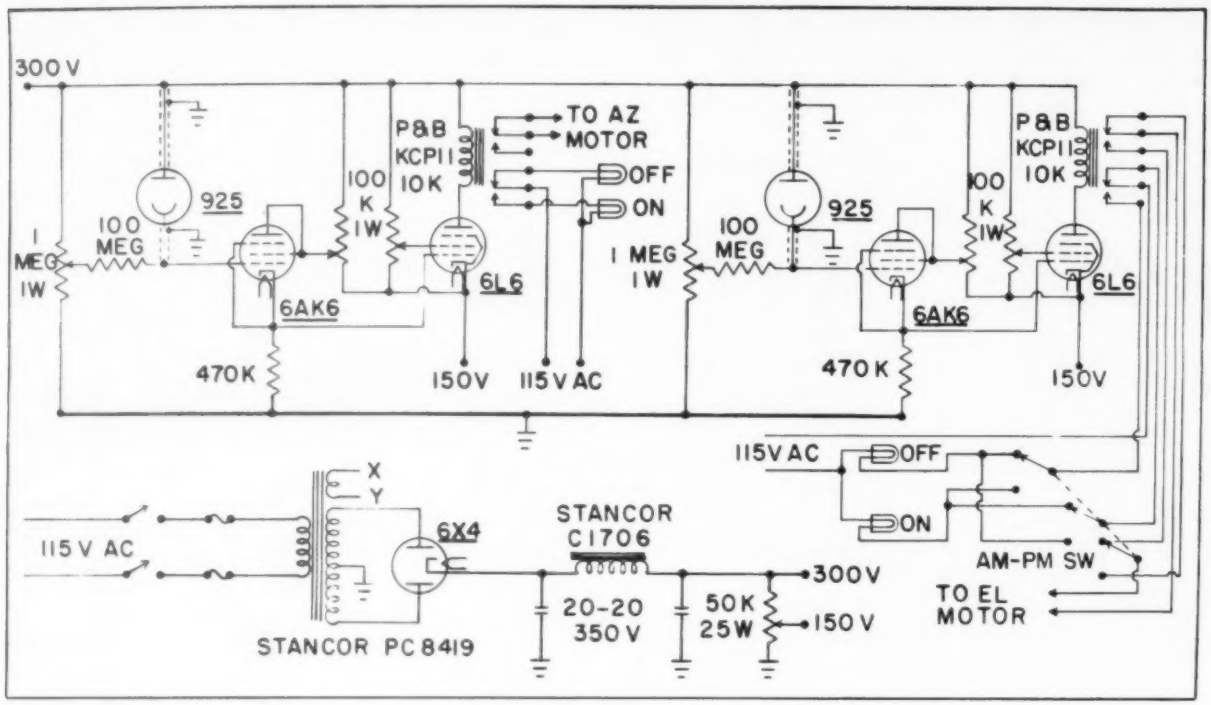


FIG. 4 — Phototube control for solar furnace.

FIG. 5 — Furnace temperature control unit.

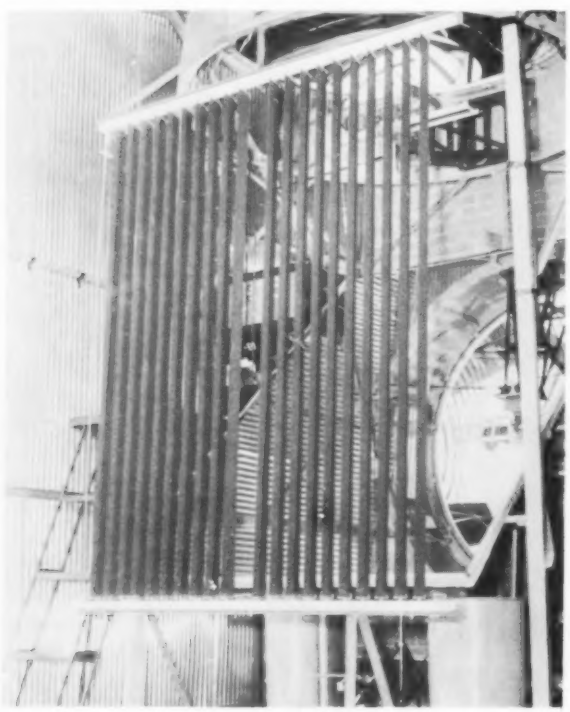

accomplished through the gear drives in the searchlight base. Backlash in the gears is taken up by applying a constant pull through a system of weights and pulleys.

The heliostat motors are controlled by plate relays which are actuated by photocells through the circuit shown in Fig. 4. This is a modification of a circuit described by Radio Corporation of America.[4] Two photocells are used, one to control the elevation and one to control the azimuth drive of the heliostat. These photocells are placed in collimating tubes mounted vertically at the periphery of the parabolic mirror. The circuit is so arranged that the azimuth motor drives until sunlight strikes the azimuth control photocell. In the morning, the elevation drive works in a similar manner. During the afternoon, however, the action is reversed and the motor drives until the sunlight no longer strikes the elevation control photocell. The small shift in the position of the focal spot in changing from morning operation to afternoon operation is easily compensated for by moving the sample mount slightly. The correction error for this control unit is of the order of plus or minus one minute of arc. A manual circuit not shown in Fig. 4 is used for initial positioning of the heliostat.

### Temperature Control and Measurement

Fig. 5 is a photograph showing the temperature control unit for the furnace. It consists of a so-called vertical blind and was obtained from a local venetian blind company for about $40. At the present time the blind is controlled



VOL. 1 1957

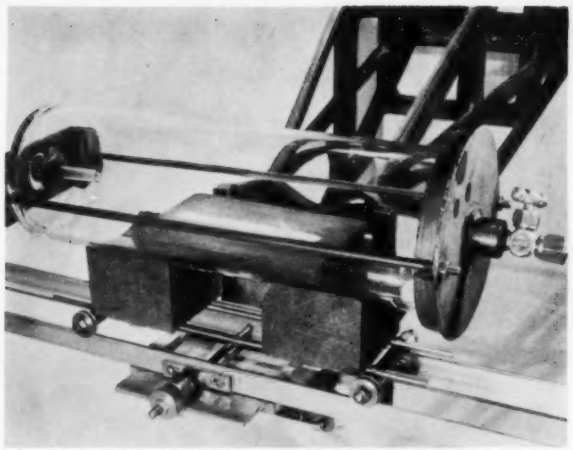

FIG. 6 — Sample chamber and mounting.

manually, but it could easily be adapted to automatic control. The center and side of the unit were left open in order to assure continued operation of the photocells. This arrangement also functions as a focusing aid when the blind is closed.

Furnace temperatures have been measured by fusing materials of known melting point. Magnesium oxide which has a melting point over 3000°K has been melted in this furnace.

### Sample Handling

Although much solar furnace work is successfully done under oxidizing conditions, this is not possible when working with metals. It was, therefore, necessary to devise a sample chamber capable of furnishing either protective atmospheres or high vacuum. In order to study zone refining techniques, it was further necessary to provide a means of passing samples through the focus. Fig. 6 is a photograph of the sample chamber and mounting. The 4-in. diameter pyrex cylinder is set upon carbon blocks and a machined carbon block is used to support the sample inside the chamber.

The original searchlight arc mount was modified to hold the chamber and allow its movement along three axes. For zone refining studies, the frame holding the sample chamber is pulled along the rails at the desired rate so that successive portions of a rod of the material being studied are passed through the focus.

### Results with the Solar Furnace

The final installation and testing of the Kennecott solar furnace was finished late in the summer of 1956; consequently, no completed projects can be reported. In order to test the amenability of the furnace to the types of research mentioned earlier, several preliminary experiments have been completed. It has been found that the furnace is capable of fusing a niobium sample, MP 2770°K, under vacuum in the chamber shown in Fig. 6. It was not possible, however, to melt rhenium, MP 3420°K. A sufficient number of zone melting experiments have been conducted on samples of fire-refined copper and on alumina to indicate that the solar furnace with its ancillary equipment is adaptable to this technique.

### Proposed Modifications

The furnace has proved itself to the extent that it is felt worthwhile to proceed with such modifications as will further improve its performance and versatility.

It was observed soon after putting the furnace into operation that the heliostat was causing a considerable amount of aberration because of misalignment of the individual mirrors. It has also been observed that a more rigid frame for supporting the heliostat is desirable so as to minimize the effect of wind. Plans are underway to correct at least partially these difficulties. Methods of measurement and control of flux and temperature are also under consideration.

In addition to Kennecott's research, interest in using the unit has been expressed by the University of Utah, and it is anticipated that the furnace will have a full schedule for many sunny days to come.

The author wishes to thank Mr. S. R. Zimmerley, Director of Research, who conceived the idea of constructing the Kennecott solar furnace, for the opportunity of undertaking this project. He also wishes to express appreciation to Mr. C. D. Michaelson, General Manager, Western Mining Divisions, Kennecott Copper Corporation, for his encouragement of the project and to the Kennecott Copper Corporation for permission to publish this paper.

## REFERENCES

1. G. Benveniste, "Solar energy furnaces." Menlo Park, Stanford Research Institute, 1955.
2. G. Benveniste and N. K. Hiester. *Mech. Eng.* 78:915, 1956.
3. W. M. Conn, *J. Franklin Inst.* 257: 1-12, 1954.
4. RCA Manufacturing Co., Inc., "Phototubes." 1940.
5. F. Trombe. (In *Proceedings of the World Symposium on Ap-Applied Solar Energy, Phoenix, Arizona, 1955,* p. 63.)

# INDUSTRIAL CONSIDERATIONS OF SOLAR FURNACES

By FRANK E. EDLIN

Engineering Department, E. I. duPont de Nemours & Co.
Wilmington, Delaware

**A solar furnace for research is compared to other furnaces above 3000°K with oxidizing or reducing environment. Lower quality reflective furnaces and heat traps are discussed for possible power generation. Plastics are considered as a material of construction for reflectors and heat traps.**

Various means are now available and others are being developed to concentrate and utilize solar energy. Typical of proposed applications at relatively low temperatures are water distillation, space heating and refrigeration, and solar engines; and these applications are being studied intensively. Solar furnaces provide a concentration of energy to produce very high temperatures, capable of melting most, if not all, known materials. Also, because of their many other advantages, such furnaces are receiving attention for research and for prospective commercialization. This paper presents some considerations for the industrial use of solar furnaces.

Let us review first what the advantages are, and compare the performance of solar furnaces with that of other high temperature furnaces. We shall discuss, from an industrial point of view, the relative value of solar furnaces in competition with more conventional equipment in high temperature chemical processing and for generation of power.

## POTENTIAL ADVANTAGES OF SOLAR FURNACES

The potential advantages of solar furnaces over conventional high temperature furnaces for high temperature research investigations have been discussed by many authors. These advantages apply, also, to industrial applications, but for industrial applications the final choice of a furnace is usually dictated by economic considerations.

Briefly, the potential advantages of the solar furnace include:

(1) prospect for reaching useful operating temperatures not yet realized with conventional furnaces;

(2) means for attaining high temperatures without restrictions heretofore imposed by available materials of construction;

(3) ability to effect rapid, controlled temperature changes in heating and quenching cycles, without limitations imposed by the heat capacity of furnace components;

(4) elimination of contamination, either by vapors from the furnace materials or by attack of the reaction mass on its container;

(5) operation in any desired atmosphere and over a wide pressure range;

(6) elimination of an electromagnetic field;

(7) high flexibility for research studies.

The maximum temperatures reported attained in seven solar furnaces are shown in Table I.

TABLE I
MAXIMUM REPORTED SOLAR FURNACE TEMPERATURES

| Furnace Location | Diameter ft. | Rim Angle ° | Temperature °K |
|---|---|---|---|
| Montlouis, Fr. | 35 | 41 | 3270 |
| Algiers | 27.6 | 36.5 | 3270 |
| Japan | 6.5 | 75 | 2370 |
| Fordham | 5 | 60 | 3610 |
| Convair | 10 | .... | 3290 |
| Ariz. St. Col. | 5 | .... | 3300 |
| Cal. Tech. | Refract. | .... | 3300 |

These temperatures are substantially lower than the maximum theoretically obtainable with geometrically perfect reflectors, and correspond to an apparent optical precision representing a comparatively poor value. Substantially better optical systems can be built at acceptable costs for research, if this proves to be the principal limitation.

There are three efforts to be made in the development of the solar furnace. The first of these would be to produce a research furnace. Although present temperatures will make possible a substantial amount of industrial research, the great advantage of the solar research furnace will be found in the achievement of higher temperatures. The second effort would anticipate commercial application, and would evaluate largeness, operation, and costs. As a process tool, it will extend the research furnace planned particularly for a specific application. A third effort should promote the evaluation and development of systems for the production of power.

A design study of the structural and component require-

VOL. 1 1957

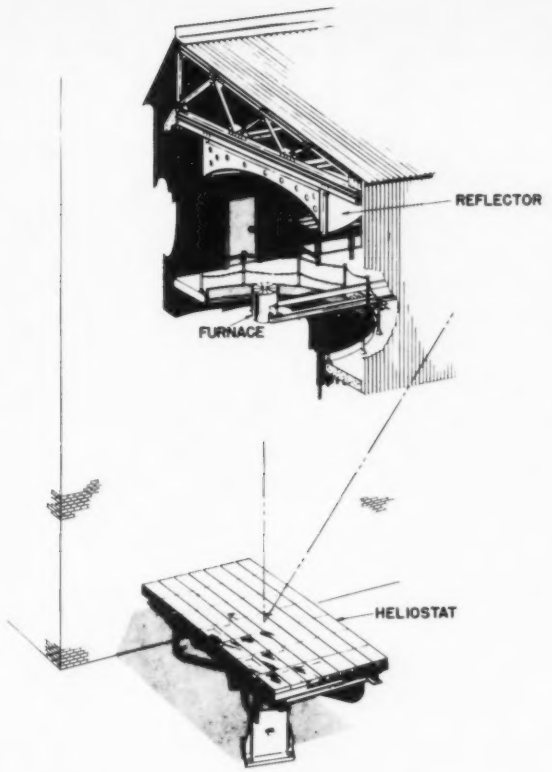


FIG. 1 — A solar research furnace designed for highest temperatures.

ments for a solar furnace capable of attaining temperatures considerably higher than those reported in Table I leads to a concept of the general arrangement of this furnace as shown in Fig. 1.

The reflector would have a minimum diameter of 100 in., to provide sufficient power for melting metallurgical test coupons and for operation of skull-type cavity furnaces. It would be rigidly mounted horizontally in a down-facing position, to minimize the problem of distribution of shell stresses, and also to permit vertical furnace construction. The reflector and mounting can be maintained at constant temperature by a circulating fluid, and by enclosing for weather and wind protection. The reflector is visualized to be one of one-piece construction, preferably of silvered metal or glass. It must be mounted about 50 ft above the heliostat to avoid noon shadow in summer.

The heliostat reflecting surface would consist of optically flat glass mirrors, approximately two feet square, individually supported in the frame for alignment and adjustment. It is of utmost importance that the heliostat frame and support be rigid, in order to maintain parallel reflection at the various tilt angles. The heliostat must maintain undistorted reflection of the sun's rays even though its deflection due to its weight will vary as its angle of tilt is changed. The slightest misalignment will result in a small but significant reduction in the apparent reflector quality.

This is typical of the many engineering and construction problems awaiting solution before a satisfactory design can be made for a large scale, high quality, high temperature furnace.

## CONVENTIONAL HIGH TEMPERATURE FURNACES

After the engineering problems have been solved, and it is demonstrated that a large, high temperature solar furnace can be designed, industrial application will still be a matter of economics. Solar furnaces for industrial uses will become a reality only if the economics are favorable when compared with other competitive means for accomplishing the ends sought. Let us review the performance of conventional high temperature furnaces, before discussing the industrial potential of the solar furnace. Fig. 2 shows a comparison of the temperatures obtainable.

Present and prospective limits for solar furnaces are indicated. The shaded zone at the upper limits for electric furnaces represents temperatures attainable only in selected applications. Such limits may be imposed, for example, by permissible contamination levels.

Prospects for attaining higher temperatures with electric resistance furnaces of graphite construction are limited by the vapor pressure of carbon and thermionic discharge from the heating element. By modification of these furnaces, the usual reducing atmosphere can be excluded from the reaction zone by the use of refractory liners, and inert or even oxidizing atmospheres can be maintained.

Resistance furnaces made entirely of refractory oxides, for use with inert or oxidizing atmospheres, are limited to temperatures lower than those attainable with graphite construction by the physical properties of the available refractory materials.

Arc furnaces are widely used for the melting of electrically conductive materials. The consumable electrode arc furnace produces a melt by an arc being established between the electrode and a bed of the same material as the electrode, contained in a cooled crucible. A skull of frozen melt is formed and maintained at the cooled wall.

FIG. 2 — Comparison of electric and solar furnaces.

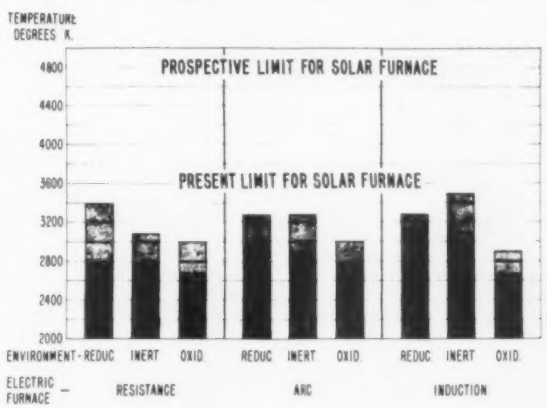

Ingots of considerable size and exceptional purity are produced in this manner.

The nonconsumable electrode arc furnace is limited in application by the very few refractory materials suitable for use as electrodes. These materials must be electrically conductive, and presence of minor amounts as a contaminant in the melt must be tolerable.

Indirect arc furnaces, wherein the arc is maintained to a crucible of refractory material containing the melt, are also limited in application to the use of electrically conductive refractories, and the melt is likewise subject to environmental contamination.

High frequency induction or dielectric heated electric furnaces are the usual choice for research investigations, because of the cleanliness and simplicity of operation. Limitations of materials of construction restrict applications, generally, to the temperature range of the other electric furnaces.

## INDUSTRIAL POTENTIAL FOR SOLAR FURNACES

The principal industrial applications for solar furnaces may well result from the high temperatures under the conditions which they alone can provide. If large expenditures are to be made for research furnaces, these furnaces should be designed to exploit the higher temperature potential.

Solar furnaces are likely to be used in some commercial applications for the processing of materials. Processing costs, at a favorable site, are expected to be nominal — perhaps a few cents per pound of product. The amortization cost must be added to this. An amortization charge of 10 cents per pound of product would amortize an investment of $150 to $200 per sq ft of reflector surface. Where the advantages of the solar furnace are required for manufacturing, such high unit costs of utilizing solar energy are not prohibitive.

The most serious limitation to the use of solar furnaces for chemical processing is the intermittent operation. Continuous processing is often desirable and most economical; but with the solar furnace, operation is intermittent, and cycles are unpredictable. Obviously, this factor must be carefully considered by management in comparing the economics of solar furnaces with other furnaces.

For industrial power applications, the solar plant must be economically competitive, as the cost of power is the only justification for selection. The economics of solar furnaces for industrial power are quite different from those for manufacturing. Based on the equivalent fuel value of the energy delivered, a reflector cost, including auxiliaries, of at the most from one to two dollars per square foot seems to be justified. For this use, facilities in this cost range appear to be a possibility.

Fortunately, extremely high temperatures, and thus high quality collectors, are not required for routine power applications. We have cast experimental paraboloidal reflectors, 3 ft in diameter, of reinforced plastic. We have been unable, as yet, to duplicate the high surface quality of the glass mold, but if it should appear that there is justification, we feel that this difficulty could be overcome. We expect that this type of reflector might be produced on a substantial scale at a cost of from one to two dollars per square foot, or even less. The development of a low-cost, small engine would stimulate the development of such reflectors.

## SUMMARY

To summarize, solar furnaces are now useful in research investigations because of their unique advantages. Prospective solar furnaces, operating at temperatures substantially higher than are attainable today, will undoubtedly provide a powerful tool for both research studies and for manufacturing, and are of greater interest to industry than are much larger furnaces of present quality.

The industrial application of solar furnaces appears promising now and certain for the future, when other fuels become more costly. Continued invention and development can lead to the successful application of solar energy to the economic production of power.

VOL.
1
1957

# DESIGNING SOLAR FURNACES FOR SPECIFIC PERFORMANCE

By RAYMOND BLISS

Institute of Atmospheric Physics
University of Arizona, Tucson, Arizona

**The basic performance equations of a parabolic solar furnace are manipulated into graphical form convenient for purposes of estimation and design analysis. It is found that slight changes in either the specified performance or the over-all efficiency of a furnace can necessitate relatively large changes in design size. A preliminary test program of experimental calorimetric measurements is considered a necessity in furnace design. The essentials of such a program are described briefly.**

## INTRODUCTION

The basic theory of the performance of parabolic solar furnaces has been treated in the literature by Cabannes and Le Phat Vinh,[1] Trombe,[2] Benveniste,[3] Benveniste and Hiester,[4] and Bliss.[5] Similar information is available in a report prepared for an aircraft company[6] and in reports prepared for various branches of the U.S. Air Force.[7,8,9,10] This paper presents, in graphical form convenient for visualization and estimation purposes, the results of manipulating the basic performance equations. The design implications of the results obtained are analyzed and discussed, and an outline is given of what appears to be the logical type of preliminary test measurements necessary for the design of any moderate- or large-sized solar furnace to specified performance.

## BASIC PERFORMANCE EQUATIONS

A paraboloidal reflector designed to produce high temperatures is a relatively simple type of solar heat collector. Most of its performance features may be summarized in two fundamental equations, one giving the diameter of the concentrated solar image, or "hot spot", produced at the focal plane by the reflector, and the other giving the radiation intensity obtainable at this hot spot:

$$d = a\alpha \qquad [1]$$

$$q_f = q_i \frac{4}{a^2} F \sin^2 \theta_1 \qquad [2]$$

The meanings of all principal symbols used in this paper are given in Table I. Fig. 1 illustrates the meanings of some of the symbols.

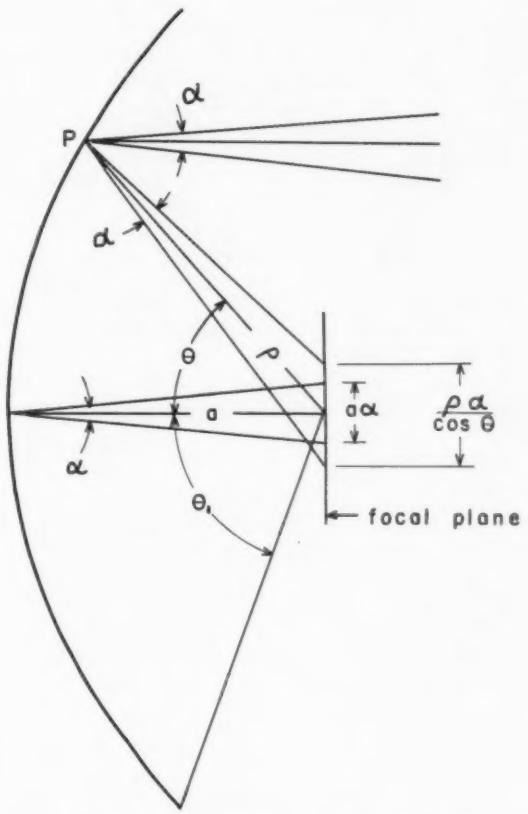


FIG. 1 — Solar image formation by a parabolic reflector.*

The quantity appearing in brackets in Equation [2] is defined as the concentration ratio of the furnace:

$$C_a = \frac{4}{a^2} F \sin^2 \theta_1 \qquad [3]$$

The "furnace factor" $F$ appearing in the above equation is the catch-all product of a series of transmissivity factors allowing for all theoretically avoidable solar energy losses

*Figs. 1, 2, and 3 in this article have been presented in a previous article by the author.[5] They are repeated here for convenience in reference.

TABLE I

PRINCIPAL SYMBOLS USED

$a$ . . . Paraboloid focal length, ft

$C_a$ . . . Concentration ratio of furnace, dimensionless

$d$ . . . Hot spot diameter, ft

$D$ . . . Paraboloid diameter, ft

$F$ . . . Furnace factor, dimensionless

$q_f$ . . . Solar radiation intensity upon hot spot, Btu/sq ft-hr

$q_i$ . . . Direct sunshine intensity at furnace site, Btu/sq ft-hr

$q_s$ . . . Radiation intensity at surface of sun, Btu/sq ft-hr

$T$ . . . Temperature, ° F absolute

$\alpha$ . . . Apparent angular diameter of sun's disc, radians

$\alpha_r$ . . . Solar absorptivity of test sample, dimensionless

$\epsilon$ . . . Emissivity of test sample, dimensionless

$\eta$ . . . Generalized furnace transmissivity factor, dimensionless

$\eta_a$ . . . Misalignment factor

$\eta_c$ . . . Flux control device shading factor

$\eta_f$ . . . Mirror segment frame shading factor, per mirror

$\eta_g$ . . . Geometrical imperfections factor, per mirror

$\eta_r$ . . . Surface reflectivity factor, per surface

$\eta_s$ . . . Hearth & supporting tower shading factor

$\eta_t$ . . . Glass transmissivity factor, per pass through glass

$\theta$ . . . Angle between principal axis and a given paraboloid "radius", degrees (see Fig. 1)

$\theta_1$ . . . Paraboloid rim angle, degrees

$\rho$ . . . Paraboloid "radius", ft (see Fig. 1)

$\sigma$ . . . Stefan-Boltzmann constant, Btu/sq ft-hr-(°F abs)$^4$

$\tau$ . . . Over-all atmospheric transmissivity factor, dimensionless

in transit through the solar furnace apparatus. The furnace factor may be expressed:

$$F = (\eta_1 \eta_2 \eta_3 \cdots \eta_n) \qquad [4]$$

in which $\eta_1$, $\eta_2$, etc., are the various individual transmissivity factors. The nature and number of these transmissivity factors depend upon the particular type of paraboloidal furnace under consideration and upon the degree to which it appears desirable to separate a given type of loss into specific components. As an example, the furnace factor of a two-mirror furnace, constructed of individual segments of back-silvered glass, may be conveniently expressed:

$$F = (\eta_{t1}^2 \eta_{r1} \eta_{g1} \eta_{f1} \eta_a \eta_c \eta_s \eta_{t2}^2 \eta_{r2} \eta_{g2} \eta_{f2}) \qquad [5]$$

The subscripts 1 and 2 in the above refer to the plane mirror heliostat and to the parabolic reflector respectively, and the meaning of each transmissivity factor is given in Table I. A rough estimate of the probable low and high values of these transmissivity factors has been made,[5] and it is concluded that a reasonably well-designed solar furnace of this type should exhibit a furnace factor ranging between 0.3 and 0.7. The furnace factor of a geometrically perfect and perfectly reflective paraboloid, coupled to an equally perfect heliostat, would, of course, be 1.00. For an actual two-mirror furnace, very careful and painstaking attention to all design details would be required to attain a furnace factor of 0.6 or higher. All large solar furnaces constructed so far appear to have furnace factors of 0.35 or lower.

It can be shown that Equation [2] may be transformed to:

$$q_f = \tau F q_s \sin^2 \theta_1 \qquad [6]$$

in which $\tau$ is a suitable transmissivity factor allowing for atmospheric depletion of direct sunshine at the furnace site, and $q_s$ is the intensity of radiation leaving the sun's surface (the sun being assumed a spherical black body at uniform temperature). The above equation indicates that, in the absence of atmospheric depletion effects (i.e. $\tau = 1.00$), and with a perfect paraboloid of rim angle 90° (i.e. $F = 1.00$ and $\sin^2 \theta_1 = 1.00$), then the radiation intensity at the hot spot would be equal to that at the sun's surface. This, of course, is the thermodynamic maximum which could be attained.

A corollary of the above finding is that no device of the same rim angle can achieve a higher concentration ratio than a given perfect paraboloid. If it could, it would be possible to combine the device with a portion of a perfectly reflecting paraboloid, and thereby achieve the thermodynamically impossible situation of producing a higher radiation intensity at the hot spot than that at the heat source. This leads to the conclusion that the image spread produced by paraboloids of large rim angle is a thermodynamic necessity, and that attempts to design devices which will have a greater concentration efficiency than a paraboloid of the same rim angle are likely to prove futile.

Certain simplifying assumptions are used in the derivation of Equation [2]. With one exception, the errors introduced by these simplifying assumptions are negligible from an engineering design standpoint. The one exception is an assumption made in the derivation that the sun's disc is of uniform intensity. From the standpoint of careful engineering, this assumption leads to an error in design calculations which is slight but not negligible.

The sun's disc is not of uniform intensity, but is relatively brighter at the center than at the edge. Approximate calculations, using available quantitative values of the relative intensity of varying portions of the sun's disc,[11] yield the result that a perfect paraboloid of rim angle 60° could be expected to have average intensity at the hot spot about 10 per cent greater than that predicted by Equation [2].

It should not be inferred from the above that an actual solar furnace operating in actual (limb-darkened) direct sunshine can be surely expected to have a higher radiation intensity at the hot spot than would be attained if the sun's disc were of uniform intensity. The solar limb-darkening phenomenon increases any losses present in the furnace due to geometrical imperfections of the reflecting surfaces. Since such geometrical imperfections are always present to some degree in a furnace, the over-all effect of the limb-darkening phenomenon may be either in the direction of very slightly increasing or of slightly decreasing the concentration ratio of a furnace as compared to that which the furnace would have if the sun's disc were of uniform intensity. Proper evaluation and understanding of the limb-darkening effect is very important when



VOL. 1 1957

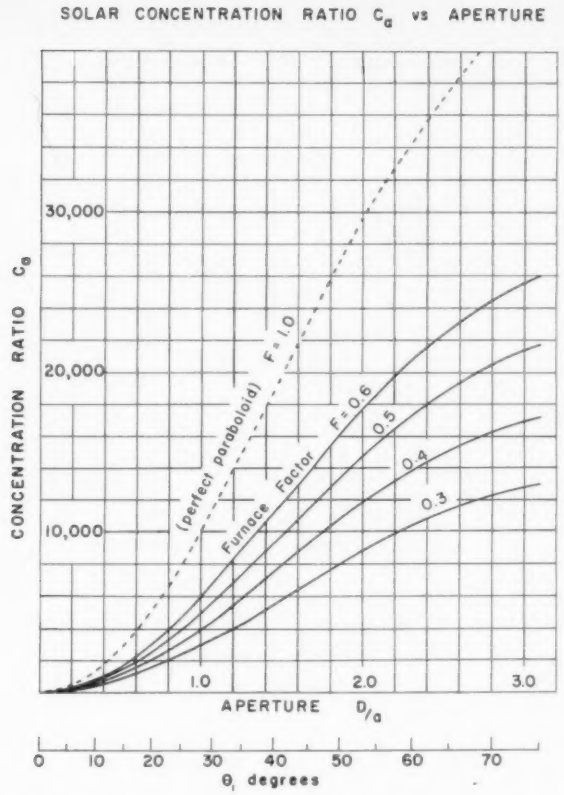


FIG. 2 — Solar furnace concentration ratio vs. paraboloid aperture ratio.

conducting preliminary tests necessary for furnace design, but the effect only slightly influences the necessary size of a solar furnace to give specified performance.

## CONCENTRATION RATIOS AND MAXIMUM ATTAINABLE TEMPERATURES

The concentration ratios attainable with furnaces of various rim angles and furnace factors are given in Fig. 2. This graph is simply a plot of Equation [3], using the average solar disc diameter $a = 0.00931$ radian. This average value of solar disc diameter is used wherever needed in plotting all graphs appearing in this paper. Because of the slight seasonal variation in solar disc diameter, the fraction $4/a^2$ appearing in Equation [3] varies in value from about 44,500 in January to about 47,500 in July, with an average value (at $a = 0.00931$ radian) of 46,200. Hence a solar furnace will have a slightly higher concentration ratio in July (when the earth is farthest from the sun) than it will have in January (when the earth is closest to the sun). This effect should be allowed for in accurate test work. Although the concentration ratio of a furnace is a function of the earth-to-sun distance, it is to be noted from Equation [6] that the radiation intensity at the hot spot is independent of the sun's distance.

The calculation of approximate maximum temperatures attainable by solar furnaces is approached by assuming that the sample presents a plane surface within the focal plane at the hot spot, and that the entire heat loss of the sample is by radiation from this plane surface facing the paraboloid. This leads to a heat balance equation between absorbed sunshine and emitted radiation:

$$a_r C_a q_i = \epsilon \sigma T^4 \qquad [7]$$

The further assumption is then made that the solar absorptivity of the sample is equal to its emissivity; in other words, that the ratio $a_r/\epsilon$ is equal to 1.00. This assumption is correct for black-body cavities and is approximately true for exposed solar furnace samples maintained at a high temperature. Thermodynamics demands that, if sample surface temperature and radiant source temperature are equal, then $a_r/\epsilon = 1.00$. A test sample in a solar furnace operating at a very high temperature is approaching, although very roughly, the temperature of the sun. Hence, for solar furnace calculations, the assumption that $a_r/\epsilon = 1.00$ is in many cases not too erroneous. Utilizing this assumption, Equation [7] becomes:

$$T = \left( \frac{C_a q_i}{\sigma} \right)^{1/4} \qquad [8]$$

Fig. 3 is a plot of the above equation for several values of incident direct sunshine $q_i$. Available regular measurements of southwestern direct sunshine intensities[12] suggest that a direct sunshine intensity of about 360 Btu/sq ft/hr can be taken as an *occasional peak value* to be attained only in clear mountainous sites at elevations of 7500 ft or more. At such high mountain sites intensities of 320 Btu/sq ft/hr can be expected fairly regularly when the sun is shining. Values of 260 Btu/sq ft/hr or slightly higher can be expected fairly regularly in nonurban areas throughout much of the Southwest.

Fig. 3 indicates that a solar furnace must have a concentration ratio of about 20,000 in order to produce a maximum temperature of 4000°C. Fig. 2 indicates that such concentration ratios are within the conceivably attainable range, but require a furnace factor of at least 0.5. Concentration ratios this large have not so far been achieved by any large solar furnace, although they may have been approached by some small furnaces of the searchlight mirror type. The maximum temperatures reported from presently constructed large solar furnaces are on the order of 3000°C, corresponding to a concentration ratio of about 7500.

## BASIC SIZING CONSIDERATIONS

From the standpoint of engineering design, the size and shape of a solar furnace paraboloid may be considered as determined by three independent variables:

(1) hot spot diameter, $d$,
(2) concentration ratio, $C_a$,
(3) furnace factor, $F$.

This section presents in graphical form several of the relations between these variables and paraboloid bowl areas, and discusses the resulting design and cost implications. Paraboloid bowl area was chosen as a parameter both because it is a convenient specific quantity to visualize and because the costs of moderate to large furnaces are probably roughly proportional to their surface areas.

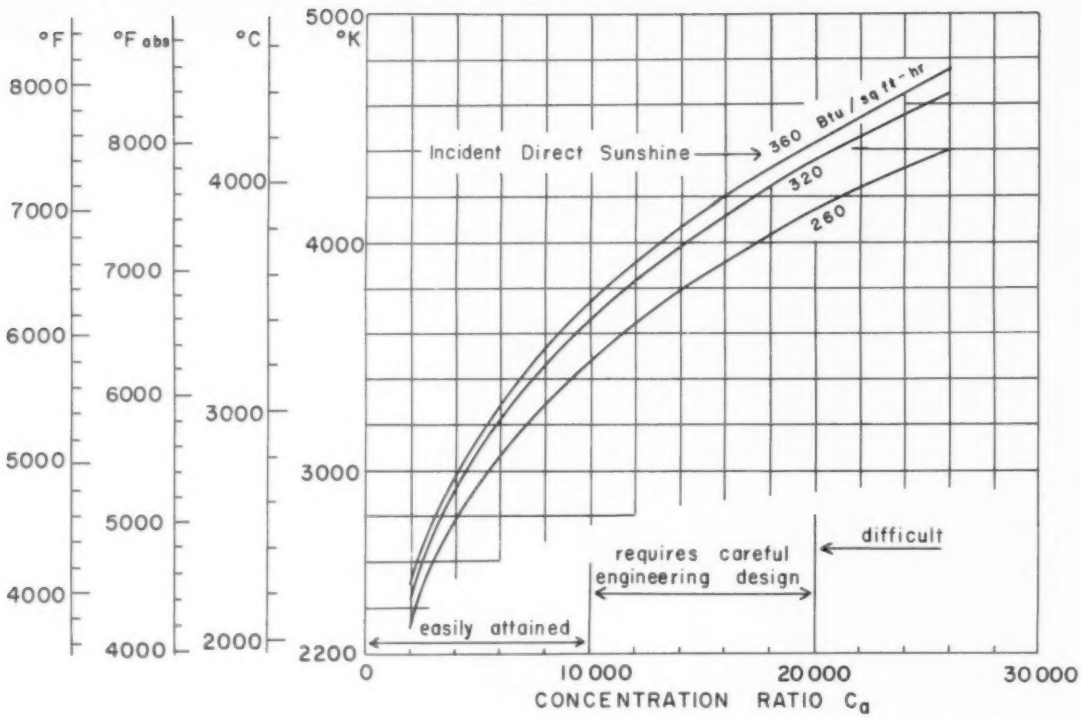


FIG. 3 — Approximate maximum temperatures attainable by solar furnaces.

Incidentally, in the range of rim angles used in solar furnace design, there is not much difference between the bowl area of a paraboloid of diameter $D$ and its projected area $\pi D^2/4$. A paraboloid of rim angle 50° has only about 5 per cent more bowl area than projected area, and one of rim angle 70° has about 11 per cent more bowl area than projected area. Hence, the relations between bowl area and other variables are substantially the same as those between projected area and the same variables.

The bowl area of a paraboloid is given by:

$$A_s = \frac{8\pi a^2}{3}\left[\frac{1 - \cos^3\frac{\theta_1}{2}}{\cos^3\frac{\theta_1}{2}}\right] \qquad [9]$$

Substitution between this equation and Equations [1] and [3] permits determination of the bowl area as a function of concentration ratio, furnace factor, and hot spot diameter. Figs. 4, 5, 6, and 7 present the results of this algebraic manipulation. Bowl areas in square feet are plotted against concentration ratios, for spot diameters ranging from 1 to 5 in., and for furnace factors ranging from 0.30 to 0.60. As noted previously, the fraction $4/a^2$ was taken at its average value of 46,200 in plotting these and subsequent graphs.

Figs. 4 through 7 portray vividly the very rapid increase in bowl area (and consequent rapid increase in cost) incident to increase in either hot spot diameter or in concentration ratio. For example, assuming preliminary tests have shown that a furnace factor of 0.50 is attainable, it will be found from Fig. 6 that a furnace having a concentration ratio of 10,000 and a hot spot diameter of 2 in. requires a bowl area of 600 sq ft. This furnace could yield a maximum temperature of about 3400°C (see Fig. 3). Now suppose that the prospective user feels that this furnace will not be adequate for his type of research work, and wishes instead to have a furnace whose concentration ratio and whose spot diameter are each twice that of the example given. In other words, he desires a furnace with a concentration ratio of 20,000 and a spot diameter of 4 in. Again assuming a furnace factor of 0.50, Fig. 6 indicates that this second furnace will require a bowl area of a little over 8000 sq ft, approximately *14 times* the bowl area of the first example. This second furnace, in addition to its larger spot size and doubled radiation intensity, could produce a maximum temperature of about 4000°C as compared with the 3400°C maximum attainable by the first furnace. But the fact that it must be 14 times larger than the first furnace suggests that it also may be a least 14 times more costly. As an intermediate size between the two examples, we might consider a furnace with a 20,000 concentration ratio and a 2-in. spot diameter. Again assuming the same furnace factor of 0.50, it is seen that such a furnace requires a bowl area of about 2100 sq ft. This is about 3½ times larger than our original example. Summing up, for the hypothetical case chosen, doubling the concentration ratio alone required increasing bowl area by a factor of 3½; doubling both concen-

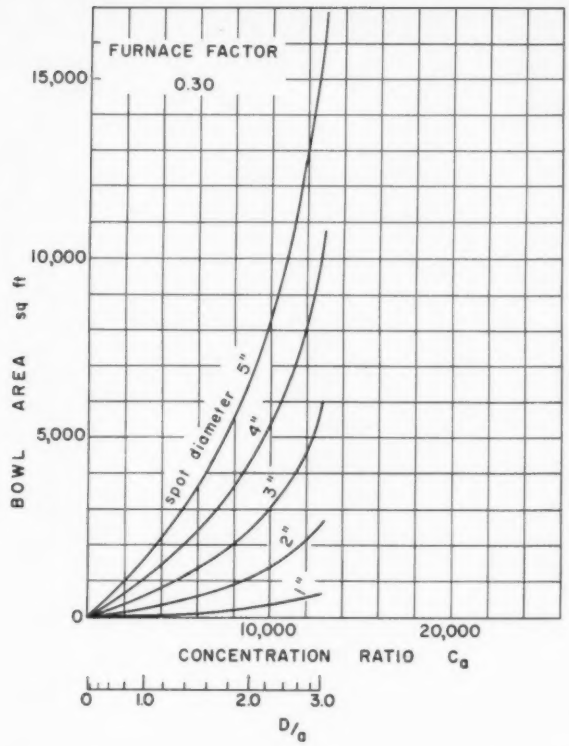


FIG. 4 — Paraboloid bowl area vs. concentration ratio, $F = 0.30$.

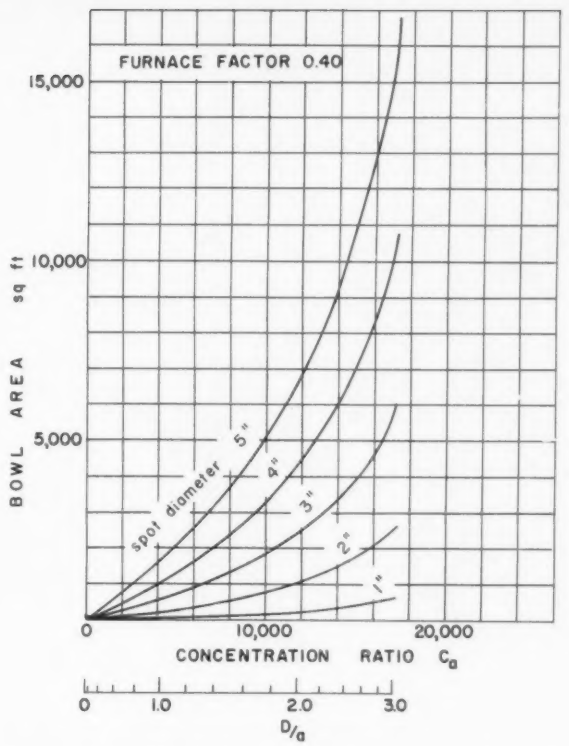


FIG. 5 — Paraboloid bowl area vs. concentration ratio, $F = 0.40$.

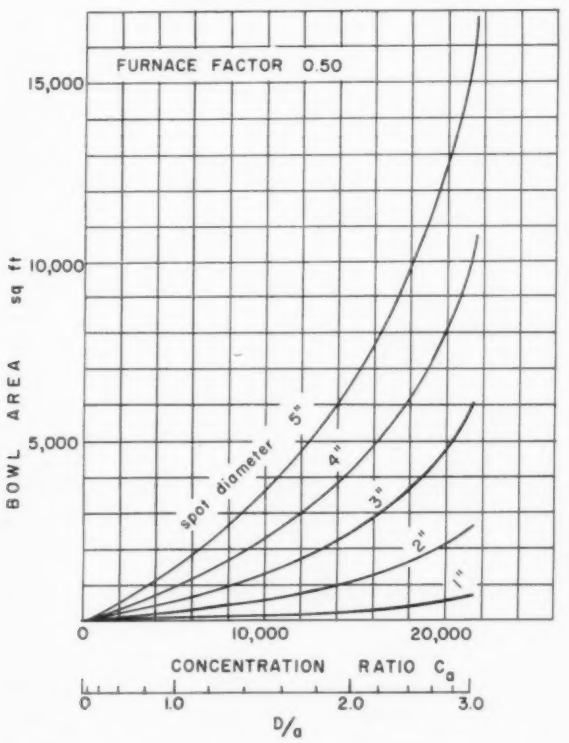


FIG. 6 — Paraboloid bowl area vs. concentration ratio, $F = 0.50$.

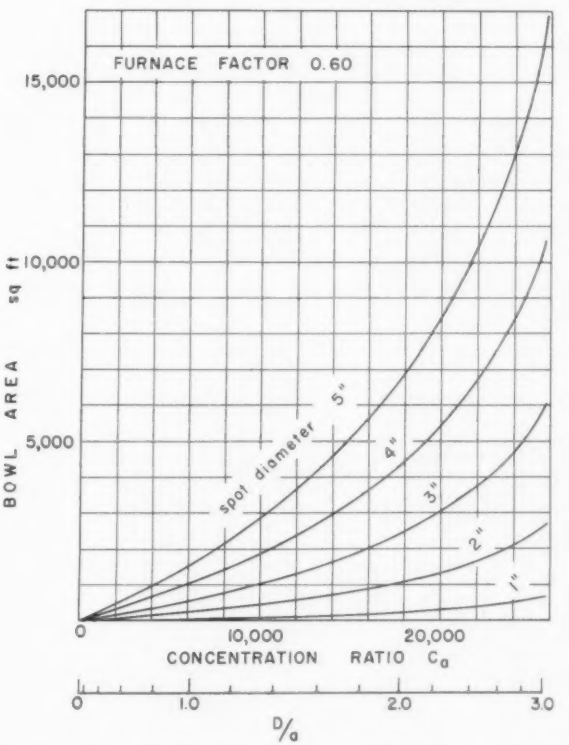


FIG. 7 — Paraboloid bowl area vs. concentration ratio, $F = 0.60$.

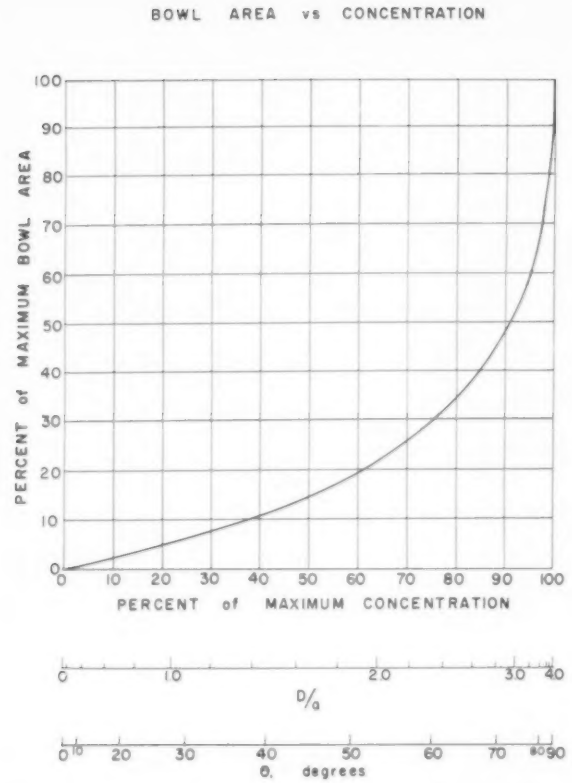


FIG. 8 — Percentage of maximum bowl area required to attain a given percentage of maximum attainable concentration ratio.

FIG. 9 — Relative concentrating efficiency of different portions of of the paraboloid bowl.

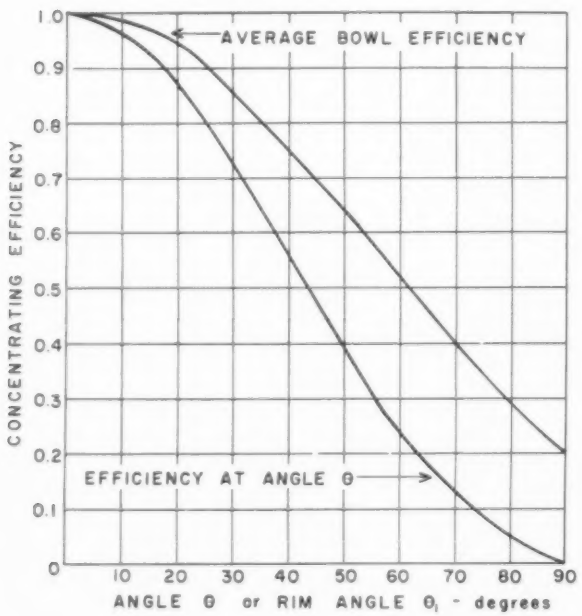


tration ratio and spot diameter increased bowl area by a factor of 14. Different figures are of course obtained depending upon the particular case chosen but, in general, bowl areas and costs increase very rapidly with increasing concentration ratios or with increasing spot diameters. This economic factor must be reckoned with both by the designer and the prospective user.

Figs. 4 through 7 suggest, correctly, that outer portions of a paraboloid are relatively less efficient in concentrating sunshine at the hot spot than are portions near the vertex. This situation is presented more clearly in Figs. 8 and 9. In Fig. 8 the per cent of the maximum bowl area is plotted against per cent of maximum concentration. It is seen that 70 per cent of the maximum attainable concentration ratio can be had with 25 per cent of the maximum bowl area. To attain 90 per cent of maximum concentration requires doubling the bowl area (to 50 per cent), and to attain the last possible 10 per cent of concentration would require again doubling the bowl area. It can be seen from this graph that a solar furnace paraboloid of rim angle around 70° represents about the extreme practicable maximum.

Fig. 9 gives the relative concentrating efficiencies of different parts of the bowl, both on an average basis and for a region at a particular angle. For example, from the upper curve of the figure, the average concentrating efficiency of an entire paraboloid of rim angle 60° is 52 per cent of that which it would have if each unit area of the bowl had the same concentrating efficiency as a unit area located at the vertex. The concentrating efficiency of a unit area located at a specific angle is given by the lower curve. A unit area located at an angle of 60°, for example, has a concentrating efficiency which is 24 per cent of that of a unit area near the vertex. In other words, slightly more than 4 sq ft of paraboloid bowl at an angle of 60° are required to reflect the same amount of energy to the hot spot as is reflected to it by 1 sq ft of bowl at the vertex. One immediate design conclusion to be drawn from this is that shading near the center of the paraboloid, though unavoidable to some degree, should be held to a minimum. For a paraboloid of rim angle 60°, every square foot of bowl which is shaded at the vertex requires the construction of 4 sq ft of bowl at the rim to compensate for the loss.

Increasing the furnace factor decreases the rim angle necessary to attain a specified concentration ratio. And, since paraboloid efficiency increases with decreasing rim angle, furnace sizing to give specified performance is very sensitive to small changes in furnace factor. This is illustrated in Fig. 10, in which bowl area is plotted against furnace factor, concentration ratios being held constant. This graph indicates the large reductions in sizing which can be attained by moderate increases in furnace factor.

For example, suppose that a furnace with a concentration ratio of 15,000 is desired. Assume that preliminary testing has shown that construction of reflecting surfaces by method A, which is relatively inexpensive per square foot of reflecting surface, can yield a furnace factor of 0.40. The tests also show that construction of reflecting

VOL. 1 1957

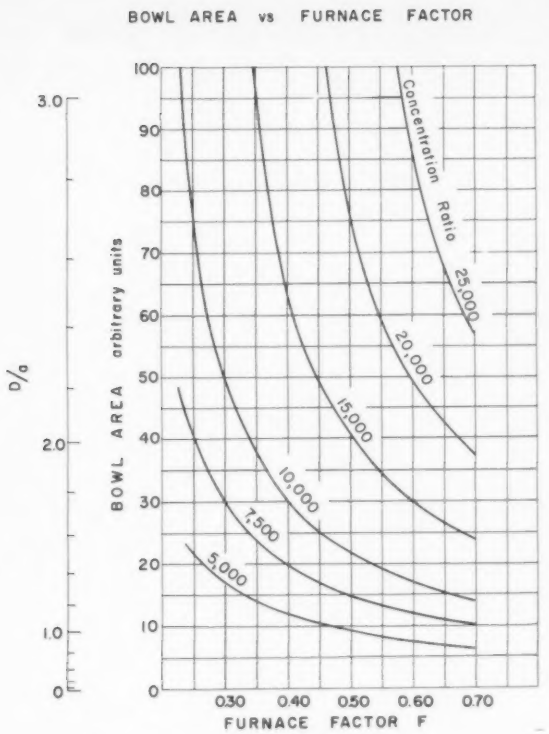


FIG. 10 — Bowl area vs. furnace factor.

surfaces by method B, more expensive per square foot of reflecting surface, can yield a furnace factor of 0.60. It will be seen from Fig. 10 that method A will require a furnace with a little more than *twice* the bowl area of method B. Method B can produce such a substantial decrease in over-all sizing that, even if the method should have considerably higher glass cost per square foot than method A, the second method should by no means be dismissed out of hand without a careful analysis of the total per square foot cost of each furnace.

In connection with this matter of rapid decrease of necessary furnace sizing with increase in furnace factor it is pertinent to point out that there are at present two general approaches to the problem of producing paraboloid reflecting surfaces for the moderate- to large-sized solar furnaces. One method is relatively cheap and relatively inefficient; the other is more expensive and more efficient. The first method is that of using thin flat glass mirrors clamped to an approximation of the desired parabolic curvature. The second method is that of using heavier mirrors preformed by slumping or grinding. There is no question that, from the standpoint of paraboloid glass cost alone, clamped flat-glass mirrors are much cheaper per square foot than slumped or ground mirrors. But it seems an open question as to which method may have the lowest total furnace cost. The large reduction in paraboloid and heliostat sizing permitted by the use of relatively high-quality mirrors may save more than the added cost of the high-quality mirrors. The question is best settled by preliminary experimental testing of various types of mirrors.

## OUTLINE OF NECESSARY PRELIMINARY TESTING

A consideration of the preceding section will show that the chief uncertainty in solar furnace performance design centers on one variable: the furnace factor *F*. The design sizing necessary to produce a specified performance is very sensitive to slight changes in furnace factor, and it is essential that the furnace factor of a proposed design be both accurately known and accurately maximized to the highest economic degree. This requires preliminary heat-transfer tests of individual furnace components and of small subassemblies prior to final determination of construction methods and details.

The furnace factor, as noted previously, is a catch-all reduction factor which includes the effects of five general types of heat losses:

(1) glass absorption,
(2) imperfect reflectivity of reflecting surfaces,
(3) geometrical imperfections of reflecting surfaces,
(4) shading effects,
(5) imperfections in alignment.

Most of these heat losses can be evaluated by a test program of suitable calorimetric-type measurements made upon sample components of the proposed furnace. Glass absorption, for instance, is conveniently measured by noting the drop in intensity indicated by a good normal incidence pyrheliometer when a test sample of glass is interposed between the sun and the pyrheliometer. This particular test for determining glass absorption requires, of course, a suitable correction for surface reflectivity of the glass; and it is susceptible of more accurate results if fairly thick glass test samples are used.

Similar calorimetric-type tests, using actual sunshine as the heat source, can be devised to measure the individual effects of imperfect reflectivity and of geometrical aberrations. Shading losses can be determined in part by calculation and in part by calorimetric tests on furnace subassemblies which include some components of shading. Shading calculations must take into account the effect of the varying efficiencies of different parts of the paraboloid. As noted previously, center shading produces the greatest relative shading loss.

The allowance for misalignment loss included in the furnace factor refers to the probability that some misalignment of furnace reflecting surfaces will occur with time. Such misalignment will occur as a result of wind, weather, thermal strains, etc. This loss is of course impossible of quick experimental measurement, but it is probable that the information gained in a preliminary test program will shed at least some helpful light on the magnitude of this factor.

Following the individual-type tests on losses due to glass absorption, imperfect reflectivity, geometrical aberrations, etc., over-all-type tests of small subassemblies of the proposed furnace construction should be made. Fig. 11 indicates the general scheme of such tests. A small test heliostat, formed of the same type of plane mirrors contemplated for the actual furnace, is used to reflect sun-

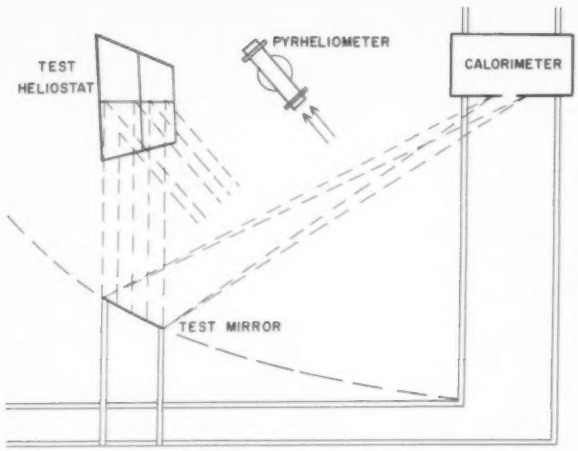


FIG. 11 — Schematic diagram of a "heat-transfer test frame" for use in preliminary testing of proposed solar furnace components.

shine directly to a subassembly of paraboloid mirror segments, these also being of the type of construction proposed for the actual furnace. These paraboloid mirror segments in turn reflect the sunshine to a concentrated image at the focal plane of the paraboloid of which the segments are a small part. A suitable continuous-flow calorimeter located at the focal plane is used to measure the radiation intensity at the "hot spot" produced by the subassembly of mirrors. This radiation intensity at the hot spot is compared with the direct sunshine intensity measured with the pyrheliometer.

This over-all-type test yields, essentially, the local concentration ratio and the local furnace factor pertaining to the small portion of the paraboloid under test. By making a short series of such tests to cover the various angular portions of the proposed furnace paraboloid, the resulting small measured concentration ratios can be suitably summed to calculate the actual over-all concentration ratio to be expected from the entire proposed furnace. In making such calculations, appropriate slight corrections will be required to properly allow for the nonuniformity of intensity of the sun's disc.

Calorimetric tests of this nature, although they do not appear to have been used in solar furnace work so far, seem the only logical procedure in designing any moderate- or large-sized solar furnace. Because of the rapid change of necessary design sizing with slight change in furnace factor, we see no alternative to preliminary tests of this general nature if the furnace factor and consequent furnace sizing are to be worked out to customary standards of engineering and economic accuracy.

## SUMMARY AND CONCLUSIONS

A parabolic reflector is a relatively simple type of solar heat collector. But, like all solar heat collectors, it has a deceptive appearance of utter simplicity. It is not quite as simple as it looks, particularly when the problem is posed of designing such a collector to definite specified performance. It appears, however, that this type of collector can be surely designed to specified performance, provided only that the furnace factor of the proposed design is accurately determined by suitable preliminary experimental measurements. From an economic standpoint, the preliminary experimental work should be in the direction not only of accurately determining the furnace factor of the proposed design, but also of maximizing it to the best possible economic degree.

Much of the information presented in this paper was developed by the author while employed as a consultant at Holloman Air Force Base. Appreciation is expressed to the Commander, Holloman Air Development Center, HAFB, New Mexico, for permission to use this material. The information presented represents the opinions of the author, not necessarily those of Holloman Air Development Center.

## REFERENCES

1. F. Cabannes and A. Le Phat Vinh, "Calcul de la répartition de l'énergie solaire réfléchie par un miroir parabolique." *J. de Physique et le Radium* 15: 817-20, Dec. 1954.
2. F. Trombe, "High temperature furnaces." (In *Proceedings of the World Symposium on Applied Solar Energy, Phoenix, Arizona, 1955*, Stanford Research Institute, 1956, pp. 63-72.)
3. Guy Benveniste, "Solar energy furnaces." Stanford Research Institute, 1955.
4. Guy Benveniste and N. K. Hiester, "The solar furnace — new tool for high temperature work." *Mech. Eng.* 78(10): 915-20, Oct. 1956.
5. R. W. Bliss, Jr., "Notes on performance design of parabolic solar furnaces." *J. Solar Energy Science and Engineering* 1(1): 22-29, 1957.
6. J. Farber and B. I. Davis, "Analysis of large aperture parabolic reflectors for solar furnaces." CONVAIR Report no. TRM-77, Jan. 28, 1954. 7 pp. + 10 figs.
7. Eugene Loh, Pol Duwez, N. K. Hiester, and T. E. Tietz, "Theoretical considerations on performance characteristics of solar furnaces." Technical Report no. 1, AFOSR TN-56-69; ASTIA Document AD 81521. Stanford Research Institute, Jan. 16, 1956.
8. Robert De La Rue, T. E. Tietz, and N. K. Hiester, "Economic and design study of solar furnaces." AFOSR TN-56-382; ASTIA Document AD 95818. Stanford Research Institute, June 21, 1956.
9. R. W. Bliss, Jr., "Notes on optical design principles, concentration ratios, and maximum temperatures of parabolic solar furnaces." Holloman AFB, N.M., Technical Memorandum HWD TN-56-1, July 1956.
10. R. W. Bliss, Jr., "Summary of parabolic solar furnace performance design." Holloman AFB, N.M., Technical Memorandum HWD TN-56-2, Oct. 1956.
11. G. Abetti, *The Sun*. D. Van Nostrand, 1938. pp. 312-17.
12. *Climatological Data — National Summary* (monthly). Weather Bureau, U.S. Department of Commerce.

VOL.
1
1957

# A SOLAR FURNACE FOR USE IN APPLIED RESEARCH

By PETER E. GLASER

Arthur D. Little, Inc., Cambridge, Massachusetts

**A description is presented of a solar furnace developed by Arthur D. Little, Inc. for research use. This furnace was developed to provide a compact, flexible research tool for exposing materials to temperatures up to 3500°C. over a circular area of 0.6 cm diameter, without the problem of contamination from sample containers or furnace walls.**

**An important feature is the sample-moving mechanism which allows the sample to be moved parallel to any of the three coordinates. Variable-speed motors, the controls for which are conveniently located at the base of the mirror support, permit regulation of the motion of the sample holder. Movement can take place either in cartesian or polar coordinates; and the sample can thus be rotated around the hot zone if desired. Measuring and optical instruments can be inserted through the hole at the back of the reflector and can be placed very close to the hot sample without being affected by the high temperature. An electronic guiding system keeps the furnace trained on the sun, while a shielding cylinder provides temperature control over the sample even at the highest temperature range.**

**This solar furnace is the first in a line of high temperature equipment which Arthur D. Little plans to make commercially available to research laboratories.**

---

The rapid advance of technology has created the need for basic information on the behavior of materials at high temperatures, and the means for generating such temperatures conveniently in the laboratory.

The harnessing of the sun's rays to obtain high temperatures, although basically no modern achievement, has provided us with an energy source eminently suitable for research purposes.

The more common methods used to achieve temperatures above 2000°K are electric-resistance heating, induction heating, electric arc, and flames. These sources of high temperature, however, have drawbacks that rule them out in a number of research problems. These drawbacks include the presence of oxidizing or reducing atmospheres and electric and magnetic fields, as well as the problem of providing a suitable container in which to heat the sample.

In the solar furnace not only are high temperatures attainable, but research conditions are ideal. Radiation is a very pure source of energy, since no objectionable products of combustion or volatile components of various furnace materials are present. The material heated in the solar furnace is its own container, and reactions between the container and the sample are eliminated.

The furnace need not be insulated, because it remains virtually at atmospheric temperature, and no reactions between the sample and other parts of the furnace can take place. Finally, the solar furnace can be used in a much higher temperature region than any conventional furnace, except, perhaps, the arc furnace.

FIG. 1 — Solar furnace — artist's conception.

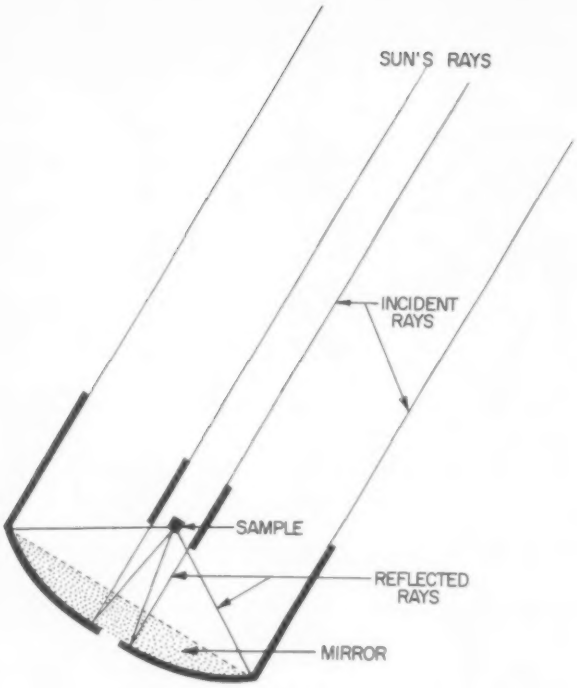


FIG. 2 — Operating principle of solar furnace.

The solar furnace, therefore, is today considered one of the most valuable tools for investigation of high temperature properties of materials.

Arthur D. Little, Inc. has designed a solar furnace which is the most recent addition to the line of research tools supplied by ADL. This furnace utilizes the principles proven by Dr. Tibor Laszlo in his research work with the solar furnace at Fordham University. It will permit scientists to conduct a wide variety of experiments, without the necessity of spending valuable research time on the construction of such a furnace. It is easy to operate and maintain, and it provides a compact, flexible tool for exposing materials to temperatures up to 3500°C. Fig. 1 is an artist's concept of the ADL Solar Furnace. Its basic component is a 60-in.-diameter parabolic mirror with the front surface plated with stellite.

The principle on which the operation of this solar furnace is based is shown in Fig. 2. The irradiated area of the sample, which can reach 3500°C, is 6 mm in diameter. Although this area is rather small, physical properties such as melting point, vapor pressure, specific heat, and thermal conductivity can be measured. In addition, for the study of crystalline properties and phase changes, no larger sample irradiation is required. It is of much greater importance to have the area of high temperature well defined and to maintain a constant temperature during a test run or to provide for a controlled temperature change. To meet these conditions, accurate sample-moving and sun-tracking mechanisms are required.

Fig. 3 shows the schematic view of the sample-moving

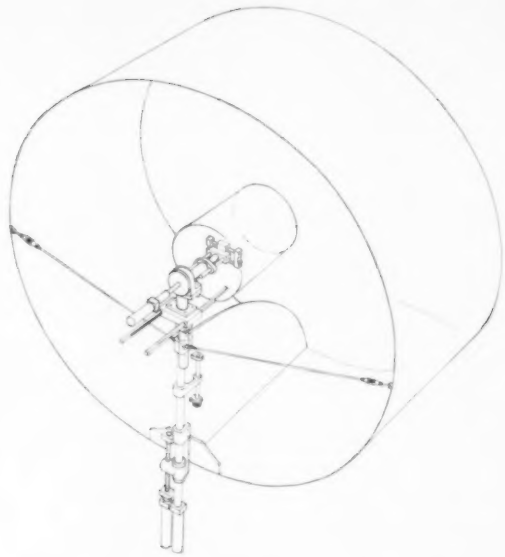

FIG. 3 — Schematic view of sample-moving mechanism.

mechanism. This mechanism must be rigid as the reflector follows the sun. We achieved this rigidity by using lightweight materials in a mechanically strong device, keeping the tolerances of the various moving parts of the mechanism within very close limits. In addition, the minimum frontal area reduces the shadowing loss.

The mechanism is constructed so that the sample can be moved parallel to any of the three coordinates. The control of the movement is such that the sample can be positioned to within 0.1 mm of a desired position. The rate of traverse can be varied by changing the speed of the motors. The controls for the motors of the sample-moving mechanism are mounted on the mirror support base so that the observer can easily control the various motions, as shown in Fig. 4.

Since the solar furnace must be mounted outdoors and there is a chance it will be exposed to adverse weather

FIG. 4 — Controls of motors of sample-moving mechanism.

VOL.
1
1957

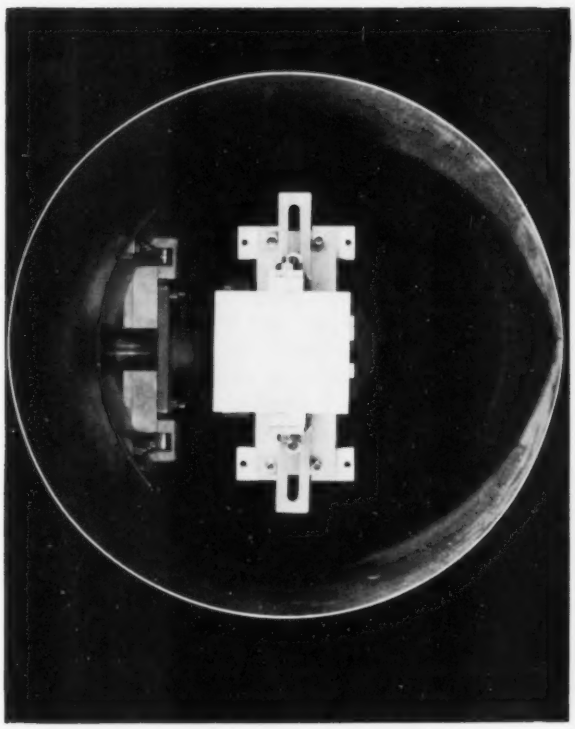

FIG. 5 — View of sample mounted in holder.

FIG. 6 — Sample-moving mechanism in swung-out position.

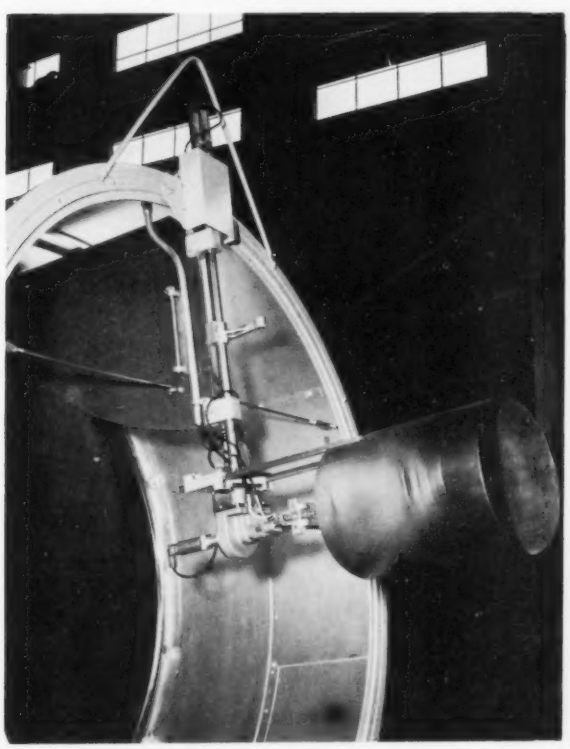

conditions, all mechanical and electrical parts are weather-resistant.

Fig. 5 shows the view of the sample mounted in its holder as seen through the hole in the parabolic reflector. For carrying out various measurements or making observations of the sample under test, instruments can be inserted through the hole at the back of the reflector. These instruments can be placed quite close to the sample without being affected by the high temperature. Accessories can be provided so that the sample can be rotated around its axis at speeds up to 20,000 rpm.

Fig. 6 shows how the whole sample-moving mechanism can be swung out. This greatly facilitates introducing the sample, and installing accessories and instruments.

Various temperatures and heat fluxes can be obtained by varying the position of the shielding cylinder. This cylinder can also be used to keep a constant temperature. For this purpose a radiamatic pyrometer is mounted near the sample and coupled by a servomechanism to the motor moving the cylinder. This provides a fine temperature control over the sample even at the highest temperature range. Further control over the temperature can be obtained by defocusing the sample. The rapid change of temperature as the sample is moved away from the focal zone is another reason for close control over the sample movement and a rigid sample support.

The stage for mounting the sample has been designed so that the sample can be tested in air, under vacuum, or in the presence of other gases. The arrangement for testing the sample in air, and in vacuum or other atmospheric work is shown in Fig. 7.

The pyrex glass or fused silica, hemisphere-type of bell jar does not have surfaces corresponding to that of the parabolic reflector; therefore, there is some loss of efficiency because of absorption and reflection of some of the rays.

Another important design feature of the solar furnace is the sun-tracking mechanism. Two motors rotate the parabolic reflector around the horizontal and vertical axes, respectively. For experiments which may extend over a

FIG. 7 — Mounting stage for work in controlled atmosphere.

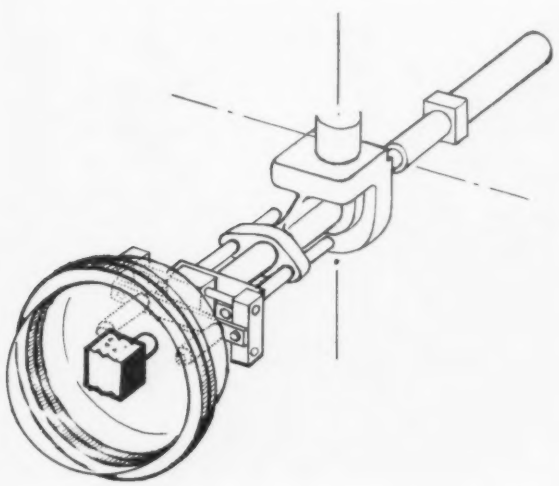

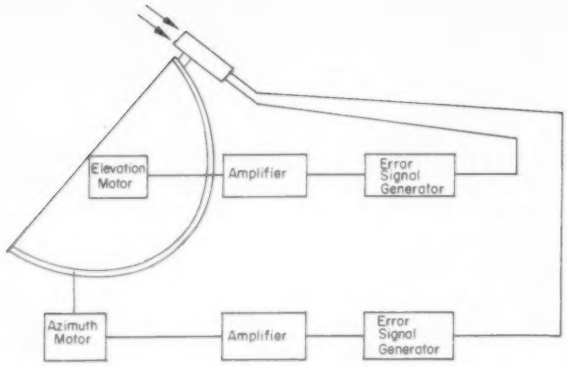


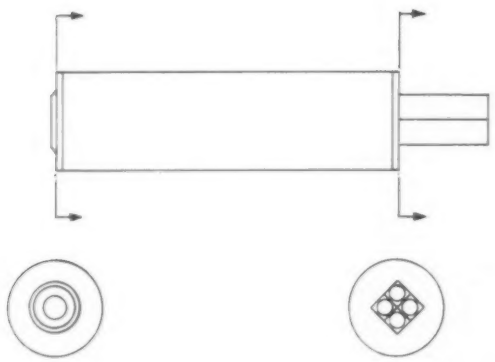

FIG. 8 — Electronic guiding system.

FIG. 9 — Manual guiding mechanism.

longer period of time, we have an electronic guiding mechanism as shown in Fig. 8. This electronic guiding mechanism is actuated by photomultiplier tubes that generate an error signal when a passing cloud prevents the reflector from following the correct tracking path. This signal after amplification is algebraically added to the basic drive current of the motor. The basic speed of the motors is adjusted so that the reflector follows roughly the motion of the sun.

For short-time experiments such an accurate guiding mechanism is not required. Therefore, as shown in Fig. 9, we have provided a manual device so that we can make the reflector follow the sun by sighting the sun in a collimating tube and using sensitive potentiometers to correct the basic tracking speed of the motors.

In carrying out experiments we have to know the physical characteristics of the solar furnace. The geometry of the furnace and the materials of construction determine the concentration ratio we can obtain. This is a ratio of the heat flux at the sun's image to the actual flux received by the reflector from the sun, at normal incidence, at the furnace site. For our furnace the theoretical concentration ratio is 25,500. The theoretical concentration efficiency is the ratio of the power concentrated within the sun's image to the total power received by the parabolic mirror, and in our case it is 40 per cent.

The potentially available energy is shown in Fig. 10. The geometrical perfection of the mirror will affect this available energy. In addition, the shape and absorptivity of the sample material will determine how much of the available energy will be absorbed.

The maximum theoretically attainable temperature is shown in Fig. 11. This assumes a geometrically perfect mirror and a black-body sample.

Since the parabolic surface reflecting the sun's rays cannot be assumed to be a geometrically perfect paraboloid, we cannot obtain the maximum theoretically attain-

FIG. 10 — Potentially available energy.

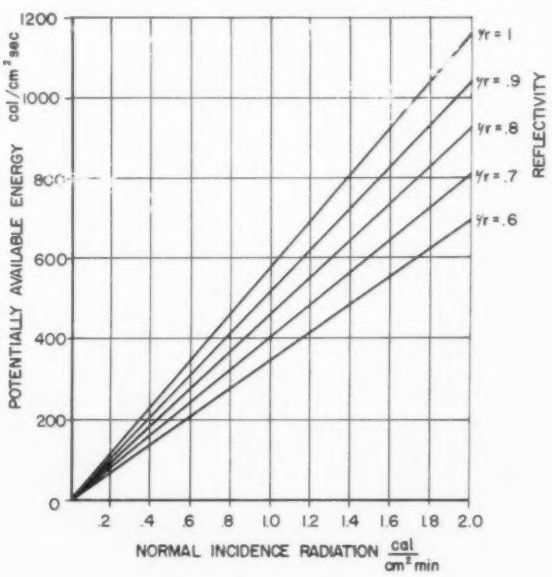


VOL.
1
1957

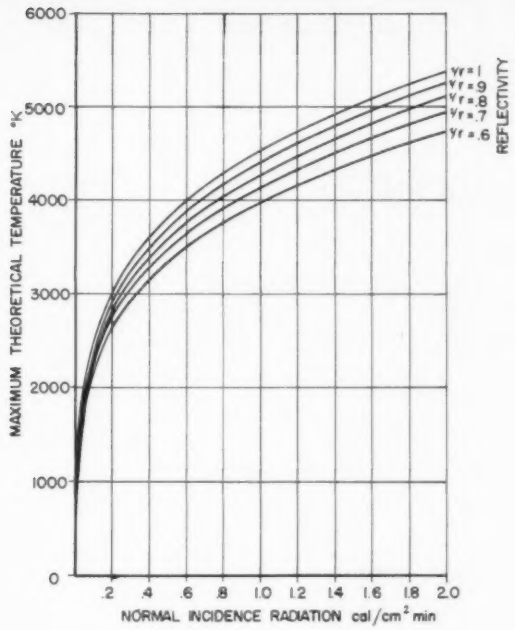


FIG. 11 —Maximum theoretically attainable temperature.

able temperature. The effects that the geometrical imperfections have on the actual maximum temperature and heat flux show that a solar furnace which is intended for high temperature research need not be quite as geometrically perfect as one in which a maximum flux is desirable.

The accurate measurement of temperature of a sample in the solar furnace is a formidable research problem. The information available to us on the measurement of temperatures at ordinary levels permits some estimate to be made of the temperatures we are encountering in the solar furnace. We cannot assume that the temperatures as measured with an optical pyrometer are accurate, due to the absence of black-body condition. In addition, the emitted and incident radiation of the sun from the surface of the sample have to be separated. One way of doing this is shown in Fig. 12.

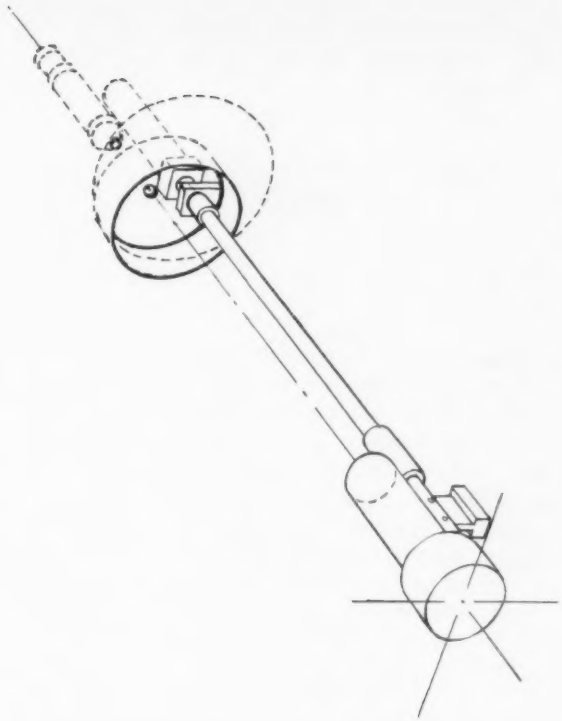

FIG. 12 —Shutter mechanism for separation of emitted and incident radiation.

We have developed the solar furnace as a means of carrying out experiments of scientific interest, and it is our hope that this furnace will permit scientists to reach new goals in the field of high temperature investigations of materials.

## BIBLIOGRAPHY

W. Conn, *Z. F. Angew. Physik* 6: 284-91, 1954.
W. Conn, *J. Opt. Soc. Am.* 44: 45-47, 1954.
T. S. Laszlo, *Science* 124: 797-800, 1956.
T. S. Laszlo, W. F. de Dufour, and J. Erdell, (Paper to be published in the *Transactions of the Tucson Conference on the Use of Solar Energy — The Scientific Basis.*)
E. Loh, P. Duwez, N. K. Hiester, and T. E. Tietz. Stanford Research Institute, Technical Report no. 1, Project no. CU-1410, AFOSR TN 56-69, ASTIA Document no. AD81521.

# THE USES OF SOLAR ENERGY

By C. C. FURNAS

Assistant Secretary of Defense for Research and Development*

The ability of the planet Earth to sustain its ever-increasing population is discussed in terms of both food and energy. The pressure of rapidly increasing population puts demands upon the world's fuel reserves which are so tremendous that we must look for other sources of energy.

The author reviews various ways by which solar energy has been used in the past. Methods of heating and cooling dwellings are discussed, and it is pointed out that one-third of our annual energy consumption is used for these purposes. It is in this field that solar energy is likely to make its most important contribution in the near future. Means of producing power by steam and other engines are described, and the need for "good old Yankee ingenuity" is stressed. Pumping water for irrigation and distillation of sea water are other fields in which solar energy has long been used and where new "break-throughs" are needed. Photoelectricity and photosynthesis also hold much promise. The development of methods by which fuels for automobiles can be produced from water, air, and sunlight is a field in which research would be most profitable. Much research is needed to bring these developments to the point of feasibility, but the rewards will be rich, and the solar energy is there for the taking.

## THE RISING TIDE

In his earliest days, man undoubtedly led the truly simple life. For food he ate the roots, nuts, and berries of wild plants — augmented by the flesh of those animals he could kill with his crude weapons. For shelter he sought a cave on the sunny side of the trail. For clothing — if any — he used pliable bark or animal skins. But even under the best of conditions, it took several square miles of territory to support one person with that level of culture. If the numbers increased above some certain low level, death by starvation, disease or exposure would intervene as a restraining force.

Before the European invasion, which began in 1492, the native American Indians north of the Rio Grande lived largely in a rooting and hunting culture. It is estimated that there were only a few hundred thousand of them, but that the land was overpopulated; it was "saturated" with people; it could not support any greater number with the techniques of living available to the inhabitants.

In other parts of the world, however, man with his inquisitiveness, restlessness, and large brain had succeeded in devising better ways of making a living. The pattern of cultural evolution was probably something like this. First, the food-yielding animals were more or less domesticated, and grazing gradually began to replace hunting as the prime means of livelihood. Then came the very important step of the planting and harvesting of crops — agriculture. You will remember the story of Cain and Abel as a conflict between two cultures. The use of beasts of burden was a very important step in supplementing man's own motive power. The next move was the harnessing of inanimate power — first, that of wind by means of windmills and sails; next, that of falling water, as for instance by the early water mills of New England; and finally that of the power of steam by James Watt, which started the Industrial Revolution. Thus evolved the industrial pattern, such as we see in America today.

With each advance in technology, the number of people who could be supported per acre or per man-hour of effort increased very substantially. Not only could more people survive, but also they could live out their span of years with a higher standard of living than their ancestors had. But all of these advances in numbers and quality of living called for more energy. Where was it to come from?

The most significant breakthrough came with James Watt's invention of the first truly successful steam engine in 1769. This and other types of heat engines constituted a new source of power which could be constant, concentrated, and dependable as long as a source of fuel was available. Fortunately for us, wood, then coal, then gas and oil have been readily available to turn the wheels of the world. Particularly in the Western World we have promoted the Industrial Revolution assiduously. We have increased our numbers tremendously and have developed an irresistable urge for an ever-increasing standard of living. These are social forces that will not be denied. Unless we can tap sufficiently large reservoirs of energy to satisfy the continuing and rising demands, civilization is scheduled for some very rough bumps.

When the steam engine was invented — less than six generations ago — the world population was about three-

* Now returned to his position as Chancellor of the University of Buffalo.



VOL.
1
1957

quarters of a billion. Today the number stands at two and one-half billion. So rapidly has our growth been in recent generations that of all the people who have existed on the face of the earth since the beginning of human beings (a few hundred thousand years), one out of 15 is alive, eating and propagating today.

As we learn to use power for industrial purposes, we can support more people. This leads to more industrialization, which leads to increased standards of living which require more power. Mathematically, this is an exponential function. It is a chain reaction which we have carried further in America than in any other part of the world.

At the present time our country contains only about one-sixteenth of the world's population; yet because we are the most highly industrialized, we utilize almost one-half the world's inanimate power and produce about 50 per cent of the world's industrial goods and services. Industrial goods and services require not only an abundant amount of inanimate energy but also numerous raw materials, such as the metals. If all the rest of the world should suddenly be raised to the same level of industrial production as the United States, at least 750 per cent increase in the use of energy, as well as of the other natural resources, would immediately be required.

But this is not even half of the situation. The explosive increase in population of the world which is now well started will not stop in the foreseeable future. Predictions[1] can be made quite accurately for at least three generations, which is just a bare 100 years. The United States at the present time has 165 million people. Within the life span of the children of the children now being born, the population of the United States will be at least 375 million — even if the rate of increase at that time has dropped to zero. Taking the world as a whole, in the next 100 years the two and one-half billion which we now have will almost inevitably increase to at least six billion and it may be as many as eight billion. It will be utterly impossible to support this number of people unless we have a quite high degree of industrialization throughout the world. The old pattern of subsistence agriculture, which held in America 200 years ago, and still holds throughout a large portion of the world, simply will not do. The first requisite for providing the industrial pattern to support all these people is the availability of an adequate amount of inanimate energy to supply the power for the various machines, vehicles, space heating, chemical processing, and metallurgical work plus some functions not yet dreamed about. Actually, as congestion increases the amount of power required goes up much more rapidly than the number of people who use it. My own estimate is that, a century from now, the world will require at least 50 times as much energy as it is utilizing today.

Until quite recently, to worry about the future energy supply of the world was very unpopular except among a few academicians. Now, however, even hard-boiled industrialists are beginning to take the matter a bit more seriously. Although we still have a great deal of oil and coal in the ground — which is there only because the sun beneficiently stored energy in luxuriant plants a couple of hundred million years ago — and though we are still finding new oil fields and have large deposits of oil shale, we are beginning to see that we have skimmed off the cream and that the whole bottle of milk may disappear quite rapidly. Our dependence on a continuing and dependable supply of energy is possibly best illustrated by the quandary in which Western Europe now finds itself because of a temporary blockage of the Suez Canal. There, the rationing of fuel has been imposed again, and it is going to be a rather grim winter. So we are beginning to worry about our energy supply for this generation and to become even more solicitous about our children's situation.

Yet while we are worrying, about 32,000 times as much energy falls on the surface of the earth each day in the form of the rays from the sun as the entire human race utilizes in that same 24 hours. As long as the sun shines, and it certainly is good for at least a few million years, we should never run out of energy — although we may always be short on the ingenuity required to utilize it.

## SHORTCOMINGS OF SOLAR ENERGY

With all this energy to be had simply for the taking, why have we not been more successful in utilizing it? There are three reasons:

(1) The energy comes to us only in the form of electromagnetic radiation. Visible light accounts for nearly half of the energy of sunlight; a very small amount is in the invisible ultraviolet end, and the remaining one-half is in the heat, or infrared, rays. Although all of this light and these heat rays are very useful — as a matter of fact, essential — they do not cover all of our needs. We very frequently, for instance, want our energy in the form of electricity.

(2) The sun itself, of course, is a very concentrated source of energy; its surface has a temperature of about 5,500°C. But the sun is 93 million miles away from the earth. Although at the outer edge of the atmosphere the heat input to the earth from the sun is about 2.0 small calories per square centimeter per minute, only about two-thirds of that energy, on the average, reaches the surface of the earth because of absorption by the atmosphere. For industrial activities, energy sources hundreds or thousands of times more concentrated than this are required. Hence, one of the basic problems in the use of solar energy is to devise ways and means of reconcentrating this energy.

(3) The third drawback is the fact that the sun's energy comes to us intermittently; the well-known phenomena of daylight and darkness and cloudy weather. Thus, if we solve the first two problems, those of getting the energy into the form we want it and of concentrating it from its low potential, we still have the problem of storage if we are going to have a source of energy that we can count on continuously.

## A LOOK AT THE RECORD

In approaching the problems of future uses of solar energy, we should first fall back on the old device of taking a look at the record, namely, running through the history of various schemes that have been advanced to tap

the energy of the sun. I shall briefly describe 15 past and present approaches. This is by no means a complete catalog, but the examples do fairly well define the possibilities and the limitations of solar energy uses.

**(1) Windmills**

One might contend that to tilt with windmills under the guise of utilization of solar energy is to evade the issue, but since winds are caused by the uneven solar heating of sections of the earth the energy of the wind actually comes from the energy of the sunlight. Windmills, of course, have long been used, but we now find them to be vanishing, even in Holland. They will probably be useful for some time in isolated areas where the winds are favorable, but here again the potential is low and the source is intermittent.

**(2) Wave Motors**

Ocean waves are one step further removed from direct utilization of solar power because they are caused by wind. A few attempts have been made to devise wave motors, but, as far as I know, none of the devices has been successfully used for very long. Although wave motors can produce a substantial amount of power when the breakers are coming in, periods of extended calm make these motors more or less useless. The final blow comes when, reversing the situation, a violent storm washes the whole installation into the sea. Wave motors have never quite made the grade and, frankly, I doubt if they ever will.

**(3) Water Power**

Power from falling water is today's most important use of solar energy — even though it is an indirect use. The old-time inefficient, overshot water wheel passed from our scene a generation ago, but, where reasonably high heads of water are available, the modern turbine-driven hydroelectric plant will certainly stay with us for the foreseeable future. Where available, water power is the least expensive source of electric power. Unfortunately, in America, only about one per cent of our energy is supplied by hydroelectric power. If we stretched every resource where a reasonable head could be obtained, we might double this amount, but the proportion will always remain small.

**(4) Heating Buildings**

Several schemes[2] for heating buildings directly with solar energy have been tried experimentally and have met with a modicum of success. The work has been stimulated by the funds of the Cabot Foundation at the Massachusetts Institute of Technology, and other institutions have also been doing good work. Though substantial progress has been made, solar-heated houses are not simple dwellings. The first requisites are that there be a central heating system, that there be some means of storing heat for darkness and for those chill and cloudy days, and that there be a stand-by method of heating for the times when sunshine is temperamentally absent for substantial periods. The results to date show that, for the middle and lower latitudes in the United States, the break-even point for solar heating is an installation which will supply 75 to 80 per cent of the total heat required for an individual dwelling. If one puts in enough storage capacity to provide about that amount, he will save a little bit of money over a period of years. If one tries to make an installation which will supply *all* of the heat by solar means, then the costs will be more than if our presently accepted methods of heating homes were used. Perhaps some ingenious trick is in the offing to change this proportion of feasible heating, but it will not be particularly earth-shaking for the individual, because the capital costs of installation will inherently be greater than for gas or oil or coal, provided we continue to require the present level of comfort. In the national picture, however, solar heating is a very worthy venture because we use about one-third of our total fuel to heat our buildings; if a substantial number of the houses were largely heated by the sun, the total savings of our natural fuel resources would be significant.

**(5) Air-Conditioning Systems**

A few attempts[3] have been made to devise air-conditioning systems using solar energy for the cooling of buildings and for food refrigeration. These systems work essentially on the principle of the gas refrigerator, in which the latent heat of the condensation of a vapor to a liquid is on one side of the cycle and the reverse latent heat of evaporating a liquid to a vapor is on the other side of the cycle. The evaporating part of the cycle cools the house. The experiments thus far have all led to quite expensive equipment, and the economics is doubtful. However, the experiments should not be abandoned at this point, because a practical, balanced system, using both solar heating in the winter and solar cooling in the summer, might work out with a fair degree of economy. If it broke even for the individual home owner, then it would be a national benefit to use solar heat, since here, again, it would save a great deal of the material in the national fuel bin.

**(6) Hot Water Heaters**

There are at least several hundred solar water heaters in homes in the southern part of the United States; some of them are homemade and some have been commercially produced. The enthusiasts claim very satisfactory performance for these heaters; that there is seldom, if ever, a shortage of hot water and that they would not be without them. Some people found, however, that they could not always have a hot bath when they wanted it. On the whole, these devices, properly installed, are beyond being a novelty and are practical; they save a modest amount of fuel and will probably come into increasing use in the lower latitudes. Their use, however, will not make any great impact on the national supply of energy.

These first six approaches I have mentioned have not embraced any particular method for the concentration of solar energy; they have used the heat of the sun at about the potential at which it arrives at the surface of the earth. The development of the flat-plate accumulator has been very useful here. This flat-plate device, which has been described in various papers,[4] essentially depends on the greenhouse effect. The heat comes in, is caught in the medium, and is not allowed to escape. For both the heating and cooling of houses and for hot water heaters, this seems

VOL.
1
1957

to be a more feasible approach than to try to build parabolic mirrors or other concentrating devices. I shall now turn to some of the devices where concentrators of various kinds have been employed.

**(7) Cook Stoves**

Some of you will have heard of, or may perhaps remember, the reflector oven which was used in times past by campers for baking biscuits around a campfire. This idea has been refined to give, through the concentrating effect of a parabolic mirror focused on a cooking utensil, a quite satisfactory source of heat for the cooking of food — when the sun is shining. Several such gadgets have been devised. It is reported[5] that a practical device has been made and marketed in India at a cost of about $14, for use in regions where about the only kind of fuel is animal dung. In such areas solar cook stoves would be of great benefit, permitting the fertilizing value of the animal excrement to be put back on the soil where it really belongs. Progress in utilizing these stoves has been rather slow. In the first place, $14 is a lot of money to the people who should be reached. Second, it breaks into old customs, and, besides, when the sun is not shining at least moderately brightly, food cannot be cooked. But here is an area that is worth pursuing. The device could probably be made and sold for about $2.98 if large-scale manufacturing methods were used.

**(8) Heat Engines**

Numerous schemes have been devised for making heat engines that rely solely on the rays of the sun and which produce a moderate amount of power. All of them, as far as I know, use concentrating devices, such as cylindrical or parabolic mirrors, to build up the temperature in the container of the working medium. Air engines, steam engines, engines using sulphur dioxide as the working fluid and probably other engines, have been devised. All of these engines will produce a small amount of power — when the sun is shining. It looks as if they might be workable for intermittent use for sizes of from one to ten horsepower, without getting too large and cumbersome. The building and maintaining of these large reflecting surfaces, plus the inherently large engine per horsepower, make the heat engine a rather expensive device, but the experiments are sufficiently close to success to justify their continuance. One can visualize quite simple machines,[6] using containers for air or some other fluid, made of the modern, inexpensive, elastic plastics which could give slow but quite decisive pulsations that could be used for various things, especially for the pumping of water. In many areas of the world, irrigation is carried on in very slow and ineffective ways by using human or bullock power. To pump water from wells or streams, a very inexpensive engine of one or two horsepower, even though it only operated intermittently, could be quite effective. I visualize that by raising water at a leisurely rate, the economic level of a great many people could be improved.

**(9) Thermocouples**

Practically everyone who is familiar with laboratory experimentation knows of the thermocouple. If the ends of two wires of different composition are twisted together and heated (the other end of the wires being kept at a lower temperature), an electric potential is produced and a small amount of current can be withdrawn. The voltage produced is, in most cases, roughly proportional to the temperature difference between the two ends of the wires. Although each couple produces only a small fraction of a volt, a great many of them in series can give a quite substantial electromotive force. This is inherently a rather expensive method and the thermodynamic efficiency is low. Experimenters[7] have been able to get about a 3 per cent efficiency from this device, and a 10 or even a 15 per cent is hoped for. At least one very ingenious motor has been invented on paper in which the windings of the motor would be the thermocouple wires themselves.[8] This might help to improve the over-all efficiency of a solar motor of this kind. In special applications, it might have some future promise.

**(10) Photovoltaic Cells**

The photovoltaic cell is in a somewhat similar state of development. This is the sort of device which one uses as an exposure meter for photographic purposes. The Bell Telephone Laboratories have recently applied their findings in the transistor art to making a photovoltaic cell for power purposes.[9] The active surface itself consists of a silicon transistor material in the form of very thin wafers. If a number of these wafers are placed in series and exposed to the sun, a potential of a few volts is obtained and the electrical energy so produced can be used directly or stored up in a conventional storage battery. This can be thought of as a very special sort of trickle charger. The Bell System is now experimenting with these devices for supplying current for telephone repeaters in a test circuit in Georgia. As to cost, one radio company has produced a power pack using this type of photoelectric cell for one of its small transistorized radios. The cost of the power pack is $185, whereas the cost of a dry cell to operate the same radio for about 100 hours would be less than a dollar. So you can see we have a long way to go before this can be an economical source of power for all except the most special purposes. Here again we, as experimenters, should not be too easily discouraged, and the work should continue.

**(11) Production of Salt**

In some of the sunnier parts of the world, including our own West Coast, one sees many shallow ponds retained by dikes where sea water is being evaporated by the heat of the sun to recover the salt. This is a very old art, and I presume it will continue to have its small and useful place. These ponds might be called "open-pan" evaporators.

**(12) Distillation of Sea Water**

In semitropical regions, on the average day, the solar energy on an acre of ground is enough to evaporate about 10,000 gallons of water. The fresh-water condensate from such an operation would cover an acre of ground to the depth of 0.4 in. of water. These data give some hope for the economical recovery of fresh water from sea water

for domestic, industrial, or even irrigation purposes. The energy is free, but the apparatus to effect the evaporation and the subsequent condensation of vapor is not. Such apparatus must be large, and hence, with the present state of the art, expensive.

The equipment tried thus far for solar sea-water distillation resembles a greenhouse. The "boiler" is under glass. It is a shallow pan with a blackened absorbing surface, filled with sea water. The "condenser" is the inclined transparent surface (glass) which allows the solar radiation to come through and which doubles as the dissipater of the heat of condensation of the vapor by cooling owing to the ambient air or wind.

Recent work[10] in this country has led to an improved design of still which has operated with an efficiency of over 60 per cent. This begins to look interesting.

Still more interesting is some recent small-scale experimentation on multiple-effect solar stills. In this process, the heat absorbed by evaporation is recaptured in condensation and made to evaporate additional water. This is an old principle, long used in steam-heated evaporators, but it has not been applied to solar stills before. It is reported that a small ten-effect experimental solar still has been developed, which requires no expensive mechanical equipment and which, from a given area exposed to sunshine, can produce about six times as much water as a single-effect still.[11] If we could just get the apparatus at a very low cost per square foot, we might begin to get somewhere.

It has been suggested that the solution to low-cost equipment may be found in some of the thin, strong, transparent, inexpensive modern plastic materials. This is worthy of further investigation. Since I have not seen it mentioned anywhere, I would like to suggest that the recently developed air-supported plastic buildings might offer some interesting possibilities for solar stills. I am speaking of the type of structure which is used for housing radar antennas, called radomes.[12] These are plastic spherical structures of large dimension and are supported solely by very small internal air pressure. I suggest that someone look into the possible adaption of this idea.

The crying need for fresh water in many parts of the world, plus the zero cost of the sun's energy, make this solar distillation idea most intriguing. We must face the fact, however, that because of high apparatus cost fresh water so produced would still cost about 10 times too much to be practical for irrigation purposes. There is a great need to devise means of reducing the cost of apparatus before solar distillation can be really practical.

### (13) Solar Furnaces

The principal theme of this meeting has been the design and use of solar furnaces. It is an intriguing subject. Principal attention is being given to the solar furnace as a research tool. By various ingenious reflector and mirror systems, it is possible to get very high temperatures in very small areas, thus taking advantage of the high surface temperature of the sun even though it is 93 million miles away. The modern solar furnaces are essentially sophisticated refinements of the old-time burning glass. With the best system[13] that has yet been designed, it should be possible to obtain spot temperatures of nearly 4,000°C. This system is much better than any laboratory devices we have to date. Further, the entire equipment can be free from atmospheric contamination, it can be carefully controlled, and it can be shut off and on almost instantly. These are great advantages in certain types of research work, but the equipment is also very expensive. For instance, the solar furnace for the U.S. Air Force, which is now being designed and which we hope will be constructed soon in New Mexico, will cost several million dollars. The specimens to be heated can only be about five inches in diameter. Don't mistake me — I think this is very worth while because the solar furnace is a unique research tool and can give results which cannot be duplicated in any other way. I simply want to point out that this type of apparatus, while of great potential value for research, is hardly practical as a power source in the ordinary sense of the word.

### (14) Biological Growth

Plants, of course, take the solar energy as it comes and, by a mysterious process which we do not yet understand, succeed in synthesizing the various types of chemical compounds which make up plants and which are eventually, in many cases, eaten by animals and by man. Most of the plants, however, are highly inefficient as energy converters. The energy storage efficiency of the average plant is probably somewhat closer to one-tenth of one per cent, even under fairly favorable growing conditions.[14] Some of the simpler forms of life, particularly those that can be handled in water suspensions, show substantially higher efficiencies. One of these, which is a favorite of experimenters, is the *Chlorella*, a genus of algae. *Chlorella* absorbs and uses wave lengths of certain parts of the solar spectrum with a fairly high efficiency. It grows very luxuriantly if the water medium is kept at the right temperature and composition. It is also a very good protein producer and looks as if might be favorable for foodstuffs, particularly for animals.

### (15) Artificial Photosynthesis

Photosynthesis represents the largest unexplored area in the field of possible utilization of solar energy. Although we need much more research on biological materials to arrive at an understanding of the photochemical process, I do not think we will satisfactorily solve our energy-capture-and-storage problem by employing living substances. They are too delicate, complicated, and inefficient to serve this particular purpose. Perhaps we will use organic but inanimate materials, or inorganic materials, or both. When we learn to produce simple sugars and alcohols and other compounds from carbon dioxide and water, through some well-understood and efficient process utilizing only solar energy and inanimate catalysts, we will have made a good start. But this may not necessarily be the best answer. It is estimated[15] that the maximum possible efficiency of solar energy storage through the organic compound route would be about 12.5 per cent. That might

VOL.
1
1957

not be too bad, but we would like to do better.

Many radiation-induced inorganic chemical reactions have been investigated. One[16] of the more interesting of these is the reduction of water, using cerous and ceric perchlorate as a catalyst, to produce gaseous hydrogen and oxygen, albeit, thus far, in only minute concentrations. Since this is a straight reduction reaction, you might not wish to class it as photosynthesis, but it serves the same purpose. If hydrogen and oxygen could be produced very cheaply from water, in large quantities, they certainly could be used for fuel.

Many other radiation-induced chemical reactions have been explored slightly, but the field is still wide open for new discoveries. In general, as far as photosynthetic and similar processes are concerned, I would say that here is a tremendous opportunity for basic research which has barely been tapped. Interest in the field is rising, but it does need the stimulus of a major national research program.

## NO PANACEA

From the foregoing examples, you may have come to the conclusion that there are several fairly interesting possibilities for the use of solar energy but that none of them represents a panacea for the future energy demands of the world. In my opinion, that is the correct impression to carry away at this time. But the situation should be a challenge and not a discouragement. There is much fruitful work that can be done at this time — even before great new basic discoveries have been made.

Hundreds of millions of people live in parts of the world where sunshine is plentiful, where the technological level of the society is low, and where other forms of power are either nonexistent or very expensive. I am thinking of portions of the agricultural areas of India, China, Indonesia, the Middle East, Africa, and Central and South America. In some of these regions, solar cook stoves and hot water heaters should be particularly helpful. A solar house heating system, even though not always adequate, would represent a great advance in the standard of living for many. An inexpensive solar refrigerator should certainly help in the preservation of food. Simple heat engines to pump water for irrigation would often be a great boon. Widespread cultivation of the special organisms such as *Chlorella* might help to remove millions from the semistarvation list. Near seacoasts or brackish lakes, solar stills for the production of fresh water could bring great benefits.

Though these are all possibilities, they will not readily become realities. In the first place, all the apparatus used must be simple and very inexpensive — preferably of the make-it-yourself variety. Secondly, the use of any of these new devices will mean changes in old customs and methods of doing things. Such changes are usually resisted and come very slowly.

Despite the barriers and drawbacks, here is one way to promote the well-being of many people in the world. I feel that this country would be well-advised, through its Mutual Aid Program, or what was formerly known as Point IV, to substantially increase its efforts in helping these countries to make fuller use of solar energy devices. It seems to be a natural way to make friends — as well as to be of great aid to the people themselves.

When we turn to our own economy, we find a very different situation. We, along with most of Western Europe and the metropolitan areas of nearly *all* the world, have built up a very complicated technology. We use an inspiring array of power-hungry machines that require a continuous, concentrated energy supply. Discounting the small percentage of hydroelectric power, we have come to rely almost entirely on the fossil fuels — coal, oil, and gas. The daily supply of sunshine is hardly a capable competitor to these sources — when they are available.

But these fossil fuels — coal, gas, and oil — will eventually be depleted and probably sooner than most people think. Every indication is that the petroleum production will begin tapering off as far as this country is concerned, in this generation. We will have to begin relying more and more on foreign petroleum sources. Remember that the use of power is rising at a rapid and exponential rate, and although we still have a lot of coal, oil, and gas in the ground, the demand is catching up with great leaps and very long bounds. So it is time for us to begin to become constructively worried about it. The fossil fuels will become too precious to use as fuel because they will have such a high value in the chemical synthesis field. They will become analagous to wood, which is now much too precious to be used to any great extent as fuel.

## THE NEWER ENERGY SOURCES

What, then, is the answer for America? Fortunately for us, we are entering the atomic age. We have a partial answer at hand now in the form of nuclear power. The fission reaction, under controlled conditions, using uranium (or thorium) is on the verge of being practical, that is, of being able to produce power at prices competitive with other sources. As you know, Great Britain is starting on a campaign of building and using a number of nuclear reactors. The current designs are already practical in Britain because the unit cost of power there is about twice what it is in the United States. I predict that within a decade the cost of electrical power produced from nuclear reactors will also be competitive with other sources in the United States. This will not come overnight; the growth of nuclear power will come relatively slowly, but it will be of increasing importance as the years go on. It has come just in time. At present it will not be possible to produce power on an economic basis except at quite large installations, but I am of the opinion that as we develop the art, we will be able to produce power economically in smaller and smaller packages which will be useful in areas of limited use, or in isolated regions.

Throughout the world, the known reserves of uranium and thorium are enough to supply the necessary energy, even with the anticipated rise in use, for some 500 years, and of course we have not yet found nearly all of the deposits which undoubtedly exist. Further, a tremendous amount of uranium and thorium is in deposits too low-grade to be usable now. For instance, the average granite,

which makes up such a large proportion of the earth's crust, contains about 4 grams of uranium per ton. If this could be extracted in some economical fashion and used in a nuclear power reactor, each ton of granite would then produce as much energy as 50 tons of coal. We still have the little research task of trying to find out how to extract that minute amount of 4 grams of uranium per ton (that's about 4 parts per million) from these forbidding rocks.

The next step will probably be the production of power from the controlled thermonuclear, or fusion, reaction — the hydrogen bomb reaction. This is going to be really difficult, but those who are working on it now seem to be breathing an air of optimism. Because of the inherent nature of the process, however, I anticipate that it can be used only in very large installations. It will be a highly specialized operation and will require very expensive equipment. It will not be a very versatile method. However, if this is successful, the power will eventually be very cheap at the source, although the distribution cost to distant places will always remain relatively high. Further, because the raw material will essentially be heavy hydrogen or deuterium, which is present in all water, including sea water, the supply will be inexhaustible. So, just in time, we seem to have tapped the sources of power which will save our industrial civilization.

## FILLING THE GAPS

You undoubtedly have the idea by now that I am being a traitor to my subject — that I am canceling out the use of solar energy for our sophisticated civilization. But wait. We still have automobiles and we still have to eat. The nuclear reactors I have been speaking of do not produce gasoline; they only produce heat and electrical power. Perhaps someone will find a way of storing electrical energy in a very economical, light, and compact manner for use in automobiles. The performance of electrochemical storage batteries has been carried to about as high a state of perfection as the laws of nature will allow, and they are still tenfold off, as far as weight and cost are concerned, as a practical means of storing energy for automobiles. The present prospects are that, for the portable power plants such as the automobile, we will still be calling for liquid fuel — at least for a long, long time. This is where artificial photosynthesis will come in.

We do not yet know what catalyst we must use; we do not yet know any of the details of the process; but after we have conducted enough research perhaps we can take carbon dioxide and water and the rays of the sun and make carbohydrates and/or hydrocarbons for liquid fuels at low cost. Then we will be well on our way to solving the problem of liquid and gaseous fuels for all time to come. This is the "blue chip" possibility. But until we do acquire that necessary research knowledge, we cannot be satisfied that we have solved the problem of the energy for the future.

Even though they may not all be blue, there are other solar chips that we might profitably pick up for playing the game of tomorrow's industrial society. By way of recapitulation, solar heating and cooling of houses and heating water will be moderately worth while where the climate is favorable. The raising of unconventional foodstuffs, such as *Chlorella,* by concentrated methods may prove to be a real necessity as the world population increases. Solar furnaces which produce high temperatures are going to be used rather extensively for research work. Photovoltaic cells will find substantial use in some special situations.

Finally, I can visualize the sun's rays as an important part if not the sole source of energy for the production of inexpensive fresh water from the sea. This is a process, however, where some combined efforts are called for. There are many valuable mineral elements in sea water, albeit in dilute concentrations. As our mineral resources approach depletion we are going to become more interested in their recovery. At present we are only recovering two, bromine and magnesium. Eventually we should recover a dozen or more. Is it feasible to think of a physical-chemical process plant where sea water and sunshine are the input materials and fresh water plus a dozen separated mineral substances are the products? By such an approach, could these necessary materials for civilization be produced economically? I do not know the answers but I trust that someone, some day, will make a serious effort to find out.

## REFERENCES AND NOTES


1. For more detail, the reader is referred to the author's analysis of P. C. Putnam's data in *Industrial and Engineering Chemistry* 46: 2446-457, Dec. 1954.
2. H. C. Hottel, "Residential uses of solar energy." (In *Proceedings of the World Symposium on Applied Solar Energy, Phoenix, Arizona, 1955,* pp. 103-12.) Harold Heywood, Austin Whillier, G. O. G. Löf, Maria Telkes and Raymond Bliss, "Solar house heating." (*Ibid,* pp. 113-58.)
3. G. O. G. Löf, "Cooling with solar energy." (*Ibid,* pp. 171-89.)
4. H. C. Hottel, "Residential uses of solar energy." (*Ibid,* pp. 103-12.) (A good summary discussion of flat-plate collectors is given in pp. 104-107.)
5. Farrington Daniels. *Science* 121: 121, Jan. 28, 1955. Also, M. L. Ghai, "Applications of solar energy heating, air conditioning, and cooking." (In *Solar Energy Research,* ed. by Farrington Daniels and John A. Duffie, Madison, Univ. of Wisconsin Press, 1955, pp. 63-67.)
6. Farrington Daniels, "The sun's energy." *Scientific Monthly* 82(5): 247-54, May 1956. Refer particularly to pp. 250 and 251.
7. Maria Telkes, "Solar thermoelectric generators." (In *Solar Energy Research,* pp. 137-42.)
8. Marcus D. O'Day, "Some new approaches to solar energy utilization." Paper presented at ARDC Science Symposium, Cambridge, Mass., Oct. 8-9, 1955.
9. G. L. Pearson, "Electricity from the sun." (In *Proceedings of the World Symposium on Applied Solar Energy,* pp. 281-88.)
10. Maria Telkes, "Distillation with solar energy." (In *Solar Energy Research,* pp. 111-18.)
11. Work of M. Telkes, "Solar distillation of saline water." *Science,* p. 1287, Dec. 18, 1956.
12. Murray Kamrass, "Pneumatic buildings." *Scientific American* 194: 131-32, June 1956.
13. Félix Trombe, "Development of large-scale solar furnaces." (In *Solar Energy Research,* pp. 169-71.)
14. Farrington Daniels, "Efficiency of photosynthesis." (In *Solar Energy Research,* pp. 175-77.)
15. A. W. Fisher, Jr., "Economic aspects of algae as a potential fuel." (In *Solar Energy Research,* pp. 185-89.)
16. Lawrence J. Heidt, "Photochemistry of cerium perchlorates in dilute aqueous perchloric acid." (In *Solar Energy Research,* pp. 203-19.)


VOL. 1 1957

# CONTROL OF THERMAL ENERGY FROM A HIGH TEMPERATURE SOURCE

By BERTRAM BUSSELL, K. G. LINDH, R. D. KOPA, and G. E. GWYNNE

University of California, Los Angeles

**A unique high temperature energy source is described in which radiation from a graphite surface at 5,000°F is controlled by means of water-cooled shutters. Since the energy source available was capable of less than 300 kw power output, storage of energy was needed and was accomplished by means of an insulated muffle. Means of controlling the heat output and of regulating the duration of the radiation pulses are described.**

## INTRODUCTION

The necessity of measuring the response of specimens of aircraft structures to transient external heating under controlled conditions has made it necessary to construct a device capable of supplying and regulating intense heat inputs to relatively large areas. The particular requirements which the heat source described herein was designed to satisfy are as follows:

(1) Short time heat input to specimen with emissivity = 1.0 is to be $10^6$ Btu/hr/ft$^2$.

(2) The surface receiving the heat input is to be a 3 ft by 5 ft plane rectangle or of such a size and shape that its boundaries will fit inside of a 3 ft by 5 ft rectangle.

(3) A system of controls shall be included which will allow the heat rate at the surface of the specimen to be various kinds of functions of time. The function of principal interest requires that the radiant flux increase from zero to maximum in a minimum of 0.20 sec.

The only significant amount of power available for the operation of such a source of thermal energy is a d.c. diesel generator rated at 288 kw (180 volts, 1600 amps), continuous operation. The power required for the specified heat flux over a 3 ft by 5 ft rectangular area is approximately 5,000 kw. It is therefore apparent that some method of energy storage and controlled release is required. The method chosen involves the storage of energy in the thermal form in an electrically heated graphite plate (or "element") insulated from the surroundings. The release of the energy to the specimen is accomplished by rapidly moving the heated graphite element from its insulated position to a position directly opposite the specimen. Control of the resulting radiation heat transfer between the element and the specimen is furnished by a system of shutter blades placed between the element and the specimen. The radiant energy received by the specimen is then a function of (1) the initial temperature of the element as it is removed from the insulation, (2) the configuration and relative positions of the element, shutter blades, and specimen, (3) the total emissivities of all surfaces involved, (4) the degree of rotation of the shutter blades, and (5) the integrated effect on the element surface temperature of all heat transfer from the element after being removed from the insulation.

## HEATING ELEMENT

The heating element, whose surface temperature is to reach 5000°F, is constructed of ¾-in. graphite sheet stock

FIG. 1 — Graphite heating element.

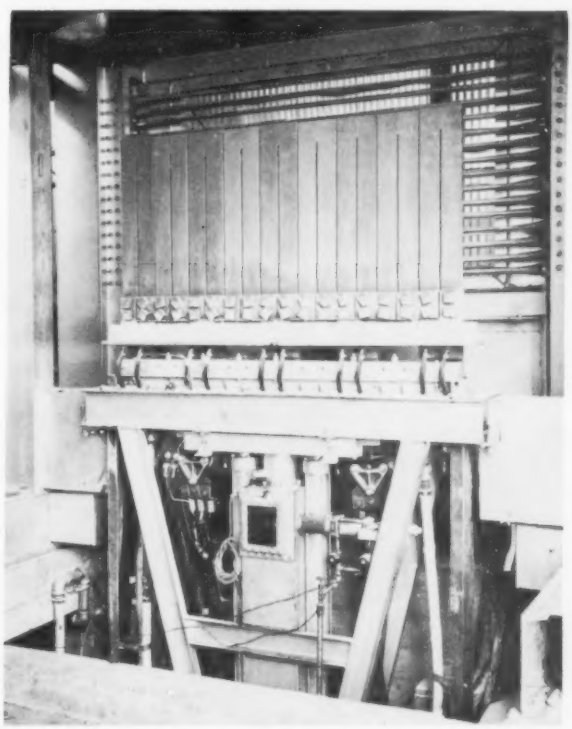

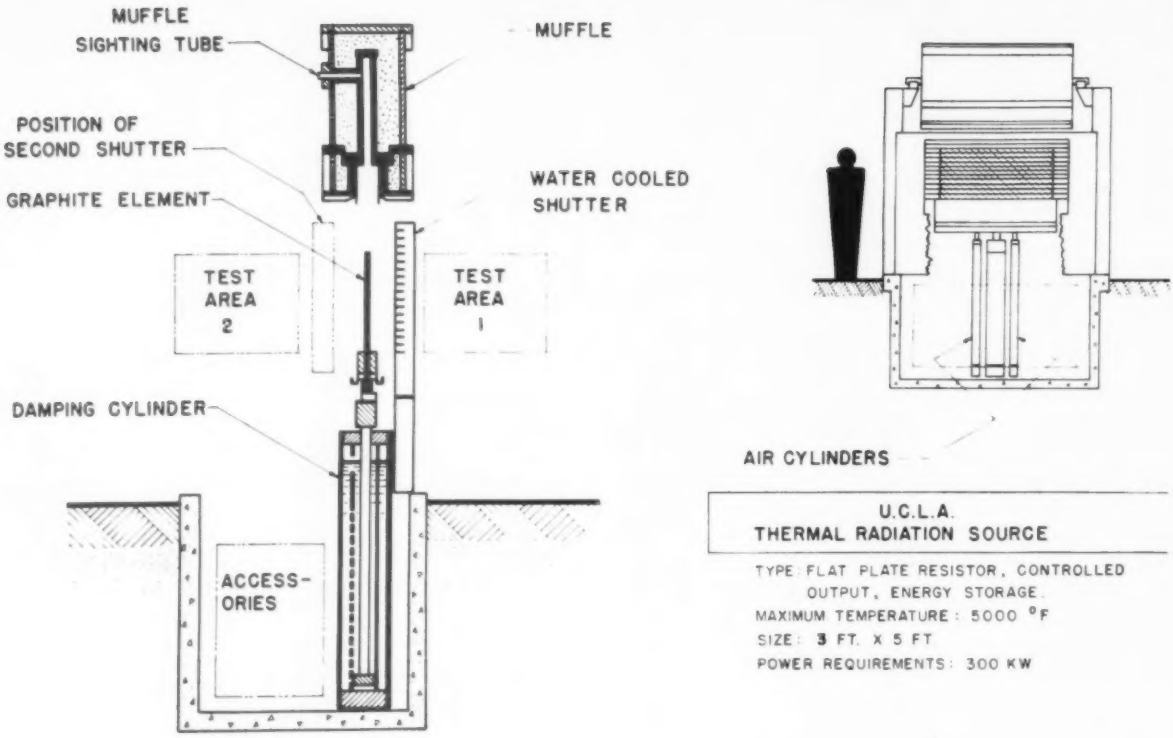


FIG. 2 — Schematic of heat source.

in such a manner that its individual elements are connected in a series path (maximum resistance) (Fig. 1). This element (approximately 4 ft x 5 ft) is held in a vertical position and is supported along its lower edge by a series of water-cooled clamps. In order to store the energy and at the same time prevent rapid evaporation of the heating element, the heating element is stored in a double-walled muffle (Fig. 2) placed above it. This muffle consists of a graphite and carbon inside liner surrounded by a transite outside shell, and the space between is filled with lampblack. During operation, the element temperature is measured with an optical pyrometer which sights through a ¼-in. hole in the muffle wall. This pyrometer has a telescope attached and is placed at a remote location for personnel safety.

In order to raise and lower the element, it is mounted on the piston rods of two vertical pneumatic cylinders which allow the element to travel 54 in. The velocity of the element in the up direction (into the muffle) is determined by the air pressure in the pneumatic cylinders and the counteracting viscous damping force in an hydraulic cylinder which also is connected to the element. This hydraulic cylinder serves two functions. The first function is that of a rigid member, giving structural support to the heating element. The second function is as a dashpot to control the free-fall drop velocity of the element and prevent shock. This cylinder is constructed in such a way that the damping is small over the initial part of the strokes, but quite large near the end of the strokes, thereby allowing rapid raising and lowering of the element without subjecting the relatively fragile graphite plates to high shock loads at the end of strokes. This downstroke can be accomplished in ¾ sec, with a maximum deceleration of $0.5g$. At the bottom of its stroke, the heated element is directly opposite the test specimen which is to receive the thermal energy input. In order to vary this input, a set of shutter blades (similar to venetian blinds) is placed between the specimen and heat source. This shutter is composed of 16 hollow aluminum blades each of which is mounted on a pair of swivel joints to allow for an angular rotation of the blades. By rotating the blades, the radiant energy falling on the specimen is varied. The blades are linked together by means of gears and lever systems actuated by a single link which is controlled by a servomechanism. In order to maintain a low temperature in the aluminum blades, cooling water is pumped through the blades at the rate of 300 gal per min. The total heat capacity of the water in this closed system coolant supply and the high flow rate assures a small temperature rise of the water, and consequently in the shutter blades. In addition, the blades themselves are polished to assure a fairly high reflectivity over the emissive spectrum of the source.

## CONTROLS FOR SHUTTER

The radiant energy falling on a test specimen is also picked up on a specially designed radiometer (Fig. 3) which is the main component of the feedback system in controlling the position of the shutter blades. The sensing element of the instrument is a coil of 0.002-in. constantan



VOL.
1
1957

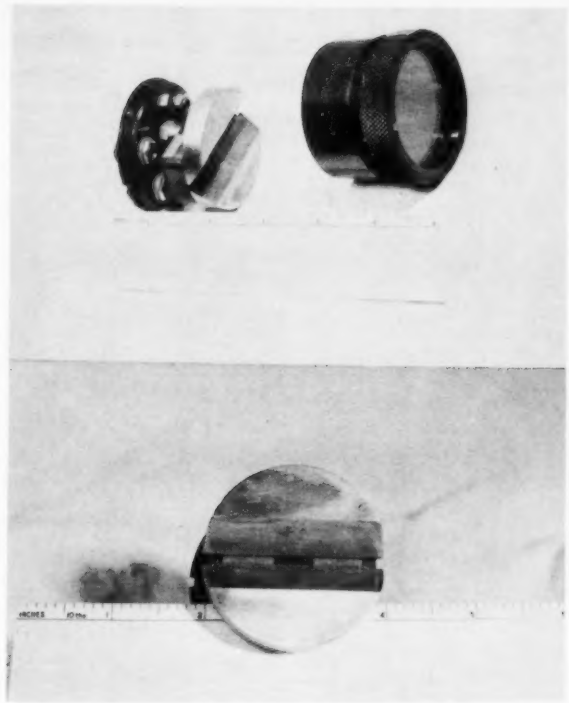

FIG. 3 — Radiation pickup device.

wire wound at 110 turns per inch about a slotted, insulated copper block. The winding is silverplated over three-quarters of the coil, so as to give 110 silver-constantan thermocouple junctions per inch on each of two sides of the copper block. The copper block is mounted in a housing so that only one set of junctions faces out, and this set is blackened to give an absorbtivity $\cong 1$. The front plate of the radiometer housing is designed to have a high reflectivity over the entire frontal area except for the area through which radiation "sees" the thermopile. This radiometer has a time constant $\cong 0.05$ sec. The output of the radiometer is fed through an amplifier and then to a gate-winding of a magnetic amplifier, where it is balanced against the input from a function generator which is signalling the desired function. The error signal is amplified and then is used to control a servomotor which positions the shutter blades. In order to prevent excessive overshooting of the shutter position, a rate pickup device is connected to the shutter mechanism, and this signal also is fed to a gate-winding in the magnetic amplifier in order to modify the information going to the servomotor. The function generator is a unit which consists of a standard oscilloscope on whose face is attached an opaque mask of the desired output waveform. A housing attached to the face of the oscilloscope tube contains a photomultiplier tube which constrains the electron beam trace to move along the edge of the mask as it traverses the screen from left to right. This is accomplished by causing the beam to rise if there is insufficient light received at the phototube, and causing it to fall if there is too much light received at the phototube. The voltage which is caused to be imposed on the vertical plates of the oscilloscope is then a linear function of the shape of the mask, and is therefore the desired signal.

## REMOTE STATION CONTROL

The entire operation is controlled from a remote station which has facilities for manual and automatic control of the various steps in a testing program. Integral with the control station are numerous safety interlocks which are used for both personnel and equipment safety. These interlocks perform such tasks as preventing the element from being withdrawn from its muffle, or de-energizing the source if an unsafe condition presents itself. The cycle of operation is as follows:

(1) The cold graphite plate is raised into its muffle.

(2) Power is turned on and the element is brought up to temperature.

(3) Power is turned off and the shutters are closed.

(4) The element is lowered rapidly to a position opposite the shutters.

(5) The shutter blades go through a specified cycle.

(6) The plate is raised into the muffle for reheating.

The tests with the source are intended as experimental tests of thermal stress studies. Other uses to which the source may be put concern the compilation of basic data in the area of physical properties of materials at elevated temperature as well as thermal stress studies of structural configurations too complex to warrant theoretical analysis.

# TEMPERATURE AND FLUX VS. GEOMETRICAL PERFECTION

By TIBOR S. LASZLO

Fordham University*
New York City

This paper describes the problems involved in determining the energy flux and temperature existing at the focus of a solar furnace. Theoretical values are readily calculated from the geometry and materials of the system, but actual measurements are much more difficult to obtain. A method is described by which brightness temperature, as measured by an optical pyrometer, and normal incident solar flux, measured simultaneously, can be converted into black-body temperatures.

TABLE I

SOLAR FURNACES IN OPERATION OR UNDER CONSTRUCTION

| Organization | Location |
|---|---|
| United States: | |
| Army Medical Corps | ——— |
| Arizona State College | Tempe, Ariz. |
| Arthur D. Little, Inc. | Cambridge, Mass. |
| Assoc. for Applied Solar Energy | Phoenix, Ariz. |
| Bureau of Mines | Morgantown, W. Va. |
| California Institute of Technology | Pasadena, Calif. |
| Convair | San Diego, Calif. |
| Conn, W. M. | Kansas City, Mo. |
| Curtiss-Wright Corp. | Wood-Ridge, N.J.* |
| | Quehanna, Pa. |
| duPont | Wilmington, Del. |
| General Electric | Philadelphia, Pa. |
| | Cleveland, Ohio |
| | Richland, Wash. |
| B. F. Goodrich | Brecksville, Ohio |
| Holloman Air Force Base | Alamogordo, N.M. |
| Kennecott Copper | Salt Lake City, Utah |
| Lockheed Aircraft | Van Nuys, Calif. |
| Mass. Institute of Technology | Cambridge, Mass. |
| National Bureau of Standards | Washington, D.C. |
| Quartermaster Research Center | Natick, Mass. |
| Sandia Corp. | Albuquerque, N.M. |
| Stanford Research Institute | Menlo Park, Calif. |
| University of California | Los Angeles, Calif. |
| University of Minnesota | Minneapolis, Minn. |
| University of Utah | Salt Lake City, Utah |
| Belgium: | |
| Inst. Royal Météorologique | Uccle |
| Canada: | |
| National Defense Research Board | Ottawa |
| France: | |
| CNRS | Montlouis |
| CSRSAA | Bouzareah, Algiers |
| Japan: | |
| Government Industrial Research Inst. | Nagoya |
| USSR: | |
| Heliolaboratory of the Acad. of Sc. | Tashkent |

*Formerly of Fordham University, New York City.

A few years ago the solar furnace was only a scientific curiosity in high temperature research. Very few investigators knew of its existence and only the researchers who used it were aware of its potentialities. In 1954 Conn[1] listed five locations in the world where solar furnaces were available. To these may be added the Russian Heliolaboratory at Tashkent. Of these six locations only two were in the U.S.A. and only one furnace was used for high temperature investigations.

In recent years the number of solar furnaces has increased considerably. In Table I are listed the solar furnaces in use or under construction at present.

In the U.S.A. the number of furnaces increased from the 2 in 1954 to 26 in 1957. When surveying this list we may divide the furnaces into two groups. The first group would contain those which are used chiefly for fundamental high temperature research. Furnaces operated by academic institutions belong to this category. In the second group we may list furnaces used for applied research by various branches of the armed forces and by industrial organizations. Obviously this division cannot be sharp, and very likely several of the furnaces are used at one time or another for both types of work.

This arbitrary grouping serves only to show why investigators turned to the use of solar furnaces in recent years. Our fundamental knowledge in the field of high temperature is very meager, while recent developments in technology require equipment capable of operating at much higher temperatures than ever before.

The suitability of solar furnaces for both fundamental and applied high temperature research has been pointed out before.[2] Less known is the fact that its performance characteristics are very little explored, and, as a consequence, our efforts to improve the performance of solar furnaces and establish them in high temperature research do not have the necessary experimental foundation.

The two performance characteristics of the greatest importance are the distribution of heat flux and the temperature at the focal zone. Before discussing the prob-

*Present address: Curtiss-Wright Corporation, Wright Aeronautical Division, Development Metallurgy Division, Wood-Ridge, N.J.

VOL. 1 1957

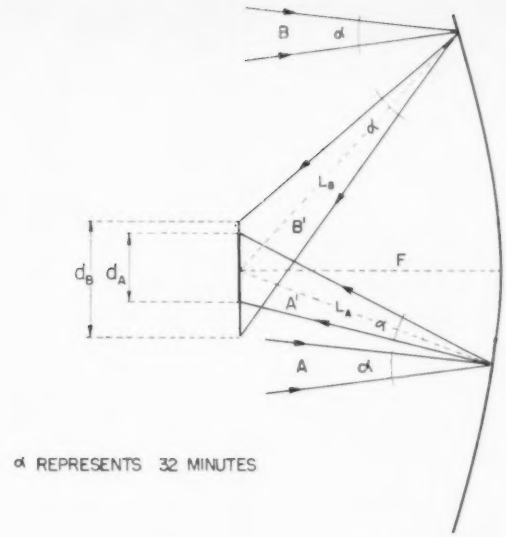


FIG. 1 — The formation of the solar image.

lem of measuring these quantities, let us review the formation of the focal zone in a paraboloidal solar collector. Fig. 1 illustrates the real path of solar radiation in a large-aperture reflector. The image of the sun is defined by an angle of 32′ at any point of the reflector. The recreated image at the focal zone is naturally defined by the same angle. At a point close to the rotational axis $F$ of the reflector, image $A$ is reflected, forming cone $A'$. The intersection of the sample with cone $A'$ forms the base of the cone, which is approximately a circle of diameter $d_A$. The axis of cone $A'$ is $L_A$. A point farther away from $F$ reflects cone $B'$. The base of this cone is an ellipse with a major axis $d_B$. Since $L_B$ (the axis of cone $B'$) is longer than $L_A$, the area of ellipse $d_B$ is greater than the area of circle $d_A$. As the total energy contents of both cones are equal, the energy density is greater in circle $d_A$ than in ellipse $d_B$.

A further temperature gradient results from the fact that the central part of the focal zone receives radiation from all points of the reflector, whereas the outer part of the zone is heated only by reflection from the peripheral portions. Accordingly, the peripheral parts of the reflector make no appreciable contribution to the highest flux zone.

It should be pointed out that in this discussion the mirror was considered as a perfect paraboloid. Even under this purely theoretical condition we find that the energy flux has a maximum value at the center of the focal zone, and it decreases sharply away from the center. This very steep flux drop gives rise to a number of advantages and disadvantages. It is an advantage, for instance, to be able to approach the heated sample very closely, but it is a disadvantage not to be able to maintain the entire heated portion of the sample at uniform temperature. The magnitude of the flux at the focus of the paraboloidal solar furnace is determined by the following parameters:

(1) normal incident solar flux,
(2) aperture of the reflector,
(3) focal length of the reflector,
(4) shadowing factor,
(5) coefficient of reflection of the optical system,
(6) geometrical perfection of the reflector.

With the exception of the normal incident solar flux, all parameters are constant for one furnace. If these constants are once determined, thereafter only the measurement of the normal incident solar flux has to be performed, in order to calculate the flux at the focal zone at any particular time. Since the flux is related to the temperature, the latter can also be calculated provided some additional information is available.

The intensity of the solar radiation, the normal incident solar flux, can be measured with thermopile-type radiometers. The Eppley normal incidence pyrheliometer is used by the U.S. Weather Bureau for such measurements. For the present measurements an Eppley thermopile was used, calibrated for normal incidence at the Blue Hill Observatory. This instrument was mounted directly on the solar furnace. The alignment was made by putting into the instrument mount a 7-in. collimator tube with a small orifice at the front end and a transparent screen with concentric rings at the back. When the image of the orifice appeared at the center of the screen the collimator tube was replaced by the thermopile. Once lined up, the thermopile remained focused on the sun during the measurement since the mirror followed the apparent rotation of the sun, controlled by an electronic guiding mechanism.[3] In Fig. 2, on the right, the Eppley thermopile is shown mounted on the furnace, while the collimator tube,

FIG. 2 — The mounting of the pyrheliometer.

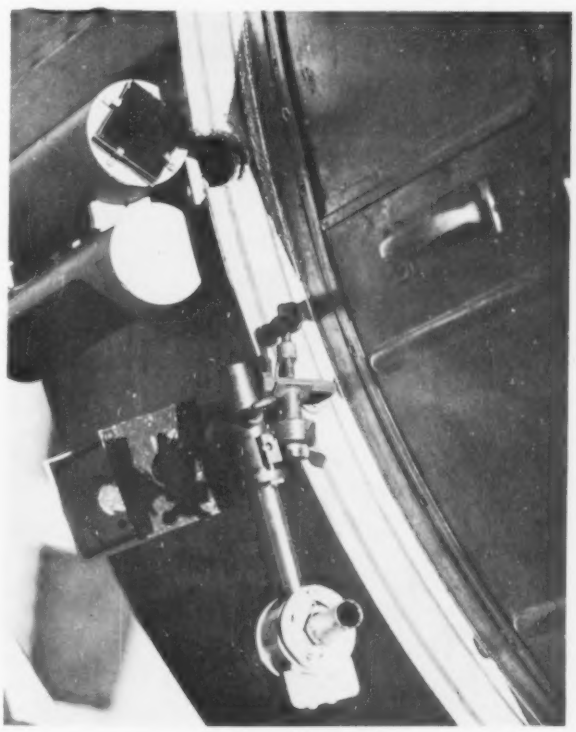

with filters for the phototube assembly of the guiding mechanism, is shown on the left.

Aperture and focal length can be easily measured. On the army searchlight mirrors the focal length is engraved on the edge.

The shadowing factor indicates how large an area of the mirror is shaded by the sample holder, temperature control, and other mechanisms necessary to operate the furnace. Efforts were made to measure this surface by mounting a photosensitive paper perpendicular to the optical axis of the mirror, but no commercially available paper could be found which would differentiate between direct sunlight and daylight and at the same time have the required low speed. Some promising experiments have been carried out at Fordham University towards the development of such a paper, but, for the present measurements, the size of the shadow was determined by hand-tracing it on a paper placed perpendicular to the mirror axis. The area of the rather intricately shaped shadow thus obtained was determined by graphical integration, and was found to be 1217 $cm^2$ or 6.7 per cent of the aperture surface of the mirror. It should be noted that this value represents a loss far greater than 6.7 per cent in flux since the central portion of the mirror which is shaded the most contributes relatively more to the high flux part of the focal zone than the peripheral portions. The shadow factor includes also the loss of reflecting surface due to the observation hole cut at the center of the mirror.

The coefficient of reflection values for stellite are available in the International Critical Tables[4] for wavelengths 0.45 to 4.00 microns. It seemed necessary, however, to measure the actual coefficient of reflection of our mirror in order to obtain a single value applicable to the spectral distribution of solar radiation and in order to determine whether the corrosion, visible on the mirror, changed the original value.

The aforementioned Eppley thermopile was used for the reflection coefficient measurements. A method had to be developed for eliminating the error due to the concentrating effect of the paraboloid mirror. The trigonometric approach used is illustrated in Fig. 3. $D$ is the radius of the receiving disc of the pyrheliometer, $x$ is the radius of the paraboloidal section which reflects on the pyrheliometric disc, and $a$ is the distance of the latter from the surface of the paraboloid. Since the focal length $(a + b)$ of the paraboloid is very large (64.77 cm) and $x$ is usually very small (0.3 cm), it is permissible to consider the paraboloidal section as a circle of radius $x$. Accordingly, the degree of concentration can be calculated in the following way:

FIG. 3 — Reflection coefficient measurement.

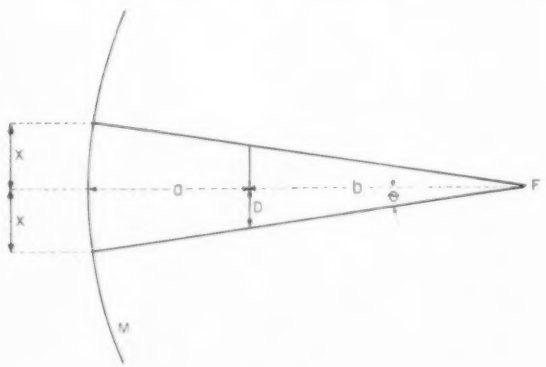


$$\tan\theta = \frac{D}{b} = \frac{x}{a+b} \qquad [1]$$

$$x = (a+b)\frac{D}{b} \qquad [2]$$

$$\text{Degree of concentration} = \frac{x^2}{D^2} \qquad [3]$$

Measuring the normal incident radiation and the radiation reflected by the mirror, the degree of concentration can be calculated and the measured reflected radiation corrected. The ratio of incident and reflected radiation gives the coefficient of reflection. The values obtained are shown in Table II. The over-all coefficient of reflection was calculated as 70 per cent, and this value was used in the flux calculations. For these measurements it was assumed that the coefficient of reflection is independent of the angle of incidence as long as this angle is less than 60°.

TABLE II

COEFFICIENTS OF REFLECTION OF THE STELLITE-COATED 60-IN. DIAMETER PARABOLOID MIRROR

| Location on the Mirror | Coefficient of Reflection |
|---|---|
| Edge | 0.68 |
| Edge | 0.66 |
| Edge | 0.66 |
| Edge | 0.62 |
| Edge | 0.68 |
| Edge* | 0.61 |
| Edge* | 0.63 |
| Edge* | 0.62 |
| Middle | 0.72 |
| Middle | 0.70 |
| Middle | 0.73 |
| Middle | 0.73 |
| Middle | 0.71 |
| Middle | 0.71 |
| Center** | 0.59 |
| Center | 0.78 |
| Center | 0.74 |
| Center | 0.66 |
| Center | 0.76 |
| Center | 0.72 |

*Stellite coating peeled off approximately 2 sq in. surface, not considered in calculation.
**Not considered in calculation.

If we assume that the mirror is a perfect paraboloid, we can calculate from these data the flux at the focal zone. It has been shown[5] that the magnitude of the flux at the image is:

$$P_{calc.} = 46.1 \times 10^3\, n\, \eta_r\, \eta_s \sin^2\theta \qquad [4]$$

where:

$P_{calc.}$ is the calculated flux at the focal zone,
$n$ is the normal incident solar flux,
$\eta_r$ is the coefficient of reflection of the reflector,
$\eta_s$ is the shadowing factor,
and $\theta$ is the rim angle of the mirror.

Since all these have been measured, the flux $P$ can be calculated. For our furnace $P_{calc.} = 382.35\, n$ cal/$cm^2$/sec.



VOL. 1 1957

The assumption that the mirror is a perfect paraboloid cannot, of course, be justified experimentally. The real flux value at the focal zone, therefore, can be expressed as:

$$P = \gamma P_{calc.} \qquad [5]$$

where $\gamma$ is the index of geometrical perfection. For the determination of $\gamma$ the flux at the focal zone has to be measured as well as calculated.

The measurement of the flux presents considerable problems. Flux measurements at the focal zone of the solar furnace were reported by Farber using a water-cooled calorimeter.[6] This method did not appear applicable to our work mainly because we intended to measure the change of flux throughout the entire focal surface. This required an instrument with a small sensing area that could be moved continuously across the focal zone. This instrument in turn requires an instrument of very fast response — a response which may be considered independent of time for the applicable speed of motion. Gardon[7] designed an instrument with fast response for measurement of high fluxes. For our measurements Dr. Gardon loaned us a water-cooled version of his instrument. The diameter of the constantan receiving disc is 0.116 cm, thus permitting a very fine measurement of the flux distribution. The instrument was calibrated at the Material Laboratory of the New York Naval Shipyard over part of its range. Although this calibration showed a linear correlation between flux and millivolt output of the instrument, we found it advisable to reduce the flux during the measurements so as to remain within the range of calibration. A filter cannot be used for this purpose because it exhibits preferential absorption in various parts of the spectrum and, accordingly, the sensitivity would vary with spectral distribution. A diaphragm cannot be used at the radiometer because it would not withstand the high flux and would increase the shadow factor.

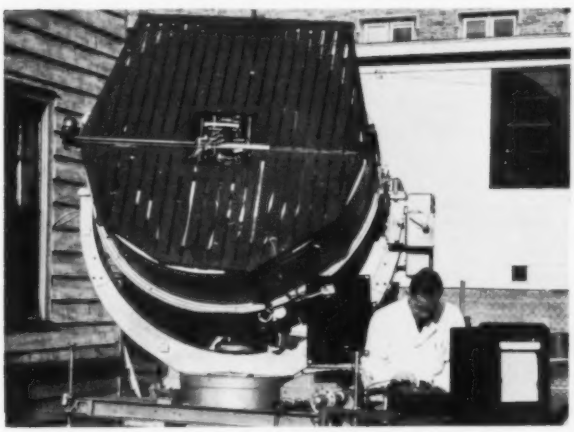

FIG. 4 — Solar furnace with diaphragm.

FIG. 5 — Radiometer output records.

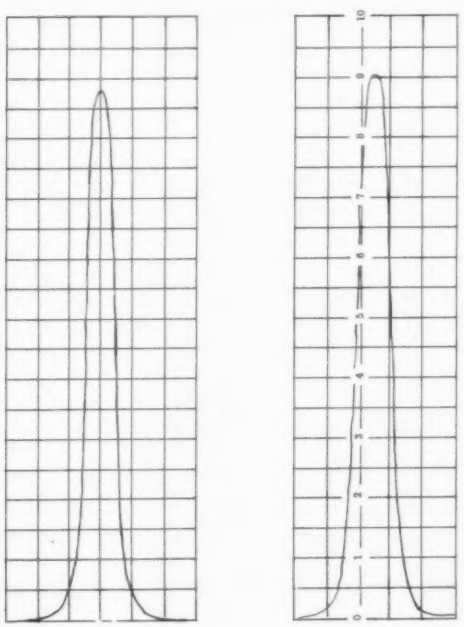

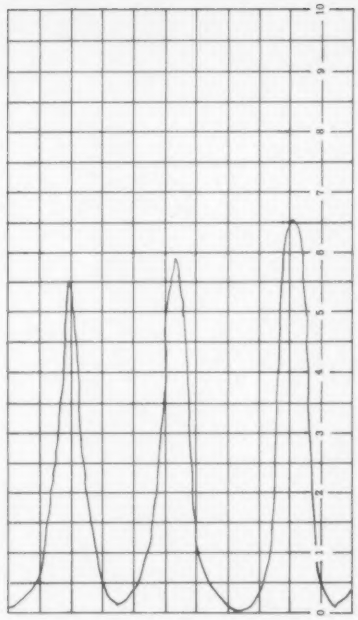

FIG. 6 — Radiometer output records.

A solution of this problem was found in placing a diaphragm on front of the mirror. An iris-type diaphragm would favor the central portions, so a Venetian-blind structure was built in such a fashion that the ratio of the center surface to the peripheral surface was not altered significantly. By varying the exposed area a value could be obtained which permits the use of the radiometer within the range of calibration.

Fig. 4 shows the 60-in. solar furnace with the diaphragm mounted. The electronic guiding mechanism is visible on the cart at the front.

The radiometer was mounted in the sample holder and moved along the three directions of space by three servomotors. A recording potentiometer was used to obtain a continuous record of the millivolt output of the instrument. Figs. 5 and 6 show parts of the original chart

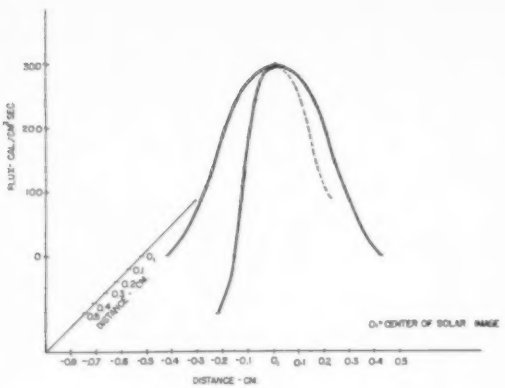


FIG. 7 — Change of flux along the horizontal and vertical coordinates.

with the recorded values of emf as obtained. The millivolt values were converted to flux and multiplied by the screen factor. Three curves were thus obtained showing the change of flux values vs. displacement along each spatial direction. From these curves, a three-dimensional diagram was constructed. Fig. 7 shows the change of flux along the horizontal and vertical coordinates.

During the flux measurements a continuous record of the normal incident solar radiation value is kept and these values synchronized with data obtained in the flux measurements. The paired values then permit the calculation of a factor

$$C = \frac{P}{n} \qquad [6]$$

where

$P$ is the measured flux at the focal zone

$n$ is the normal incident solar flux

$C$ is the concentration factor, specific for the mirror.

Once $C$ is determined the numerical value of the flux at the focal zone may be obtained by measuring only the normal incident solar radiation (a very simple measurement) and multiplying this value by $C$, the concentration factor.

The results of our measurements indicate that

$$C = \frac{P}{n} = 293$$

and

$$\gamma = \frac{P_{\text{calc}}}{P_{\text{meas}}} = 76 \text{ per cent}$$

an unexpectedly high value which requires further checking.

The temperatures $T$ obtainable at the focal zone are usually of wider interest than the flux. The two are correlated by the Stefan-Boltzmann law:

$$P = \sigma T^4 \qquad [7]$$

This correlation can be used only when the target in the solar furnace approximates black-body conditions. For nonblack-bodies the emissivity of the target has to be introduced:

$$P = \epsilon_t \sigma T^4 \qquad [8]$$

$\epsilon_t$, the total emissivity, is not only a function of the material but also of the temperature and surface conditions of the target. To specify the latter, the substance is prepared in some well-defined manner to assure that the emissivity is reproducible and that it is characteristic of the substance and not the condition of its surface.

Emissivity values for materials above 2000°C are very scarce and mostly calculated ones. There is a great need for measurements of such data for materials which are of interest in fundamental and applied high temperature research. The knowledge of emissivity is needed for temperature determinations when working with a solar furnace. There are two ways open to the investigator to overcome this difficulty. One is to use the assumption that emissivity does not change much with the change in temperature and wave length and therefore the available data are satisfactory. The second method requires the determination of the emissivity of the target under experimental conditions; e.g. at the temperature where the planned experiment will take place, on the sample to be used, and applying the same optical pyrometer which will be used. This second method can be followed on the solar furnace without undue complications.

From the Kirchhoff law it can be shown that

$$\epsilon_t = a \qquad [9]$$

i.e. the total emissivity for any radiator is equal to its absorptivity for black-body radiation at the same temperature.

It also follows from Kirchhoff's law that

$$1 = \rho + a \qquad [10]$$

where $\rho$ is the reflectivity and $a$ the absorptivity. This relation is valid if the material is opaque for radiant energy.

Substituting $\epsilon_t$ from Equation [9]:

$$\epsilon_\lambda = 1 - \rho_\lambda \qquad [11]$$

a correlation which can be used to calculate the emissivity from reflectivity measurements.

The reflectivity of a substance can be measured in the solar furnace by application of the method described above for flux determination.

From normal incidence data the flux at the focal zone can be calculated using Equation [6]. The reflected flux is measured with the radiometer and from the incident and reflected flux values the total reflectivity $\rho_t$ and the total emissivity $\epsilon_t$ of the target can be calculated.

For optical pyrometry $\epsilon_\lambda$ is of greater importance, where $\lambda$ is the effective wave length of the pyrometer. This value ($\lambda_e$,) can be calculated from:

$$\frac{\int_0^\infty J(\lambda T_1)\, K_\lambda\, T_R\, d\lambda}{\int_0^\infty J(\lambda T_2)\, K_\lambda\, T_R\, d\lambda} = \left[\frac{J(\lambda T_1)}{J(\lambda T_2)}\right] \qquad [12]$$

where $J(\lambda T)\, d\lambda$ is the radiant intensity for wave-length interval $\lambda$ to $\lambda + d\lambda$, $T_R$ is the spectral transmission of the red glass, and $K_\lambda$ is the spectral luminosity, so that $\int_0^\infty J(\lambda T_1)\, K_\lambda\, T_R\, d\lambda$ is the luminous intensity from the



VOL. 1 1957

source at temperature $T_1$ that is transmitted by the glass. $T_R$ values are usually obtainable from the manufacturer of the instrument. Reference 8 gives details of the calculation.

Once the effective wave length and the spectral transmission are known for an optical pyrometer and $\rho_t$ has been determined for a substance, $\rho_\lambda$ can be calculated. Substituting $\rho_\lambda$ into Equation [11] $\epsilon_\lambda$ is obtained.

Thus the emissivity of the substance to be used in high temperature investigations can be determined in advance for all contemplated operating temperatures, for the very same surface conditions and for the principal wave length of the optical pyrometer to be used.

The true temperature of a sample in the focal zone can be calculated either using Equation [8] with the known value of the flux or from the brightness temperature measured with the optical pyrometer, using the following form of the Wien equation:

$$\frac{1}{T} - \frac{1}{S_\lambda} = \frac{\lambda}{c_2} \ln \epsilon_\lambda \qquad [13]$$

where $T$ is the true temperature, $S_\lambda$ the brightness temperature, $c_2$ the second radiation constant (1.4320 cm deg), $\lambda$ the effective wave length of the optical pyrometer, and $\epsilon_\lambda$ the corresponding emissivity.

In all these considerations it is tacitly assumed that the target receives and loses energy only by radiation. This assumption may be justified by proper mounting of the sample. Heat losses from conduction can be reduced by using the smallest possible target and applying an insulator between target and sample holder. Convection losses are most difficult to reduce, but are far less in significance because of the great difference in order of magnitude between radiation traffic on one hand and convection values on the other hand at temperatures above 1200°C.

Since the temperature is a function of the flux, the geometrical perfection of the mirror will have an influence on the temperature values as well. From Equations [5] and [7]:

$$\frac{P}{P_{calc.}} = \frac{T^4}{T^4_{calc.}} = \gamma \qquad [14]$$

Under operating conditions the values of $P_{calc.}$ and $T_{calc.}$ are such that with increased geometrical perfection, the temperature will increase much more rapidly than the flux. This must be borne in mind when designing solar furnaces for specific performances.

The reported methods and instruments appear suitable for flux and emissivity measurements in the solar furnace. It is realized that the methods need further refinements and the reported data more experimental foundation before their application in precise measurements can be recommended.

The author wishes to express his appreciation to Dr. Joseph M. McGreevy and Mr. J. Carter of the Materials Laboratory of the New York Naval Shipyard for the loan and calibration of radiation instruments, to Dr. Robert Gardon of the Mellon Institute of Industrial Research for the design and construction of the water-cooled radiometer, to Mr. Charles V. Cunniff at the Blue Hill Observatory for the calibration of the thermopile, to Dr. Norman O. Smith of Fordham University for suggestions concerning the manuscript, to the Curtiss-Wright Corporation for permission to complete this work, and to the National Science Foundation for the financial support he received throughout his efforts.

## REFERENCES

1. W. M. Conn, "Recent progress in solar furnaces for high temperature research and development work." *J. Franklin Inst.* 257(1): 1-12, Jan. 1954.
2. T. S. Laszlo, "Solar furnace in high temperature research." *Science* 124: 797-800, Oct. 26, 1956.
3. T. S. Laszlo, W. deDufour, and J. Erdell, "Guiding system for solar furnaces." (To be published in the *Transactions of the Tucson Conference on the Use of Solar Energy — the Scientific Basis.)*
4. *International Critical Tables* 5: 253, 1926.
5. E. Loh, P. Duwez, N. K. Hiester, and T. E. Tietz, "Theoretical considerations on performance characteristics of solar furnaces." Technical Report no. I, Report no. 3, Stanford Research Institute, Menlo Park, Calif.
6. J. Farber, "Images of very high temperature sources." (In *Proceedings of the Symposium "High Temperature — A Tool for the Future", Berkeley, California, 1956,* pp. 1-9.)
7. R. Gardon, "An instrument for the direct measurement of intense thermal radiation." *Rev. Sci. Inst.* 24: 266, 1953.
8. W. E. Forsythe, *Measurement of Radiant Energy.* McGraw-Hill, 1937. p. 360.

# MATERIALS AND SURFACES FOR SOLAR FURNACES

By RALPH H. WIGHT

J. W. Fecker, Inc., Pittsburgh, Pa.

**The nature of the reflecting material and the paraboloidal surface used in solar furnaces, and the methods by which such a surface may be approximated, are here discussed with a view to determining how the highest possible performance efficiency may be attained. A second-surface silver reflector, a first-surface aluminum reflector, and a silicon monoxide-overcoated aluminum reflector are compared, and the silvered mirror, used with water-white plate glass, is shown to give the best performance. Five methods of approximating a paraboloidal surface for large furnaces are considered, and a combination slumping, grinding, and polished technique is found to be the most economical and accurate. The effect of vignetting losses on over-all efficiency are discussed. Efficiencies of a series of possible solar furnace design combinations are computed, and formulas are given to determine exact paraboloidal efficiency with a true solar surface rather than with a uniform solar disc brightness.**

## INTRODUCTION

The application of solar heat collectors has received considerable emphasis of late from current high temperature research. Solar furnaces as such are not historically new. The first military application of such a device is described in an apocryphal tale in which Archimedes is related to have used reflectors to destroy the enemy fleet during the siege of Syracuse in 212 B.C. Later references to solar energy devices are given by Pliny who cites the use of solar burning glasses in the cauterization of wounds.

After the fall of Rome and the beginnings of the Middle Ages, no new achievements in the line of solar energy devices were reported. In fact, even some of the previously considered valid information on solar devices took on the character of legend, to the point that Descartes considered Archimedes' mirrors to be a fable.

Benveniste[1] has reported the history of the solar furnace from Archimedes to the present date.

Interest in modern solar furnaces can be considered to have begun with the work of Stock and Heyneman, who built a two lens furnace with an adjustable mounting in 1909. Since that time, several furnaces have been built. One which captured particular attention was the installation at Montlouis in the French Pyrenees.[2]

This renewed interest in solar energy collecting devices and solar furnaces in particular stems from the particular advantages to be gained in high temperature research from the use of a solar heating device. Those advantages are:

(1) an entirely "pure" and uncontaminated source of heat,
(2) a heat source of high quantity and quality,
(3) an accurately controllable heat flux,
(4) a comparative facility of manipulation of the work.

Geometry indicates that a paraboloidal mirror should be the most efficient method of concentrating the sun's rays. As in the case of an astronomical telescope used to concentrate the rays from celestial objects, the paraboloidal mirror of the solar furnace can be made to track the sun. This presents considerable difficulties with regard to maintaining sample position and orientation. Another approach is to maintain the focal spot fixed, and to maintain centration of the solar image by tracking the sun with an auxiliary mirror or heliostat. While the former approach may be shown to give somewhat higher values of possible concentration ratios, solar furnaces as they are envisioned today are to be considered as research tools, and it is the over-all usefulness of these tools that must be considered, not merely the efficiency of some abstract object.

Most current thinking with regard to large solar furnaces presupposes the use of a two-mirror paraboloid-heliostat combination solar furnace. Unless otherwise specified, the comments in this report are intended to be applicable to that type of furnace.

In the case of small furnaces, such as several built in this country utilizing surplus searchlight paraboloids, there is little that can be done to increase their efficiency. In the case of large solar furnaces however, strict attention to design detail is necessary if the ultimate in performance is to be achieved.

The nature of the surfaces used in the furnaces may be separated into two portions:

(1) the nature of the reflecting surfaces or material itself,
(2) the nature of the paraboloidal surface and the way

VOL. 1 1957

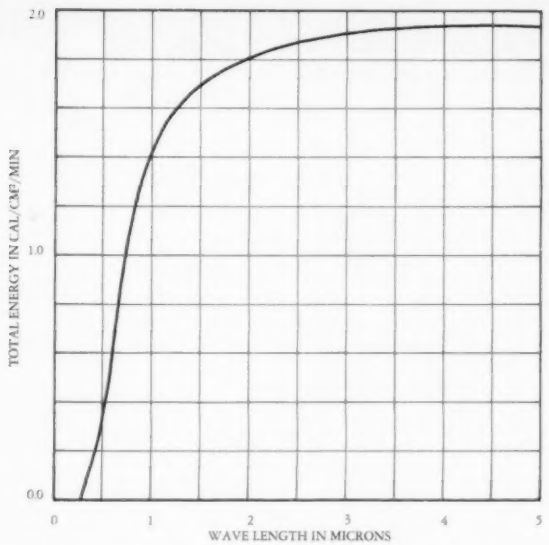


FIG. 1 — Energy distribution of solar radiation outside the atmosphere.

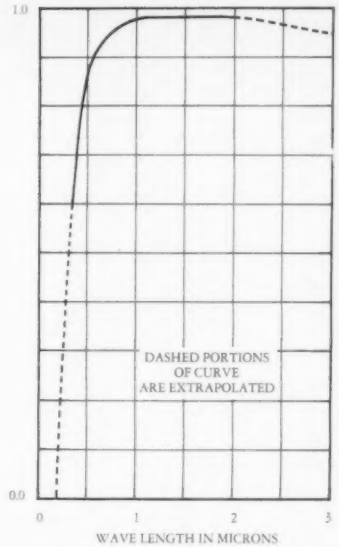


FIG. 2 — Atmospheric transmission coefficient (average for Table Mt., Calif.).

in which a sufficient approximation of this surface is obtained.

Before any accurate analysis with regard to the concentration of solar energy can be made, a description of this solar energy and of the conditions under which it is to be used is necessary.

## AVAILABLE SOLAR ENERGY

The distribution of solar radiation as a function of wave length has been given by Moon.[3] A plot of this energy distribution has been made in which the summation of energy is shown plotted against the wave length of the incident radiation in microns. This plot is shown in Fig. 1.

Because of the absorption of the atmosphere, not all of this energy striking the outside of our air envelope is available for use with solar furnaces located at the surface of the earth. Abbot[4] reported a long series of measurements made at widely separated, selected stations by the astrophysicists of the Smithsonian Institution on the total intensity of solar radiation and the spectral distribution of this radiation.

The atmospheric transmission coefficients for various wave lengths are reported by Aldrich and Hoover[5] for Table Mountain, California. The arithmetic average for high and low values at this location are shown plotted as a function of wave length in Fig. 2. It will be noted that in the range of from 0.70 to 2.25 microns, the curve is shown smooth without reference to the water vapor absorption bands. The curve is extrapolated below 0.34 microns and above 2.25 microns.

Combining the data shown in Figs. 1 and 2, it is possible to obtain the energy distribution of solar radiation at the surface of the earth. To arrive at this combination, the incremental amounts of energy between two wavelength values is multiplied by the transmission coefficient. A series of such energy products is then summed to give the energy distribution curve in exactly the same way as the increments of energy were summed to give the energy distribution outside the atmosphere. A curve showing the distribution of solar radiation at the surface of the earth as a function of wave length is shown in Fig. 3.

It is obvious from Fig. 3 that a preponderance of the energy reaching us from the sun lies between the wave length region of 0.4 to 2.0 microns. For purposes of this discussion it will be considered that "solar energy" consists of that band of radiant energy reaching us from the sun between the wave-length limits of 0.40 to 2.0 microns. The distribution to be assumed in all cases will be that shown in Fig. 3.

FIG. 3 — Energy distribution of solar radiation at the surface of the earth.

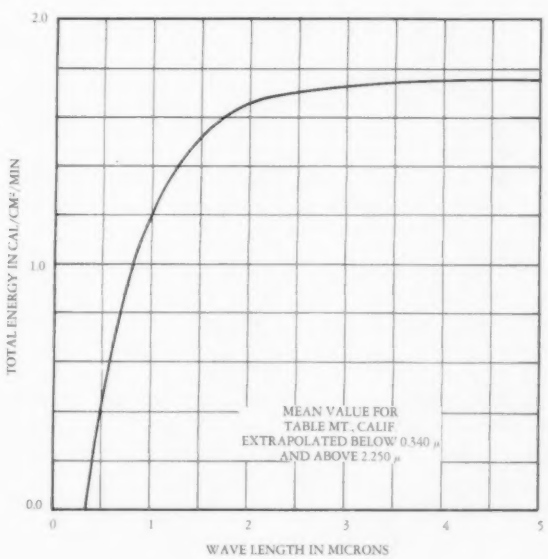

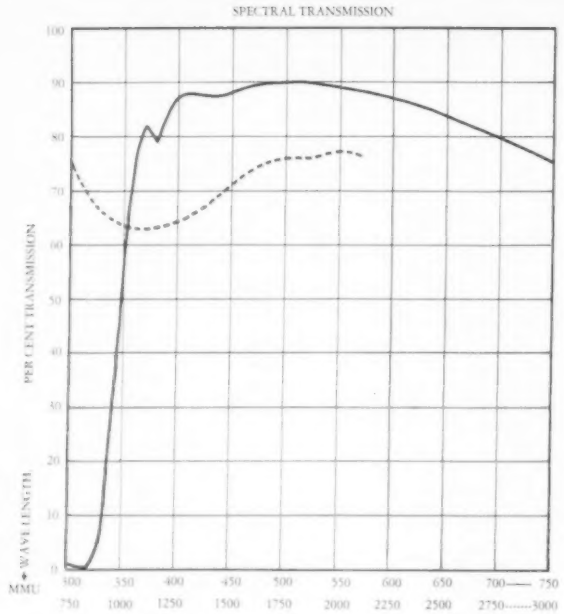


FIG. 4 — Radiant energy transmission, ¼-in. regular polished plate glass.

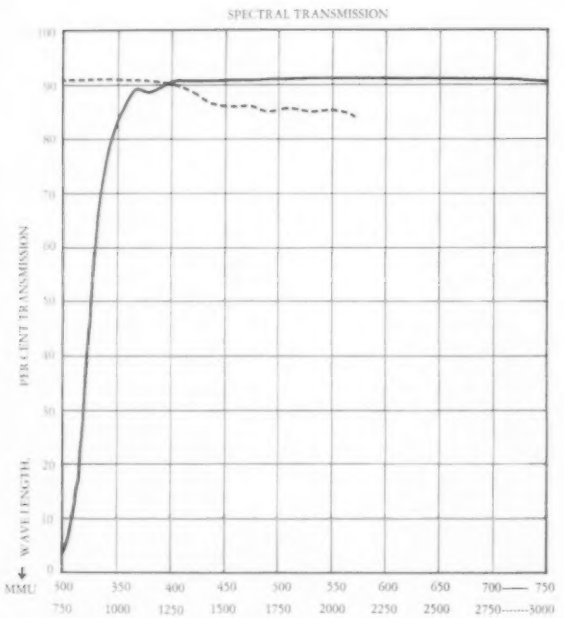


FIG. 5 — Radiant energy transmission, ¼-in. water-white polished plate glass.

TABLE I

RADIANT ENERGY TRANSMISSION

| | ¼-in. regular polished plate glass | ¼-in. water-white polished plate glass |
|---|---|---|
| Thickness of sample | 265 in. | 239 in. |
| Total solar light | 88.2%* | 91%* |
| Total solar energy (calculated) | 77.4%* | 90%* |
| Total solar ultraviolet | 66.3%* | 83%* |
| Total solar infrared | 67.8%* | 90%* |

*Average

| Wave length ($m\mu$) | Per cent transmission: ¼-in. regular polished plate glass | Per cent transmission: ¼-in. water-white polished plate glass |
|---|---|---|
| *Ultraviolet* | | |
| 300 | 1.1 | 3.5 |
| 310 | 0.3 | 12.0 |
| 320 | 0.3 | 35.3 |
| 330 | 6.2 | 58.5 |
| 340 | 29.4 | 74.6 |
| 350 | 57.4 | 83.0 |
| 360 | 74.8 | 86.9 |
| 370 | 81.7 | 89.0 |
| 380 | 79.3 | 88.3 |
| 390 | 83.7 | 89.5 |
| *Visible* | | |
| 400 | 87.2 | 90.5 |
| 420 | 87.5 | 90.6 |
| 440 | 87.3 | 90.8 |
| 460 | 88.7 | 90.8 |
| 480 | 89.3 | 91.1 |
| 500 | 89.4 | 91.1 |
| 520 | 89.5 | 91.1 |
| 540 | 89.3 | 91.1 |
| 560 | 88.7 | 91.1 |
| 580 | 88.0 | 91.1 |
| 600 | 87.0 | 91.2 |
| 620 | 85.6 | 91.3 |
| 640 | 84.4 | 91.1 |
| 660 | 83.0 | 91.1 |
| 680 | 81.3 | 91.1 |
| 700 | 79.6 | 91.1 |
| 720 | 77.9 | 91.0 |
| 740 | 76.1 | 91.0 |
| 750 | 75.3 | 91.0 |
| *Infrared* | | |
| 800 | 71.4 | 91.0 |
| 900 | 65.8 | 91.0 |
| 1000 | 63.4 | 90.9 |
| 1100 | 62.9 | 90.7 |
| 1200 | 63.8 | 90.4 |
| 1300 | 68.6 | 89.7 |
| 1400 | 69.9 | 87.3 |
| 1500 | 71.1 | 85.8 |
| 1600 | 73.8 | 86.0 |
| 1700 | 75.5 | 84.9 |
| 1800 | 75.9 | 85.6 |
| 1900 | 76.1 | 84.5 |
| 2000 | 77.1 | 85.1 |
| 2100 | 76.3 | 84.1 |

## CHARACTERISTICS OF REFLECTING MATERIALS

A choice of reflecting materials is available to the solar furnace designer. Since high heat fluxes are one of the primary reasons for the fabrication of a solar furnace in the first place, it is taken for granted that high efficiency is one of the chief aims of the designer. This being the case, the choice of reflecting materials is considerably narrowed. In fact, except for the case of small furnaces, it is limited to two materials, i.e. silver and aluminum. If it were not for the corrosive effects of our atmosphere, a first-surface, silvered mirror would be nearly as efficient as could be desired by even the most hopeful solar furnace designer.

Unfortunately, silver is subject to very deleterious chemical attacks, to such an extent that anything but an extremely fresh silver film would be even lower in reflectivity than such durable metals as chromium and rhodium.

VOL. 1 1957

Fortunately, it is possible to utilize a silver reflector in a second-surface application where the silver is protected by an impermeable layer of glass. When such a superstrate is used in combination with the reflecting silver film, the solar radiation to be concentrated must pass through the glass, be reflected from the silver glass interface, once again traverse the glass, and in the case of a two-mirror type of furnace, repeat the entire sequence once again.

The transmission of whatever glass might be used as a superstrate in combination with the reflecting silver film, therefore, takes on the utmost importance.

The spectral transmissions of two types of plate glass are shown in Figs. 4 and 5 and Table I. The values shown are uncorrected, i.e. they include losses by reflection at two glass-air interfaces. In order to obtain the true transmission of the glass without regard to reflection losses at glass-air interfaces, it is necessary to compute the internal transmission $T_i$. This is done in accordance with the following formula:

$$T_i = \frac{T}{T_o} \qquad [1]$$

where:

$T_i$ = internal transmission,
$T$ = transmission including reflection losses,
$T_o$ = transmission considering reflection losses only.

$$T_o = 1 - \frac{2(N-1)^2}{(N+1)^2} + \frac{(N-1)^4}{(N+1)^4} \qquad [2]$$

(normal incidence)

where:

$N$ = the refractive index of the glass at the wave length given.

The over-all transmission throughout the range of "solar energy" is so much better in the case of the water-white polished plate glass shown in Fig. 5, that this material has been arbitrarily selected for further use in the computations of this report. Utilizing the data computed in accordance with Equation [1], the internal transmission for ¼-in. water-white glass is shown in Fig. 6.

It appears that between the region of 0.40 and 1.40 microns, this material is nearly perfectly transparent. In the region from 1.40 to 2.0 microns, its internal transmission drops to as low as 92½ per cent, but even this is sufficiently high to warrant further consideration of the material, especially since this low point in transmission occurs where not too much is being added to the total of the solar energy received at the earth's surface.

The reflection of any metal film in contact with a superstrate, whether such superstrate be either air or other transparent material of known optical characteristics, may be calculated from the following formula:

$$R = \left( \frac{N - n + i\,n\,k}{N + n - i\,n\,k} \right)^2 \qquad [3]$$

$R$ = fraction of incident light reflected,
$N$ = index of refraction of the superstrate,
$n$ = index of refraction of the metal,
$k$ = the absorption index of the metal,
$i$ = the square root of $-1$.

This may be reduced to:

$$R = \frac{(N-n)^2 + n^2 k^2}{(N+n)^2 + n^2 k^2} \qquad [4]$$

The optical constants of the metal, $n$ and $k$, are the refractive index and absorption index of the metal respectively. Values of these optical constants for silver have been determined at a wide range of wave lengths by many investigators. Table II gives values for the optical constants of silver over a range from 0.2 to 4.50 microns. Utilizing these data and combining them with the internal transmission of water-white plate glass, it is possible to compute quite accurately the total reflectivity of this particular metal superstrate combination.

FIG. 6 — Internal transmission ($T_i$) for ¼-in. water-white plate glass.

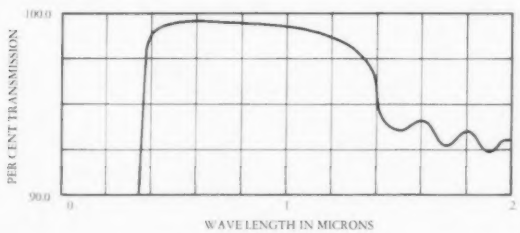


TABLE II

OPTICAL CONSTANTS OF SILVER

| $\lambda(\mu)$ | $n$ | $k$ | $nk$ | $R$% | Authority |
|---|---|---|---|---|---|
| 0.226 | 1.41 | 0.75 | 1.11 | 18 | |
| 0.293 | 1.57 | 0.62 | 0.97 | 17 | |
| 0.316 | 1.13 | 0.38 | 0.43 | 4 | |
| 0.332 | 0.41 | 1.61 | 0.65 | 32 | |
| 0.395 | 0.16 | 12.32 | 1.91 | 87 | Minor |
| 0.500 | 0.17 | 17.1 | 2.94 | 93 | |
| 0.589 | 0.18 | 20.6 | 3.64 | 95 | |
| 0.750 | 0.17 | 30.7 | 5.16 | 97 | |
| 1.00 | 0.24 | 29.0 | 6.96 | 98 | |
| 1.50 | 0.45 | 23.7 | 10.7 | 98 | Ingersoll |
| 2.25 | 0.77 | 19.9 | 15.4 | 99 | |
| 3.00 | 1.65 | 12.2 | 20.1 | — | Först- |
| 4.50 | 4.49 | 7.42 | 33.3 | — | Freed |

In the case of a solar furnace, parallel light from the sun first strikes the heliostat mirror. A certain fraction of this light is reflected at the air-glass interface in the case of a second-surface silvered mirror. The amount of this light that is reflected is dependent upon the angle of incidence and the refractive index of the glass. A typical series of values for this reflection is shown in Table III.

This table gives the percentage $R$ of light reflected by one surface of glass having a refractive index 1.55 relative to air. The angle of incidence is $i$, and the angle of refraction is $r$. The two components of polarized light are marked according to the electric vector of the vibration. Values were computed in accordance with the formula given by Fresnel.

TABLE III
REFLECTION OF LIGHT BY GLASS IN AIR

| $i$ | $r$ | $\parallel$ | $\perp$ | $R$ |
|---|---|---|---|---|
| 0 | 0° 0′ | 4.65 | 4.65 | 4.65 |
| 10 | 6°26′ | 4.84 | 4.47 | 4.66 |
| 20 | 12°45′ | 5.45 | 3.92 | 4.68 |
| 30 | 18°49′ | 6.64 | 3.00 | 4.82 |
| 40 | 24°30′ | 8.77 | 1.75 | 5.26 |
| 50 | 29°37′ | 12.54 | 0.46 | 6.50 |
| 60 | 33°58′ | 19.35 | 0.12 | 9.73 |
| 70 | 37°19′ | 31.99 | 4.00 | 18.00 |
| 80 | 39°27′ | 55.74 | 23.34 | 39.54 |
| 90 | 40°11′ | 100.00 | 100.00 | 100.00 |

It must be noted that in the case of a solar furnace this reflection "loss" is not lost. The amount of light reflected from the first surface of either the heliostat or paraboloid, when second-surfaced mirrors are used, is combined in the final image and is directly added to the total sum of collected energy. With this concept in mind, the formula for the total reflectivity of the metal superstrate combination for one reflection may be derived. The formula for this computation is:

$$R = I_o\left\{T_i^2\, C\left[I_o - \frac{(N-1)^2}{(N+1)^2}\right] + \frac{(N-1)^2}{(N+1)^2}\right\} \qquad [5]$$

where:

$R$ = total reflectivity for the combination,
$I_o$ = intensity of illumination,
$T_i$ = internal transmission of superstrate,
$C$ = reflection (fraction) of metal-superstrate combination,
$N$ = refractive index of the superstrate.

Using the data computed in accordance with this formula, the reflectivity of silver in contact with water-white plate glass is shown as a function of wave length in Fig. 7. Normal incidence is assumed in the case of the data plotted in Fig. 7.

FIG. 7 — Reflectivity of silver in contact with water-white plate glass ($N_d$ 1.525).

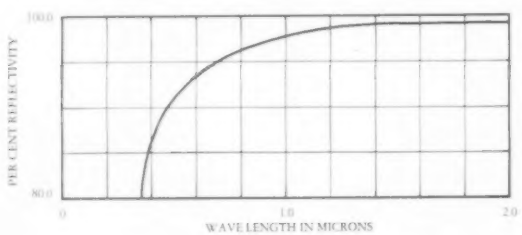


FIG. 8 — Total reflectivity for a silver mirror made on ¼-in. water-white plate glass.

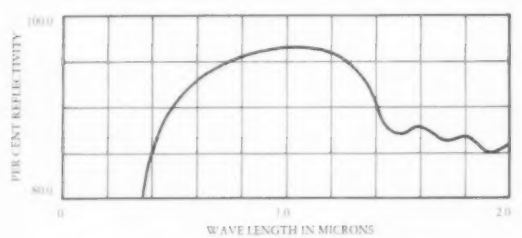


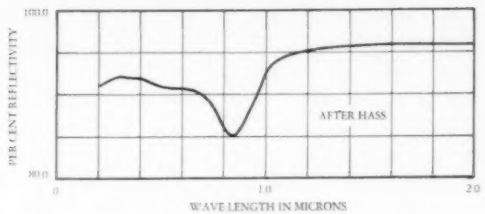


FIG. 9 — Total reflectivity of fresh aluminum film.

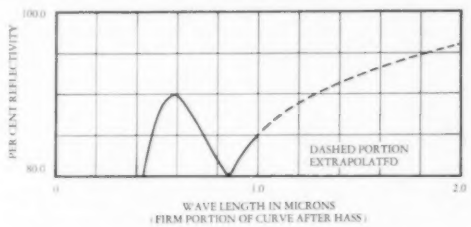


FIG. 10 — Total reflectivity of fresh aluminum with SiO overcoating.

Combining the plot shown in Fig. 7 with that for the internal transmission for ¼-in. water-white plate glass shown in Fig. 6, the total reflectivity for a second-surface silver mirror made on ¼-in. water-white plate glass may be obtained. A plot of this reflectivity as a function of wave length is presented in Fig. 8.

The spectral reflectivities of aluminum films have been experimentally investigated by many authorities. Among the most reliable results are those reported by Hass.[6] These results, later experimentally confirmed by Jupnik,[7] are reproduced in part in Fig. 9. It must be noted that the results given are for a fresh aluminum film. It is anticipated that some deterioration of this reflecting power would follow field use.

An unprotected front-surface aluminum film, even when put down under the best conditions, is a fragile thing. In order to add durability to aluminized films, various overcoatings have been added. One of the most popular of these is silicon monoxide. Unfortunately, the addition of a silicon monoxide overcoating to an aluminum film reduces its reflectivity. Hass[6] shows the effect of adding silicon monoxide overcoating to an aluminum film. The total reflectivity of a fresh aluminum film with silicon monoxide overcoating is shown as a function of wave length in Fig. 10. The undashed or firm portion of the curve is as according to Hass. The transmission is then extrapolated to 96 per cent at 2 microns. This extrapolation is not entirely arbitrary; it is based on an average of certain results obtained by Jupnik.[7]

A complete picture of the efficiency of a given reflecting combination cannot be obtained from a glance at the total reflectivity curves between the limits of 0.40 and 2.0 microns. This is due to the fact that the slope of the total solar energy versus wave length curve is much

VOL.
1
1957

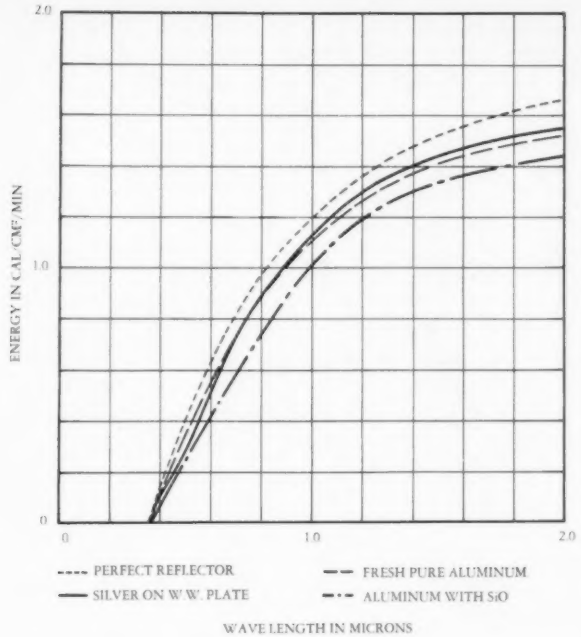


FIG. 11 — Total solar energy available from various reflectors after a single reflection.

steeper in the shorter wave length portion of the curve. Otherwise expressed, this means that in the shorter wave length range energy is being added more rapidly for a given addition to wave length than it is in the longer wave length range. For example, between 400 and 600 millimicrons, there is a total solar energy gain of 0.40 cal/cm²/min. Between 1.80 and 2.0 microns there is a gain of less than 0.1 cal/cm²/min. Utilizing the same integrating technique used to compile the total solar energy versus wave-length curves shown in Figs. 1 and 3, the total solar energy available from various reflectors after a single reflection has been plotted and is presented in Fig. 11. It may be seen that in the wave-length region of from 0.40 to 0.80 microns the fresh aluminum reflector and the second-surface silver reflector are essentially equivalent. Below 0.80 microns the aluminum reflector is more efficient than the second-surface silver reflector. Beyond 0.8 microns however, the second-surface silver reflector maintains superiority. The silicon monoxide overcoated aluminum reflector is inferior to either the second-surface silver reflector or the first-surface pure aluminum reflector.

The conclusions that may be drawn from Fig. 11 are obvious. If, on an over-all basis, a fresh aluminum coat or an aluminum coat with silicon monoxide overlayer had been shown to be somewhat more efficient than a second-surface silver mirror, then there would be an opening for debate. Even if the former were the case, the much greater durability of a second-surface silver mirror would argue much in its favor. However, since the second-surface silver mirror is even more efficient as a concentrator of energy than is the first-surface aluminized or aluminized and protected reflector, there can be little choice.

It should be pointed out that the silvering process used in the fabrication of these second-surface silver mirrors should be the very best obtainable. Careful quality control of the reflectivities of the silvered mirrors must be established. Water-white plate glass should be used whenever very high efficiencies are desired while ordinary or "tank" plate should be used only when comparatively low concentration ratios are needed. The same general cautions apply to the use of aluminized mirrors if such should be chosen for certain applications. The reflectivity values given in this report are those achieved when the aluminizing was done by those extremely proficient in this art. The conditions of evaporation and the thickness of the aluminized film determine to a large extent the reflectivities that can be expected. Here again, careful application of best techniques and suitable quality control would be required before the ultimate in performance could be expected.

## CHARACTERISTICS OF PARABOLOIDS

Once a material for the reflector is chosen, it remains to decide by what method the paraboloid is to be approximated. In the case of small furnaces, a single-piece paraboloid of metal or glass construction may be employed. A number of furnaces have been built utilizing surplus searchlight paraboloids, and these have proved quite successful. As long as it is possible to remain content with the size available in a searchlight, the reflector may be obtained rather economically. If it were decided to make a one-piece paraboloid of dimensions other than those standard for searchlights, a master would be required, and the cost of this would most likely be prohibitive.

For larger furnaces, where a mosaic type arrangement is imperative, five methods exist whereby the paraboloid may be approximated. The first of these is that used by Trombe.[8] It consists of clamping and bending flat glass mirrors to an approximation of desired paraboloidal curvature. Comparatively thin glass is usually employed, with a resultant small gain in transmission efficiency. This gain is usually more than offset by the additional shadowing produced by the clamps. Second, the paraboloid may be approximated by a series of spherically ground mirrors. These may be made, in the case of the first-surface reflectors, from nearly any glass. Third, the paraboloid may be approximated by toroidally ground mirrors. Much in the same way that it can be approached by small spherical segments, the paraboloid can also be approached, even more closely, by toroidally ground and polished mirrors. Fourth, an approximation to the paraboloid may be obtained by slumping flat glass into either a spherical or toroidal approximation of the paraboloid. Fifth, a combination of the slumping and grinding and polishing techniques may be made, so that no great amount of glass may need to be removed during the grinding and polishing. This results in a considerable saving of time and effort as compared to grinding and polishing alone and offers a great increase in accuracy of surface over the precision slumping methods used alone.

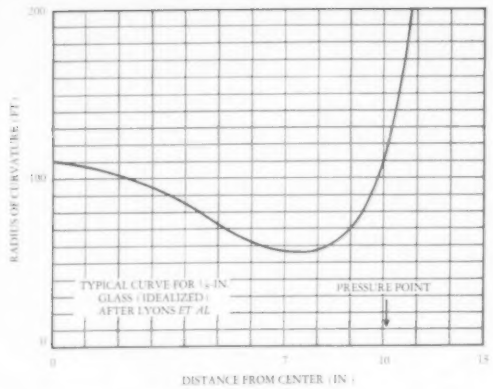


FIG. 12 — Variation of radius in stressed glass.

Lyons[9] has reported the change in radius of curvature of glass plates under load. The variation in radius of curvature, shown somewhat idealized from the original data, for a piece of 1.8-in. glass is shown in Fig. 12. Assuming that the change in radius shown in Fig. 12 could be improved upon with a series of pressure points, etc., it would still appear to be quite dubious as to whether or not the curve obtained by bending the glass plates could be maintained over a range of temperature and stress conditions.

The variations of radius of curvature for slumped and slumped, ground, and polished spherical segments are shown in Fig. 13. The near order-of-magnitude difference between the variations of radius shown by these segments and by the stressed section shown in Fig. 12 will serve to illustrate the advantage of using a fixed curve segment. While no measurements are available on toroidal sections, it is anticipated that similar accuracies would be possible in that instance.

The efficiency of the spherical segment approximation of the paraboloid has been determined experimentally. Utilizing the test arrangement shown schematically in Fig. 14, the efficiencies of two sizes of spherical paraboloidal approximations were measured. The test mirrors used in this investigation have projected square sides equal to 0.042 and 0.021 times the focal length of the paraboloid of which they were assumed to be a portion. The results of this test are shown in Fig. 15. Here it is assumed that a total paraboloid has an efficiency of 100 per cent, and the two spherical segments are shown in comparison with that perfect paraboloid out to rim angles of 70°. It is apparent that if an over-all optical efficiency in excess of 95 per cent is desired, it is necessary to use projected squares of 0.021 *f* from rim angles of 40° on to the edge. It is not, however, necessary to use such small segments throughout the entire paraboloid. In the case of a 30° rim angle furnace, 0.042 *f* side squares could be used with an over-all efficiency of nearly 95 per cent, and in a 60° rim angle furnace it would be necessary to use only the smaller size segment in the last 15° to 20°.

FIG. 13 — Variation of radius in spherical glass sheets.

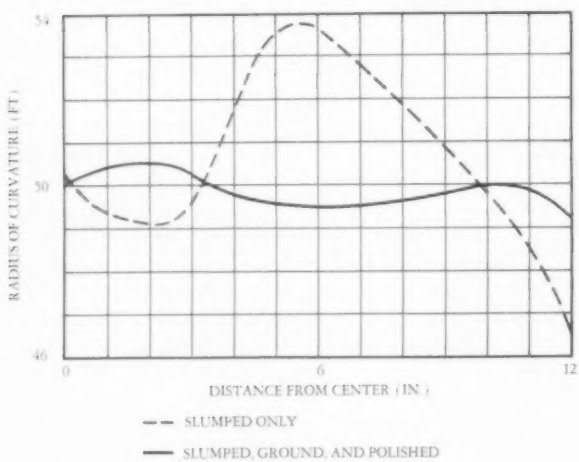


FIG. 14.

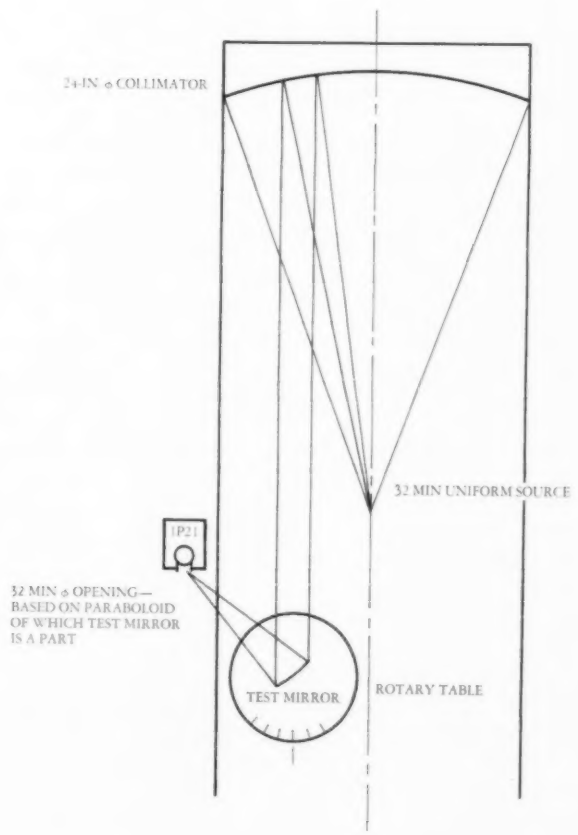
24-IN. ⌀ COLLIMATOR
32 MIN UNIFORM SOURCE
1P21
32 MIN ⌀ OPENING— BASED ON PARABOLOID OF WHICH TEST MIRROR IS A PART
TEST MIRROR
ROTARY TABLE

VOL. 1 1957

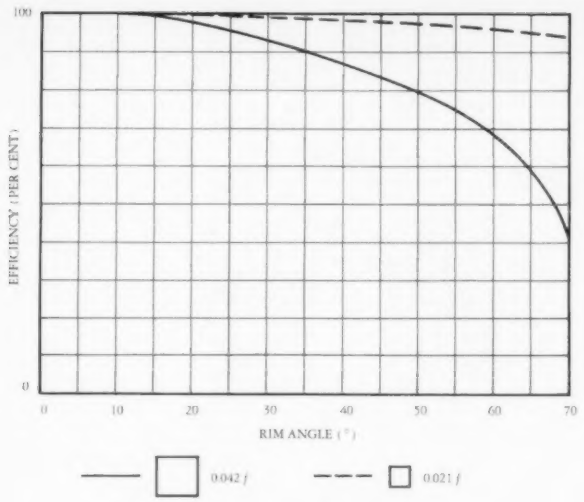


FIG. 15 — Efficiency of spherical segments.

## THE VIGNETTING PROBLEM

A point frequently not sufficiently considered in the design of furnace structures is the part played in the over-all efficiency of the furnace by the occulting produced by the structure itself. This occulting or vignetting effectively robs the furnace of a certain portion of its area. It is essential that in any high efficiency solar furnace design, strict attention be paid to this occulting problem, and the amount of vignetting allowable held to an absolute minimum.

A practical analysis of the vignetting problem leads to an estimate of 15 per cent for the minimum vignetting possible in a large mosaic-type furnace. While 15 per cent allowable vignetting leaves only a minimum of space for supporting structure and test platforms, the losses produced from this amount of vignetting are greater than the reflection losses from two reflections in the case of a second-surface silvered mirror type of furnace. This example points out the seriousness of vignetting losses. All possible efforts should be made to keep these at an absolute minimum.

Using the figure of 15 per cent accumulated vignetting, the furnace factors, or relative efficiencies in comparison to a theoretically perfect paraboloid, have been computed for a series of possible two-mirror furnaces. These efficiencies are shown in the bar chart given in Fig. 16.

The first is a silver on water-white plate glass, slumped, ground, and polished paraboloid with a silver on water-white plate glass second-surface silver mirror heliostat. The computed efficiency for this furnace is 71.5 per cent. The second is an aluminum and silicon monoxide-overcoated reflector on slumped, ground, and polished plate glass in the paraboloid, with an aluminum and silicon monoxide-overcoated reflector on flat plate glass for the heliostat. The computed efficiency of this combination is 60.7 per cent. The third system is silver on water-white plate glass slumped only, without additional grinding and polishing, used with a silver on water-white plate-glass heliostat. The computed efficiency for this system is 60.0 per cent. The fourth arrangement is silver on water-white plate glass stressed and bent into an approximation of the paraboloid. In this case the 15 per cent vignetting figure might be somewhat optimistic; however, it was maintained for the sake of consistency in a preparation of this chart. The over-all efficiency for this in combination with a silver on water-white plate glass heliostat is 52.5 per cent. The fifth arrangement is a combination of aluminum and silicon monoxide on slumped plate glass in the case of the paraboloid and aluminum and silicon monoxide on flat plate glass in the case of the heliostat. The efficiency of this combination is 51.0 per cent. The sixth arrangement is aluminum and silicon monoxide on glass bent into the approximation of the paraboloid used in combination with aluminum and silicon monixide over flat glass on the heliostat. The efficiency for this combination is 44.7 per cent. Bars 7 and 8 in Fig. 16 represent the efficiencies which would be expected for a small furnace utilizing an aluminized and quartz-overcoated paraboloid used in conjunction with a water-white plate glass second-surface silver mirror heliostat. Vignetting here is assumed to be 5 per cent. Bar 8 illustrates what could be expected in the case of a single aluminized mirror of high accuracy with 2 per cent vignetting.

FIG. 16 — Estimated furnace factors for various combinations.

1. Silver on w.w. plate — slumped, ground, and polished
2. Aluminum on plate — slumped, ground, and polished (SiO-coated)
3. Silver on w.w. plate — slumped only
4. Silver on w.w. plate — stressed
5. Aluminum on plate — slumped only (SiO-coated)
6. Aluminum on plate — stressed (SiO-coated)
7. One piece paraboloid: aluminum with SiO coat, heliostat silver on w.w. plate
8. One piece paraboloid: aluminum, no heliostat

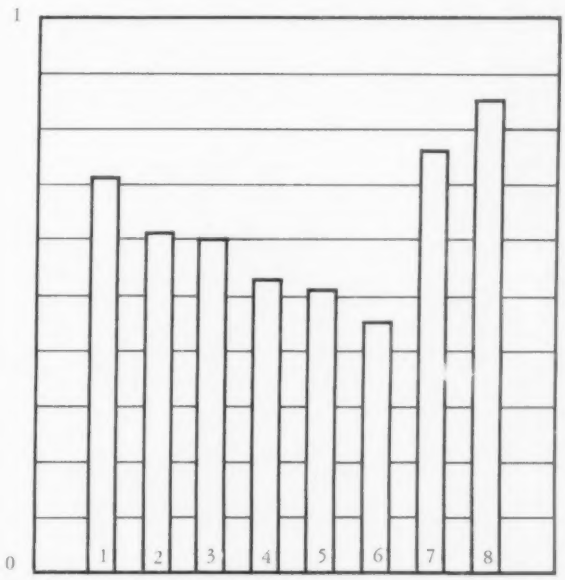

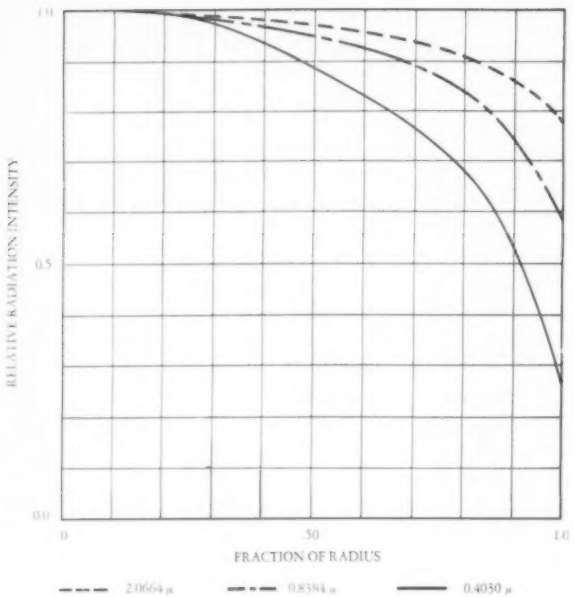


FIG. 17 — Distribution of radiation intensity over the solar disc.

## PARABOLOID EFFICIENCY

The collective efficiency of a paraboloidal energy concentrator is somewhat greater than can be derived mathematically using the assumption that the solar disc is uniformly illuminated. Cavanaggia and Chalonge[10] have reported appreciable variations of radiation intensity across the solar disc. While the fall-off in intensity towards the rim of the sun is especially noticeable in the ultraviolet and violet regions, it is nonetheless quite noticeable even at 2 microns. The relative radiation intensity as a function of a fraction of the solar radius from the center toward the limb is shown graphically in Fig. 17. This effect is extremely advantageous to the designer of solar furnaces. The reason for this is that a larger portion of the solar energy available can be concentrated through a given aperture than can be calculated assuming uniform solar disc intensity.

A geometrical representation of a paraboloid and the notation used in the derivation of the efficiency formula is shown in Fig. 18. The formulas used to compute paraboloidal efficiency presented by Bliss[11] are based upon the assumption of uniform solar disc brightness. They are also somewhat generous compared to the exact formula. While they are sufficiently accurate to be used as a basis of preliminary design prerequisites, final design criteria should be based upon the exact forms, as follows:

$$\phi_o = 2f \tan \phi/2 \qquad [6]$$

$$A_o = \pi\,(f \tan \phi/2)^2 \qquad [7]$$

$$d = \frac{(4f^2 + y^2)^2 \sin \phi}{4f\,(4f^2 - y^2)} \qquad [8]$$

$$b = 2\,\rho \tan \phi/2 \qquad [9]$$

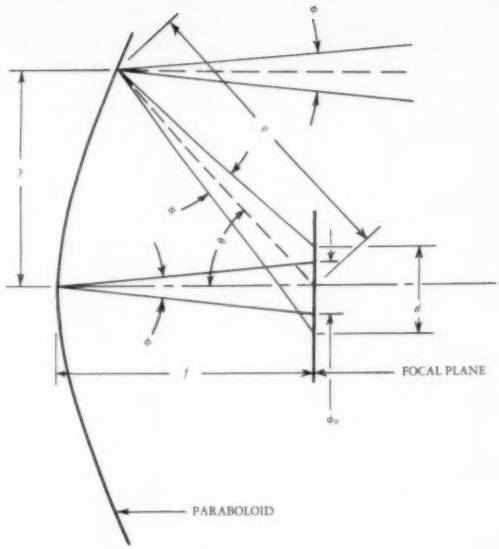


FIG. 18 — Paraboloid notation.

$$\rho = \sqrt{\left(\frac{4f^2 - y^2}{4f}\right)^2 + y^2} \qquad [10]$$

$$A_y = \frac{\pi d\,(\rho \tan \phi/2)}{2} \qquad [11]$$

$$E = \frac{2\,(f \tan \phi/2)^2}{d\,(\rho \tan \phi/2)} \qquad [12]$$

The quantities are self-explanatory with the exception of $b$, which is the minor axis of the ellipse constituting the solar image in the focal plane with major axis $d$. $E$ is the efficiency of the paraboloid as a concentrating mechanism at a particular point $y$ above its optical axis. A plot of the

FIG. 19 — Efficiency of a perfect paraboloid.

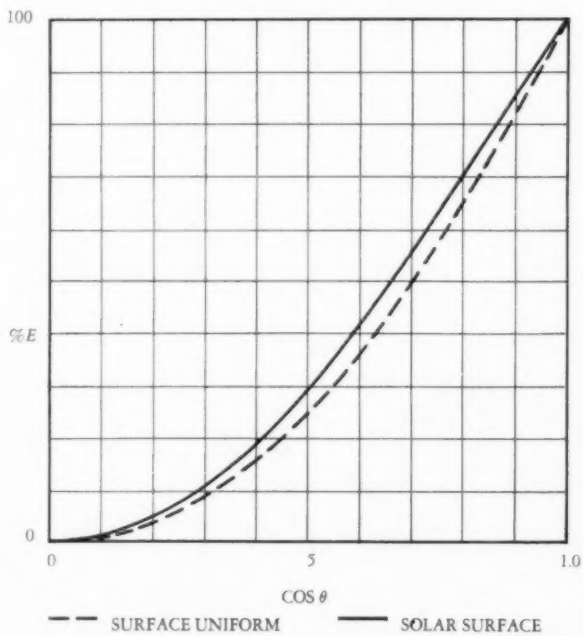




VOL. 1 1957

efficiency of a paraboloid as a function of the cosine of the rim angle $\theta$ is shown as the dashed curve in Fig. 19. If the true solar surface is considered, instead of the uniformly bright approximation, the solid curve shown in Fig. 19 results. In that area of the curve in which solar furnace designers will be most interested there is a difference of nearly 5 per cent efficiency between the uniformly illuminated and true solar surfaces.

## CONCLUSIONS

It would appear that further work on solar furnace surfaces could advance along three lines: First, ways of reducing the occulting or vignetting below the previously considered irreducible minimum of 15 per cent should be investigated. Second, methods of obtaining a constructive interference superstrate which would also act as a protective coating on silver should be studied. The same approach should be taken in an attempt to increase the efficiency of aluminized surfaces. Third, the techniques used in the precision slumping and grinding and polishing of spherical and toroidal paraboloidal approximations should be developed with particular reference to economics of solar furnace construction. As a result of such research and development, we should be able to produce solar furnaces, the performance of which will approach those limits unfortunately set by nature on the performance of such devices.

The author wishes to thank Mr. Russell Whittemore of the Pittsburgh Plate Glass Company for furnishing the spectral transmission data for their water-white and tank-quality glass. Thanks are also expressed to Dr. Helen Jupnik of the American Optical Company for assistance in the preparation of the reflectivity values for aluminized surfaces.

## REFERENCES

1. G. Benveniste, "Burning glasses: from Archimedes to Lavoisier." *The Sun at Work* 1 (2): 4-6, June 1956.
2. F. Trombe, "L'utilisation de l'énergie solaire: état actuel et perspective d'avenir." *J. Rechehches CNRS,* Dec. 25, 1953.
3. P. Moon. *J. Franklin Inst.* 230: 583, 1940.
4. C. G. Abbot, "Solar radiation and weather studies." *Smiths. Misc. Coll.* 94 (10), 1935.
5. L. B. Aldrich and W. H. Hoover, "Table 809." *Smithsonian Physical Tables,* p. 719, 1954.
6. G. Hass, "Filmed surfaces for reflecting optics." *J.O.S.A.* 45 (11), 1955.
7. H. Jupnik, unpublished results of measurements on aluminized mirrors.
8. F. Trombe, "High temperature furnaces." (In *Proceedings of the World Symposium on Applied Solar Energy, Phoenix, Arizona, 1955,* Menlo Park, Stanford Research Institute, 1956, pp. 63-72.)
9. D. H. Lyons, R. D. Cooper, and E. S. Cotton, "Solar furnace design." Report T-7, Pioneer Research Division, Quartermaster Research and Development Center, Natick, Mass., 1956.
10. Cavanaggia and Chalonge. *Ann. d'Astrophys.* 9: 143, 1946.
11. R. Bliss, "Notes on optical design principles, concentration ratios, and maximum temperatures of parabolic solar furnaces." Holloman Air Development Center, Holloman Air Force Base, New Mexico.

# FLUX DISTRIBUTION NEAR THE FOCAL PLANE

By ROBERT E. DE LA RUE, Jr., EUGENE LOH, JOEL L. BRENNER, and NEVIN K. HIESTER

Stanford Research Institute
Menlo Park, California

**In the focal plan of a parabolic concentrator, the assumption of a sun's disk of uniform flux intensity leads to a sharply defined image. However, in planes parallel and adjacent to the focal plane, the heat flux distribution is much less uniform. Further away from the focal planes, the heat flux distribution is again more uniform, but is reduced in intensity. For these cases, the effect of a nonuniform flux intensity across the sun's disk, as well as a uniform sun disk, is considered. Typical flux distribution curves are presented.**

## INTRODUCTION

In the design of a solar furnace, the desired or specified heat flux at the focal plane usually is the main factor in determining the size and characteristics of the furnace. Further, in the operation of the designed solar furnace, there is little control over the flux received by the target, except by use of various mechanical methods. Among these methods would be (1) using a control shutter placed between the focal plane and the concentrator, (2) shading a portion of the concentrator and/or heliostat, or (3) if possible, changing the focal length by position adjustment and deformation of the individual mirror segments of the concentrator. Although these methods would be satisfactory, it would be interesting to know if flux control could be attained by off-focus operations. Knowledge of the heat flux distribution near the focal plane would be useful in determining the extent to which the flux received by a target could be controlled by off-focus operations. Secondly, it would show the extent to which proper positioning of the targets is necessary for them to receive specified levels of flux intensity and uniformity. Also, knowledge of the flux distribution would serve as a guide in estimating the degree of precision needed in the construction of target positioning devices to obtain desired operating characteristics.

The problem with which this paper mainly concerns itself is the calculation of the heat flux distribution at and near the focal plane of parabolic concentrators of various angular openings, for the case of nonuniform flux intensity across the sun's disk.

In order to account strictly for all the complexities of the problem, including variation with wave length of the radiation flux distribution across the sun's disk, it would be necessary to perform an unpleasant number of multiple integrations. The method used compromised with accuracy by substituting, in the place of a portion of the numerical work, pictures of ellipses of various sizes and shapes being intersected by various circles which represented zones of the target. The amount of area common to the various ellipses and parts of circles was estimated. The effect of the nonuniformity of the flux across the sun's disk was also estimated. Therefore, although the results cannot be claimed to be exact, they are realistic and give a reasonable picture of the effect of changing the position of the target from the focal plane to a position nearby and parallel to it.

## MATHEMATICAL APPROACH

In a determination of the heat flux distribution across the sun's image at and near the focal plane of a paraboloid, the calculations are obscured, not to say complicated, by a number of factors. For one thing, the sun is not a point source of heat, but a disk, the angular diameter of which is approximately 32 minutes of arc. For another thing, the heat flux from various points on the sun's disk varies.[1] The third complication is common to all optical instruments, namely, the images reflected from various points on a parabolic surface cannot be congruent, and hence do not coincide. To calculate the heat flux over the image of the sun, it is therefore necessary to average in some manner the heat fluxes over the many different images which are reflected from the various zones of the paraboloid.

To calculate the heat flux received at the focal plane and parallel planes, the parabolic mirror was divided into many concentric rings of equal area, so that they were zones of approximately equal insolation. For each of these zones, the extremities and therefore the average lengths of the major axis of the reflected ellipses were determined at the focal plane and at other planes of interest as a function of the angle, $\theta$ (see Fig. 1), the distance from the focal plane to the plane of interest, $\delta$, and the focal length of the parabolic mirror, $f$. If the origin is at $F$, and $\theta$ is the angle $AFB$, then from the geometry of the parabola

$$\overline{FB} = \frac{2f}{1 + \cos\theta} \qquad [1]$$



VOL.
1
1957

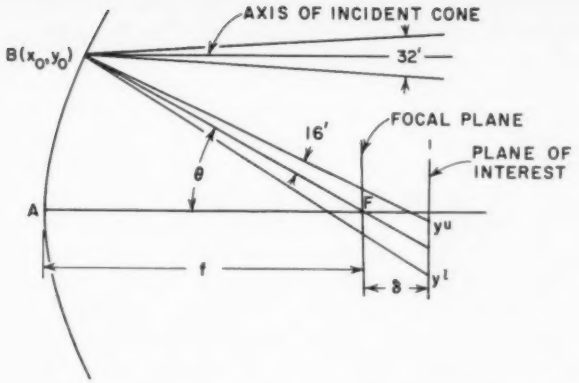


FIG. 1 — Schematic diagram showing parabolic concentrator with incident cone being reflected to plane of interest.

and $$x_o = -\overline{FB}\cos\theta = \frac{-2f\cos\theta}{1+\cos\theta} \qquad [2]$$

also $$y_o = \overline{FB}\sin\theta = 2f\tan\frac{\theta}{2} \qquad [3]$$

The equation of $\overline{PC}$ is [4]

$$\frac{y-y_o}{x-x_o} = -\tan(\theta+16')$$

Therefore, the extreme $y^l$ is

$$y^l = 2f\tan\frac{\theta}{2} - \tan(\theta+16')\left[\delta + \frac{2f\cos\theta}{1+\cos\theta}\right]$$

or

$$\frac{y^l}{2f} = \tan\frac{\theta}{2} - \tan(\theta+16')\left[\frac{\delta}{2f} + \frac{\cos\theta}{1+\cos\theta}\right] \qquad [5]$$

Similarly, for the other extremity of the major axis of the ellipse the coordinate $y^u$ is given by

$$\frac{y^u}{2f} = \tan\frac{\theta}{2} - \tan(\theta-16')\left[\frac{\delta}{2f} + \frac{\cos\theta}{1+\cos\theta}\right] \qquad [6]$$

Combining equations [5] and [6], the average length of the major axis, $a$, of the ellipse is, for any zone of equal insolation,

$$a = \frac{1}{2}\left[\frac{y^l - y^u}{2f}\right]$$

or

$$a = \frac{\tan(\theta-16') - \tan(\theta+16')}{4f}\cdot\left[\frac{\delta}{2f} + \frac{\cos\theta}{1+\cos\theta}\right] \qquad [7]$$

Also from geometry, the minor axis, $b$, of any ellipse is

$$b = a\sqrt{1-e^2} \qquad [8]$$

where $e$ is an eccentricity, which was shown by Lange[2] to be given by

$$e = \sin\theta$$

To determine the heat flux contribution from each ring element of the mirror to the various circular regions on the planes, parallel to the focal plane, two factors had to be estimated. These were, first, the ratio of the areas of the ellipses reflected from the ring elements to the area of each circle centered on the axis and in the plane of interest; and, second, the effect of the nonuniformity of the heat flux over the sun's disk in the portion of the plane which is common to a typical ellipse and a typical circle. Sometimes the common area was an entire ellipse or an entire circle; sometimes it was a portion of each.

In order to avoid the lengthy numerical calculations, which would have been necessary to determine the area common to various ellipses, circles, and circular annuli, reasonably accurate pictures of ellipses of the size and shapes determined by equations [7] and [8] were drawn, and these were intersected by circles representing zones of the target. Then, the ratio of the common area to the total area of the ellipse was estimated graphically. A typical example showing the intersection of an ellipse by a circle is drawn in Fig. 2. Fig. 3* shows the profiles, on various planes parallel to the focal plane, of the ellipses which are formed when the cone of light from the sun's disk is reflected from certain zones of the paraboloid.

Fig. 2 suggests, and Fig. 3 shows, that the effect of nonuniformity of the heat flux across the sun's disk becomes more important as the target plane moves away from the

FIG. 2 — Schematic diagram showing intersection of a typical ellipse by a circle on the plane of interest.

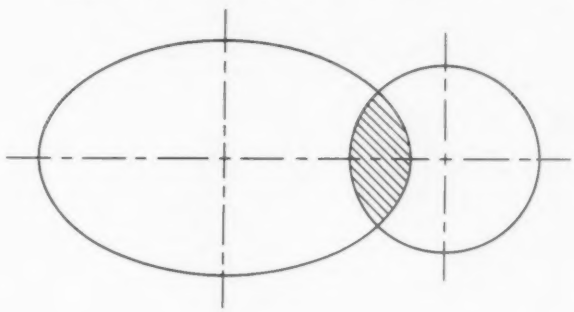

FIG. 3 — Profiles of typical ellipses for planes parallel to the focal plane.

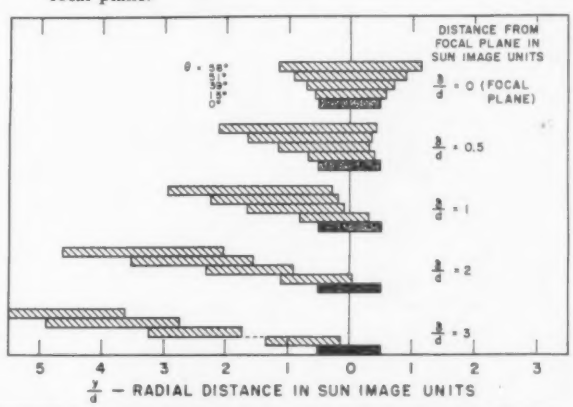


* The distance $d$ is defined as the diameter of the circular image in the focal plane produced by the central portion of the parabolic concentrator. This image is called the "sun image" and is given by

$$d = 2f\tan 16' = \frac{f}{107.3}$$

where $f$ is the focal length of the paraboloid.

focal plane. This is true because the average flux across the sun's disk is fairly uniform over the central region, but decreases rapidly to 65-75 per cent of this uniform value at the edges. As the target plane moves away from the focal plane, the relative contribution of the outer, low-flux portion of the ellipse increases.

To estimate the effect of nonuniformity of heat flux across the sun's disk on the flux received by the circles of interest, the data of Tables 813, 814, and 815[1] were scanned to determine the average flux intensity at various portions of the sun's disk. From these tables, estimated correction factors were obtained, and these factors were applied to the ratio of the areas of the portion of the ellipses which are illuminated by the circles of interest on the target planes.

In the actual calculations, the area factor and the heat-flux factor were applied to several (up to 40) zones of the paraboloid, and the contributions from each zone were summed. The circle on the target plane was divided into as many as 10 concentric rings in each calculation of the heat flux at a particular plane of interest.

## RESULTS AND DISCUSSION

Before presenting the results of the present calculations it should be acknowledged that calculations of a similar nature, at least for a sun's disk of uniform radiation intensity, have been made by Cabannes and Le Phat Vinh.[3] The purpose of their calculations was to determine the variation of heat flux around the focal plane of the 34-ft solar furnace located at Montlouis, which has an apparent rim angle of 47°. Fig. 4 is adapted from their reported results. This figure shows the heat flux distribution at the focal plane and on parallel planes near the focal plane for a parabolic concentrator having a rim angle of 47°.

FIG. 4 — Heat flux distribution for planes parallel to focal plane for parabolic concentrator having $\theta = 47°$.

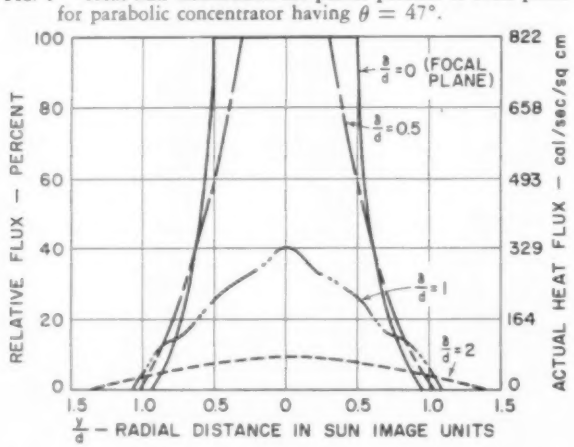


FIG. 5 — Heat flux distribution for planes parallel to focal plane for a parabolic concentrator having $\theta = 60°$.

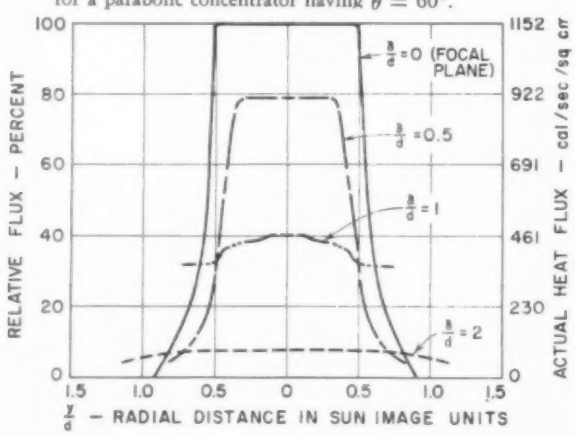


Fig. 5 shows the results of our calculations for the case of a parabolic concentrator having a rim angle of 60°, in which the nonuniform flux intensity across the sun's disk was considered.*

In comparing the two cases, Figs. 4 and 5, two major differences are apparent. These are the differences between the average heat flux values, in the areas of relatively uniform flux distribution, for planes of relatively equal distance from the focal plane, and second, between the shapes of the flux distribution curves for planes of relatively equal distance from the focal plane.

In the first place, Fig. 5 (nonuniform sun disk) does not allow as great a flux at any point near the axis of an off-focal plane as at the corresponding point in the focal plane, whereas Fig. 4 (uniform sun disk) does suggest that maximum central heat flux is not decreased by moving the target one-half sun image unit from the focal plane. In the second place, Fig. 5 gives larger central regions of uniform heat flux (that it, smaller gradients of heat flux) in off-focal planes than does Fig. 4. This last difference is due on the one hand to the fact that the rim angles used for the calculations were different, and on the other hand to the fact that the central portions of the curves in Fig. 5 are flatter than they would be if the radiancy of the sun's disk were assumed uniform. In particular, the difference between the relative values for a plane one-half a sun image unit away from the focal plane is large. The values for this plane are 100 per cent over about 0.7 of a sun image diameter for Fig. 4 as compared with 79 per cent for Fig. 5. In Fig. 5, the actual heat fluxes at the centers of all planes are greater than the corresponding ones in Fig. 4 because of the larger rim angle used in the calculations; these figures would of course be still greater if the sun's brightness had been assumed uniform across the disk. The percentage decrease in heat flux in off-focus planes one-half, one, and two sun image units from the focal plane should be slightly less for a 47° mirror than for a 60° mirror. The actual heat flux values were calculated assuming an ideal case, that is, an optically perfect paraboloid with no reflective, transmissive, or other losses, where the flux received by the concentrator was equal to the solar constant.

Fig. 6 bears on this point. It pictures calculations made

* It should be stated that the results presented in Fig. 5 are only strictly valid for planes to the right of the focal plane, as pictured in Fig. 1. Although the flux distribution is not symmetrical around the focal plane, the difference is small, being in the order of 1 to 2 per cent for planes one sun image from the focal plane on the mirror side.



VOL. 1 1957

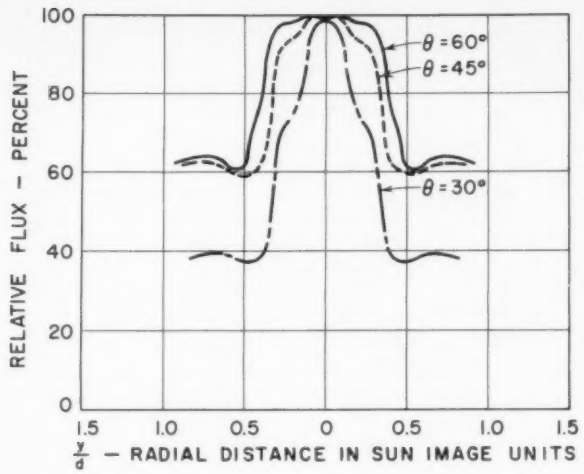


FIG. 6 — Flux distribution at a plane one sun image unit from the focal plane for a parabolic concentrator of various rim angles.

in the plane one sun image unit to the right of the focal plane and shows the flux distribution as produced by concentrators of various rim angles but of equal focal length. The total amount of flux received and the average value of the flux increases with increasing rim angle of the concentrator. Also, it can be seen that the flux becomes more uniform in the central region of the plane with increasing rim angle. For a 60° rim angle the region of uniform flux is a circular area having a diameter of approximately 0.65 sun images.

If the average flux values and the peak values in Fig. 5 are compared for various planes, it is evident that the flux distribution again becomes more uniform and the uniform area extends over a larger region at a plane two sun images from the focal plane. The region of uniform flux distribution for this plane is a circular area having a diameter of approximately two sun images.

Because the flux distribution is fairly uniform in the central region of a plane two sun images from the focal plane, and also because the flux distribution should become more uniform over a larger region of a plane as the distance between the plane of interest and the focal plane increases, it would be useful to know if the average flux value for the central region of uniform flux distribution is related to the flux at the sun image on the focal plane. Calculations using the inverse area law, which relates the integrated average flux value received by a plane of interest to the flux at the focal plane by using circular areas formed by the intersections of the focal plane and the plane of interest with the cone of rays from the parabolic concentrator were made to determine if a relationship exists.

The results of these calculations showed that the integrated average flux for the entire flux spot on an off-focus plane can be related to the flux at the focal plane by the inverse area law, but not the average value of the flux for the central regions of uniform flux distribution. The reason that the inverse area law is not valid for determining the average flux value in the central region is that the area of the total flux spot of an off-focus plane is much greater than the area of the central region of uniform flux distribution. Therefore, the average integrated flux value is lower than the value for the central region. For example, with a plane at a distance of two sun images from the focal plane, the area of the total flux spot was found to be 25 times greater than the area of the central uniform flux region, and the integrated average flux value to be one-fourth as great as the average flux in the central region.

To illustrate the effect off-focus positioning has on the temperature a target can attain, the temperatures an ideal black body should reach at various positions relative to the focal plane of a 100-ft, 60° parabolic solar furnace were determined, using Fig. 5. The calculations were made for two cases: ideal and practical. In the calculations for the ideal case, three assumptions were made: (1) the body receiving the flux is an ideal black body; the heat flux absorbed by the body is equal to the flux emitted by the body, or

$$T = \sqrt[4]{p/\sigma}$$

where $T$ is the absolute temperature of the body, $p$ is the heat flux, and $\sigma$ is the Stefan-Boltzmann constant; (2) the flux received by the concentrator is equal to the solar constant; and (3) the solar furnace is optically perfect. There are no reflective, transmissive, or other losses. Therefore, the flux received by the target at the focal plane is given by Loh,[4]

$$p = 46.1 \times 10^3 \, p_o \sin^2 \theta$$

where $p_o$ is the solar constant.

The assumptions made in the calculations for the practical case were: (1) the target loses 20 per cent of the radiation received by poor emissivity, convection, and conduction; (2) the efficiency of transmission of direct solar radiation through the earth's atmosphere, $\eta_a$ is equal to 85 per cent of the solar constant; and (3) the total operating efficiency, $\eta$, of the solar furnace is 60 per cent. The operating efficiency includes inefficiences due to reflectivity losses of the mirrors, shadowing losses, and losses due to the imperfections of the mirrors or furnace. Therefore the flux received by the target at the focal plane is for this case

FIG. 7 — Variation of temperature with distance from focal plane of a 100-ft, 60° parabolic concentrator.

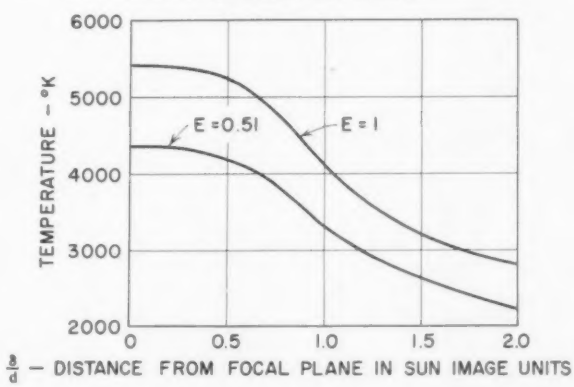

$$p = 46.1 \times 10^3 \, E \, p_o \sin^2 \theta$$

where $E$ is the total efficiency with which the solar constant is concentrated by the solar furnace, $E = \eta\eta_a$. The results of these calculations are given in Fig. 7.

A few remarks concerning Fig. 7 are in order. First, the rapid decrease of the temperature a target can attain, when it is moved from the focal plane to a distance of one sun image away, should be noticed. Although this distance is only approximately 5 in. for a 100-ft solar furnace, compared with a focal length for the furnace of 43.3 ft, the temperature the targer can attain for the practical case decreases by about 1000°C when the target is moved this much off focus. Second, from the shape of the curve it can be seen that in order to obtain a temperature within 5 per cent of the maximum attainable temperature, the target must be placed within a distance of approximately one-half sun image from the focal plane, which in this case is approximately 2.5 in. It should be remembered that the area of maximum heat flux decreases noticeably when the target is displaced even by this amount. Also, for furnaces of smaller sizes, the size of the sun image decreases, and therefore these distances decrease.

## SUMMARY AND CONCLUSIONS

Off-focus operation can be used to control flux and thus the temperature of a target, instead of the various possible mechanical methods. Although the size of the area of uniform flux decreases as the plane of interest moves away from the focal plane, it again increases in size and uniformity at a distance of over two sun images from the focal plane. Also, the average flux received by the central uniform region of an off-focus plane cannot be determined by the inverse area law.

To obtain the maximum flux delivered by a parabolic solar furnace, the target must be positioned properly. To obtain temperatures within 5 per cent of the maximum attainable temperatures, a target must be placed within a distance of one-half of a sun image unit from the focal plane.

The authors wish to express their appreciation for the invaluable assistance in the numerical calculations by Dr. Clay Perry, Ralph Kierstad, Jean Waters, and Sally Hornig of Stanford Research Institute.

### NOMENCLATURE

- $a$ . . . Major semi-axis of an ellipse
- $b$ . . . Minor semi-axis of an ellipse
- $d$ . . . Diameter of the circular image in the focal plane produced by the central portion of the parabolic concentrator. This image is called the "sun image."
- $E$ . . . Total efficiency with which the solar constant is concentrated by the solar furnace, $E = \eta\eta_a$
- $f$ . . . Focal length of the paraboloid
- $p_o$ . . . Solar constant, measured above the atmosphere, 2 cal/cm²/sec
- $T$ . . . Absolute temperature, °K
- $y$ . . . Distance measured radially from axis of paraboloid
- $\delta$ . . . Distance from the focal plane to the plane of interest
- $\sigma$ . . . Stefan-Boltzmann constant
- $\theta$ . . . Angular aperture or rim angle of a parabolic concentrator
- $\eta$ . . . Operating efficiciency factor, the product of the index of geometrical perfection, the over-all reflectivity efficiency factor, and the shadowing efficiency factor
- $\eta_a$ . . . Fraction of ideal solar constant which is available at the furnace site, taking into account losses through the atmosphere

## REFERENCES

1. W. E. Forsythe. *Smithsonian Physical Tables*, 9th ed., 120: 722-33, 1954.
2. L. Lange. *Amer. Math. Monthly* 63: 488-81, 1956.
3. F. Cabannes and A. Le Phat Vinh. *Jour. de Phys. Radium* 15: 817, 1954.
4. E. Loh, P. Duwez, N. K. Hiester and T. E. Tietz, "Theoretical considerations on performance characteristics of solar furnaces." ASTIA Document no. AD81521, AFOSN TN-56-69, Jan. 16, 1956. (Accepted for publication by *Jet Propulsion*.)

VOL. 1 1957

# CONSTRUCTION AND OPERATION OF THE ARIZONA STATE COLLEGE SOLAR FURNACE

By C. J. KEVANE

Arizona State College at Tempe

**A description is given of the solar furnace installed early in 1956 on the roof of the Science Building at Arizona State College at Tempe. In common with many contemporary furnaces, a converted searchlight reflector is used in a stationary mounting. The yoke which originally held the searchlight has been converted and serves as a mounting for the heliostat. A photoelectric system is used to make the heliostat follow the sun throughout the day. The furnace is now in use in a program of high temperature studies for which accurate temperature control is needed. This has been accomplished by means of adjustable sleeves, rotating segments, and other devices.**

The Arizona State College solar furnace is mounted on the roof of the Science Building on the Arizona State College campus at Tempe. Just below the furnace platform is a small laboratory room which is used for instrumentation and storage. The location assures full sunlight from sunrise to sunset throughout the year.

The furnace is a horizontal, fixed-focal-spot furnace composed of a parabolic focusing reflector, a flat mirror or heliostat, and an automatic tracking device for driving the heliostat.

The solar furnace is built around a military searchlight reflector. The paraboloidal reflector is mounted in a fixed position with its axis oriented horizontal. Light from the sun is directed to the curved reflector by reflection from the movable flat mirror, or heliostat.

The reflecting surface of the heliostat consists of four plate glass mirrors which are back-silvered. These mirrors

FIG. 1 — Arizona State College solar furnace showing heliostat (left) and parabolic reflector.

FIG. 2 — View of the tracking system sensing element. The image of the sun is shown at the center of the screen at the rear of the tracking telescope.

are mounted in a large steel frame which permits independent adjustment of each mirror for proper orientation. Each mirror can also be set for best flatness by means of an adjusting screw. The purpose of these adjustments is to insure that all parts of the heliostat reflecting surface reflect light in the same direction; in other words, that all parts are flat and parallel.

The total reflecting surface of the heliostat is 86 in. square. At the latitude of Tempe this permits full illumination of the curved reflector from sunrise to sunset over half the year and for a somewhat lesser time the rest of the year.

The large frame holding the flat mirrors is mounted on the original yoke which held the searchlight. This yoke provides for independent rotation of the heliostat reflecting surface about both horizontal and vertical axes. The movable parts are counterbalanced so that the assembly may be smoothly driven by small electric motors.

The purpose of the heliostat is to direct light from the sun to the curved reflector along its optic axis. This condition affords the sharpest focus and, consequently, the highest heat flux and temperature.

This is accomplished by means of a servomechanism control system. A telescope mounted on the frame of the curved mirror forms an image of the sun on a screen. The screen is constructed so that, if the image is not in its proper position on the screen, light is reflected to a photoelectric cell and a signal is sent to an electronic circuit. The circuit controls the heliostat drive motors in such a way that the sun's image is driven back to its proper position on the screen. Through the action of this servomechanism, the light from the sun is always directed along the optic axis of the curved reflector; as the sun executes its apparent motion across the sky, the heliostat drive system automatically maintains the correct orientation of the heliostat.

The curved mirror which focuses the sun's rays is a paraboloid of revolution 60 in. in diameter which was originally part of a military searchlight. In this installation it is mounted with its optic axis horizontal. The focal spot is approximately 25½ in. from the center of the curved reflector and this focal spot, which is that position where the sun's rays are most concentrated, remains fixed in space through the action of the heliostat. The focal spot is theoretically 0.23 in. in diameter for this furnace; in actual fact, it is slightly larger, depending on how the focal spot is defined.

FIG. 3 — Parabolic reflector showing sample support framework or spider. Experimental apparatus is mounted on the platform.

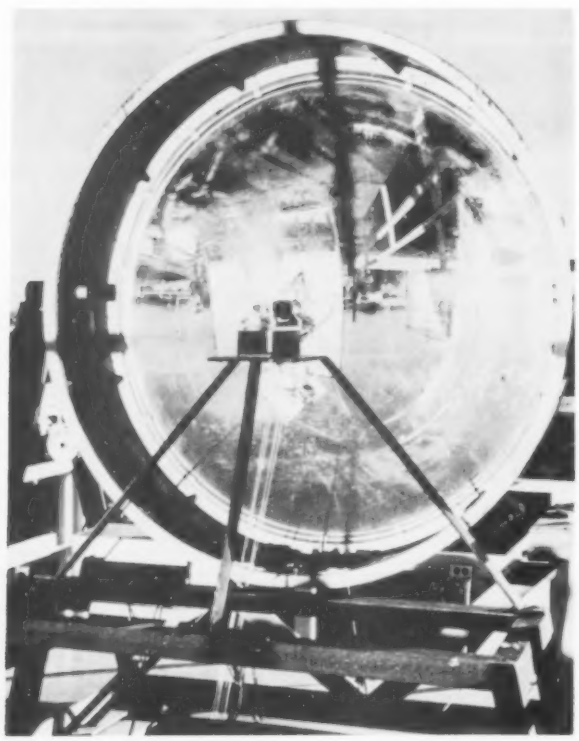

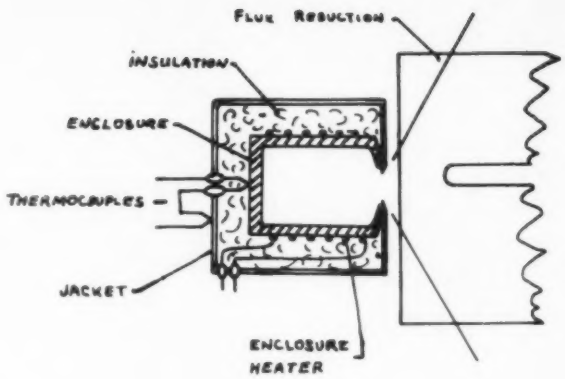


FIG. 4 — Schematic diagram of the calorimeter used to determine heat flux at the focal spot. The heat flux is reduced to keep calorimeter temperatures low.

The paraboloidal reflector is made primarily of copper, on the surface of which is plated a rhodium coating. On the Arizona State College furnace, this rhodium layer has been covered with aluminum with the intention to increase the optical reflectivity of the surface.

An important property of a focusing device is the aperture, which is a measure of the ability of the device to form a bright image. For reflectors such as this, a parameter which is sometimes used to specify the aperture is the angle between the rim of the reflector and the optic axis, as measured at the focal spot. For the furnace being described, this aperture angle is approximately 65°.

A permanent structure for supporting experimental apparatus at the focal spot is mounted under the focal spot position. It is a welded steel framework designed for rigidity and low shadowing factor. This supporting structure, along with typical experimental apparatus, shadows about 5 per cent of the total reflecting surface of the paraboloid.

Other auxiliary apparatus consists of a prism for viewing the focal spot from the side of the reflector; recording potentiometers, which are located in the small laboratory under the furnace platform; an optical pyrometer and a recording radiation pyrometer for temperature measurements; and a radiometer for monitoring the heat flux from the heliostat.

The heat flux to the focal spot is an extremely important parameter and this has been measured using a calibrated copper calorimeter. The calorimeter consists of a blackened copper enclosure with an aperture at one end which is the size of the theoretical focal spot, i.e. 0.23 in. in diameter for this furnace. Radiation from the curved reflector enters the enclosure aperture and is absorbed by the blackened interior. The resulting temperature rise of the copper enclosure is measured by means of a thermocouple attached to the wall of the enclosure.

Surrounding the copper enclosure is an electrical heater-

VOL. 1 1957

winding which is used in calibrating the calorimeter. This is done by making a curve of enclosure temperature as a function of heat input; in use, the heat flux is determined from the enclosure temperature when the enclosure is receiving heat flux from the furnace. The entire structure is surrounded by a polished metal jacket.

Obviously, if the full heat of the furnace entered the copper enclosure, it would quickly melt. To prevent this, and to permit operation at lower temperature, only a fraction of the furnace heat flux is permitted to enter the enclosure. The flux reduction is accomplished by means of a sector which effectively shadows all but a known fraction of the paraboloidal reflector. This sector is rotated so that the flux received by the enclosure is the average flux over the entire paraboloidal reflector.

Measured in this way, the heat flux to an aperture of theoretical focal spot size is approximately 325 watts when the incident heat flux is 1.1 cal/cm$^2$/sec. This corresponds to a heat flux density, or illuminance, of approximately 300 cal/cm$^2$/sec, about 1070 Btu/ft$^2$/sec at the focal spot.

Detailed studies of the maximum attainable temperatures have not been made, but melting has been performed on zirconia and magnesia.

Another property of a solar furnace which is of interest is the variation of heat flux density with distance off the optic axis. Aside from some theoretical calculations, no detailed study of this variation has been made. However, a qualitative record of this variation has been made using the moon as a source and a photographic film as receiver.

The resulting picture shows several lobes about the central spot. These lobes are believed to be caused in part by departure from a parabolic surface which occurs near the edge of the reflector. This is believed to be a common effect in such searchlight reflectors, but it does not involve a large part of the reflecting surface. Some distortion is no doubt introduced by small misalignments and departure from flatness of the heliostat mirrors.

Radiometric measurements performed in connection with the heat flux determination indicate that the heliostat mirrors have an average effective reflection coefficient of about 75 per cent. This reflection coefficient was determined by measuring the heat flux to a radiometer with and without reflection from the heliostat.

In solar furnace operation, an important consideration is the constancy of the solar heat flux to the furnace. Several studies have been made to determine the amplitudes and frequencies of the variations in direct insolation which can be expected to occur. In these measurements, the output of a radiometer receiving radiation by reflection from the heliostat was recorded over several hours time. A typical curve for a clear day shows that no variation greater than about 2 per cent occurs over a time shorter than one minute. Larger changes occur, but only over time spans of an hour or greater. In work where constant enclosure temperatures are an important consideration, as in the work we are doing, it appears from this that incident heat flux variations are not as serious a problem as is that of variations in heat transfer from the enclosure.

Another factor which affects the uniformity of experimental conditions is the stability of the focal spot position. In our experience, the factor most strongly affecting focal spot stability is wind loading of the heliostat. Random wind loading of the heliostat leads principally to lateral movements of the focal spot about the optic axis of the paraboloid, with some accompanying defocusing and large changes in heat flux to a receiver of small aperture.

A series of tests was made to determine the seriousness of the wind loading problem in relation to the prevailing wind conditions in this locality. The position of the focal spot was observed over several hours on days of varying wind conditions. It was found that, with a nominal 2 knot wind velocity and with 5 knot gusts, the center of the focal spot varied in position up to about 10 per cent of the diameter of the focal spot. Winds with 10 knot gusts led to serious shifts of the focal spot up to 50 per cent of the focal spot diameter. Fortunately, the more serious wind conditions are rare and have caused no difficulty with present programs. The wind loading problem could certainly be alleviated by giving some additional attention to the heliostat drive mechanism or by providing a wind shield for the heliostat.

The intention in using the solar furnace here has been to attempt to make it a part of fundamental studies of the properties of materials and to develop techniques for determining these properties by using the solar furnace. The solar furnace undoubtedly has an important place as a piece of laboratory equipment as well as a piece of industrial equipment. The intention here is to expand its place as laboratory equipment and consequently, perhaps, to enhance its importance as industrial equipment.

# A METHOD FOR MANUFACTURING PARABOLIC MIRRORS

By PAUL B. ARCHIBALD

University of California Radiation Laboratory
Livermore, California

**A simple method is described for producing parabolic mirrors by revolving a horizontal pan of liquid plastic and allowing it to harden into the parabolic shape which has been assumed by the plastic. This surface can be plated without further polishing into a mirror of a quality suited to various laboratory and industrial applications.**

Among the most interesting surfaces of solid geometry is the paraboloid. This surface, generated by revolving a parabola about its axis, is widely used for reflectors such as telescopes, searchlights, automobile headlights, and solar furnaces. The well-known characteristic of the paraboloid which accounts for its use is its ability to reflect all light parallel to the principal axis onto a common focal point.

The forming of a paraboloid surface presents certain problems requiring extensive and specialized equipment and a very large amount of labor in the final polishing operation. This paper describes a process for the manufacture of paraboloids from a synthetic resin which requires no extensive machinery and where the polishing is completely eliminated.

The principle utilized is that a liquid in a revolving horizontal pan takes the shape of a paraboloid, and that a liquid resin suitably catalyzed to harden after this form is taken will retain the shape. The possible reason this simple method has not been developed in the past has been the absence of a suitable resin.

With the development of the epoxy resins, which has occurred on a commercial scale only within the last several years, a satisfactory material has been made available. These resins are characterized by high strength, low shrinkage, and, of special interest, an extremely smooth glass-like surface when set. This surface may be plated to produce a mirror without polishing.

The focal length is controlled by the speed of rotation of the pan. The density and the viscosity of the resin have no effect on the focal length of the paraboloid. The formula for the focal length may be simplified to $\sqrt{f} = 38.4/\text{rpm}$ where $f$ is the focal length in feet. Thus a paraboloid of the general appearance of an automobile headlight is formed at 180 rpm while a 36 in. focal length requires a speed of only 22.7 rpm.

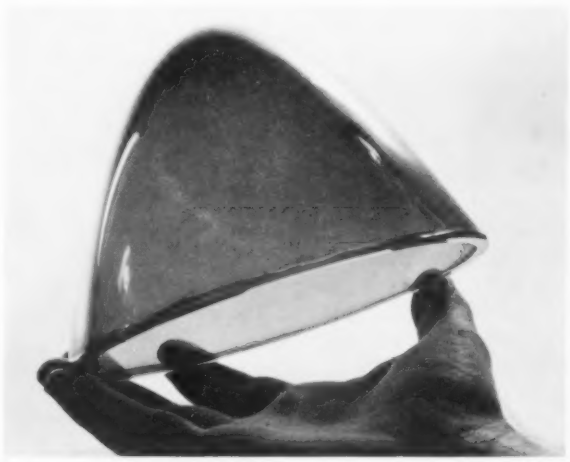

FIG. 1 — Paraboloid shape of epoxy resin cast on revolving surface of mercury.

While various epoxy resin-catalyst systems might be employed, a suitable resin, Epon 828 catalyzed with 5 per cent piperidine and cured at 80-90°C, has been found to give satisfactory results. The principal problem has been to devise a suitable turntable which would be free of harmful vibrations.

In 1900 R. W. Wood, an American inventor, investigated the use of a revolving pan of mercury as a parabolic astronomical mirror. Further development of this idea was handicapped by the lack of a vibration-free turntable. Very fortunately, in so far as vibration is concerned, the requirements for producing a plastic or resin mirror are much less severe than those for producing a smooth surface on a revolving pan of mercury. Thus good resin surfaces up to 10 in. in diameter were produced from a turntable mounted directly onto the slow speed shaft of a gear-reduction motor. The production of 36 in. mirrors, which is currently under way, has been attended by some difficulty, the problem being aggravated somewhat by the easy success of the smaller turntables. These difficulties centered on the proper selection of bearings, reduction gears, motor, etc.

VOL.
1
1957

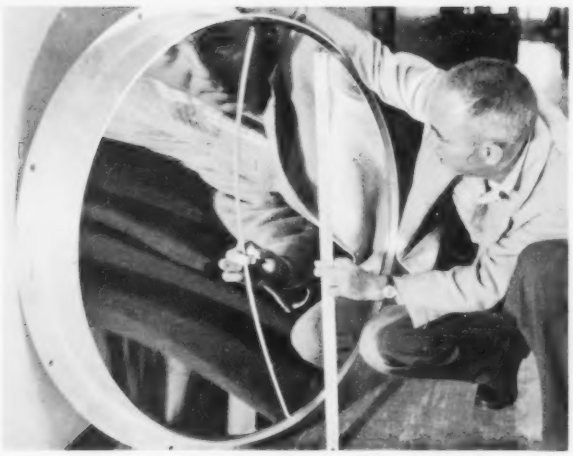

FIG. 2 — *f*1 36-in. Epoxy resin mirror, vacuum-plated with aluminum.

The actual production of a mirror is a relatively quick and simple process. The resin (warmed) and catalyst are mixed together and poured into a pan on the turntable. A lid is placed over the pan to prevent entrance of dust and the resin is allowed to cure for a period of from 5 to 6 hours. Additional resin may be poured onto this surface after it has set. In general, superior surfaces are obtained on the second or third pour. Inasmuch as the quantity of resin required on these additional pours is much less than the first pour, a considerable saving in resin is possible. This also serves as a means for introducing reinforcing material into the resin without affecting the mirror surface.

Mirrors up to 36 in. in diameter with a 36 in. focal length have been produced with the techniques described. The first mirror of this size cracked after cooling. Several layers of fiberglass cloth were placed on the surface and a new surface poured. This reinforced mirror appears to be much less subject to thermal shock. Subsequent *f*1 36-in. mirrors have been produced with a foamed-in-place plastic backing and a fiberglass reinforcement. This reduced the weight of the mirror to 25 per cent of the solid one of the same size. These mirrors have been successfully plated with vaporized aluminum under high vacuum.

The possibility of producing a thin mirror by pouring resin onto a spinning pan of mercury was also investigated. A primary form was first cast from plastic to minimize the amount of mercury required to cover the surface, and then liquid resin was added and allowed to set. This produced a thin-walled paraboloid with a mirror surface on both sides. The use of fiberglass reinforcement with this system would appear to present no great difficulty.

While epoxy resins are characterized by a relatively low shrinkage of 3-4 per cent compared to 10-12 per cent for the polyester resins, the actual shrinkage does not apparently cause the surface to depart from its parabolic shape. Surface tension causes a slight meniscus to form near the edges; however, the effect of surface tension on the rest of the surface appears to be negligible. In any event, mathematical analysis indicates that surface tension would tend to form a paraboloid which, added to the one already present, would serve only to shift the focal point.

At the present stage of development, the process described would appear to be well suited for producing mirrors of short focal length for use in solar furnaces and other light-gathering devices. At the present time, no apparent size limit for this process is evident except that of producing large vibration-free turntables.

The quality of the mirrors produced to date is better than anything now available without the use of grinding and polishing techniques. Whether astronomical quality mirrors can be made by this process awaits further refinements in the technique.

# MEASUREMENT OF THE SPECTRAL INTENSITY DISTRIBUTION OF A CONVERGENT HIGH INTENSITY LIGHT BEAM WITH A MAGNESIUM-OXIDE-SMOKED PLATE*

By F. W. BROWN, III**

Nucleonics Division, U.S. Naval Radiological Defense Laboratory
San Francisco, California

The absolute spectral intensity distribution at the center of the focused image of a carbon arc was determined in the region of 3000-9000 A. The basic optical system (used in studies of thermal radiation damage) consisted of a high intensity carbon arc at the focus of a 36-in. paraboloidal searchlight mirror, and a similar condensing mirror which focused the reflected beam in a cone of vertex angle 120°. The intensity at the focus of the condensing mirror was approximately 100 cal/cm$^2$/sec. The high intensity and convergence of the beam at the focus led to the adoption of a new technique for the spectral analysis. A magnesium-oxide-smoked plate was inserted into the beam at the focus, and the light reflected normally from the plate was focused upon the slit of a spectograph. Absolute intensities were obtained by comparison with a standard pyrometric arc. The results are compared with absolute black-body measurements of the total intensity at the focus. The observed differences in spectrum between arc and image are discussed.

## INTRODUCTION

The U.S. Naval Radiological Defense Laboratory employs a high intensity Navy searchlight with two 36-in. paraboloidal reflectors for studies of the effect of thermal radiation on materials. The searchlight and auxiliary equipment used in these studies have been described previously.[1]

The spectral intensity distribution curve presented in Reference 1 (and shown here as part of Fig. 8) was furnished by the National Carbon Company. It represents the intensity distribution of the radiation emitted by the arc. The intensity distribution at the focus of the optical system is not identical with that at the arc since the optical path between arc and image involves two reflections from aluminized mirrors and passage through two glass plates. It was thought desirable to measure the spectral intensity distribution of the image itself, since it is the image which is of importance in our experiments.

The proposed measurement presented serious difficulties owing to the high intensity and convergence of the beam at the focus. The intensity of the image, about 100 cal/cm$^2$/sec, is 5,000 times that of normal noon sunlight. Furthermore, the use of a rotating step sector for the photographic measurements necessitated exposure times of at least 10 sec to ensure reproducibility. Exposure times of this length also serve to average short-time fluctuations in the arc intensity. These exposure times in conjunction with the high intensity would result in film exposures of the order of $10^6$ times those normally used in spectroscopic measurements.

The beam converges toward the focus in a cone of half-angle of approximately 60° (vertex angle 120°). The only spectrograph which was available, the Hilger Medium Quartz Spectrograph, is an f:12 system,[2] which accepts at most the light converging from a cone of half-angle 5°. If the slit of the spectrograph were placed at the focus, many exposures would be required for a complete sampling of the beam, and the opportunity for error would be correspondingly great.

Methods for the attenuation of the beam by a factor of $10^6$ were investigated. Since the primary purpose of this investigation was to determine the *absolute* spectral intensity distribution of the focused beam, the amount of the attenuation had to be accurately known. The calibration of a single screen to effect an attenuation of this magnitude with accuracy is extremely difficult. If several *(N)* wire screens were used, the attenuation of each would have to be known to an accuracy of the *N*th root of the accuracy desired of the experiment. Neutral density filters

* The opinions or assertions contained herein are the private ones of the writer and are not to be construed as official or reflecting the views of the Navy Department or the Naval Service at large.

** Lieutenant Commander, Medical Service Corps, U.S. Navy. Now at Medical Research Department of U.S. Navy Mine Defense Laboratory, Panama City, Florida.



VOL.
1
1957

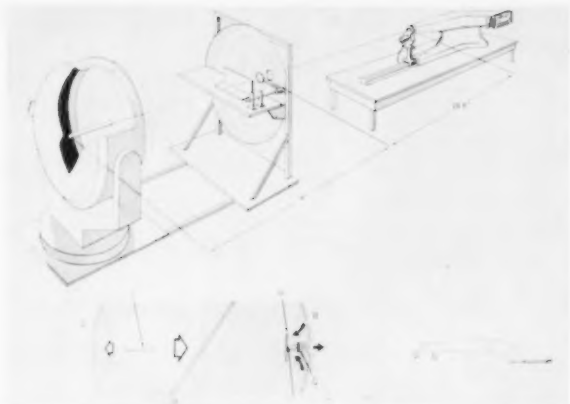

FIG. 1 — Experimental arrangement: *C*, positive carbon; *A*, searchlight mirror; *M*, monitor glass (not shown in perspective view); *B*, condensing mirror; *I*, image of arc; *P*, magnesium-oxide-smoked plate; *Q*, quartz lens; *D*, sector disk; *S*, spectograph slit.

are objectionable because their transmission is not actually independent of wave length.

To meet the requirements imposed by the degree of attenuation necessary and by the convergency of the beam, it was decided to make the spectral measurements on the light reflected from a magnesium-oxide-smoked plate inserted at the focus of the beam. Such a plate is widely used as a standard of reflectance in spectrophotometry.[3,4] Light incident upon a magnesium-oxide-smoked plate is diffusely reflected according to Lambert's Cosine Law to within one per cent,[5,6] and the intensity of the light reflected normally to the plate is independent of the illuminating angle up to about 60°.[6,7] Consequently, it was considered feasible to place a magnesium-oxide-smoked plate at the focus and to image the light reflected normally from a small area at the center of the image upon the slit of the spectograph by means of a quartz lens. By this method contributions from the entire beam could be sampled at the same time, and would be attenuated sufficiently to make convenient spectrographic exposures possible.

## EXPERIMENTAL METHOD

As shown in Fig. 1, an image *I* of the positive carbon *C* of the arc was formed on a magnesium-oxide-smoked plate *P* by the condensing mirror *B*. An area of 0.4 mm x 3.3 x $10^{-4}$ mm at the center of this image was focused on the slit of the spectrograph *S* by means of a quartz lens *Q* of 10-in. focal length. A sector disc *D*, placed directly in front of the slit of the spectrograph, was adjusted to give graded relative exposures on the spectrographic plate differing by a factor of 2 between adjacent steps. Thus it was possible, for each wave-length interval of interest, to plot the photographic characteristic curve[8] for the light reflected by the magnesium-oxide-smoked plate.

The magnesium-oxide-smoked plate was then removed, and two comparison spectra of the standard pyrometric arc[9] were recorded. This standard pyrometric arc has a well-known energy distribution and was used as an absolute standard. It should be noted that the geometry of the observing spectrograph system remained unchanged; the only difference was that the positive carbon of the standard pyrometric arc, rather than the magnesium-oxide-smoked plate, served as the emitting surface. Therefore, direct comparison of intensity was possible. Fig. 2 shows the spectrum of the searchlight image (center), with the spectrum of the standard arc above and below it (top and bottom). The characteristic curves for both the searchlight image spectrum and the spectra from the standard pyrometric arc were then plotted and are shown in Fig. 3.

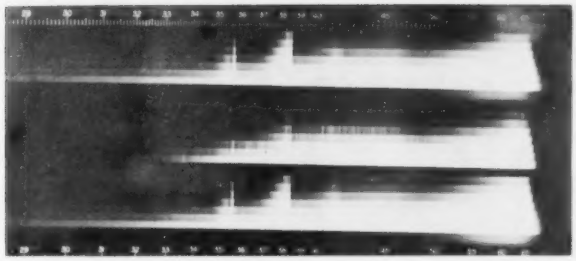

FIG. 2 — Spectra of searchlight image (center) and standard arc (top and bottom).

The large number of emission lines in the searchlight image spectrum (see Fig. 2) necessitated some integration over a definite wave-length interval. The use of a wide (1-mm) spectrograph slit caused the discrete lines to overlap to form a continuum, but the irradiation of the spectrograph plate was so intense that satisfactory exposures were not feasible. As a result, it was necessary to use a narrow (10-micron) slit. Since this gave a large number of fine lines, it was necessary to measure the density over a small (2-mm) region of the spectrographic plate centered about the wave-length region of interest and thus average the density fluctuations caused by the individual lines. This was done by using a 2-mm slit in the microdensitometer with its long direction parallel to the long width of the spectrum. (The 2-mm slit represents a $\Delta\lambda$ of 20 A at 3000 A and of 500 A at 9000 A.) Uniform results could be obtained in this way.

FIG. 3 — Photographic characteristic curves for searchlight image and standard arc at 5000 A.

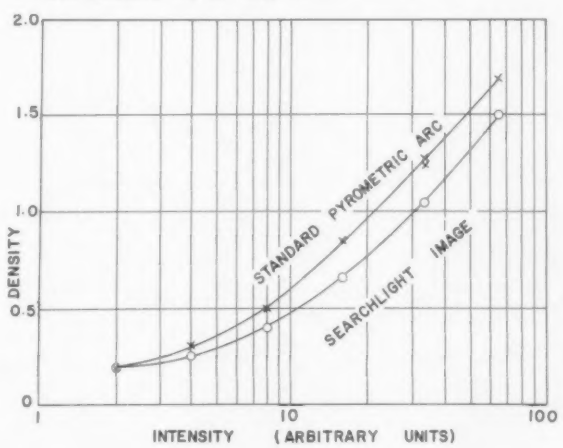

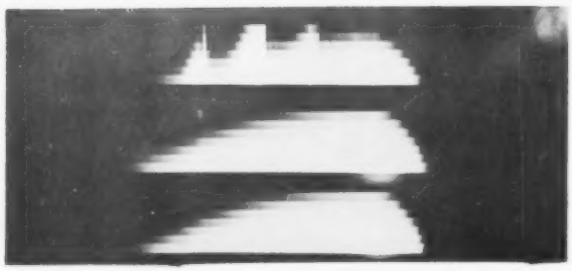

FIG. 4 — Spectra of the standard arc in air (top) and in an atmosphere of carbon dioxide (center and bottom).

## RESULTS

The intensity ratio between the standard pyrometric arc and the unknown flux was measured at several points on the straight-line portion of the photographic characteristic curves, giving an average ratio factor of $a_\lambda$, between the intensity of the standard pyrometric arc, $I_{p\lambda}$, and that of the searchlight image, $I_\lambda$, at wave length $\lambda$. The absolute spectral intensity of the arc image at wavelength $\lambda$ is then given by

$$I_\lambda = \frac{\pi\, a_\lambda}{r_\lambda} I_{p\lambda}$$

where $r_\lambda$ is the reflectance of magnesium oxide at $\lambda$, and the factor $\pi$ appears because magnesium oxide is a Lambert Cosine Law reflector. Using this equation, the absolute spectral intensity of the searchlight image was calculated in the spectral region from 3000 to 9000 A.

Some difficulty was experienced in the region of the cyanogen bands because the MacPherson[9] data did not give the absolute spectral emission at the band heads. Since the intensity data was incomplete, it was necessary to determine the energy in the cyanogen band region for the standard pyrometric arc. This arc was burned, first in air, and then in an atmosphere of carbon dioxide. In the latter case the cyanogen bands were not present. In Fig. 4, the top exposure is the spectrum of the standard pyrometric arc being burned in air; for the center and bottom exposures the arc was burned in an atmosphere of carbon dioxide.

FIG. 5 — Spectral intensity distribution of standard pyrometric arc.

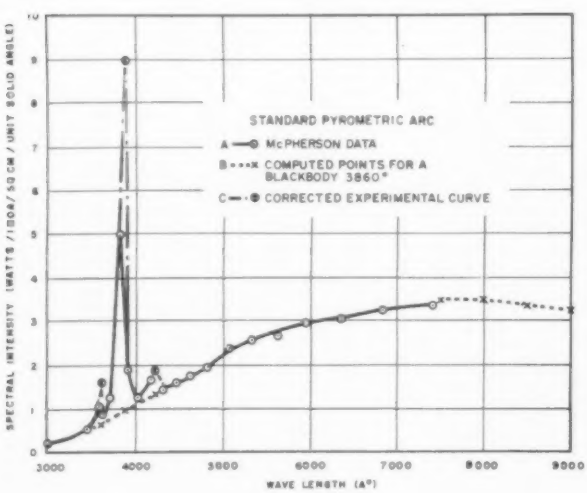
STANDARD PYROMETRIC ARC
A —● McPHERSON DATA
B ···× COMPUTED POINTS FOR A BLACKBODY 3860°
C —·● CORRECTED EXPERIMENTAL CURVE
SPECTRAL INTENSITY (WATTS / 100A / SQ CM / UNIT SOLID ANGLE)
WAVE LENGTH (A°)

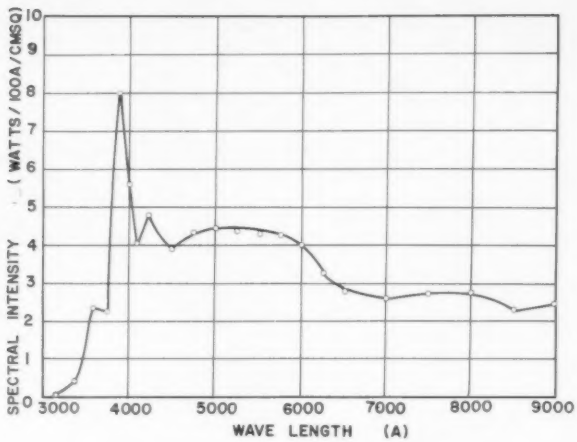


FIG. 6 — Absolute spectral intensity distribution of searchlight image.

The emission of the standard pyrometric arc, while being burned in carbon dioxide, is that of a black body at 3860°K. The spectral emission of a black body at 3860°K was computed, and since Finkelnberg[10] has found that there is no significant difference in the brightness of a solid carbon arc burning in air and in carbon dioxide, we can obtain the absolute value for the emission of the standard pyrometric arc in the cyanogen band region. If one plots the spectrum of the standard pyrometric arc being burned in air and draws a smooth curve by ignoring the cyanogen band region, Fig. 5, the computed points fit this curve nicely. The MacPherson data[9] did not go beyond 7400 A; however, considering this data, one is justified in computing the emission at longer wave lengths by considering the arc to be a black body of temperature 3860°K. Fig. 6 shows the spectral intensity distribution curve of the flux at the focus of the thermal source used in this Laboratory.

The possibility that the reflectivity of the magnesium-oxide-smoked plate would change as a result of irradiation was investigated. First, a spectrographic exposure of 10 sec was made on freshly smoked plate. Then the plate was irradiated for 1 min and other 10-sec exposure was made. This was repeated six times with 1-min irradiation intervals occurring between successive exposures. At several wave lengths the density of the spectrographic plate, Fig. 7, was measured. There was no significant difference

FIG. 7 — Spectrum of magnesium-oxide-smoked plate after each of seven consecutive 1-min irradiations.

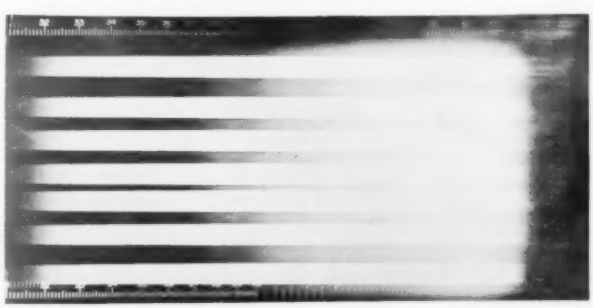

VOL. 1 1957

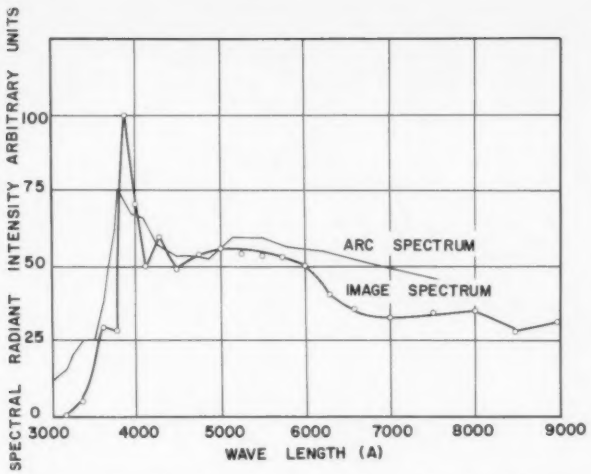


FIG. 8 — Normalized spectral intensity curves for arc and image.

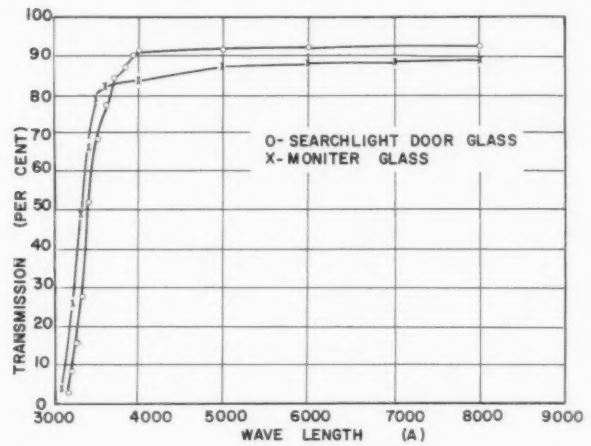


FIG 9 — Spectral transmission of searchlight door and monitor glass.

between the successive exposures. The spectral reflectance of the irradiated magnesium-oxide-smoked plate was measured with a Cary Recording Spectrophotometer in the wave-length region 3000-8000 A. A similar measurement on a freshly smoked unirradiated plate gave identical results. It is concluded that, except for the possible occurrence of a reversible reaction during exposure, the reflectance of the magnesium-oxide-smoked plate is not significantly changed by 6 min of irradiation at the rate of 100 cal/cm²/sec.

## DISCUSSION

It was desirable to check the accuracy of the results with respect to the total energy in the region from 3000 to 9000 A. The spectral intensity distribution curve (Fig. 6) was integrated with respect to wave length from 3000 to 9000 A, yielding a total intensity in this region of 45.9 cal/cm²/sec. Other measurements, for which a black-body calorimeter was used as the detector, gave 100± 6 cal/cm²/sec as the intensity at the center of the image. Using a filter, it was found that approximately 56 per cent of the energy of the searchlight lies in the region of 3000 to 9000 A. These figures yield 56 cal/cm²/sec as the total flux incident at the focus of the condensing mirror in the region from 3000 to 9000 A, which compares favorably with the values obtained by integration of the spectral intensity curve. The spectral intensity distribution curve for the arc, furnished by the National Carbon Company, is shown in Fig. 8, together with our spectral intensity distribution curve at the focus, the two curves being normalized at 5000 A. (The curve for the arc does not include the cyanogen band heads.) One can see that the energy curve at the focus is deficient both in the ultraviolet region below 3825 A and the red beyond 6000 A. Fig. 9 shows the spectral transmission of the searchlight door glass and of the monitor glass. Their transmission falls off rapidly below 3750 A. This would account for the differences between the arc and image spectra in the ultraviolet. The discrepancy in the red portion may be partially assigned to the selective reflectivity of the aluminized mirrors which, according to Strong,[11] is 90 per cent at 4000 A and falls to 85 per cent at 8000 A.

To complete this work and to extend it, the spectrum should be observed with an infrared spectrometer to the limit of the transmission of the glass, about 2.5 microns. It would be of interest to measure the spectra of portions of the image other than its center as there exist large temperature differences in the positive carbon, and correspondingly different spectral intensity distributions can be expected. It will also be desirable to repeat all measurements with a number of different carbons to obtain a measure of the variation of the spectrum from carbon to carbon.

## REFERENCES

1. R. I. Condit, C. P. Butler, A. B. Willoughby, and F. W. Brown, III, "USNRDL thermal radiation studies, progress in physics, January 1950-51." *USNRDL Restricted Report* AD-306(RP), March 27, 1951.
2. A. C. Hardy and F. H. Perrin, *The Principles of Optics*. N.Y., McGraw-Hill, 1932. p. 73.
3. F. Benford, *et al. J. Opt. Soc. Am.* 38: 445, 964, 1948.
4. *Paper Trade Journal* 124(26): 51-52, June 26, 1947.
5. Hardy and Perrin, *op. cit.*, p. 154.
6. W. W. Barkus. *Proc. Phys. Soc.* (London) 51:274, 1939.
7. D. Smith (Interchemical Corp. Research Lab.), private communication.
8. G. R. Harrison. *J. Opt. Soc. Am.* 19:268, 1929.
9. H. G. MacPherson. *J. Opt. Soc. Am.* 30:189, 1940.
10. *The High Current Carbon Arc.* FIAT Final Report 1052 — PB-81644. Washington, D.C., Dept. of Commerce, 1947. p. 82.
11. J. Strong, *Procedures in Experimental Physics*. N.Y., Prentice-Hall, 1938. p. 375.

# DESIGN PROBLEMS OF A SOLAR FURNACE

By NOBUHEI HUKUO and HISAO MII

Government Industrial Research Institute, Nagoya
Nagoya, Japan

Errors are likely to take place in the construction and use of a solar furnace, and these errors, to a greater or less degree, interrupt the concentration of solar radiation on the heating surface of a specimen. In the present paper, the energy concentration of solar radiation incident to the focal plane given by an ideal parabolic reflecting mirror is first analyzed theoretically with reference to the aperture ratio. Next, the effect on the concentration of the solar radiation of the accuracy of the mirror, of the precision of the sun-tracking mechanism, and of the precision related to the placing of the specimen, is discussed quantitatively.

The main source of error interrupting the energy concentration of the solar radiation is the accuracy of the mirror. The accuracy must be of such a degree that the diameter of the circle in which the focus scatters is less than half of the diameter of a solar image produced by its paraxial ray. The other two factors do not play such important roles, both being readily controllable within a permissible limit. An aperture ratio of 2 to 3 is recommended. The temperature a specimen will reach does not necessarily depend on the accuracy of the mirror alone. It is also closely related to the physical properties of the specimen, i.e. size, shape, reflective power, absorptive power, heat capacity, thermal conductivity, and heat radiation. It is rather difficult to cover this subject completely; however, a numerical survey of attainable temperatures is given under several energy conditions.

## INTRODUCTION

Since the temperature of the heating surface of a specimen in a solar furnace is affected by its physical and chemical properties such as size, shape, reflective power, absorptive power, heat capacity, thermal conductivity, heat radiation, etc., it is rather difficult to generalize in the discussion of temperature; however, a higher concentration of solar radiation is definitely needed for obtaining still higher temperatures.

The question of how high a concentration of solar radiation it is desirable to achieve must be answered in the design and construction of a solar furnace. This concentration is affected by three errors which occur in the construction and use of the solar furnace; namely, the error in the surface of the mirror, the error caused through the improper setting of the specimen, and the error caused by improper sun-tracking with the mirror.

In this paper the effects of these errors on the concentration of solar radiation are discussed in detail. The results will be most useful in the design, construction, and utilization of solar furnaces.

## THE IDEAL PARABOLIC MIRROR

An ideal, error-free parabolic mirror will be considered first. The section in Fig. 1 is depicted in a distorted manner. The symbols in this paper are defined as follows:

- $D$ . . . aperture of the parabolic mirror (cm)
- $f$ . . . focal length (cm)
- $n = D/f$ . . . aperture ratio
- $d$ . . . diameter of the solar image by paraxial ray (cm) $d = af = 0.0093f$, ($a = 2 \tan 16'$)
- $\beta$ . . . angle between the optical axis of the mirror and a reflecting ray
- $\gamma$ . . . reflectivity of the mirror
- $E_n$ . . . incident solar radiation per unit area in the plane perpendicular to the solar ray (watts/cm²)

FIG. 1 — Section of a parabolic mirror.

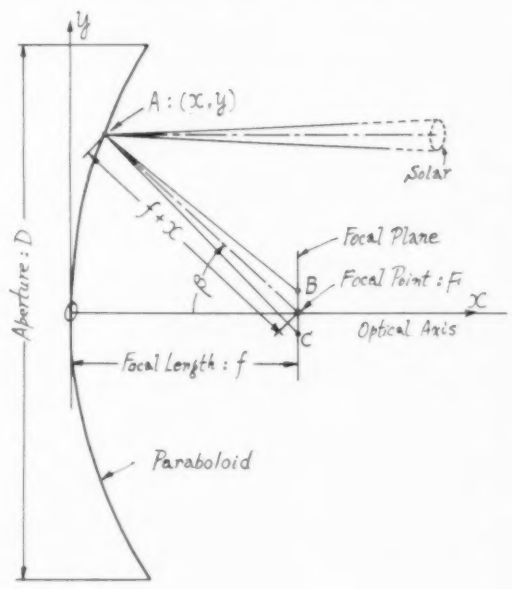

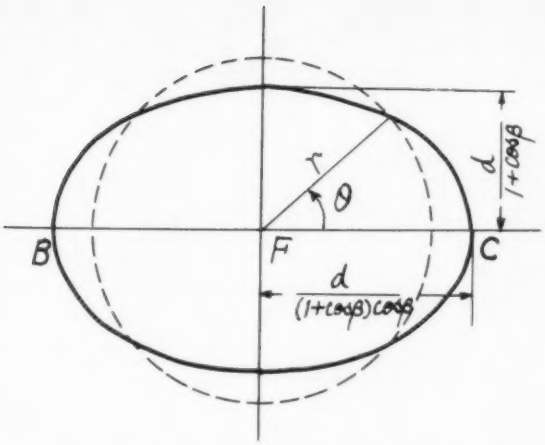


FIG. 2 — Solar image produced by a ray which is reflected by the paraboloid with the angle $\beta$.

The solar image on the focal plane is represented as a function of $\beta$, i.e. an ellipse as shown in Fig. 2. Since the major axis of the ellipse lies in the same plane as the plane of the rays of incidence and reflection, the area of this ellipse is:

$$\pi a^2 f^2/\{(1+\cos\beta)^2\cos\beta\} \qquad [1]$$

The increment of the area of the mirror perpendicular to the optical axis at $\beta$ is

$$4\pi f^2 \{2\sin\beta/(1+\cos\beta)^2\}\, d\beta \qquad [2]$$

The solar radiation on the focal plane is obtained by dividing Equation [2] by Equation [1] and multiplying by $\gamma E_u$, or

$$2(4\gamma E_u/a^2)\sin\beta\cos\beta\, d\beta \qquad [3]$$

FIG. 3 — Maximum density of the heat flux and maximum temperature of the heating surface of a black body.

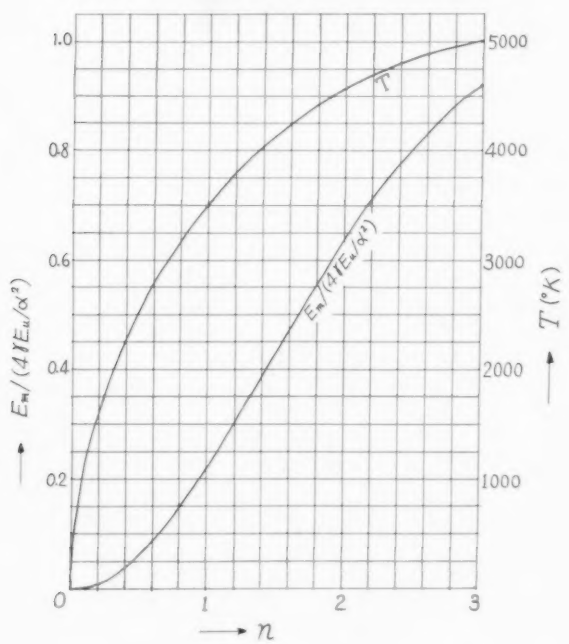


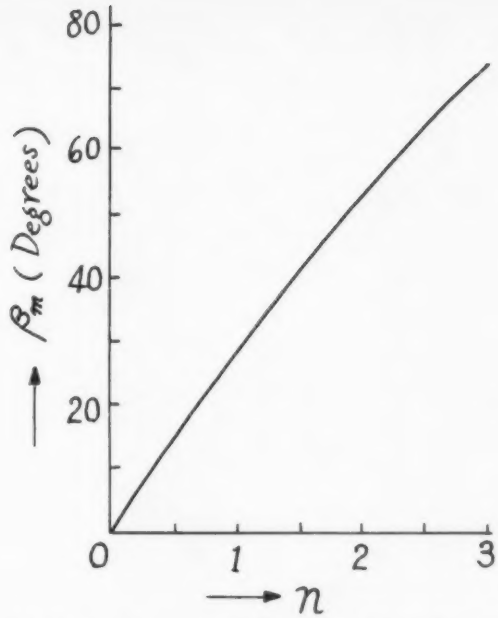


FIG. 4 — Relation between the aperture ratio $n$ and the maximum value of $\beta$.

The ellipse shown in Fig. 2 always involves the paraxial solar image, that is, a circle, the center of which is the focal point $F$, and the diameter of which is $d$. In this circle, the incident radiation per unit area, $E_m$, is determined by the following integral;

$$E_m = (4\gamma E_u/a^2)\int_0^{\beta_m} 2\sin\beta\cos\beta\, d\beta \qquad [4]$$

$$= (4\gamma E_u/a^2)\sin^2\beta_m$$

where $\beta_m$ represents the maximum value of $\beta$.

The aperture ratio $n$ is represented by a function of $\beta_m$, or

$$n = \sqrt{(1-\cos\beta_m)/(1+\cos\beta_m)} \qquad [5]$$

Figs. 3 and 4 show the results of Equations [4] and [5] respectively.

Assuming that the specimen is a black body (exclusive of convection losses, etc.), the temperature $T$°K of the heating surface of the specimen is expressed as a function of $E_m$ in accordance with Stefan-Boltzmann's law of radiation;[1]

$$T = \sqrt[4]{E_m/5.735}\times 10^3 \qquad [6]$$

The Equation [6] is represented in Fig. 3 as the curve $T$, assuming that $\gamma = 0.85$ and $E_u = 0.1$ watts/cm$^2$.[2]

The above results are established only in the range $r < d/2$, where $r$ is defined as the distance from the focal point to a point on the focal plane. In the range $r > d/2$, we can also obtain the distribution of the radiation, in a similar manner.

The incident radiation per unit area at the point which is $r$ distant from $F$ is expressed by,

$$E = (4\gamma E_u/a^2)\int_0^{\beta_m} 2(2\theta/\pi)\sin\beta\cos\beta\, d\beta \qquad [7]$$

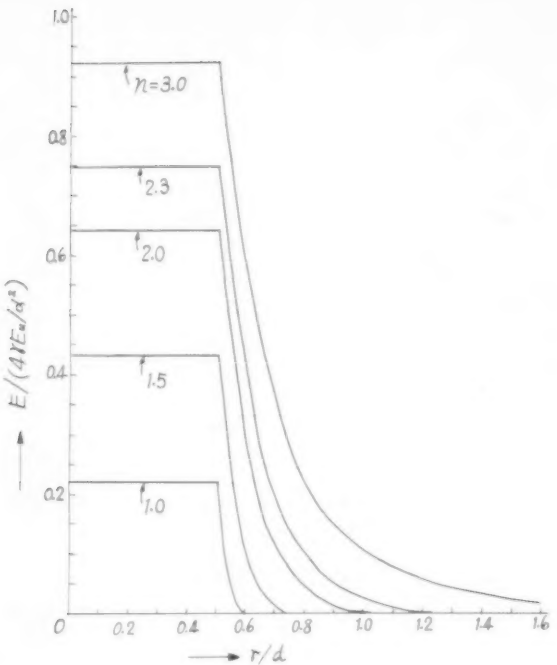


FIG. 5 — Distribution of solar radiation on the focal plane for various values of $n$.

where $\theta$ is an angle as shown in Fig. 2. According to whether $r > d/(1 + \cos\beta)\cos\beta$ or $r < d/(1 + \cos\beta)$, $\theta$ is either 0 or $\pi$ respectively, while $d/(1 + \cos\beta) < r < d/(1 + \cos\beta)\cos\beta$ has such values as

$$\tan\theta = \sqrt{\frac{\{1/(1+\cos\beta)\}^2 - (r/d)^2\cos^2\beta}{(r/d^2 - \{1/(1+\cos\beta)\}^2}}$$

We can evaluate Equation [7] by means of a planimeter or through numerical integration. Fig. 5 shows some results computed by a planimeter for various values of $r/d$.

## EFFECTS OF THE OPTICAL ERRORS CAUSED BY THE MIRROR SURFACE

The mirrors used in a solar furnace are parabolic and heliostat mirrors, and they are likely to have errors in their surface due to the imperfect machining and finishing. In this paper the errors are assumed to be as follows:

In the case of an ideal mirror without error the parallel rays which are incident upon the mirrors in parallel direction to the optical axis are concentrated at one point, the focal point. By the existence of errors, however, the parallel rays are not concentrated at the focal point, but scatter into an irregular shape or pattern on the focal plane. For the sake of simplicity we will assume that this irregular shape forms a circle and that the illumination in this circle is everywhere uniform.

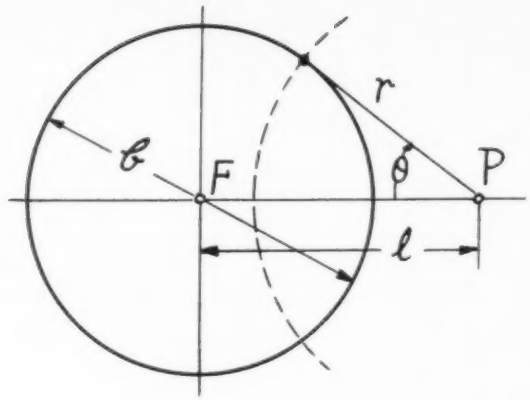


FIG. 6 — Scattering circle.

These assumptions are in approximate agreement with an ordinary searchlight mirror, where the diameter of the scattering circle is about one per cent of the focal length.

Provided that such mirrors are used in the solar furnace, the centers of the ellipses shown in Fig. 2 will be scattered in the circle mentioned above. It is then concluded that the center of the ideal heat flux shown in Fig. 5 is scattered in this circle.

Under these assumptions it is possible to evaluate the density of heat flux at a point $P$ which is $l$ distant from $F$ on the focal plane.

Letting

$$\lambda = l/d, \sigma = r/d \qquad [8]$$

and the diameter of the scattering circle equal $b$, the probability that the distances from $P$ to points situated in the scattering circle are equal to $\sigma$ is shown as

$$\{2\theta\,\sigma/\pi\,(b/2d)^2\}\,d\sigma \qquad [9]$$

where $\theta$ is an angle as shown in Fig. 6. Thus the density of the heat flux at $P$ becomes

$$(2/\pi)(2d/b)^2 \int \theta\,\sigma\,E(\sigma)\,d\sigma \qquad [10]$$

where $E(\sigma)$ represents the density of the ideal heat flux at $\sigma$ as shown in Fig. 5. In the same manner as Equation [7] the integration is evaluated as follows:

(A) $\lambda > (b/2d)$,

(i) for $\lambda - (b/2d) > \sigma$ and $\lambda + (b/2d) < \sigma$, $\theta = 0$,

(ii) for $\lambda - (b/2d) < \sigma < \lambda + (b/2d)$,

$$\tan\theta = \sqrt{(b/2d)^2 - \xi^2}/(\lambda - \xi), \xi = (\sigma^2/\lambda) - \lambda. \qquad [11]$$

(B) $\lambda < (b/2d)$,

(i) for $(b/2d) - \lambda > \sigma$, $\theta = \pi$,

(ii) for $(b/2d) + \lambda < \sigma$, $\theta = \pi$,

(iii) for $(b/2d) - \lambda < \sigma < (b/2d) + \lambda$, $\theta$ has the same value as in Equation [11].

The results computed by means of a planimeter are shown in Figs. 7(a) to 7(d).

In the case $(b/d) < 1$ the maximum value of the density of the heat flux is equal to that of $(b/d) = 0$, where the density is uniform in the range $2\sigma \leqq 1 - (b/d) \equiv$



VOL. 1 1957

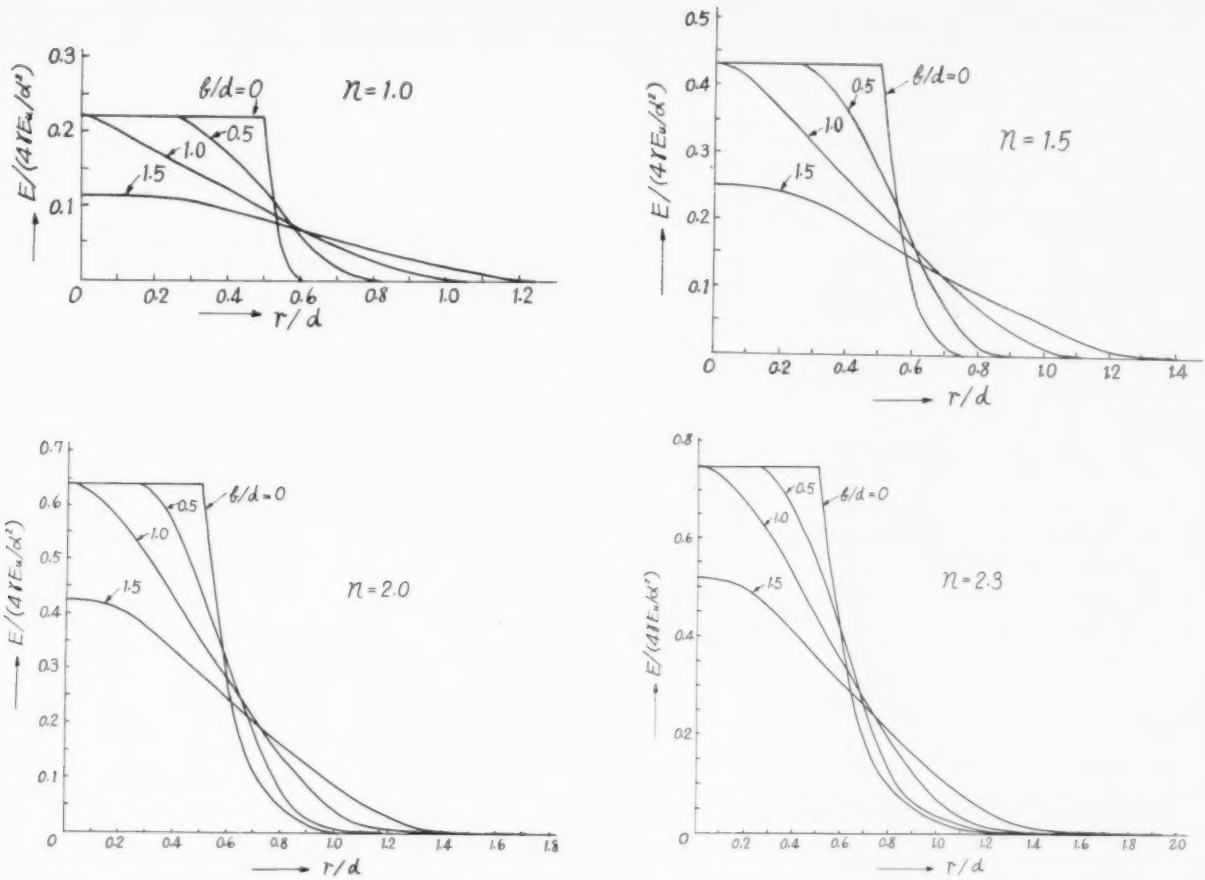


FIG. 7 — Distribution of solar radiation on the focal plane for various values of $b$ when $n = 1.0$ (Fig. 7a), 1.5 (Fig. 7b), 2.0 (Fig. 7c), and 2.3 (Fig. 7d).

FIG. 9 — Error caused through the improper setting of a specimen.

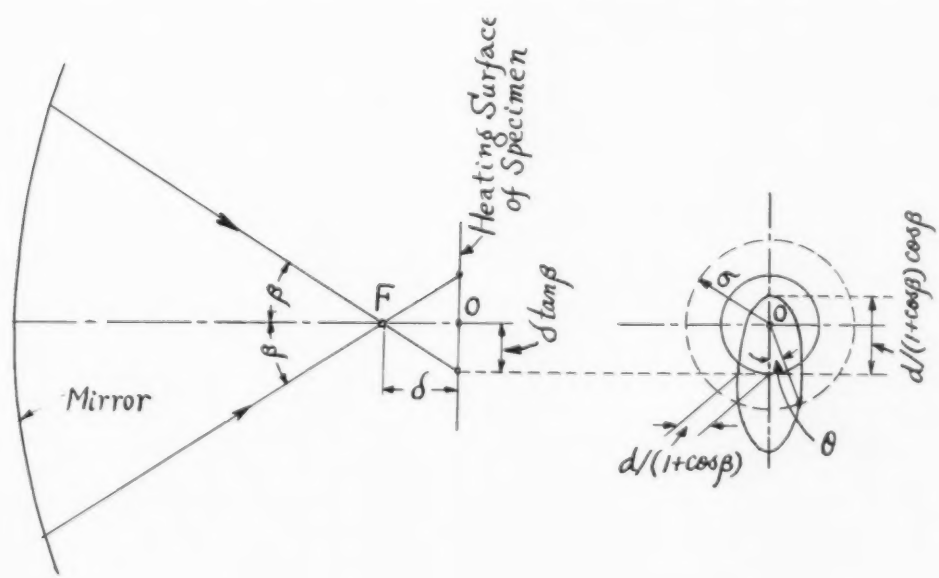

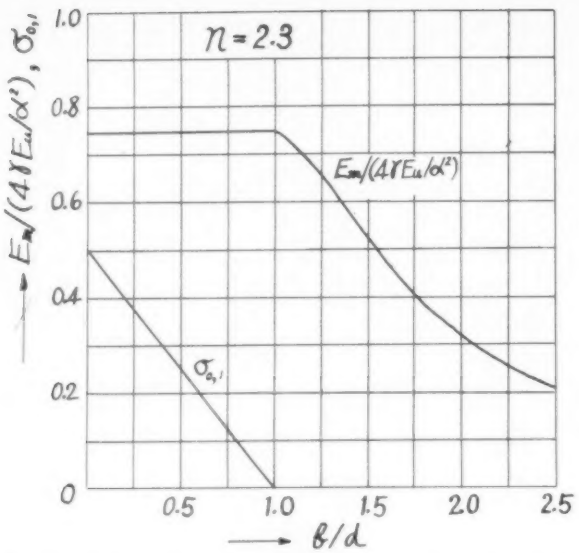


FIG. 8 — Relation between maximum density of the heat flux and $b/d$ when $n = 2.3$.

$\sigma_{0,1}$. In the case $(b/d) > 1$, the maximum occurs at $\sigma = 0$, and its value $E_m$ is obtained by the following equation:

$$E_m = 2\,(2d/b)^2 \int_0^{b/2d} \sigma E(\sigma)\, d\sigma \qquad [12]$$

Fig. 8 shows $E_m$ and $\sigma_{0,1}$.

## EFFECTS OF THE ERROR CAUSED THROUGH THE IMPROPER SETTING OF A SPECIMEN

In order to heat a specimen in the solar furnace, it is necessary to set the heating surface of the specimen so as to coincide with the focal plane. In actual practice, however, this is almost physically impossible and some error will thus occur.

The heating surface of the specimen and the focal plane are assumed to be $\delta$ distance apart and both planes are assumed to be parallel.

In the same manner as introduced in Equations [7] and [10], the density of the heat flux at a point which is $\sigma$ distant from the optical axis on the heating surface is evaluated with reference to Fig. 9 as follows.

$$E = (4\,\gamma\,E_u/a^2) \int 2\,(2\,\theta/\pi)\,\sin\beta\,\cos\beta\,d\beta \qquad [13]$$

where $\theta$ is such an angle as indicated in Fig. 9.

An example of the many possible numerical results is shown in Fig. 10.

In the same manner as introduced in Fig. 8, Fig. 11 is obtained by the following method: The maximum value is equal to $(4\,\gamma\,E_u/a^2)\,\sin^2\beta_c$, where $\beta_c$ is a value to satisfy $d/(1+\cos\beta)\,\cos\beta = \delta\,\tan\beta$. $\sigma_{0,2}$, the value corresponding to $\sigma_{0,1}$ in Fig. 8, is obtained by $\sigma_{0,2} =$ Min. $[\{d/(1+\cos\beta_m)\,\cos\beta_m\} - \delta\,\tan\beta_m]$.

FIG. 10 — Distribution of solar radiation on the heating surface of a specimen when $n = 2.3$ and $\delta/d = 0.5$.

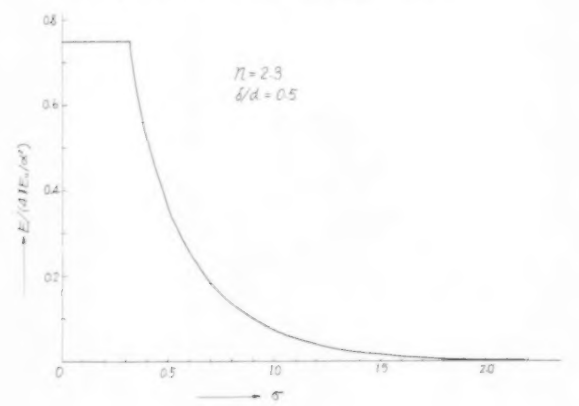


## EFFECTS OF THE ERROR CAUSED BY THE SUN-TRACKING MECHANISM

The error caused by the sun-tracking mechanism of the solar furnace may be represented by $\epsilon$, an angle between the optical axis and the incident solar rays. When the parallel rays are exactly incident to the sun-tracking mirror, a cone $APBF$ as shown in Fig. 12 will be generated by the reflected rays. The rays which incline at an angle $\epsilon$ with the optical axis due to the sun-tracking error are assumed to lie in a plane parallel to this figure. Then the points at which the reflected rays intersect the focal plane lie in the line $FF'$ in the figure. The angle $\psi$ between the line $FF'$ and the generating line $PF$ of the cone $APBF$ is represented by

$$\sin\psi = \sqrt{1 - \sin^2\beta\,\cos^2\phi} \qquad [14]$$

where $\phi = \angle POB$.

Provided that a ray inclined at an angle $\epsilon$ is reflected at $P$ and intersects $FF'$ at $Q$, $\angle FPQ$ is equal to $\epsilon$ and the mean value of the length $PQ$ is approximately equal to the length $PF$, $2f/(1+\cos\beta)$. The length $FQ$, $z$, is obtained by applying the sine formula for $\triangle PFQ$;

$$z/d = (2\sin\epsilon/a)\,\{1/(1+\cos\beta)\,\sin\psi\} \qquad [15]$$

Provided that this ray is a solar ray, the image on the focal plane becomes an ellipse as shown in Fig. 2, $Q$ being its center and $\phi$ the angle between $FF'$ and its major

FIG. 11 — Relation between maximum density of the heat flux and $\delta/d$ when $n = 2.3$.

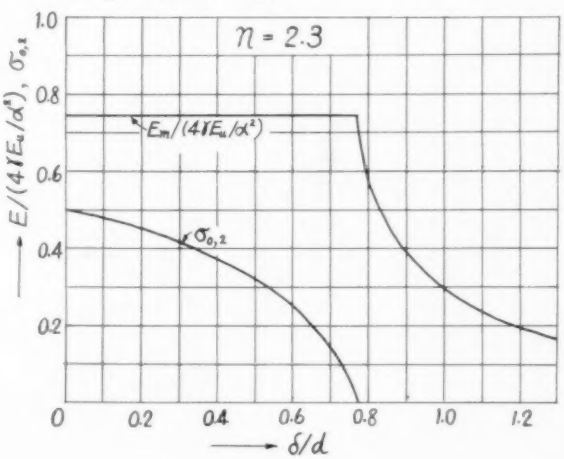




VOL. 1 1957

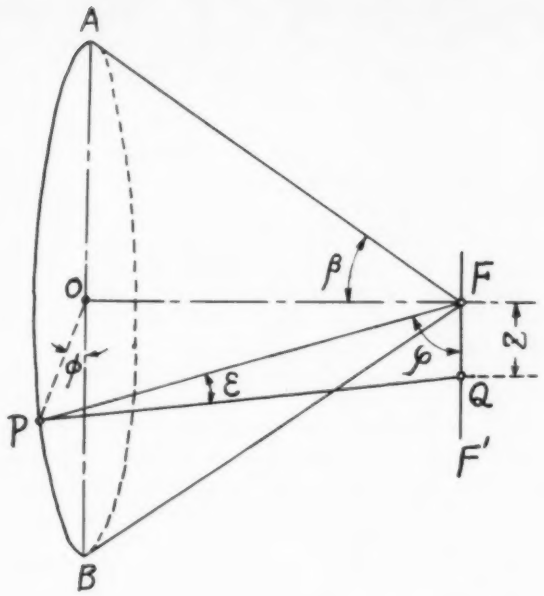


FIG. 12 — Sun-tracking error measured by the angle $\epsilon$.

axis $BC$. The length of the chord, $2\rho$, which is formed by the intersection of the ellipse and the line $FF'$, is shown by

$$\rho/d = 1/(1 + \cos\beta)\sqrt{1 - \sin^2\beta\cos^2\phi} \quad [16]$$

From Equations [14], [15], and [16] the following equation is obtained:

$$z = (2\sin\epsilon/a)\,\rho \quad [17]$$

The range in which the solar radiation is incident upon $FF'$ is $z - \rho < \sigma < z + \rho$, and the following is obtained:

$$z \pm \rho = \rho\{(2\sin\epsilon/a \pm 1\} \quad [18]$$

Considering $z \pm \rho$ to be a function of $\beta$ and $\phi$, and letting the maximum value of the lower limit be $\Gamma_l$ and the minimum of the upper limit $\Gamma_u$, the value of the maximum density for values of $\epsilon$ satisfying $\Gamma_l < \Gamma_u$ is equal to that of the maximum density when $\epsilon = 0$; but throughout the range $\Gamma_l \leqq \sigma \leqq \Gamma_u$ the level of the density is always the same.

Fig. 13 shows the results obtained under these conditions. The shadowed range represents the region in which the maximum density is equal to that of $\epsilon = 0$, and the dotted lines show the limits of the incoming radiation.

## DISCUSSIONS AND CONCLUSIONS

In the practical design and construction of a solar furnace it is necessary to determine the amount of each of the above errors by applying the above analytical results. The following five important items of design and construction are discussed with the assumption that the sole consideration is to obtain the very highest possible temperature from the solar furnace.

**(i) Determination of the Aperture $D$ and the Aperture Ratio $n$**

As the analytical results are represented in dimensionless form, the aperture $D$ and the focal length $f$ do not affect the density of the heat flux provided that the aperture ratio $n$ is the same. The amounts of $D$ and $f$, however, affect the area of the heating surface.

With the increase of the value of the aperture ratio $n$, the rate of solar radiation which affects the increase in the maximum density of the heat flux becomes small, as shown in Fig. 3, while an $n$ value larger than 4 becomes impossible because $\beta$ becomes greater than 90°.

Considering the difficulty of finishing a mirror to

FIG. 13 — Effects of the error measured by the angle $\epsilon$ caused by the sun-tracking mechanism.

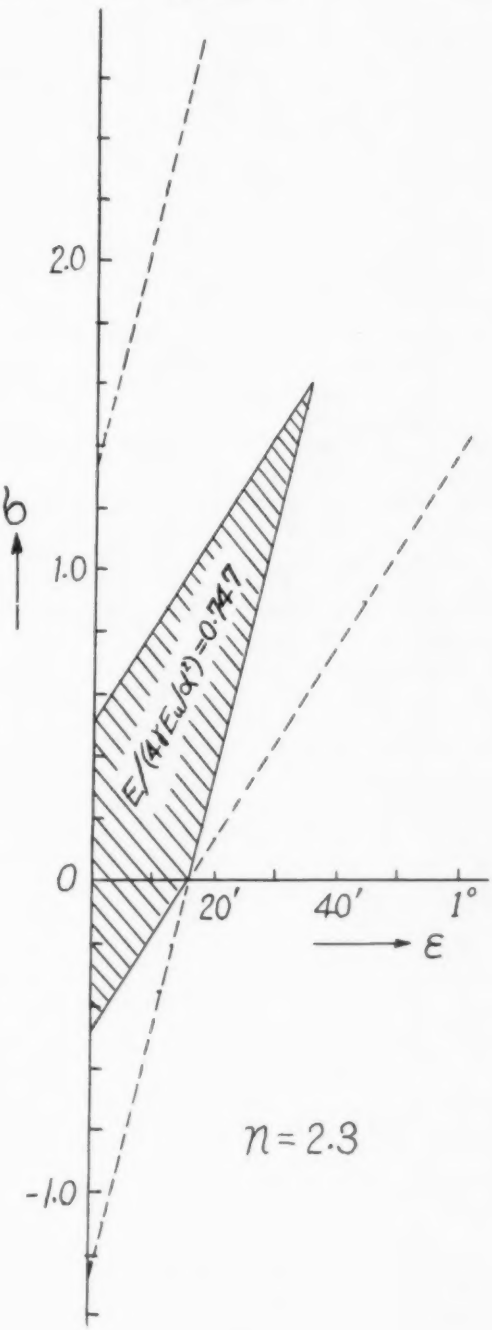

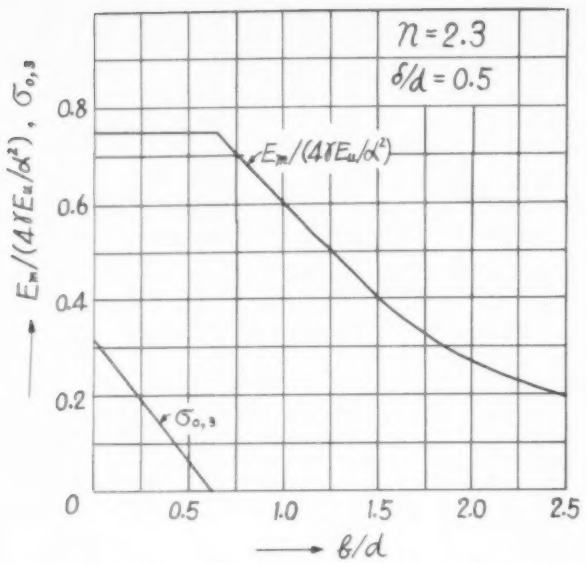


FIG. 14 — Relation between maximum density of the heat flux and $b/d$ when $n = 2.3$, $\epsilon = 0$, and $\delta/d = 0.5$.

an ideal paraboloid, and because it was thought that 2 to 3 is a suitable value for $n$, in this paper, $n = 2.3$ was used since it is the standard taken in producing an ordinary searchlight mirror.

**(ii) Determination of the Error Caused through the Improper Setting of a Specimen, $\delta$**

It is recommended that the value of $\delta$ be smaller than 0.5 $d$, as shown in Fig. 11. It is not so difficult to attain such an accuracy because 0.5 $d$ is of the order of 2.5 mm to 5 mm for an $f$ of the order of 50 cm to 100 cm respectively.

**(iii) Determination of the Error Caused by Improper Sun-tracking with the Mirror**

It is recommended that the value of $\epsilon$ be smaller than 16 minutes as shown in Fig. 13. This also is not so very difficult to accomplish.

**(iv) Determination of the Optical Error in the Surface of the Mirror**

The optical error is the main cause for the interruption of the concentration of the heat flux. It is recommended that the diameter $b$ of the scattering circle be smaller than 0.5 $d$. To attain such an accuracy at low cost, however, is very difficult. For example, $b$ in the ordinary searchlight mirror is approximately 1.0 to 1.5 $d$. In the heliostat type solar furnace, the value for $b$ becomes larger as compared with the single mirror type because the total error is the sum of the errors found in the heliostat and parabolic mirrors.

Using the values of $n = 2.3$, $\delta/d = 0.5$ *and* $\epsilon = 0$, as a reference, the maximum density of the heat flux for various values of $b/d$ is shown in Fig. 14, which is obtained by applying Equation [12] to Fig. 10. $\sigma_{0,3}$ is a value corresponding to $\sigma_{0,1}$ in Fig. 8.

**(v) Temperature of the Heating Surface of the Specimen**

Though it is very difficult to generalize in the discussion of how high a temperature may be produced on heating surface of a specimen as explained at the outset, the following numerical survey of attainable temperatures using several rough assumptions is given.

Example (1): When $n = 2.3$, $\delta/d = 0.5$, $\epsilon = 0$, $b/d = 2.0$, $\gamma = 0.85$, $E_u = 0.1$ watts/cm$^2$, and the total loss of energy from various causes is 30 per cent, from Fig. 14, $E_m/(4\ \gamma\ E_u/a^2) \approx 0.274 \times 0.7$ is obtained. Then from the curve $T$ in Fig. 3, 3400°K as the maximum temperature may be estimated.

Example (2): If 10 per cent is added to the thermal loss in the above example, the temperature is about 3000°K.

Example (3): When the value of $b/d$ changes to 1.0 under the conditions of Example (1), the temperature is 4100°K.

Example (4): When the value of $b/d$ changes to 0.5 under the conditions of Example (1), then the temperature becomes 4350°K.

It is desirable that the errors which occur in the design and construction of the solar furnace be limited to $b/d < 0.5$, $\delta/d < 0.5$ and $\epsilon < 16$ minutes.

## REFERENCES

1. Frederick E. Fowle, *Smithsonian Physical Table*, p. 313, 1933.
2. *Loc cit.*, p. 609.

VOL.
1
1957

# A SURVEY OF SOLAR FURNACE INSTALLATIONS IN THE UNITED STATES

By RAYMOND K. COHEN and NEVIN K. HIESTER

Stanford Research Institute
Menlo Park, California

Prior to the Solar Furnace Symposium in Phoenix in January 1957, efforts were made by the Association for Applied Solar Energy to compile information about all existing solar furnace installations in the United States. At the Association's request, Stanford Research Institute mailed a questionnaire in October 1956 to all organizations known to have a solar furnace. Each organization also received a copy of the questionnaire distribution list, and was asked to suggest any possible additions. The response was quite good, and the information received in the survey forms the compendium presented in this paper.

The compendium includes information from the following organizations and covers a total of 17 furnaces:

(1) A. D. Little, Inc., Cambridge, Mass.
(2) Arizona State College, Tempe, Ariz.
(3) Association for Applied Solar Energy, Phoenix, Ariz.
(4) Bureau of Mines, Morgantown, W. Va.
(5) California Institute of Technology, Pasadena, Calif.
(6) Convair, Fort Worth, Tex.
(7) Convair, San Diego, Calif.
(8) E. I. duPont de Nemours & Co., Wilmington, Del.
(9) Fordham University, New York, N.Y.
(10) General Electric Co., Philadelphia, Pa.
(11) Kennecott Copper Corp., Salt Lake City, Utah
(12) Massachusetts Institute of Technology, Cambridge, Mass.
(13) National Bureau of Standards, Washington, D.C.
(14) Quartermaster Research & Development Command, Natick, Mass.
(15) Stanford Research Institute, Menlo Park, Calif.
(16) University of Minnesota, Minneapolis, Minn.
(17) W.M.C. Precision Works, Kansas City, Mo.

Four additional solar furnaces are reported to be in existence in this country, but detailed information about these was not received in time for inclusion in the compendium.* These additional furnaces are located at:

(18) Sandia Corp., Albuquerque, N.M.
(19) University of Utah, Salt Lake City, Utah
(20) General Electric Co., Cleveland, Ohio
(21) General Electric Co., (presumably a third installation)

*Editor's footnote: Further information about these furnaces and others not reported above would be welcome for later inclusion in the *Journal*.

TABLE I

CLASSIFICATION OF INSTALLATIONS BY TYPE OF CONCENTRATOR AND BY TYPE OF MOUNTING

**36-in. Parabolic Mirror**

HELIOSTAT MOUNTING
Parabolic in Vertical Position (i.e., axis horizontal)
Association for Applied Solar Energy, Phoenix, Ariz.

**60-in. Parabolic Mirror**

ALTAZIMUTH MOUNTING
A. D. Little, Inc., Cambridge, Mass.
Bureau of Mines, Morgantown, W. Va.
Convair, San Diego, Calif.
E. I. duPont de Nemours & Co., Wilmington, Del.
Fordham University, New York, N.Y.
General Electric Co., Philadelphia, Pa.
University of Minnesota, Minneapolis, Minn.

EQUATORIAL MOUNTING
W. M. C. Precision Works, Kansas City, Mo.

HELIOSTAT MOUNTING
Parabolic Mirror in Vertical Position (i.e., axis horizontal)
Arizona State College, Tempe, Ariz.
National Bureau of Standards, Washington, D.C.
Parabolic Mirror in Horizontal Position (i.e., axis vertical) – Directly over Heliostat
Stanford Research Institute, Menlo Park, Calif.
Parabolic Mirror in Horizontal Position (i.e., axis vertical) – Mounted over Second Plane Mirror Inclined at 45° Angle
Kennecott Copper Corp., Salt Lake City, Utah

**120-in. Parabolic Mirror**

EQUATORIAL MOUNTING
Convair, Ft. Worth, Tex.

**Other Types of Concentrators**

ARRAY OF SPHERICAL MIRRORS – HELIOSTAT MOUNTING
Quartermaster Research and Development Command, Natick, Mass.

ARRAY OF PLANE MIRRORS – SPECIAL MOUNTING
Massachusetts Institute of Technology, Cambridge, Mass.

SYSTEM OF 18 PLANE MIRRORS AND 38 LENSES – EQUATORIAL MOUNTING
California Institute of Technology, Pasadena, Calif.

In Table I, the solar furnace installations are classified according to type of concentrator and also on the basis of type of mounting. In 12 of the 17 furnaces listed, a 60-in. parabolic mirror is used as the concentrator, emphasizing the fact that much of the solar furnace construction was undertaken within the last few years when surplus military searchlights were an inexpensive source of para-

bolic mirrors. The large number of altazimuth-mounted parabolics is an indication that many of the investigators chose to use the searchlight carriage as the means for sighting the paraboloid at the sun. There are indications that in some of the more recent installations, as well as in revamping of earlier installations, more use is being made of a heliostat mounting, so that advantage may be taken of the stationary paraboloid and the fixed focal spot.

Detailed descriptions of the furnaces, as well as details of their operation and applications, are presented in Table II. It is shown that the maximum temperature obtained with a 60-in. parabolic furnace was of the order of 3500°C. Uses of the furnaces range from high temperature investigations of metals and ceramics in the parabolic furnaces to studies of the effects of radiation upon materials in the larger array-type furnaces. The dates of initiation of the various installations are of interest in that they indicate that the number of solar furnaces in this country appears to have doubled since the World Symposium on Applied Solar Energy, which was held in Phoenix in November 1955.

It should be pointed out that, at the time when this survey was made, many of the installations were still in the design and construction stages. Consequently, in some instances the furnaces may have advanced to such a stage of development that the data in this compendium do not indicate current methods of operation, or latest experimental findings.

VOL.
1
1957

OL.
1
957

## TABLE II
## SURVEY OF SOLAR FURNACE INSTALLATIONS

| Organization | Fordham University | Arizona State College | General Electric Co. | QM Research & Development Command | *Massachusetts Institute of Technology | A. D. Little, Inc. | Bureau of Mines | Kennecott Copper Corp. |
|---|---|---|---|---|---|---|---|---|
| Principal investigator | T. S. Laszlo | C. Kevane | J. Farber<br>J. Metzger | J. M. Davies<br>E. S. Cotton | H. C. Hottel | A. Emslie<br>E. Kreidl<br>P. Glaser | Special Problems Section (P. G. Salgado) | W. M. Tuddenham |
| Furnace location<br>Date initiated | New York, N.Y.<br>Spring 1955 | Tempe, Ariz.<br>March 1956 | Philadelphia, Pa.<br>Oct. 1956 | Natick, Mass.<br>1955 | Cambridge, Mass.<br>July 1951 | Cambridge, Mass.<br>Jan. 1957 | Morgantown, W. Va.<br>Nov. 1955 | Salt Lake City, Utah<br>Summer 1956 |
| Furnace description<br>Main mirror:<br>Mounting<br>Mirror material<br>Reflecting surface material<br>Reflecting surface<br>Aperture<br>Focal length<br>Rim angle<br>Theoretical image diameter | <br>Altazimuth<br>Bronze<br>Stellite<br>Front<br>60 in.<br>25.5 in.<br>60.8°<br>0.238 in. | <br>Fixed; axis horiz.<br>Copper<br>Aluminum<br>Front<br>60 in.<br>29.5 in.<br>65°<br>0.256 in. | <br>Altazimuth<br>Copper<br>Rhodium<br>Front<br>60 in.<br>25 in.<br>60°<br>0.25 in. | <br>Fixed; axis horiz.<br>Glass<br>Aluminum<br>Front<br>28 ft. x 28 ft.<br>35.8 ft.<br>32°<br>4 in. | <br>Special<br>Glass<br>Silver<br>Back<br>———<br>———<br>———<br>3 in. | <br>Altazimuth<br>Copper<br>Stellite<br>Front<br>59.5 in.<br>25.6 in.<br>60°15'<br>0.236 in. | <br>Altazimuth<br>Copper<br>Rhodium<br>Front<br>60 in.<br>26 in.<br>———<br>0.25 in. | <br>Fixed; axis vert.<br>Copper<br>Rhodium<br>Front<br>60 in.<br>25.8 in.<br>60°<br>0.24 in. |
| Auxiliary mirrors and lenses:<br>No. of auxiliary mirrors<br>No. of lenses<br>System | None<br>None<br>——— | One<br>None<br>Heliostat | None<br>None<br>——— | One<br>None<br>Heliostat | One<br>None<br>Special | None<br>None<br>——— | None<br>None<br>——— | 2<br>None<br>Heliostat |
| Furnace operation<br>Guiding<br>Type<br>Other details | <br>Phototubes<br>——— | <br>Phototubes<br>——— | <br>Manual<br>——— | <br>Phototubes<br>——— | <br>None<br>——— | <br>Manual<br>(Electronic optional) | <br>Manual<br>(Considering phototubes) | <br>Phototubes<br>——— |
| Temperature control:<br>Type<br>Sensing device<br>Other details | <br>Manual<br>Optical pyrometer<br>Cylinder | <br>Manual<br>———<br>Cylinder | <br>Manual<br>Thermocouple; Rad. pyrometer<br>Cylinder | <br>None<br>———<br>——— | <br>None<br>———<br>——— | <br>Manual<br>———<br>Cylinder (automatic w/rad. pyrometer optional) | <br>———<br>Rad. pyrometer<br>Cylinder | <br>Manual<br>———<br>Shades |
| Flux control<br>Type<br>Sensing device<br>Other details | <br>———<br>———<br>——— | <br>Manual<br>———<br>——— | <br>———<br>Calorimeter & std. norm. inc. pyrheliometer<br>——— | <br>None<br>———<br>——— | <br>None<br>———<br>——— | <br>———<br>———<br>——— | <br>None<br>———<br>——— | <br>(Incomplete) |
| Temperature measurements:<br>Sensing device<br>Other details | Optical pyrometer<br>——— | Optical pyrometer<br>Device for excluding inc. energy | Pyrometer, thermocouple, spectroscope<br>Rotating tubes for excluding inc. energy | None<br>——— | ———<br>——— | Optical pyrometer<br>——— | Optical pyrometer<br>Rotating disc for excluding inc. energy | Optical pyrometer<br>——— |
| Flux measurement:<br>Type instrument<br>Means for obtaining flux profile<br>Other details | Water-cooled radiometer<br>———<br>——— | Copper calorimeter<br>None<br>——— | Water-cooled calorimeter<br>Flux vs. angle by movement of calorimeter & cylinder<br>——— | Calorimeter<br>Radiometer<br>——— | Calorimeter & radiometer<br>———<br>——— | ———<br>———<br>——— | None<br>———<br>——— | <br>(Incomplete) |
| Specimen holder:<br>Materials of construction<br>Type of traversing mechanism | Aluminum, carbon, $ZrO_2$<br>Elec. motors for all 3 axes | ———<br>——— | Steel; ½-in. Jacobs chuck<br>Geared; hand-operated | No details yet<br>——— | ———<br>——— | Stainless steel & aluminum<br>3 variable speed motors | Stainless steel & refractory<br>Manual crank & rack & pinion | Carbon blocks<br>Cart on wheels with control |
| Applications & experimental results<br>Use of furnace | (See below) | Determine thermal diffusivity of solids | (See below) | Effect of irradiation on QM materials<br>Determine protection to personnel by QM items | ——— | Basic and applied high temperature research | Refractory testing | Pyrometallurgical research |
| Maximum temperature obtained | 3500°C | ——— | To be determined soon | ——— | ——— | ——— | *2760°C | 2800°C |
| Maximum flux measured | (Underway) | 300 cal/cm²/sec (est.) | To be determined soon | ——— | ——— | ——— | Not determined | ——— |
| Average local solar constant | ——— | 1.1 cal/cm²/min | To be determined soon | ——— | 1.5 cal/cm²/min | 1.3 (June air mass = 1.0) | ——— | ——— |
| *Reflectivity efficiency factor | 70% (measured) | 75% (heliostat) | To be determined soon | ——— | 66% (est.) | 75% (est.) | Unknown | 70% (est.) |
| **Shadowing loss factor | 96% measured | 96% | To be determined soon | ——— | ——— | 96.4% | 85% (est.) | Approx. 95% |
| General type of research | Performance measurements for design of large solar furnace; investigations of physical & chemical properties of matter at high temperatures | High temperature materials research | High temperature chemistry<br>Spectroscopic studies<br>Heat flux effects on materials | ——— | Ignition of materials by radiation | Client—confidential | ——— | Zone refining<br>Vacuum fusion<br>Fusion in controlled atmos. |

*Takes into account losses by reflectivity and/or absorptivity of all optical parts of furnace. (100 per cent would denote no losses.)

**Takes into account losses due to shadowing of mirror by devices for mounting mirrors, targets, etc. (100 per cent would denote no shadowing.)

*Information from article:
R. Gardon, "A segmented-mirror solar furnace for high intensity thermal radiation studies," Rev. Sci. Instruments 25:459, 1954.

*May be higher—temperature measuring device not yet completed

| | Convair | Convair | E. I. du Pont de Nemours & Co. | W.M.C. Precision Works & R.M.F. Steel Products Division | National Bureau of Standards | University of Minnesota | California Institute of Technology | Association for Applied Solar Energy | Stanford Research Institute |
|---|---|---|---|---|---|---|---|---|---|
| | B. I. Davis<br><br>San Diego, Calif.<br>Sept. 1952 | B. I. Davis<br><br>Ft. Worth, Tex.<br>Sept. 1952 | C. M. Cooper<br><br>Wilmington, Del.<br>May 1956 | W. M. Conn<br><br>Kansas City, Mo.<br>1956 | S. Zerfoss<br><br>Washington, D.C.<br>May 1956 | E. R. G. Eckert<br>T. F. Irvine, Jr.<br><br>Minneapolis, Minn.<br>July 1956 | P. Duwez<br><br>Pasadena, Calif.<br>1932 | J. I. Yellott<br><br>Phoenix, Ariz.<br>Oct. 1956 | N. K. Hiester<br>R. K. Cohen<br><br>Menlo Park, Calif.<br>1956 |
| | Altazimuth<br>Copper<br>Co-Ni alloy<br>Front<br>60 in.<br>25.5 in.<br>60°<br>0.24 in. | Equatorial<br>Aluminum<br>Same<br>Front<br>120 in.<br>34.5 in.<br>82°<br>0.32 in. | Altazimuth<br>Copper<br>Rhodium<br>Front<br>60 in.<br>———<br>———<br>——— | Equatorial<br>Copper<br>Rhodium<br>Front<br>60 in.<br>26.3 in.<br>———<br>0.236 in. | Fixed; axis horiz.<br>Copper<br>Rhodium<br>Front<br>60 in.<br>26 in.<br>60°<br>0.25 in. | Altazimuth<br>Copper<br>Rhodium<br>Front<br>60 in.<br>———<br>———<br>——— | Equatorial<br>———<br>———<br>———<br>———<br>———<br>0.50 in. | Fixed; axis horiz.<br>Stellite<br>Stellite<br>Front<br>36 in.<br>14.4 in.<br>65°<br>0.134 in. | Fixed; axis vert.<br>Copper<br>Rhodium<br>Front<br>60 in.<br>26 in.<br>———<br>0.25 in. |
| | None<br>None<br>——— | None<br>None<br>——— | None<br>———<br>——— | None<br>———<br>——— | One<br>———<br>Heliostat | None<br>———<br>——— | 18<br>38<br>——— | One<br>———<br>Heliostat | One<br>———<br>Heliostat |
| | Manual<br>——— | Astron. controller<br>——— | Manual<br>Selsyn motor | ———<br>Motor plus tubes | ———<br>Phototubes | Manual<br>——— | ———<br>Astron. controller | Manual<br>——— | Automatic<br>4 phototubes |
| | Manual<br>———<br>Annular rings, $\theta$ = 20°, 30°, 45°, 60° | Manual<br>———<br>Cylinder | Manual<br>———<br>——— | ———<br>Thermocouple<br>Cylinder | Manual (auto. later)<br>———<br>Diaphragm | ———<br>———<br>——— | None<br>———<br>——— | Manual<br>———<br>Iris diaphragm | ———<br>———<br>——— |
| | Manual using cylinder<br>Eppley norm. inc. pyrheliometer<br>——— | Manual or motor cylinder<br>Eppley norm. inc. pyrheliometer<br>——— | ———<br>———<br>——— | ———<br>———<br>——— | Shade (manual)<br>Not yet<br>——— | ———<br>———<br>——— | ———<br>None<br>——— | ———<br>None yet<br>——— | ———<br>———<br>——— |
| | Optical pyrometer<br><br>Rotating shutter for excluding inc. energy (under dev.) | Optical pyrometer<br><br>Rotating shutter (effect on measurements not fully resolved) | Optical pyrometer<br>——— | Thermocouple/optical pyrometer<br>Sectors for shutting off incident energy | Pyrometer<br><br>Modified Conn device<br>Filter rather than shutters | ———<br><br>——— | ———<br>——— | ———<br>——— | ———<br>——— |
| | Convair-developed, water-cooled black cavity calorimeter<br>By varying rim angle<br>——— | Water-cooled black cavity calorimeter<br>By varying rim angle<br>——— | Cavity calorimeter<br><br>Reflective orifice<br>——— | Calorimeter<br>———<br>———<br>——— | Calorimeter<br>———<br>———<br>——— | ———<br>———<br>———<br>——— | Water-cooled radiometer<br><br>Rotary table<br>——— | None yet<br>———<br>———<br>——— | ———<br>———<br>———<br>——— |
| | Jacobs chuck<br>Rack & pinion | Jacobs chuck<br>Motor-driven screw | Various<br>Manual | Metal plus plastics<br>——— | ———<br>Motors | ———<br>——— | ———<br>——— | ———<br>——— | ———<br>——— |
| | Study of refractories<br>Heat transfer studies<br>Emissivities at high irradiance<br>Enthalpies of molten ceramics | Study of refractories<br>Heat transfer studies<br>Emissivities at high irradiance<br>Enthalpies of molten ceramics | Study of furnace optics<br>Study of atmos. conditions<br>Dev. of "skull melting" technique | Research & testing | ——— | High temperature emissivity measurements | Melting refractories | Demonstration of furnace principles and uses | ——— |
| | 3050°C | 2800°C | 3000°C | 3000°C | 3300°C | ——— | Thoria M.P.<br>3200±100°C | 1500°C | ——— |
| | 629 cal/cm²/sec | 139 cal/cm²/sec | ——— | ——— | ——— | ——— | 170 cal/cm²/sec | ——— | ——— |
| | 1.3 cal/cm²/min | 1.3 cal/cm²/min | Being evaluated | ——— | ——— | ——— | ——— | 0.9-1.4 cal/cm²/min | ——— |
| | 80% | 85% | Being evaluated | 86% | ——— | ——— | ——— | ——— | ——— |
| | 90% | 63% | Varied | 95% | 85-90% | ——— | ——— | ——— | ——— |
| | ——— | ——— | ——— | Rates of reaction in high temperature materials research | ——— | Total normal emissivity measurements<br>Heat transfer under high heat flux | ——— | ——— | High temperature processes, material preparation and testing rate studies, corrosion studies |
| | | | | | | | | | |